2023-08-01

Increases In Uvr Exposure: Local Adaptation Of A Bdelloid Rotifer

Maribel J. Baeza
University of Texas at El Paso

INCREASES IN UVR EXPOSURE: LOCAL ADAPTATION OF A BDELLOID ROTIFER

MARIBEL J. BAEZA

Doctoral Program in Ecology and Evolutionary Biology

APPROVED:

Elizabeth J. Walsh, Ph.D., Chair

Vanessa Lougheed, Ph.D.

Kyung-An Han, Ph.D.

Wiebke J. Boeing, Ph.D.

Stephen L. Crites, Jr., Ph.D.
Dean of the Graduate School

INCREASES IN UVR EXPOSURE: LOCAL ADAPTATION OF A BDELLOID ROTIFER

by

MARIBEL J. BAEZA, B.S., M.S.,

DISSERTATION

Presented to the Faculty of the Graduate School of

The University of Texas at El Paso

in Partial Fulfillment

of the Requirements

for the Degree of

DOCTOR OF PHILOSOPHY

Department of Biological Sciences

THE UNIVERSITY OF TEXAS AT EL PASO

August 2023

Acknowledgements

Primarily, I would like to express my profound gratitude to my mother Maria Baeza. Her constant belief in my abilities, her unwavering support, and her unconditional love have been my pillars of strength throughout this endeavor. Her sacrifices and tireless dedication to my well-being have shaped me into the person I am today. To my father Jose Baeza, though you have passed, I will forever carry the numerous lessons you taught me. I am forever indebted not only to them but also to my sisters Elvia, Azucena, Arjelia and niece Lizzette and nephew Ismael. Your unwavering support and belief in my abilities have been invaluable. Your presence during the challenging moments, both academically and personally, has provided me with the reassurance and motivation I needed. Thank you for always being there, cheering me on and reminding me of my capabilities. To my nephew Isaac and niece Savannah you have brought immense joy and inspiration into my life. Your innocence and genuine enthusiasm for the natural world have reminded me of the importance of my research. I dedicate this achievement to you and hope it serves as a testament to the pursuit of knowledge and the beauty of science.

I am indebted to my academic advisor, Dr. Elizabeth J. Walsh for her guidance, expertise, and unwavering support throughout my research. Her mentorship has been transformative, shaping not only my scientific understanding but also my approach to life. I want to express my heartfelt appreciation to Hueco Tanks State Park & Historic Site rangers, employees especially to Maria Rita Valles, for notifying me after rain, or snow to let me know when to go sampling. Samples were collected from June 2017 to February 2021, under permit numbers 2016-03, 2017-R1-19, 12-20, 7-21 (E. Walsh). A special thanks to Dr. Vanessa Lougheed for the use of Shimadzu TOC (Total Organic Carbon) L series analyzer and Dr. Raed

Aldouri for the use of Topcon GR-3 GPS GLONASS RTK Base & Rover 915 US GSM Receiver & GPS Systems. I also thank Panfeng Liang, Robert McCreary and Dr. Amy Wagler for their help with statistical analysis. As well as to the rest of my doctoral committee members Drs. Kyung-An Han, and Wiebke J. Boeing and to an honorary committee member Jonathon E. Mohl for their feedback on the project. I would also like to extend my gratitude to David Mark Welch, Bette Hecox-Lea, and Robert Wallace for extending their expertise and providing valuable guidance and feedback in developing my project.

I would like to extend my gratitude to the faculty and staff of the Department of Ecology and Evolutionary Biology, colleagues, and fellow researchers, both within my department and beyond, for their insightful discussions, constructive feedback, and camaraderie. I also want to express my heartfelt appreciation to Hueco Tanks State Park & Historic Site rangers, employees especially to Maria Rita Valles, for notifying me after rain, or snow to let me know. To Joseph McDaniel, Vanessa Blevines, Rachael Apodaca, and Maite Martin for their assistance in sample and data collection. All my friends and loved ones who but especially Julia Bustamante, Deidra Garcia, Bobbie Walsmith, Alejandra Sanchez-Avila, and Jennifer Wilhite who have stood by my side, provided me with untiring support, understanding, and encouragement. Your belief in my abilities, patience during challenging times, and celebratory moments of triumph have made this journey all the more fulfilling.

Additionally, funding for this research was supported in part by two UTEP Dodson grants, Research Assistant Fellowship from the University of Texas at El Paso Office of the Provost and Graduate School, a UTEP Frank B. Cotton Trust Scholarship, and a 3-year fellowship from the Hispanic Alliance for the Professoriate in Environmental Sciences and Engineering

Fellowship, UTEP graduate school travel grant, Biology department travel grant. Additional funding was provided by the National Science Foundation DEB 1257068 (E. Walsh), National Institute on Minority Health and Health Disparities (NIMHD), a component of the National Institutes of Health (NIH) 5U54MD007592, Border Biomedical Research Center (BBRC) 5G12RR008124, and supplement to US Department of Education Grant Minority Science and Engineering Improvement Program.

Finally, I must thank my precious cats, Soda, Alley, and Açai, due to the simple fact that one of my drivers is to provide my cats with a better life. Catface and Turtle although you have passed, I grew and learned so much from having you in my life. To all those mentioned above and countless others who have played a role in shaping my academic and personal growth, I offer my sincerest thanks. Your contributions have been invaluable, and this accomplishment would not have been possible without your love, support, and belief in me, in particular in those times I did not believe in myself. Thank you.

Abstract

Aquatic species living in ephemeral habitats without a continual influx of dissolved organic carbon (DOC) are at increased risk of the effects of ultraviolet radiation (UVR) as the climate changes. Climate change is predicted to cause changes in DOC, some habitats will experience extended periods of drought and reduced input from DOC sources, and other environmental features that increase UVR reaching aquatic habitats. UVR can cause damage to cellular structures and biomolecules such as DNA, proteins, and lipids. The pigmented bdelloid *Philodina* sp. (*Philodina*) found in rock pools in the Chihuahuan Desert naturally experiences high UVR, yet it appears to thrive. Here I: (1) Examine the relationship between DOC and pigmentation in bdelloids, (2) Determine whether red pigmentation provides protection from UVR, (3) Investigate the consequences of transgenerational UVB exposure, and how this affects offspring, and (4) quantify gene expression in response to UVB exposure highly pigmented and non-pigmented bdelloids using a combination of field and laboratory approaches.

I observed that highly pigmented bdelloids were found in a subset of rock pools at Hueco Tanks State Park and Historic Site, El Paso Co. TX. Both DOC and red pigmentation are known for their ability to absorb and attenuate UVR. To determine whether the presence of pigmented bdelloids was correlated to DOC concentration, I sampled 12 rock pools and found that bdelloids were more prevalent in rock pools with lower concentrations. From these results, I inferred that in habits with low DOC concentrations, bdelloids increase pigmentation to offset the damaging effects of UVR.

To further determine the photoprotective qualities of red pigmentation, I cultured *Philodina* in the laboratory to obtain individuals with varying levels of coloration. Individuals

were exposed to three levels of UVR (low, corresponding to local winter levels; mid, corresponding to fall levels; high corresponding to summer levels) in both the active and dormant form. I varied the length of dormancy since it is known that bdelloids become inactive in response to environmental stressors and that the longer they remain dormant, the less likely they are to recover. Comparing highly pigmentated (HP) to non-pigmented (NP) *Philodina*, HP bdelloids were twice as likely to survive UVB exposure. When bdelloids were desiccated for one day, the HP treatment was four times more likely to survive UVB exposure than the NP treatment. However, odds of surviving decreased as desiccation time increased. These results provide additional support for hypothesized the photoprotective capabilities of the red pigmentation.

The consequences of transgenerational UVB radiation exposure were investigated by exposing three non-consecutive generations of *Philodina* to the same levels of UVB and determining survival of the parental, F2, and F4 generation. Life table experiments were used to quantify responses to repeated UVB exposure. Interestingly, both lifespan and net reproductive rate increased in low (117%, 233%) and mid (50%, 205%) UVB treatments when compared to the control. Similar responses to these UVB levels were seen in the F_5 generation offspring. These results suggest that *Philodina* has locally adapted to regional UVB intensities.

Lastly, I determined changes in gene expression after UVB exposure in both HP and NP *Philodina*. In HP bdelloids, ~50 genes showed differential expression while in the NP treatment >10,000 genes showed differential expressed when exposed to regional levels of UVB radiation. These observations further support the photoprotective properties of the pigmentation seen in *Philodina*.

In this study, I have demonstrated that the pigmentation observed in *Philodina* provides effective photoprotection and that it may be a viable means to mitigate UVR-induced damage in invertebrates inhabiting shallow waters. Furthermore, I have provided evidence for local adaptation of *Philodina* to regional levels of UVB radiation. These findings could potentially serve as a model for understanding how other invertebrate species might respond to shifts in UVR levels as the climate changes.

Table of Contents

List of Tables

List of Figures

Chapter 1: General Introduction

Climate change has emerged as a major global concern, with rising temperatures and changing weather patterns threatening the ecological balance of our planet. One of the factors intensifying the effects of climate change in arctic, mid latitude, and high elevation areas is the increase in ultraviolet radiation (UVR) (Alton & Franklin 2017; Bais et al. 2018, Barnes et al. 2019, Cordero et al. 2022). As the planet continues to warm, interactions between temperature and several factors augment the risk of UV radiation exposure due to the continued use of ozone depleting substances (Bais et al. 2018; Barnes et al. 2019; Polvani et al. 2020), natural variations in atmosphere thickness (Cordero et al. 2022), and changes in weather patterns (Bais et al. 2018; Goutam et al. 2022). For each environmental variable (e.g., temperature, UVR intensity), there is a range within which individuals in a population can survive and reproduce. However, the capacity of animals to adapt to the changing climate varies among species, and the rate of climate change can sometimes exceed the ability of organisms to adapt, leading to challenges and vulnerabilities (Dam 2013; Orr 2000, 2005; White & Butlin 2021).

Various aquatic invertebrates that live in environments with high levels of UVR have evolved the production of UV absorbing compounds or can repair damage (Alcocer et al. 2020; Ekvall et al. 2015; Garcia et al. 2008; Mojib et al. 2014; Nevalainen et al. 2016). These adaptations help minimize the negative effects of UV radiation, such as DNA mutations or tissue damage, and improve their chances of survival and reproductive success in UV-rich environments (Alcocer et al. 2020; Fischer et al. 2013; Marcoval et al. 2020; Oexle et al. 2016). In general, species with higher levels of pigmentation possess a survival advantage in high UVR habitats (Alcocer et al. 2020; Hansson 2004; Hylander et al. 2009; Sen & Mallick 2021).

The rock pool environment at Hueco Tanks State Park and Historic Site (hereafter: Hueco Tanks), located in the Chihuahuan desert, presents a unique set of challenges to invertebrate survival due to the harsh climate. Invertebrates residing in rock pools are subjected to a range of selection pressures, including high UV intensity, large fluctuations in temperature, and seasonal water availability, which may lead to changes in genetic traits over time (Dam 2013; Fox et al. 2019; Stábile et al. 2021).

Solar radiation refers to the energy emitted by the sun as electromagnetic waves. It includes a range of wavelengths, from gamma rays to radio waves excessive exposure to certain wavelengths of solar radiation, such as UVR can cause cellular damage as noted above (Häder 2011, McKenzie et al. 2011, Williamson et al. 1994). UVR is composed of four wavelengths: UVV (100 – 200 nm), UVC (200 – 280 nm), UVB (280 – 315 nm), and UVA (315 – 400 nm) (McKenzie et al. 2011; Williamson et al. 1996). All UVV and most UVC rays are absorbed or reflected by the Earth's atmosphere, while UVB and UVA can reach the Earth's surface (Erickson et al. 2015; Williamson et al. 2016). UVB radiation damages tissue causing DNA mutations, which may reduce lifespan and fecundity (McKenzie et al. 2011; Williamson et al. 1996; Williamson et al. 2001), slow locomotion, and increase the toxicity of certain pesticides (Bais et al. 2018; Kim et al. 2011, 2015).

At the equator, solar radiation enters the atmosphere directly (zenith angle 0), resulting in particularly high UVR intensities (Cordero et al. 2022; Polvani et al. 2020; Williamson et al. 2016). In addition to the solar zenith angle, the amount of UVR that reaches a habitat is also affected by season, time of day, and latitude (Fig. 1.1; Bais et al. 2018; Blumthaler & Ellinger 1997; Häder 2011; Pinceel et al. 2018; Wang et al. 2014). This results in UVR, in general, being

highest during midday in the summer in most places in the world. UVR intensity reaching aquatic communities is also dependent on cloud coverage, pollution, water calmness, albedo, clarity, and depth of the water body, as well as the concentration of dissolved organic carbon (DOC) (Fig. 1.1; Allen et al. 1998; Williamson et al. 2016).

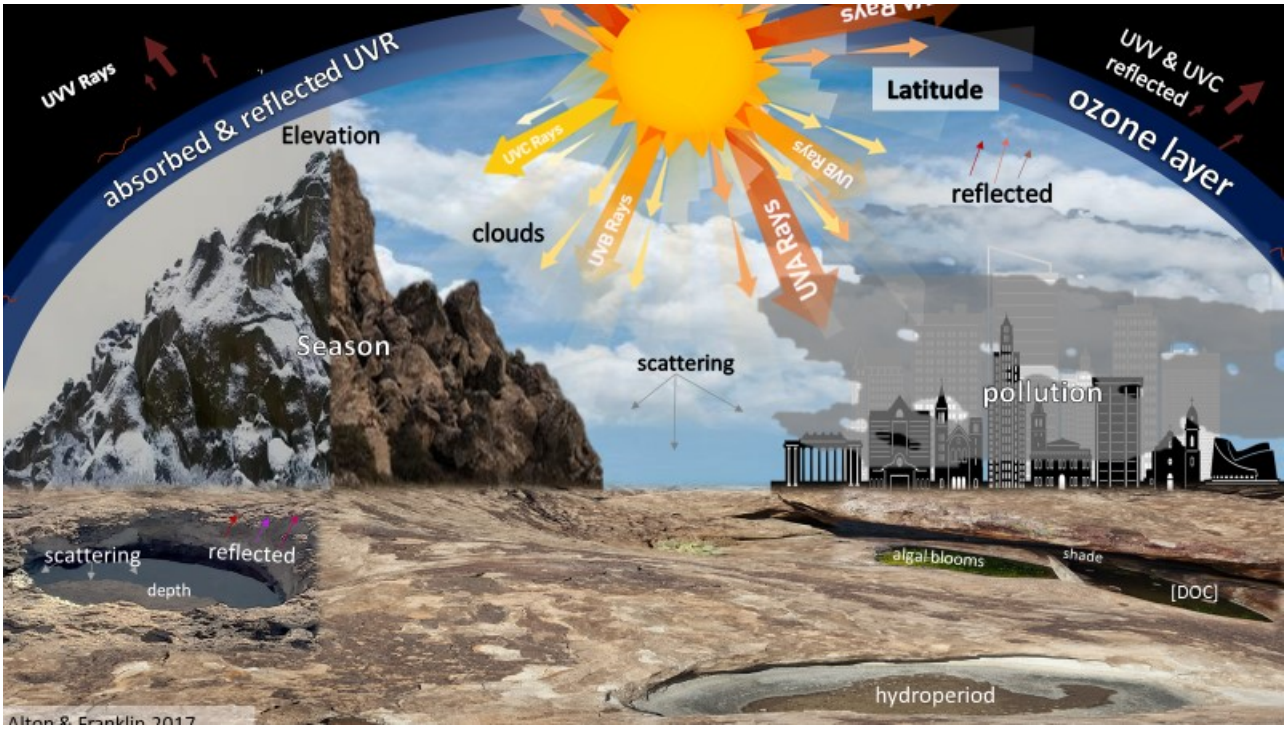

Figure 1.1. Factors that affect ultraviolet radiation intensity reaching aquatic environments in ephemeral rock pools. Diagram based on model from Alton & Franklin 2017.

Before significant ozone had accumulated, life on Earth experienced dangerous levels of UVR (Cockell 1998); to cope with this threat three main strategies evolved: avoidance, photoprotection, and DNA repair (Cockell 1998; Williamson 1994). Diel vertical migration (DMV) is the act of moving to greater depths during the day to avoid the high-intensity UVR in surface waters (Boeing et al. 2008), this is only effective in deep bodies of water that are able to absorb, reflected or refract UV radiation (Leech & Williamson et al. 2000). Avoidance is also possible in shaded habitats or in those with high concentrations of DOC, which can absorb UVR.

However, in conditions of low DOC, some organisms have evolved photoprotection as a means of avoiding UVR damage (Hansson et al. 2007; Hylander et al. 2009; Rautio & Tartarotti 2010).

Photoprotection can be an adaptive trait that has evolved in response to UVR exposure, in environments without visual predators (Hansson 2004; Hylander et al. 2009). Certain zooplankton species, such as cladocerans, can synthesize melanin, a pigment that provides photoprotection (Mojib et al. 2014; Nevalainen et al. 2016) or mycosporine-like amino acids (Nevalainen et al. 2016; Sen & Mallick 2021). Mycosporine-like amino absorbs UV light, dissipates its energy as heat, and prevents damage (Alcocer et al. 2020; Ekvall et al. 2015; Garcia et al. 2008; Sen & Mallick 2021). On the other hand, copepods acquire photoprotectants from their food sources (Alcocer et al. 2020; Andersson et al 2003; Chatragadda et al. 2021). It is physiologically costly to synthesize protective pigments for photoprotection. Thus, aquatic invertebrates only engage in this resource- and energy-intensive synthesis when it is necessary for their survival (Hansson et al. 2007; Nevalainen et al. 2016). This allocation of resources highlights the trade-offs and selective pressures that organisms face when balancing survival strategies in their environments.

Regions with lower humidity, such as deserts, tend to receive greater UVR intensity, as water droplets in the atmosphere can absorb or scatter solar radiation (Fig. 1.1; Bais et al. 2018; Häder 2011; Pinceel et al. 2018; Wang et al. 2014). The Chihuahuan Desert, the largest desert in North America, is home to a wide range of plant and animal species, many of which are found nowhere else in the world (Briggs et al. 2019; Dinerstein et al. 2000; Schmidt 1979). Hueco Tanks State Park and Historic Site (31.93° N, 106.04°W) is located within the Chihuahuan Desert, is named for the hundreds of small rock pools (huecos) that are found on the rocky

outcrops (Schröder et al. 2007; Walsh et al. 2014). The outcrops in the area are the result of volcanic and tectonic activity. The shape and dimensions of rock pools are the result of the local climate eroding depressions on outcropping rock layers composed of igneous and metamorphic rocks (Henry 1981).

Shallow rock pools in the Chihuahuan Desert represent a unique and challenging environment for organisms to survive. Rock pools are subjected to high levels of solar radiation due to their shallow depth (Havstad et al. 2006) and the low concentrations of dissolved organic carbon (Alonso et al. 2004; Tapia-Torres et al. 2015), which provide little protection from UVB damage (Blumthaler & Ellinger 1997; Tapia-Torres et al. 2015; Ríos-Arana et al. 2019). Several species have adapted to these harsh conditions and have developed various mechanisms to cope with UVR exposure, including the production of pigments that act as photoprotectants or changes in behavior to avoid high UVR exposure during the peak hours of the day (Schröder et al. 2007; Walsh et al. 2014). These adaptations are long-term effects of selection, phenotypic plasticity, and maternal effects (Dam 2013; Fox et al. 2019; Orr 2000).

Fitness is a function of lifetime fecundity and survival. These life history traits are used to interpret possible biological and/or ecological behavior in any given habitat (Dam 2013; Fox et al. 2019). The interaction between genotype and environment varies from individual to individual and directly affects potential evolution in any given population. Phenotypic variation refers to the observable differences in traits and characteristics among individuals within a population (Dam 2013; de Villemereui et al. 2020; Fox et al. 2019). Adaptations, on the other hand, involve changes in traits and characteristics across generations that enhance an organism's fitness within a specific environment. These changes are driven by natural selection,

where individuals with advantageous traits are more likely to survive and reproduce, passing on those traits to their offspring (de Villemereui et al. 2020; & Butlin 2021). Over time, this process can lead to the accumulation of traits that are adapted to the specific environmental conditions of a population's habitat.

Members of the phylum Rotifera are microscopic, multicellular invertebrates found in freshwater, marine environments, and damp soils (Ricci 2016; Walsh et al. 2014). This phylum consists of four monophyletic classes: Acanthocephala, Seisonidea, Monogononta, and Bdelloidea. Rotifers are essential members of the aquatic food web since they consume bacteria, fungi, and algae (Snell et al. 2014; Wallace 2002). They are also key food sources for many large aquatic animals, including fishes, amphibians, and invertebrates (Snell et al. 2014; Wallace 2002). In addition to their role in nutrient cycles, they consume and recycle nutrients that might otherwise be lost in the system, thereby contributing to the overall health and productivity of the ecosystem (Wallace 2002, Wallace et al. 2015).

Rotifers are used in laboratory experiments to study various biological processes. Rotifers are excellent model organisms because of their small body sizes (100 – 1600 µm; Ricci and Melone 2000), high reproduction rates, ease of cultivation, large population sizes, and short lifespans (Dahms et al. 2011; Ricci and Melone 2000; Gladyshev et al. 2008; Snell et al. 2014). In studying aging and longevity, members of Rotifera have been studied due to their short lifespan and display of senescence (Snare et al. 2013; Snell et al. 2012, 2014; Stelzer 2005). It is possible to use the sensitivities of rotifers to water quality changes and their response to environmental stressors such as pollutants, pH, and UVR variations to assess the

health of aquatic ecosystems (Dahms et al. 2011; Declerck & Papakostas 2017, Wallace et al. 2023).

In natural environments, rotifers may be exposed to UVR due to fluctuations in water depth, water clarity, and atmospheric conditions. Resistance of monogonont rotifers to varying intensities of UVR has been investigated by several researchers (Kim et al. 2011, Wang et al. 2011). For instance, when the monogonont *Brachionus urceus* (Linnaeus, 1758) was exposed to low intensities of UVB radiation for increasing time intervals, fecundity was negatively affected as UVB dose increased. Initially UVB exposure enhanced reproduction by stimulating egg production. However, when the rotifer was exposed to the same UVB intensity for longer periods of time, both lifespan and fecundity were negatively affected (Wang et al. 2011).

Bdelloidea and Monogononta, two distinct groups within the Rotifera, demonstrate different reproductive strategies (Wallace 2002; Wallace & Snell 2010). Monogononta undergoes both sexual and asexual phases, with parthenogenesis occurring during the asexual phase. In the sexual phase, mictic females and males are produced in response to environmental cues, and fertilization of mictic females results in the formation of dormant diapausing embryos (Snell 2014; Wallace 2002; Wallace et al. 2015). These dormant eggs contain a thick protective layer, which protects them from biotic or abiotic stressors (Snell 2014; Stelzer 2005; Wallace 2002).

Bdelloids reproduce through parthenogenesis, which occurs in the absence of chromosome pairing or meiosis, and where a diploid egg is formed by two successive mitotic divisions of resting oocytes (Debortoli et al. 2016; Hespeels et al. 2014; Mark Welch & Meselson 2000; Ricci 2016). The unique degenerative tetraploid genome structure of bdelloid rotifers

prevents the pairing of homologous chromosomes and the segregation or homogenization of alleles through processes like conversion or mitotic crossing-over (Eyres et al. 2015; Flot et al. 2013; Signorovitch et al. 2015). However, there is evidence of a meiotic-like parthenogenetic reproduction in *Adineta vaga* (Davis, 1873), which showed inter-allelic divergence levels equivalent to those seen in sexually reproducing species at the nucleotide level (Eyers et al. 2015; Flot et al. 2013; Simion et al. 2021). Recombination, whether mitotic or meiotic, might enhance gene conversion in asexual lineages, potentially correcting mutations (Signorovitch et al. 2015; Simion et al. 2021). Bdelloidea has no known instances of males and has likely been asexual for the last 35 – 40 million years (Hespeels et al. 2014; Mark Welch & Meselson 2000; Ricci 2016).

It is thought that asexual organisms are not able to diversify into distinct species since there is no way to maintain cohesion beyond the individual level (Fontaneto et al. 2007; Gladyshev et al. 2010; Mark Welch & Meselson 2000). However, there are 3 orders, 4 families, 19 genera, and over 460 described species of bdelloid rotifers (Mark Welch & Meselson 2000; Ricci 2016). Due to the lack of sexual recombination, it is suspected that bdelloids make use of foreign DNA to bypass the lack of genetic recombination caused by asexuality (Bininda-Emonds et al. 2016; Hecox-Lea & Mark Welch 2018; Luijckx et al. 2018; Signorovitch et al. 2015). Horizontal gene transfer (HGT) in asexual prokaryotes could be acting as a form of asexual recombination allowing for non-sexual transfer of genetic material between two organisms. This process can lead to the removal of mutations and fixation of beneficial genes (Eyers et al. 2015; Fontaneto et al. 2007; Signorovitch et al. 2015; Simion et al 2021). The ability to acquire genetic material from other sources through HGT provides bdelloids with a unique and

alternative strategy for genetic exchange and adaptation without traditional sexual reproduction.

Scope and aims of study

Bdelloid rotifers are well-suited for studying rapid evolutionary change due to their short generation time, high reproductive rate, and remarkable ability to repair DNA damage caused by environmental stressors. These characteristics make rotifers ideal candidates for investigating adaptations (Declerck, & Papakostas 2017). The overall goal of this study is to understand how pigmentation aids UVR resistance and/or adaptation in a rock pool bdelloid. There were four overall aims of the study:

(1) Confirm the relationship between rock pools with low concentrations of dissolved organic carbon and the presence of pigmented bdelloids.

(2) Test the hypothesis that pigmentation aids in reducing damage caused by UVR. Bdelloids with varying degrees of pigmentation (highly pigmented (HP), moderately pigmented (MP), lightly pigmented (LP), or non-pigmented (NP)) were exposed to regional UVB intensities (low, mid UVB) in addition to an extreme scenario (high UVB). In addition, bdelloids were desiccated for an increasing amount of time (0, 1, 7, 32 days) to determine the interaction between dormancy and pigmentation in protection from UVR.

(3) The effects of long term UVB exposure were explored by monitoring recovery of F_0, F_2, and F_4 generations and by measuring life histories traits in the F_1 and F_5 generations using life table experiments.

(4) Through *de novo* transcriptome assembly and analysis, this study aimed to investigate how pigmentation influences genes that respond to UVB exposure by comparing differentially expressed genes in pigmented and non-pigmented *Philodina*.

Chapter 2: Does pigmentation provide protection to bdelloid rotifers in a high UVB environment?

Introduction

Desert, ephemeral aquatic communities are highly susceptible to high temperatures, long periods of drought, and high ultraviolet radiation (UVR) levels (Kadad et al. 2020; Wallace et al. 2005; Walsh et al. 2014). Current climate models predict a 4° C increase in ambient temperatures by the year 2070 (Hoffmann & Beierkuhnlein 2020). Increasing temperatures will, no doubt, lead to warming of water bodies and increased evaporation, as well as fluctuations in dissolved organic carbon (DOC) (Hoffmann & Beierkuhnlein 2020; Zhou et al. 2018). Warmer temperatures may result in shallower mixing of water columns causing greater intensities of UVR reaching planktonic communities (Boeing et al. 2004; Watanabe et al. 2011; Williamson et al. 2001). UVR has a wide range of damaging effects on aquatic organisms, including tissue damage and DNA mutation, both of which will reduce lifespans (Fischer et al. 2013; Mojib et al. 2014; Ulbing et al. 2019). Synergistic effects of increasing temperatures and UVR levels on aquatic species are relatively unknown but emerging as a research imperative as the climate continues to change (Bais et al. 2018; Pinceel et al. 2018; Watanabe et al. 2011).

The intensity of UVR that reaches aquatic inhabitants depends on a range of factors including angle of the sun, elevation, latitude, calmness, albedo of water, and concentration of DOC (Leech & Williamson 2000; Watanabe et al. 2011). For most aquatic species, DOC acts as a protectant against UVR; its sources include both living and decaying organic matter. (Erickson et al. 2015). Components of UVR that cause damage to aquatic species are UVA and UVB wavelengths, both of which can break down DOC (Erickson et al. 2015; Leech & Williamson

2000). Thus, if DOC is not replenished periodically, UVA/UVB wavelengths are able to penetrate up to 30 m below the water surface (de Los Rios 2005; Williamson et al. 2001; Williamson et al. 2016). Unfortunately, some of the environments whose inhabitants are the most susceptible to UVR damage are those that live in shallow, freshwater habitats (Boeing et al. 2004; de Los Rios 2005; Solomon et al. 2015).

The Chihuahuan Desert of the southwestern USA and northern Mexico is recognized for its high biodiversity and numerous ephemeral waterbodies, including rock pools and shallow playas (Briggs et al. 2019; Brown et al. 2022; Dinerstein et al. 2000; Wallace et al. 2005; Walsh et al. 2014). Rock pools are usually filled by groundwater, surface water, precipitation, or snowmelt. As the water begins to evaporate in the rock pools, changes in conductivity, pH, and temperature can occur rapidly; this erratic environment limits the type of species that inhabit these sites (Brendonck et al. 2010; Joćque et al. 2010). Another physical challenge that these habitats face is increased exposure to UVR (Walsh et al. 2014); this is because shallow waters bodies (<1 m) with low concentrations of DOC (<10 mg/L) offer little to no protection from UVR damage (de Los Rios 2005; Tapia-Torres et al. 2015).

To avoid or reduce damage, many aquatic species use photoprotective chemicals that may take the form of conspicuous pigmentation (Hansson 2004; Hansson et al. 2007; Hylander et al. 2009; Rautio & Tartarotti 2010). Aquatic species that utilize photoprotective pigments include cladocerans, copepods, and tardigrades (Alcocer et al. 2020; Hairston 1976, 1979). These photoprotectant agents may be synthesized by the animal (Marcoval et al. 2020) or are derived from carotenoids and/or mycosporine-like amino acids found in phytoplankton, algae, bacteria, or other food sources (Bonifacio et al. 2012; Garcia et al. 2008; Schneider et al. 2016).

Carotenoids are the primary constituents of red photoprotectants in invertebrates and possess potent antioxidant activity that enables them to counteract the detrimental effects of oxidative stress (Bashevkin et al. 2020; Brüsin et al. 2016; Suma et al. 2020). Aquatic species that are not able to avoid UVR or obtain a source of pigmentation must repair UVR damage (Tartarotti et al. 2013).

Bdelloid rotifers are microinvertebrates found in remarkably diverse aquatic and limnoterrestrial habitats, including extreme habitats such as cryoconitic holes in Antarctica (Cakil et al. 2021) to temporary habitats in deserts (Wallace et al. 2005; Walsh et al. 2014). In addition, they are well known for their ability to repair oxidative stress such as single and double DNA breaks after extended periods of desiccation (Ricci et al. 2003; Ricci & Fontaneto 2009) and when exposed to ionizing radiation (Gladyshev et al. 2008; Hespeels et al. 2020; Krisko et al. 2012). The overall robustness of bdelloids has been attributed to their ability to undergo anhydrobiosis at any life stage (Ricci et al. 2003; Ricci & Caprioli 2005). As conditions become unfavorable, bdelloids contract their head and foot into their trunk, and reduce metabolic activity to the lowest detectable levels of basal activity (Caprioli & Ricci 2001; Ricci et al. 2003; Wallace et al. 2008). In this compact anhydrobiotic state called a xerosome (Wallace et al. 2008), bdelloids can avoid damage from environmental stressors (Caprioli & Ricci 2001; Ricci et al. 2003). Although, prolonged desiccation time (≥7days) has been shown to cause oxidative stress in the form of DNA breaks (Hespeels et al. 2014, 15; Ricci & Caprioli 2005).

The combined effects of desiccation and UVR exposure increased mortality and caused genome instability through DNA breaks in dormant *Adineta vaga* (Davis, 1873). The number of breaks increased with increasing doses of UVR. In contrast, the same study found that in the

dormant form neither proton radiation nor gamma rays had a significant effect on survival or DNA damage (Hespeels et al. 2014). Martin (2017) found that pigmented bdelloids from rock pools exhibited greater resistance to UVB radiation compared to unpigmented species collected from consistently hydrated locations. Bdelloid rotifers are valuable models for investigating the protective role of pigmentation against UVR due to their capacity to withstand extreme conditions in both the hydrated and xerosome states. Given their resilience to ultraviolet exposure and adeptness at thriving in challenging environments, they present promising subjects for deeper exploration into the impacts of UV radiation.

Many bdelloid rotifers exhibit a distinct red color (Table S1), including several species of *Philodina* species commonly found in rock pools in Texas, USA (Walsh et al. 2014). As noted above, pigmentation often in a red color increases resistance to UVR damage in copepods, daphnids, and tardigrades. However, the photoprotective qualities of the red color has not been the focus of a study using rotifers. Xerosomes have been shown to be more resistance to UVB radiation than hydrated bdelloids (Fischer et al. 2013). In addition, there is little information on concentrations of DOC in rock pools. Thus, the aims of this study were to (1) evaluate the presence of pigmented bdelloids in rock pools with varying DOC concentrations and (2) determine whether pigmentation provides protection against UVB exposure when bdelloids are in the anhydrobiotic state.

Methods

Site characterization

Hueco Tanks State Park and Historic Site (hereafter Hueco Tanks) is located in El Paso Co., TX, USA (Fig. 2.1, S2.1; Tables 2.1,2.2). The park is named for the hundreds of small rock pools that are found on the rocky outcrops (Schröder et al. 2007; Walsh et al. 2014). These shallow rock depressions collect rainwater that rapidly evaporates in the hot, arid, desert environment, but they are the habitat of brightly pigmented micrometazoan including the rotifer *Philodina* sp. (hereafter: *Philodina*). Because the rocky outcrops at Hueco Tanks reach elevations of approximately 1,350 m, this area is subject to high intensities of UV radiation (Williamson et al. 2001)..

Rotifer culture

El Paso has mean summer temperatures of 36 °C and receives ~22 cm of rainfall each year, the majority of which is received during the summer monsoon season. Water samples were taken from Hueco Tanks 24 to72 h after a significant rainfall event (≳0.5 cm). In the laboratory, rotifers were washed free of sediment and fed a mixture of algae consisting of *Chlamydomonas reinhardtii* (Dangeard, 1888) (Culture Collection of Algae at the University of Texas at Austin (UTEX) strain 90), and *Chlorella vulgaris* Berijerinck, 1890 (UTEX strain 30) in modified MBL media (Stemberger, 1981). Samples for this study were collected after rainfall events from June 2017 to February 2020.

Dissolved organic carbon (DOC)

Water samples for DOC analysis were collected at least twice during the monsoon season in the Southwest (mid-June – September) and dry season (October to early June; NOAA NWS, 2020). The presence of highly pigmented (HP) *Philodina* was recorded at the time of collection. When sufficient water was present, we took duplicate samples to assess instrumentation and sampling error. Prior to collection, plastic lids were soaked in 2% HCL overnight, rinsed with DI water; then collection vials were heated to 500° C for 2 h. Plastic vial lids and GF/F glass fiber filter were heated to 100° C for 1 h. This process was done to eliminate any organic residue or contamination. In the field, water samples were filtered and stored in vials, when sealed ambient air which could lead to degradation of DOC. Vials were transported on ice and stored in the dark at 4° C until analyzed using a Shimadzu TOC (Total Organic Carbon) L series analyzer.

Pigmented *Philodina* were collected from eight rock pools: Al, Edge, Enrique, Jaime, Luisa, Paw, Sergio, and Walsh (n = 8, Table S2.2). Because pigmented rotifers have not been found in Heart, Kettle 4, North Temp, and South Temp rock pools (n = 4, Table S2.2), these locations were used as controls to compare DOC concentrations in rock pools with and without pigmented bdelloids (Fig. 1; Table S2.2). To investigate if the presence of pigmented bdelloids is related to the concentration of DOC in rock pools, and if DOC concentration varied between monsoon or dry season, a generalized linear model (glm) analysis was conducted. Differences in DOC concentrations were compared using a Tukey contrast using the Bonferroni method. Analyses were done using R version 3.4.3 and RStudio version 1.0.136 (R Core Team, 2015).

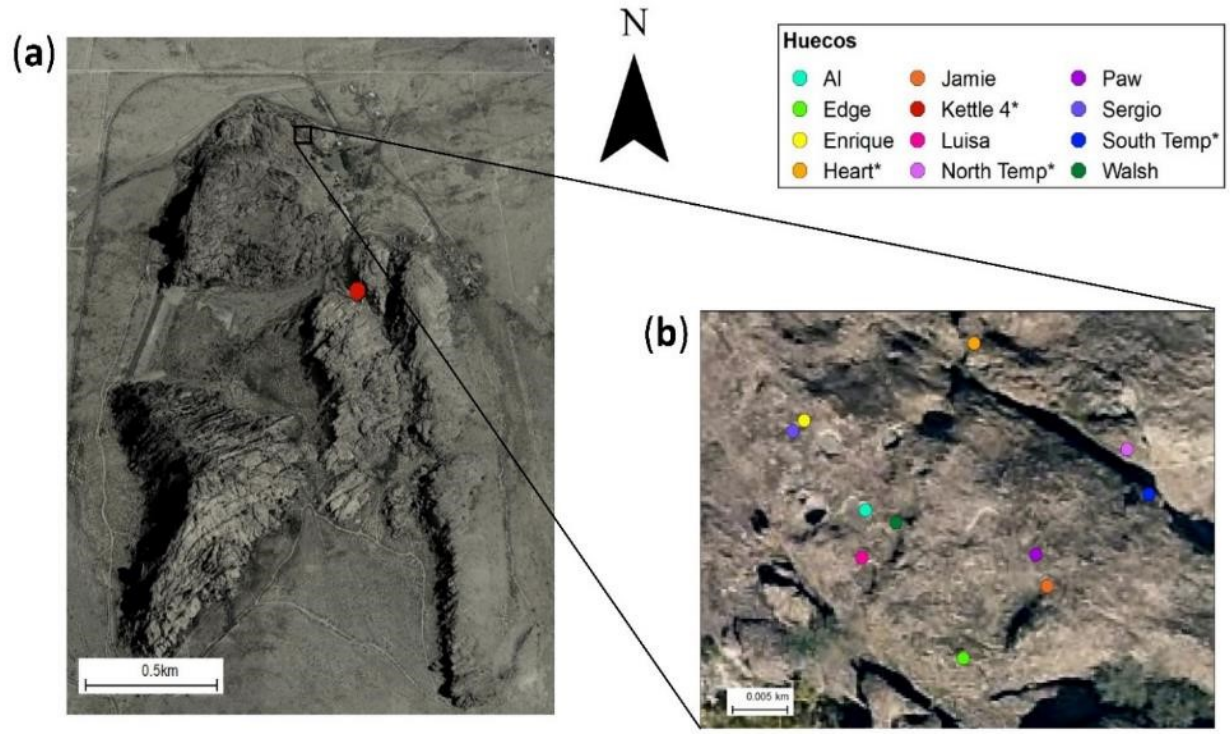

Figure 2.1. Hueco Tanks State Park and Historic Site (El Paso Co., TX). (a) Aerial view with an inset of North Mountain (b). Rock pools, or huecos, sampled for this study are depicted by colored circles. *Indicates rock pools without pigmented *Philodina* sp.

Degree of pigmentation

The intense pigmentation seen in the field collected *Philodina* was retained for some time, but it gradually dissipated after being maintained on the green algal mix. To confirm these observations, bdelloids were induced to form a xerosome through the addition of 10 drops of 1X Dulbecco's phosphate-buffered saline (DPBS; Hecox-Lea and Mark Welch 2018). Xerosomes were analyzed every three days between pigmentation levels: highly pigmented (HP), moderately pigmented (MP), lightly pigmented (LP), or non-pigmented (NP), until significant difference was found. After four months in culture being maintained on a green algae diet, bdelloids were considered pigmentation level NP. Once a difference was found 50 xerosomes were analyzed prior to desiccation or UVB exposure. Images were captured using a SPOT Imaging Insight CMOS camera and SPOT software version 5.6 (Fig. 2). Images were analyzed

using ImageJ version 1.33 and the RGB plug-in downloaded from the NIH website (https://imagej.nih.gov/ij/plugins/; Schneider et al. 2012; Vrekoussis et al. 2009). The RGB plug-in converts images to digital numbers (DN) corresponding to red, green, or blue channels. The percentage of red DN in any given pigment level was calculated using the following formula (Vrekoussis et al. 2009):

$$\% \, Red \, DN = \frac{\text{Red DN}}{(\text{Blue DN+Green DN +Red DN})} \times 100. \qquad (2.1)$$

An Analysis of Variance (ANOVA) treatments followed by a Tukey HSD comparison test were used to identify significant differences between pigmentation levels. Statistical analyses were conducted using R version 3.4.3 and RStudio version 1.0.136 (R Core Team, 2015).

Experimental procedure: Pigmentation, desiccation and UVR exposure

All desiccation and UVR treatments, including controls, consisted of 16 replicates. Each replicate contained five pieces of approximately 1x1 cm GF/F glass fiber filter paper (0.45 μm) containing 10 rotifers in a 60 x 15 mm glass Petri dish. Desiccations times and UVB intensities followed Martin (2017) and Caprioli & Ricci (2001). Briefly, dishes containing bdelloids were kept in a humidity chamber at 97 ±2 % relative humidity for 48 h, after which the relative humidity was dropped to between 45 and 35 % for 1, 7, or 32 days. After desiccation, rotifers were exposed to UVB radiation (295 – 320 nm) that was emitted from a Spectroline® XX-15B lamp (120 v, 60 Hz, 0.7 AMPS) suspended above Petri dish bottoms in a low temperature, diurnal illumination incubator (VWR). All sources of white light were removed by lining the incubator surfaces with black plastic. Incubation temperature was maintained at 25 ±1° C. UVB intensities used for 2 h exposures were: 1.3 ± 0.05 (low), 3.7 ± 0.05 (mid), or 5.0 ± 0.05 (high) W/m^2. For low UVB treatments, radiation intensities were adjusted using a glass filter that

absorbs wavelengths between 295 to 305 nm thus reducing UVB intensity. A quartz glass, which allowed wavelengths from 295 to 320 nm to reach bdelloids, was used for mid and high UVB intensity; the intensity was increased by reducing the space between Petri dishes and UVB lamp (18.5 cm (low/mid) to 16 cm (high)). A UVA/B light meter (Sper Scientific 850009) with the corresponding glass filter was use verify UV intensities. Negative controls consisted of rotifers prepared in the same manner as those in exposure treatments but placed in a Styrofoam box covered in black plastic during exposures. Post-UVR exposure, desiccated bdelloids were rehydrated using 5 mL of MBL medium and cultured under ambient light and temperature. In addition, to study the resiliency of hydrated bdelloids, active rotifers also were exposed to the same UVR treatments. Recovery of bdelloids was recorded 48 h after exposure and hydration. Bdelloids that emerged from xerosomes or showed any visible movement of the trophi (jaws) were counted as recovered; otherwise, they were counted as dead.

The probability of survival for each pigmentation level using pairwise combinations of pigmentation level, desiccation time, and UVB exposure as explanatory variables was tested using a logistic model and following methodology of Agresti (2018). Briefly, (1) accuracy and predictive power of the logistic model were confirmed using receiver operating characteristic (ROC) and calibration curves, (2) standardized Pearson residuals were used detect outliers that were removed from visualization in downstream analyses, (3) a Joint test was used to determine whether explanatory variables were correlated (are included in Table S2.6 & 2.7), (4) Maximum likelihood estimates of survival were used to determine the Wald Chi-square probability, and (5) an Odds Ratio test of bdelloid survival was performed for the model conditioned on each explanatory variable. These analyses were conducted using SAS/STAT

software version 14.3 for Windows 10 (SAS Institute Inc. 2016©, Cary, NC, USA. SAS® proprietary software 9.4 (TS1M5) licensed to University of Texas System - SFA T&R, Site 70080468).

Results

Dissolved organic carbon (DOC)

Pigmented rotifers were found in rock pools with DOC concentrations of 6.2 ± 3.4 mg/L (mean ± standard deviation) during the monsoon season and 3.7 ± 1.8 mg/L in the dry season (Table 2.1a). Rock pools with DOC concentrations in the range of 8 – 30 mg/L and/or found in shaded areas (heart, North Tempt) had no instances of pigmented bdelloids. Pigmented bdelloids were found in rock pools with concentration range of 7 – 11 mg/L (Tables 2.1 & 2.2; estimate (est) ± standard error (SE) = -0.40 ± 0.11, z value, $p < 0.0001$). Regardless of the presence of pigmented bdelloids, DOC concentrations varied between the monsoon and the dry season in rock pools (6.3 mg/L, Table 2.1 & 2.2; est ± SE = 1.19 ± 0.72, z value = 1.65, p = 0.98; Table S2.3). The presence of pigmented bdelloids in rock pools was not affected by season (est ± SE = 1.19 ± 0.72, z value = 1.65, p = 0.98; Table S2.3).

Table 2.1. Dissolved organic carbon (DOC) concentrations of rock pools with highly pigmented bdelloids. DOC samples were taken during the monsoon season (MS; mid-June to September) and dry season (DS; October to early June). Mean and standard deviation (±SD) reported for rock pools with (**a**) and without (**b**) pigmented bdelloids.

	Rock Pool	MS DOC	DS DOC
(**a**)	Al	14.4 ± 0.6	3.0 ± 0.3
	Edge	4.1 ± 0.1	3.5 ± 0.0
	Enrique	3.8 ± 0.0	3.2 ± 1.7
	Jamie	5.9 ± 0.4	5.6 ± 0.2
	Luisa	6.5 ± 2.0	4.5 ± 2.2
	Paw	4.5 ± 2.2	3.9 ± 1.4
	Sergio	3.6 ± 0.1	3.3 ± 1.8
	Walsh	5.4 ± 1.4	3.7 ± 0.9
	Mean	***6.2 ± 3.4***	***3.7 ± 1.3***

(**b**)	Heart	10.8 ± 0.9	5.7 ± 3.2
	Kettle 4	8.2 ± 0.2	27.6 ± 0.6
	North Temp	8.8 ± 0.1	3.5 ± 0.6
	South Temp	29.6 ± 3.7	5.6 ± 0.3
	Mean	***17.3 ± 8.7***	***11.0 ± 9.9***

Table 2.2. Seasonal concentration of dissolved organic carbon (DOC) in rock pools and its relation to occurrence of pigmented bdelloids collected during the summer monsoon or dry season. Results of multiple comparison test given in Table S3. Estimate (est) ± standard error (SE).

Treatment	**est ± SE**	**z value**	**Pr(>|z|)**
intercept	2.64 ± 0.65	4.05	< 0.0001
DOC	-0.40 ± 0.11	-3.62	< 0.0001
Monsoon	1.19 ± 0.72	1.65	0.9827

Degree of pigmentation

The pigmentation levels of each treatment were determined using 50 images of xerosomes analyzed using RBG plug-in. This plug-in converted images to red, green pixels. Low DN numbers represent bright regions in the images. The darker the image the higher the digital number (total number of pixels) (Vrekoussis et al. 2009), dark regions are likely green algae. Immediately after collection bdelloids were classified as highly pigmented (HP) and had the highest %red DN (mean ± standard deviation (SD): 45.8 ± 2% (Fig. 2.2a; Tables 2.3, S2.4). Rotifers that were considered as moderately pigmented (MP) had a %red DN of 39.3 ± 1.7 (Fig. 2.2b; Tables 2.3, S2.4). This coloration persisted for up to one additional week (Table S2.3) when rotifers lost most pigmentation, except for a red-orange tint that remained in the lining of their gut; these rotifers were classified as lightly pigmented (LP; Fig. 2.c) and had a %red DN of 37.1 ± 1.2 (Table 3; Table S2.4). After more than 20 weeks in the lab, bdelloids retained a weak trace of orange in the lining of their gut and were classified as non-pigmented (NP; Fig. 2.2d)

and the %red DN was 36.1 ± 0.8 % (Table 2.3; Table S2.4). The HP treatment contained 6.5, 8.7 and 9.7% more red pixels when compared to other pigmentation levels (MP, LP, NP, respectively) (Table 2.4). A statistical difference in %red DN was seen among all four pigment levels (ANOVA: F = 30.6, df = 6, p <0.0001; Tukey HSD pairwise comparisons are given in Table S2.5).

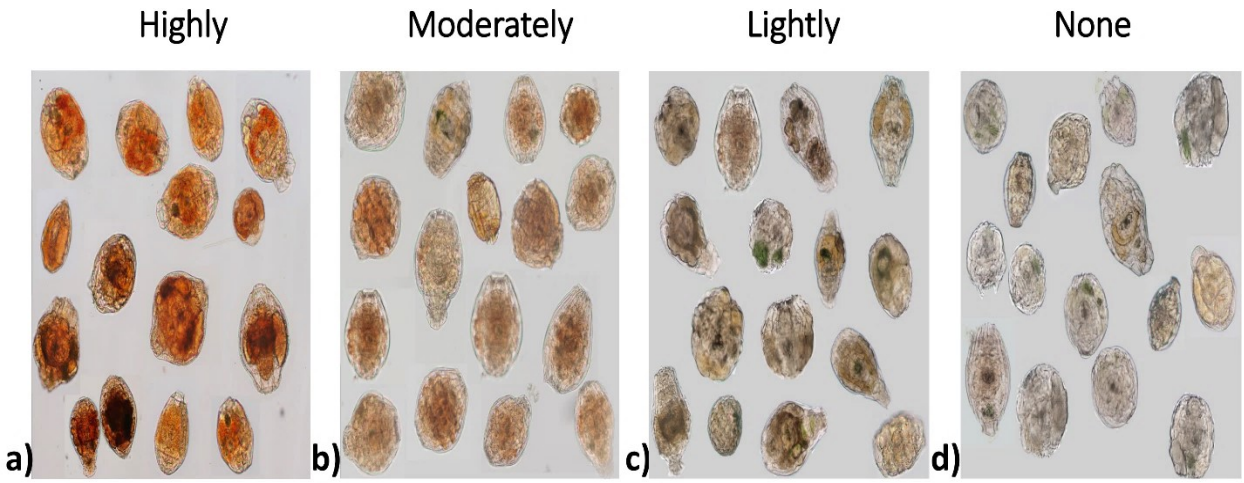

Figure 2.2. Levels of pigmentation in *Philodina* sp. xerosomes. Pigment levels (a) naturally occurring, highly pigmented (HP; 46%), (b) moderately pigmented (MP; 39%), (c) lightly pigmented (LP; 37%), or (d) non-pigmented (NP; 36%).

Table 2.3. *Philodina* sp. xerosome digital numbers as a function of pigmentation level: highly pigmented (HP), moderately pigmented (MP), lightly pigmented (LP), or non-pigmented (NP). Images were converted to digital numbers (DN). n = 50, mean and standard deviation (SD) are reported.

Pigment level	total DN mean ± SD	% red DN ± SD
Highly	356.9 ± 51	46.0 ± 23
Moderately	487.3 ± 38	39.3 ± 19
Lightly	538.3 ± 49	37.2 ± 15
None	629.6 ± 29	31.9 ± 13

Table 2.4. Comparison of pigmentation levels of *Philodina* sp. xerosomes using ANOVA and a post-hoc Tukey analysis (Table S5). Digital numbers (DN) for the red channels were compared for the four pigment levels (highly, moderately, lightly, and non). df, degrees of freedom.

	df	F-value	p-value
Pigmentation level	3	402.2	<0.0001
Channel DN	1	8674.9	<0.0001
Pigmentation level: CH DN	3	173.2	<0.0001

Pigmentation, desiccation and UVR exposure

Philodina survival 48 h after desiccation and UVB exposure is shown in Fig. 2.3. A downward trend in survival was seen as degree of pigmentation decreased and as desiccation time and UVB intensity increased. The controls, not desiccated or exposed to UVB radiation, had the highest survival (97 ± 3%). Outliers were identified by having Pearson residual values below -3 and above +3 (Table S2.6-S2.8) and these were removed from the analysis (are included in Table S.6- 8). The appropriateness of the logistic regression model was confirmed from the ROC curve (0.86) and calibration curve (slope = 0.997) (Fig. S2.2). There were significant correlations within and between treatment and treatment levels (pigmentation level, desiccation time, and UVB intensity) (Table 2.5). When desiccated for 32 days, almost no bdelloids recovered (2 ± 5%). This resulted in increasing the type I error of the regression model (e.g., introduced skew), thus this treatment was removed from the odds ratio visualization (Figures 2.4- 2.6).

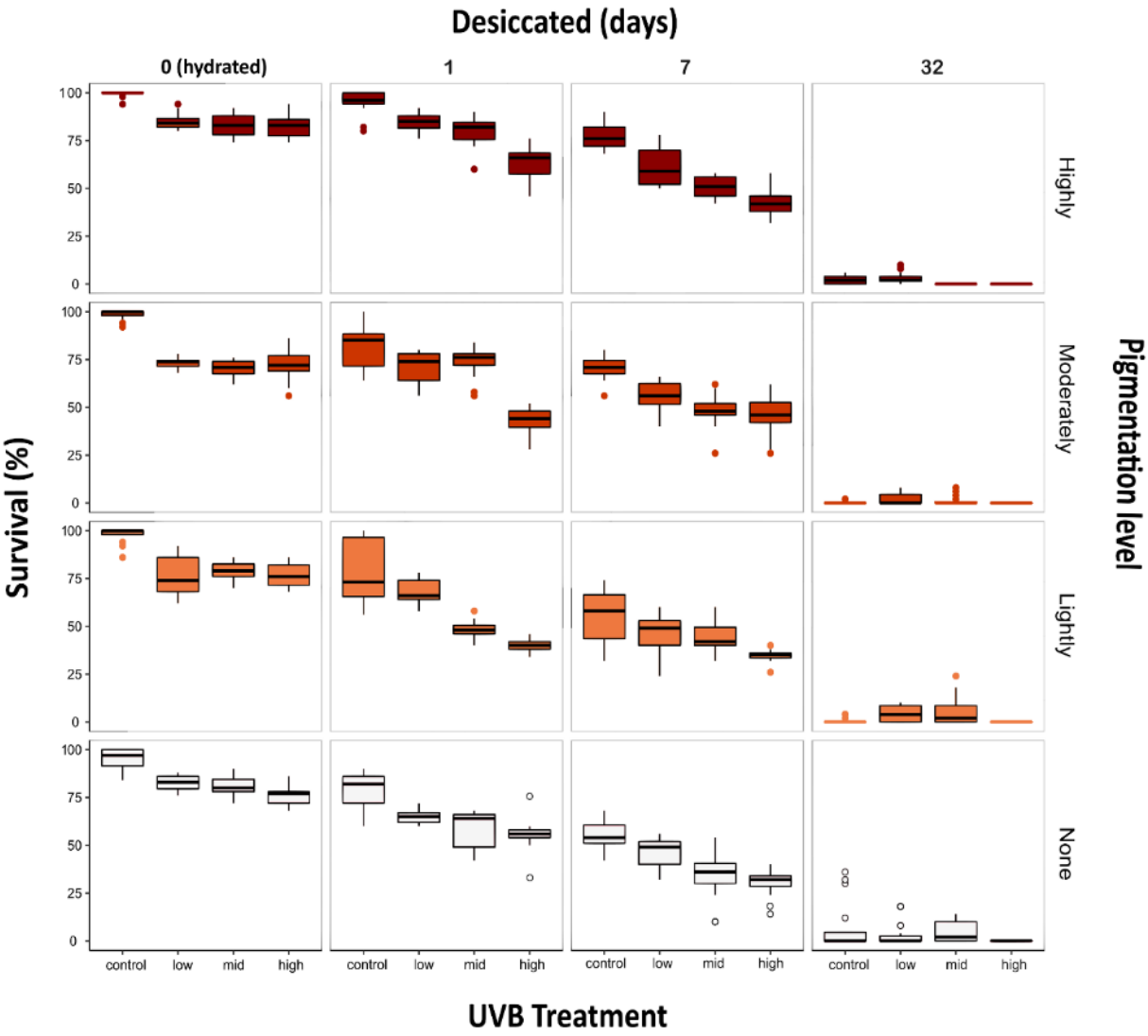

Figure 2.3. Survival of *Philodina* sp. after being desiccated for 0, 1, 7, or 32-days and then exposed to UVB intensities of 1.3, 3.7 or 5.0 ± 0.5 W/m^2, and a control. Vertical panels are divided by desiccation times of 0, 1, 7, or 32-days. Pigment levels are: Highly Pigmented (HP), Moderately Pigmented (MP), Lightly Pigmented (LP), Non-Pigmented (NP) bdelloids. Outliers are represented by dots.

Table 2.5. The effects of pigmentation level, desiccation time, and UVR exposure on *Philodina* sp. survival after 48 h. degrees of freedom (df), probability (Pr).

	df	Wald Chi-Square	Pr > Chi Sq
Pigmentation level	3	99.0	< 0.0001
Desiccation time	3	1618.4	< 0.0001
UVB intensity	3	331.5	< 0.0001
Pigmentation * Desiccation	9	343.4	< 0.0001
Pigmentation * UVB	9	66.3	< 0.0001
Desiccation * UVB	9	361.1	< 0.0001

The odds ratio estimates with 95% confidence intervals were plotted for each treatment to identify the most significant factors that determine *Philodina* survival. If the confidence interval crosses the line of null effect (odds ratio = 1.0), there is no association between treatments and bdelloid survival. First, to interpret the effect that degree of pigmentation had on bdelloid survival, the odds ratio was restricted to comparing desiccation times and UVB intensities (Fig. 2.4). There is no difference in surviving UVB exposure for hydrated bdelloids of the three lowest pigment levels, though when desiccated for 7 days MP treatments are 1.5 times more likely to survive than LP or NP treatments (Fig. 2.4a & b). No difference in survival between the LP and NP pigmented bdelloids was seen when bdelloids were hydrated or desiccated for 7 days, as shown by nearly all confidence intervals crossing the null line (Fig. 2.4c). The odds ratio for highly pigmented hydrated bdelloids increased by ~2 times when compared to LP (Fig. 2.4d), NP (Fig. 2.4e), and MP (Fig. 2.4f) pigment levels. The highest pigmentation level did not provide extra protection when the time desiccated was increased to 7 days followed by exposure to UVB radiation (Table S2.7). Overall, HP treatments had the highest odds of surviving desiccation and/or UVB exposure. The only exception was the 7-day desiccation treatment, where there was no significant difference between HP and MP bdelloids survival (Odds Ratio ≅ 1: Fig. 2.4, Table S2.6- S2.8).

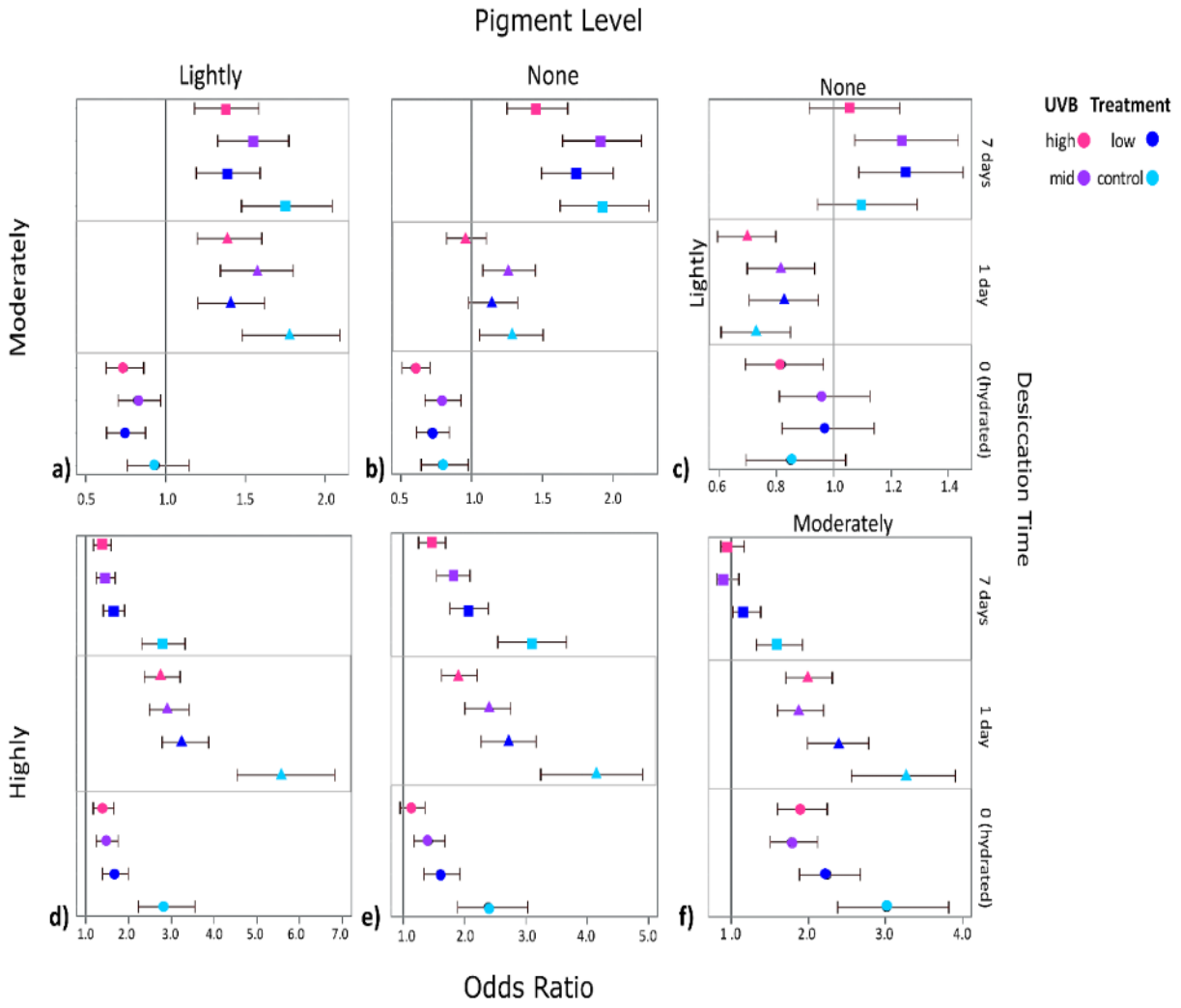

Figure 2.4. The Odds ratio comparing survival at four pigment level after desiccation and UVB exposure. The solid-colored point is the ratio estimate, and the horizontal line represents the 95% confidence interval. The null line (odds ratio = 1) indicates no significant effects on survival. Values >1.0: the treatment on the x-axis has a greater affected on survival; <1.0: the y-axis has a greater impact.

Next to investigate how desiccation impacts the survival of *Philodina* at the four-pigmentation levels and UVB intensities, odds ratio was adjusted to view desiccation time as an explanatory variable of the outcomes of UVB exposure. To focus specifically on the effect of desiccation, the odds ratio analysis was limited to three desiccation levels: 0 days (hydrated), 1 day, and 7 days. The odds ratio estimate revealed that the odds of survival for hydrated bdelloids and those desiccated for 1 day under UVB exposure were nearly identical (Fig. 2.5a).

This suggests that there was no significant difference in survival between bdelloids that were hydrated and those that underwent desiccation for 1 day when exposed to UVB radiation. *Philodina* that were desiccated for 1 day were also 2.5 times more likely to survive when compared to those that were desiccated for 7 days prior to UVB exposure (Fig. 2.5b).

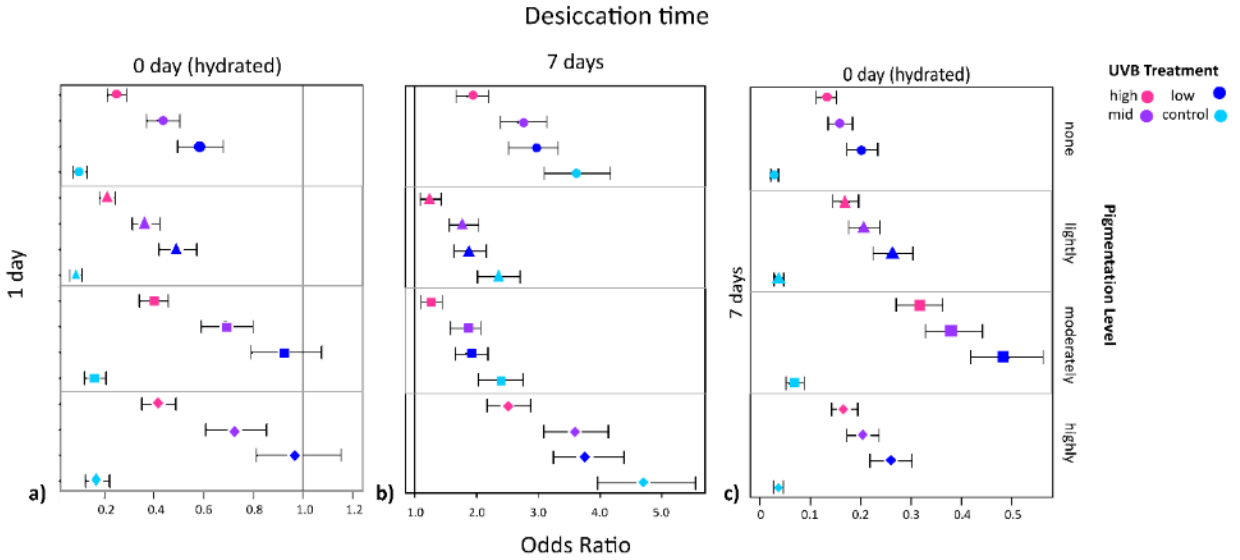

Figure 2.5. Odds ratio analysis for desiccation effects on survival and at each UVB intensity. The solid-colored point is the ratio estimate, and the horizontal line represents the 95% confidence interval. The null line (odds ratio = 1) indicates no significant effects on survival. Values >1.0: the treatment on the x-axis has a greater affected on survival; <1.0: the y-axis has a greater impact.

Finally, with UVB intensity as the explanatory variable the impacts of UVB exposure regardless of pigmentation levels and desiccation times were studied. The results showed that as the intensity of UVB radiation increased, the survival of bdelloids decreased (as depicted in Fig. 2.6). When bdelloids were exposed to low (Fig. 2.6a), mid (Fig. 2.6b), or high (Fig. 2.6c) levels of UVB intensity and subjected to desiccation for 1 or 7 days, they were more likely to die compared to the controls. Bdelloids were 1.2 or 2.0 times more likely to survive exposure to

low UVB radiation when compared to mid or high UVB intensity. The odds of survival decreased as pigmentation level decreased and desiccation time increased (Fig. 2.6d-f).

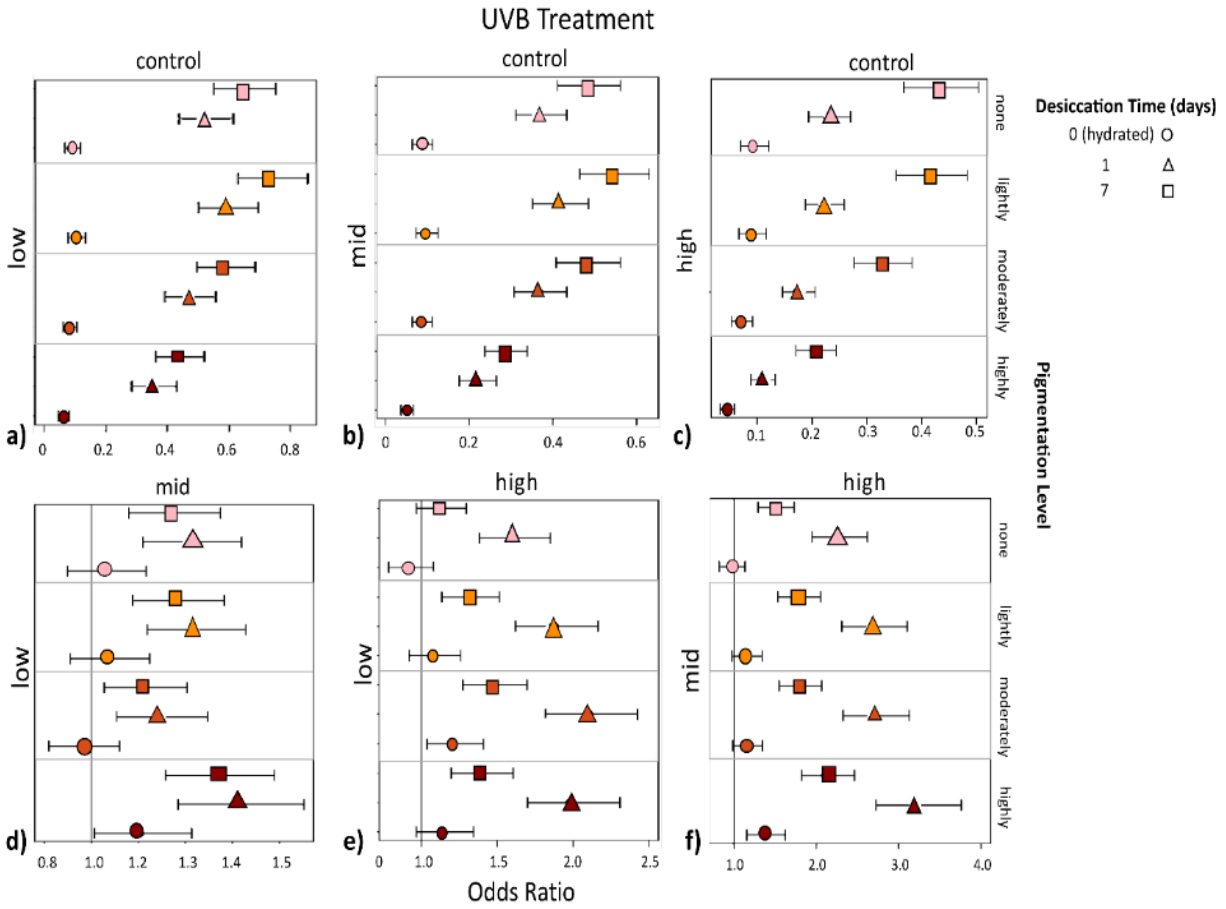

Figure 2.6. Odds ratio analysis of UVB radiation intensities effect on survival with varying pigmentation levels and desiccation times. The solid-colored point is the ratio estimate, and the horizontal line represents the 95% confidence interval. The null line (odds ratio = 1) indicates no significant effects on survival. Values >1.0: the treatment on the x-axis has a greater affected on survival; <1.0: the y-axis has a greater impact.

Discussion

The current climate change has caused changes in temperature, decreased cloud coverage, extreme precipitation events and prolonged periods of drought (Bais et al. 2018; Erickson et al. 2015; Kadad et al. 2020). In addition, increasing unpredictability of the climate is gradually leading to reduced DOC concentrations in water bodies, resulting in greater

intensities of UVR reaching planktonic communities (Boeing et al. 2004; Leech & Williamson 2000; Williamson et al. 2016). In arid environments, where rainfall is <50 cm a year, DOC concentrations in freshwaters are often much lower than in humid settings or temperate regions; however, even low concentration should offer some protection from regional UVR intensities (Tapia-Torres et al. 2015). The high pigmentation seen in *Philodina* doubles the odds of survival when hydrated, this value doubles (4X) when bdelloids were in the formant form for 1 day (Figs. 2.4 & 2.5). In invertebrates, the red photoprotective agents are often made up of carotenoids or melanin, both of which have been shown to possess remarkable antioxidant properties that function to neutralize oxidative stress caused from UVR. Bdelloids employ antioxidants to combat desiccation stress (Fischer et al., 2013; Hespeels et al. 2014, 2015) it is possible that additional antioxidants found in carotenoid would further increase bdelloids anhydrobiotic abilities.

In lieu of photoprotection, many aquatic animals rely on DOC and/or diel movements for protection from UVR damage (Alonso et al. 2004; Boeing et al. 2004; Leach et al. 2015). Long periods without replenishing sources of DOC in an aquatic habitat will leave inhabitants that rely on it for protection vulnerable. In this study the rainfall during the monsoon seasons between June 2017 and February 2020 caused DOC concentrations to increase by 2.5 and 6.3 mg/L in rock pools with and without pigmented bdelloids, respectively. However, seasonal variation in DOC did not affect in which rock pools pigmented bdelloids were found. The increase in DOC was seen in all rock pools analyzed, except for the one rock pool. Degrading leaves have been observed in this rock pool year-round (Martin 2017), which may have contributed to the high concentrations found outside of the monsoon season. Bdelloids from

this rock pool, a different species from those included in this study, showed similar levels in recovery to bdelloids in the LP treatments used here (Martin 2017; data not shown). The hypothesis that pigmented bdelloids would be found in rock pools with lower DOC concentrations, was supported by the negative correlation between DOC concentrations and presence of pigmented bdelloids. Generally unpigmented bdelloids were found in rock pools with high DOC concentration, or that were in shaded areas, which would limit exposure to UVR. This may negate the need for acquiring photoprotection by microinvertebrates in these rock pools.

As demonstrated here and in other studies (Bashevkin et al. 2020; Brüsin et al. 2016; Suma et al. 2020), photoprotection in the form of red pigmentation can reduce damage acquired from UVR exposure but variation in degree of pigmentation can affect its efficiency. It is well known that the degree of pigmentation varies seasonally in copepods and cladocerans (Bashevkin et al. 2020; Brüsin et al. 2016; Schneider et al. 2016). These fluctuations in pigmentation have been attributed to latitudinal and seasonal variation in the intensity of UVR exposure (Hansson 2004; Hansson et al. 2007; Kadad et al. 2020) and/or presence of planktonic fishes (Bashevkin et al. 2020; Brüsin et al. 2016; Hylander et al. 2014). Loss of pigmentation can cause DNA damage in the form of cyclobutane pyrimidine dimers after UVB exposure in the cladoceran *Daphnia melanica* Hebert, 1995 (Ulbing et al. 2019) and the copepods *Diaptomus castor* (Jurine, 1820) and *Eudiaptomus gracilis* (Sars G.O., 1863) (Brüsin et al. 2016). In these studies, animals with more melanin showed greater resistance to ecologically relevant levels of UVR damage. Suma et al. (2020) noted that the red-brownish pigmented tardigrade *Paramacrobiotus* sp. fluoresced under UV light, indicating that the pigments could be

transforming damaging UVR to unharmful rays. *Philodina* shows similar fluorescence (pers. obs.). Although seasonal variation in natural pigmentation levels were not evaluated in this study, we noted highly pigmented bdelloids collected in the summer retained coloration for 5 to 7 days in the laboratory when collected during summer months, whereas those collected in the winter retained high red coloration for a shorter period (3 – 5 days). Cladocerans and copepods have been known to adjust pigmentation in response to environmental factors; it is possible that the same is true for *Philodina*.

To study the effects of a stressor on invertebrates, animals are often cultured in the laboratory for several generations. This process establishes a stable population with consistent genetic and environmental backgrounds (Declerck & Papakostas, 2017; Hoffmann & Ross, 2018; White & Butlin 2021). In nature, populations have adapted to specific environmental conditions over time that enables them to survive and thrive in their environment (Dam, 2013; Declerck & Papakostas, 2017; Fox et al., 2019). Thus, the use of cultured samples may not provide an accurate representation of how some aquatic animals such as copepods, tardigrades, and bdelloids incorporate pigment to reduce reactive oxygen species or other UVR induced damage will be important in learning how they may adapt to increased UVR which maybe a byproduct of climate change in some habitats. The use of cultured animals minimizes maternal effects; however, the results may provide an accurate representation of the degree of resistance to UV. Here, the use of pigment level is a reflection of length bdelloids were cultured in the lab.

The red pigmentation seen in *Philodina* is inferred to be photoprotectant, possibly carotenoids with antioxidant capabilities (Fischer et al. 2013). The reduction of pigmentation in other studies has been linked to the reduction in carotenoids and/or melanin, which are known

to act as antioxidants that reduce UVB damage caused by oxidization (Alcocer et al. 2020; Marcoval et al. 2020; Oexle et al. 2016). Organisms with higher pigmentation levels are likely to have a survival advantage in regions with high UVB intensity (Brüsin et al. 2016; Ubling et al. 2019). Samples corresponding to pigmentation categories HP (46.0 ± 23% red DN; cultured for <5 days) and MP (39 ± 19% red DN; cultured for ~2 weeks) demonstrated the greatest odds of surviving desiccation and regional UVB exposure and their combined effects. In the study Fischer et al. (2013), a laboratory culture of the red-pigmented bdelloid *Philodina roseola* (Ehrenberg, 1832) was exposed to UVB radiation when hydrated and desiccated for 3.5 days. In the hydrated state, the bdelloid demonstrated lower resistance to UVR intensity. The authors speculate that *P. roseola* was able to repair DNA damage as it emerged from the xerosome, leaving hydrated samples more vulnerable to UVB. In contrast, in this study highly and moderately pigmented xerosomes that were desiccated for one day were not more resilient than hydrated samples when exposed to UVB intensities. It should be noted that in the study by Fischer et al. (2013) the level of pigmentation of *P. roseola* nor the length of culture prior to during UVR exposure were reported.

Researchers have hypothesized that resistance to stressors by bdelloids is a by-product of the evolutionary adaptation of anhydrobiosis, although DNA damage is still acquired during prolonged desiccation (Gladyshev et al. 2008; Hespeels et al. 2014; Rebecchi et al. 2020). Evidence of DNA breaks have been reported in *A. vaga* when desiccated for 7 days, while no damage or increased mortality was seen in those that were desiccated for 1 day (Hespeels et al. 2014; Ricci & Caprioli 2005). In this study, HP bdelloids had three times the odds of surviving 7 days desiccation than LP or NP treatments; the odds of survival decreased to twice when

exposed to UVB (Fig. 4). Pigmented tardigrades have also demonstrated greater resistance to UVR both in desiccated and hydrated states (Altiero et al. 2011). Survival of unpigmented tardigrades coated in red pigment extracts doubled after UVR exposure when compared to those that were not coated (Suma et al. 2020). Similarly, when the monogonont rotifer *Brachionus manjavacas* was fed red algal extracts, its lifespan was extended UVB exposure (Snare et al. 2012). Those authors hypothesized that this was due to enhanced antioxidants and anti-mitotic activities found in the carotenoid extracts (Marcoval et al. 2020; Snare et al. 2012). The relationship seen in these studies between pigmentation levels and reduction of oxidative stress lends merit to the hypothesis proposed here; pigmentation aids in resistance to both desiccation and UVB stress.

The low and mid UVB intensities used in this study were designed to mimic regional winter and summer UVB intensity means in the environs of west Texas. The high UVB treatment represented an extreme UVB scenario, which exposed *Philodina* to an intensity 1.4 greater than mean UVB intensity received in summer months. Extreme UVR events, such as the one simulated here, have occurred. For instance, on December 29, 2003, UVB intensity was recorded at peaks of 8.15 W/m^2 in Licancabur, Bolivia (Cabrol et al. 2014). This extreme UVB event was attributed to reduced ozone in the tropics, high elevation (> 5900m), clear skies, and unprecedented solar flares (Cabrol et al. 2014). These extreme events are currently rare but may become more frequent with the changing climate.

Future Directions

Red pigmented bdelloids are commonly observed in nature and have been identified in all four bdelloid families and 13 genera (Table S2.1). Nearly all pigmented bdelloids are found in

temporary habitats (fresh and marine), such as rock pools, that are likely exposed to higher intensities of UVR. Similar to copepods and tardigrades, red pigmentation seen in bdelloids is likely from their food source. This was supported by the observation that coloration was not retained after *Philodina* was removed from their environment and fed a mixture of green algae. However, after 20 weeks in culture *Philodina* retained some red pigment around the epithelial lining of the gut. From that observation it was inferred the possibility that bdelloids themselves can produce this pigment. Further research is still required to test the hypothesis that bdelloids acquire pigmentation through their food source. In this study humidity was adjusted as bdelloids entered the dormant form, but not as they exited. To optimize the number of bdelloids that successfully emerge from their xerosomes, future studies could gradually adjust nutrient availability and temperature along with humidity as bdelloids enter and exit the dormant stage. Finally, in addition to *Philodina* many inhabitants of rock pools are brightly pigmented including flatworms, nauplii of fairy shrimp, clam shrimp, tadpole shrimp and ostracods. It would be interesting to compare whether the findings here hold across this broad array of phylogenetically diverse taxa.

Chapter 3: Local adaptation? Enhanced fitness under regional UVB intensities in a rock pool bdelloid rotifer

Introduction

How animals respond to global climate change will depend on their ability to adapt to environmental stressors. Climate change is predicted to affect weather patterns, prolong droughts, increase temperatures, and directly and indirectly increase the intensity of ultraviolet radiation (UVR) (Bais et al. 2018; Salawitch et al. 2019). Directly, climate change can increase UVR intensity through the breakdown of ozone from greenhouse gases. While indirectly, changes in weather patterns will decrease cloud coverage, leading to longer periods of exposure to UVR (Bais et al. 2018; Salawitch et al. 2019). The intensity of UVR experienced in any environment fluctuates naturally throughout the day, and by season, latitude, and elevation (Häder et al. 2007; Mckenzie et al. 2011). During the summer, when the sun is at its peak, the intensity of UVR increases by 8 – 10% every 1,000 m above sea level (Blumthaler & Ellinger 1997; Piazena 1996; Williamson et al. 2001). This makes high-altitude portions of the Chihuahuan Desert (>1,000 m) more prone to enhanced UVR. In such habitats UVR could be acting as a selective force favoring individuals which are capable of coping with or preventing damage (Fernández et al. 2018; Häder et al. 2006; Marinone et al. 2006). This is especially true in shallow ephemeral rock pools found at high elevations which are vulnerable to many aspects of climate change, including increased UVR, increased temperatures, and prolonged droughts (Schröder et al. 2007; Walsh et al. 2014).

Bdelloid rotifers, common rock pool inhabitants, are a diverse class of rotifers that have successfully adapted to a wide range of environments, including those with high levels of UVR

(Cakil et al., 2021; Lukashanets & Maisak 2023; Wallace et al. 2005). Bdelloids most commonly avoid damage from stressors (e.g., desiccation, starvation, freezing, anoxia) by entering dormancy as a xerosome (Wallace et al. 2008). Xerosomes have also have a demonstrated resistance to ionizing radiation (Gladyshev et al. 2008; Krisko et al. 2012; Latta et al. 2019) and X-rays (Hespeels et al. 2020, 2023). However, exposure to UVR can have significant effects on life history traits, physiology, and behavior and may contribute to population declines of bdelloids in under certain conditions (Fischer et al. 2013; Zhu et al. 2021). Bdelloids from ephemeral habitats likely experience increased exposure to UVR as the environment dries and they undergo anhydrobiosis (Fischer et al. 2013; Ricci 1983). However, as bdelloids emerge from xerosomes, numerous DNA repair mechanisms are activated, repairing cellular damage including that caused by UVR exposure (Fischer et al. 2013; Hespeels et al. 2014, 2023). This has led to conflicting results on the impacts of UVR damage. For instance, the active form of *Rotaria rotatoria* (Pallas, 1766) was adversely affected by UVB radiation with increasing radiation intensity by having a later age of first reproduction and reduced fecundity and longevity (Zhu et al. 2021).

Through the process of natural selection, certain adaptations allow species to optimize their fitness to their habitats and locally adapt (Dam 2013; Fox et al. 2019; Stábile et al. 2021). Local conditions such as food availability, predator pressure, temperature, or UVR intensity, can affect life history components such as survival, growth, and fecundity, disguising patterns of local adaptation (Hanson et al. 2004; Mousseau & Fox 1998; Vehmaa et al. 2012; Yampolsky et al. 2014; White & Butlin 2021). Adaptation to UVR stress has been demonstrated in *Daphnia pulex* Leydig, 1860 in a series of experiments by Fernández et al. (2018, 2020). They found that

when comparing populations originated from low and high UVR habitats that the population from the high UVR environment exhibited increased fecundity and a younger age of first reproduction, while the population from low UVR exposure had shorter lifespans and lower fecundities (Fernández et al. 2018). Furthermore, the population from the low UVR environment produced photoprotective pigments in response to UVR, while the high UVR, which was pigmented took refuge in deeper parts of the lake (Fernández et al. 2020). Based on their findings, Fernández et al. suggest that these populations have adapted to a high UVR environment (Fernández et al. 2018, 2020). However, the response to UVR has shown varying results in *Daphnia magna* (Straus, 1820) (Huebner et al. 2009; Sha et al. 2020). After two consecutive generations of exposure to UVB radiation, there was no evidence of adaptation in F_2 offspring (Huebner et al. 2009). In contrast, clones of *D. magna* collected from a low UVR habitat had an earlier age of first reproduction and an increase in fecundity in the F_2 generation (Sha et al. 2020). Enhanced fecundity after low doses of UVR exposure has also been found in the copepod *Tigriopus californicus* (Baker, 1912) (Heine et al. 2019) and the monogonont rotifer *Brachionus urceus* (Linnaeus, 1758) (Wang et al. 2011).

As noted above, another factor that influences the amount of UVB damage incurred by aquatic invertebrates is the presence of photoprotective pigments. Many species found in shallow, high elevation habitats are highly pigmented, including bdelloid rotifers. However, despite the presence of potential protective carotenoids, the bdelloid *Philodina roseola* Ehrenberg 1832 showed reduced reproductive output when exposed to UVB radiation (Fischer et al. 2013).

In this study, a highly pigmented *Philodina* species (hereafter referred to as *Philodina*) was used to investigate the effects of UVB exposure on life history traits over multiple generations. Specifically, we assessed survival of individuals from the parental, F_2, and F_4 generations and the life history traits of their offspring (F_1 and F_5 generation). Our hypothesis was that certain life history traits, such generation time (T) would increase with UVB intensity. Furthermore, we predicted that exposure to UVB over multiple generations would have cumulative negative effects on lifespan and reproduction that would be progressively worse in subsequent generations. To test these hypotheses, we exposed rock pool bdelloids to three levels of UVR and conducted life table experiments.

Methods

Collection and culture

The parental generation (F_0) of *Philodina* was collected from rock pools at Hueco Tanks State Park and Historic Site (El Paso Co., TX, hereafter Hueco Tanks). Water samples were collected 48 – 72 hr after a significant rain event (≳0.5 cm; Table S3.1). To account for possible acclimation to environmental UVB intensities, rotifers were exposed to UVB treatments according to the season they were collected. Individuals for the control and low UVB treatments were collected in the winter (February 2020, January 2021) when regional intensities are ~1.4 W/m^2, those for the mid UVB treatments were collected when regional UVB intensity ~3.5 W/m^2, in early in the fall (October 2020) and those for high UVB treatments were collected at the end of summer (September 2019). In the laboratory, rotifers were washed free of debris using modified MBL media (Stemberger, 1981) and then fed green alga

Chlamydomonas reinhardtii (Dangeard, 1888; Culture Collection of Algae at the University of Texas at Austin strain 90). Cultures were maintained in an 18:6 hr L:D cycle at 25 ± 1°C.

Generational UVR exposure

Three non-consecutive generations of bdelloids were exposed to environmentally relevant levels of UVB, as well as an extreme case scenario. The parental generation was exposed within 72 hr of collection, while F_2 and F_4 were exposed at the end of their juvenile period, when they were at 10 - 14 days old (Caprioli & Ricci 2001; Ricci 1998; Ricci & Covino 2005). However, after intensity of red coloration decreased under laboratory conditions. Pigmentation levels were determined based on analysis of twenty xerosomes images before each UVB exposure. The percentage of red in each image was calculated using ImageJ version 1.33 along with the RGB plug-in (https://imagej.nih.gov/ij/plugins/; Vrekoussis et al. 2009). The RGB plug-in converts images to digital numbers (DN) corresponding to red, green, or blue channels. The percentage of red DN in any given pigment level was calculated using the following formula (Vrekoussis et al. 2009):

$$\%\ Red\ DN = \frac{\text{Red DN}}{(\text{Blue DN+Green DN +Red DN})} \times 100 \quad (3.1).$$

The F_0 females (16 replicates; n=50 bdelloids) were exposed to UVB radiation in 2 mL of MBL and at UVB intensities of: low (1.3 ± 5 W/m^2), mid (3.7 ± 5 W/m^2), or high (5.0 ± 5 W/m^2) for 2 hr at 25 ± 1°C. UVB radiation was emitted from a Spectroline® XX-15B UVR lamp that was suspended above the Petri dishes in a low-temperature, diurnal illumination incubator (VWR Signature Model 2015). A glass filter which filtered out low intensities of UVB (≥305nm) was used for the low treatment, this was substituted by a quartz glass filter in the mid and high UVB treatments. Intensities were verified using a UVA/B light meter (Sper Scientific 850009).

Negative controls were treated the same but placed in a Styrofoam box during exposures. After 48 hr, individuals that showed visible trophi (jaw) movement were considered recovered. Survivors (F_0, F_2, and F_4) were cultured with algal food. Eggs laid (F_1, F_3, and F_5 offspring, respectively) within a week of UVB exposure were moved to a separate Petri dish with algal food. Bdelloids of the F_1 or F_5 generation that hatched within a 6 hr period were selected for lifetable experiments. Survival of bdelloids in the F_0, F_2, and F_4 generations exposed to the three UVB intensities were compared using an ANOVA followed by a post hoc Tukey test. Statistical analyses were conducted using R version 3.4.3 and RStudio version 1.0.136 (R Core Team, 2015).

Life history characteristics

Lifetable experiments were done in replicates of 3 (F_1: control, mid, high; F_5: control) or 5 (F_1: low; F_5: low and mid) in a 9-well plate with one female per well. Rotifers were fed 250,000 ± 25,000 cells/mL of *C. reinhardtii* and culture under a 18: 6 hr L:D cycle at 25 ± 1°C. Daily, algae were counted, diluted to the appropriate concentration, and replaced in each well. An additional set of 3 replicates per UVR treatment were also followed but non-fed (NF), allowing them to serve as a control to determine the effects of food. The number of surviving females, and eggs laid and hatched were recorded every 24 hr. Females were moved to a new 9-well plate weekly to prevent the overgrowth of algae or accumulation of bacteria. Using life table data, age-specific survivorship (l_x), fecundity (m_x), the net reproductive rate (R_0), generation time (T), and the intrinsic rate of population increase (r) were calculated using Equations 3.2 – 3.6:

$l_x = \frac{n_x}{n_0}$ (3.2) $m_x = \frac{b_x}{n_x}$ (3.3) $R_0 = \sum l_x m_x$ (3.4) $T = \sum \frac{x l_x m_x}{R_0}$ (3.5) $r \sim \frac{\ln (R_0)}{T}$ (3.6).

Where x is time (day), n_0 number of starting females, n_x is the number of survivors on a given day, b_x is the number of offspring produced per day (Caswell 1989).

he Cox regression (Kragh Andersen et al. 2021) was used to investigate the interaction between maternal UVB exposure and lifespan or generation time. Effects of on lifespan and generation time were conducted using the *Survival Analysis* package version 3.3-1 (Therneau 2022) and the mixed effects Cox Models R package *coxme* version 2.2-18.1 (Therneau & Grambsch 2000A, B). Net reproductive rates (R_0) and intrinsic rate of change (r) were analyzed using a linear mixed effects (lme) model, which included random effects to account for variability in the experimental process. The Kenward-Roger correction was used to reduce the likelihood of type I errors and increase the power of the lme. These analyses were done using the lme4 package (Bates et al. 2015). Statistical analyses were conducted using R version 3.4.3 and RStudio version 1.0.136 (R Core Team 2022).

Results

Generational UVR exposure

The parental generation of *Philodina* (F_0) had a red digital number of 46.8 ± 3.3% (Table S3.2). Eggs laid by the parental generation were also brightly pigmented, but pigmentation decreased after one week of laboratory culture. In this case pigmented, neonates hatched and left behind a clear eggshell for the first two weeks of culture. Analysis of pigmentation in F_2 offspring resulted in an average of 37.4 ± 3.9 % red pixels, indicating that nearly 10% of the red

coloration had been lost (Table S3.2). In the F_4 offspring, a slightly red coloration remained in the intestinal lining, however at this point *Philodina* still contained 35.5 ± 1.7% red (Table S3.2).

The number of survivors in unexposed treatments in the F_0, F_2, and F_4 generations were between 17 – 69% greater than in UVB exposed treatments; thus, the loss in survival can be attributed to UVB exposure. Negative effects of UVB intensity became more apparent in the F_4 generation with survival decreasing by 22, 50, and 59% for bdelloids in the low, mid, or high UVB treatments, respectively (ANOVA, F = 29.6, df = 6, p>0.0001; Tables 3.1 & 3.2). Bdelloid survival also significantly decreased when comparing the F_4 to the F_0 generation (Table 3.2). Survival decreased to 14% and 7% in the high UVB treatments for the F_2 and F_4 generation offspring, respectively. After F_4 offspring were exposed to high UVB, the number of offspring produced was too low to conduct lifetable experiments.

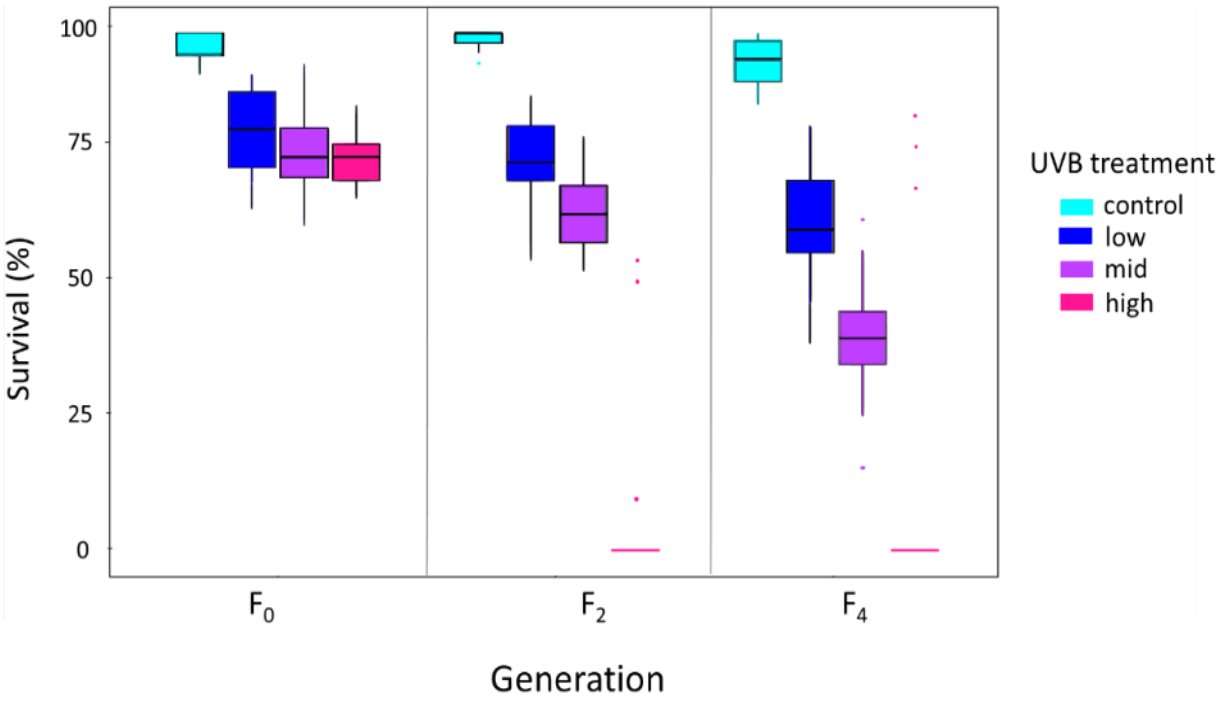

Figure 3.1. Effects of three levels of UVB exposure (1.3, 3.7,5.0 W/m^2) on survival of *Philodina* over three generations (F_0, F_2, and F_4 offspring). In the box plots, the horizontal bar represents the median, the top of the box represents the third quartile, and the bottom of the box represents the first quartile. Outliers are indicated by dots.

Table 3.1. The effects of UVB exposure on survival across three non-consecutive generations of *Philodina* (F_0, F_2, and F_4). Tukey's Honest Significance Difference (HSD) results are given in Table S3.3. df, degrees of freedom.

	df	F-value	p-value
UVB intensity	3	208.9	<0.0001
Generation	2	88.1	<0.0001
UVB intensity: Generation	6	29.6	<0.0001

Table 3.2. Percent difference in mean survival for three generations (F_0, F_2, and F_4) of Philodina after 3 levels of UVB exposure. Values above the diagonal show the percent difference in survival between treatments; significance at p<0.05 is indicated by an * below the diagonal. (Table S3.3).

	ctrl F_0	ctrl F_2	ctrl F_4	low F_0	low F_2	low F_4	mid F_0	mid F_2	mid F_4	high F_0	high F_2	high F_4
ctrl F_0		2	1	-17	-23	-35	-21	-33	-61	-23	-45	-68
ctrl F_2			-1	-18	-25	-36	-22	-34	-61	-24	-46	-69
ctrl F_4		*		-17	-24	-35	-21	-34	-61	-23	-45	-69
low F_0	*	*			-8	-22	-5	-20	-52	-7	-34	-62
low F_2	*	*	*	*		-15	3	-13	-49	1	-28	-59
low F_4	*	*	*	*	*		22	3	-39	19	-15	-51
mid F_0	*	*				*		-90	-87	-93	-96	-91
mid F_2	*	*	*	*		*			-41	16	-17	-53
mid F_4	*	*	*	*	*	*	*	*		96	40	-20
high F_0	*	*	*			*		*	*		-28	-59
high F_2	*	*	*	*	*	*	*	*	*	*		-43
high F_4	*	*	*	*	*	*	*	*	*	*	*	

Life history characteristics

The Cox regression model was established by comparing the mean differences in UVB exposed treatments to the F_1 control, for either fed (Table 3.3 – 3.6) or unfed treatments (Tables 3.7, S3.3 – 3.4). The impact of single or multiple maternal (F_1, F_5) UVB exposures on lifespan and generation time were assessed using multivariate Cox models. Due to high variability in lifespan between high UVB and the other UVB treatments the Cox model resulted in biased estimates, and large standard errors, skewing the results (Table S3.4). To correct this, and to interpret the effects of environmentally relevant UVB intensity on bdelloids, the high

UVB treatment was excluded from the lifespan analysis (Table 3.4), but not from other life history parameters.

As compared to the other treatments, the low UVB treatment for the F_1 generation had the longest lifespan (mean ± standard error (SE), 69.6 ± 5.5 days; Table 3.3), with nearly 4% of rotifers living over 100 days (regression coefficient (coef) ± standard error (SE): coef = 23 ± 0.6, z = 0.003, p<0.0001; Table 3.4). In the F_5 generation, the mean lifespan increased by 22% in the control treatment (Fig. 3.2a, Table S3.5) and by 46% in the mid UVB treatment (Fig. 3.2a, Table S3.5) and decreased by 16% in the low UVB treatment (Fig. 3.2a, Table S3.5). While lifespan decrease in the low F_5 treatment, 9 individuals lived for > 70 days (coef = 2.5 ± 6.0, z = 4.3, p <0.0001; Table 3.4, Fig. 3.2a). Generation time (T) in the F_1 generation was longest in low UVB treatment (19.8 days: Table 3.3) followed by mid UVB treatment for the F_5 generation (18.1 days, Table 3.3). The fastest generation time of 7.0 ± 2.2 days was in the high UVB treatment (coef = -2.2 ± 7E3, z = 0.003, p <0.0001, Table 3.4), and in the control, the mean was 9.7 ± 0.3 days (coef = 23 ± 0.6, z = 0.003, p <0.0001, Table 3.4). In the F_5 generation, mean generation time increased by 27% in the control and by 10% in the mid UVB treatments (Fig. 3.2b) and decreased by 13% in the low UVB treatments (Fig. 3.2b).

Table 3.3. Lifespan and generation time (days, mean ± standard error) of two generations (F_1 & F_5) of Philodina after maternal exposure to low, mid, high, and control UVB radiation (0, 1.3, 3.7, or 5.0 W/m^2). N/A – data not recorded due to low reproduction of F_4 females. ND = no data

	Control	low	mid	high
F_1 Lifespan	32.1 ± 9.8	69.6 ± 35.0	38.4 ± 6.4	21.5 ± 9.0
F_5 Lifespan	39.1 ± 11.1	58.7 ± 25.1	55.9 ± 21.7	ND
F_1 Generation time	9.7 ± 0.5	19.8 ± 3.6	16.4 ± 1.5	7.0 ± 3.7
F_5 Generation time	12.3 ± 2.1	17.3 ± 2.0	18.1 ± 1.3	ND

Table 3.4. Survival analysis of the effects of maternal UVB exposure at environmentally relevant levels (1.3, 3.7,W/m^2) on lifespan and generation time based on Cox proportional hazard regression. The model compared UVB treatments to the F_1 control. N/A – data not recorded due to low reproduction of F_4 females. Results from the high UVB treatment are given in Table S3.3. Post-hoc test results are given Table S3.4.

		coefficient ± SE	z value	Pr(>|z|)
Lifespan	F_5 vs F_1	-1.6 ± 0.5	-3.2	0.001
	F_1 low	-22.6 ± 0.6	-39.0	<0.0001
	F_1 mid	-1.9 ± 0.5	-3.9	<0.0001
	F_1 high	ND	ND	ND
	F_5l ow	2.5 ± 6.0	4.3	<0.0001
	F_5 mid	-18.1 ± 0.6	-31.1	<0.0001
	F_5 high	ND	ND	ND
Generation Time	F_5 vs F_1	-26 ± 1.0	-0.3	0.79
	F_1low	-2.2 ± 1.3	-1.7	0.08
	F_1mid	-2.5 ± 7E3	-4.0E-3	0.99
	F_1high	-2.2 ± 7E3	-3.0E-3	0.99
	F_5low	4.2 ± 1.6	2.7	0.01
	F_5mid	0.8 ± 1.5	0.5	0.60
	F_5high	ND	ND	ND

The mean net reproductive rate (R_0) for the F_1 generation was the highest for bdelloids in the low UVB treatment (32.3 ± 1.1 offspring per female; linear mix model estimate (est) ± standard error (SE), est = -11.5 ± 3.5, t = -5.41, p =0.004; Tables 3.5 & 3.6), and the lowest R_0 (8.6 ± 1.1 offspring per female) was seen in bdelloids in the high UVB treatment (est = -1.1 ± 2.6, t = -0.43, p =0.673; Tables 3.5 & 3.6). After two additional maternal exposures, means for R_0 was the highest in the F_5 mid UVB cohort (34.4 ± 1.0, est = 22.7 ± 2.3, t = 9.78, p <0.0001; Tables 3.5 & 3.6). Net reproductive rate was compared between the F_5 and F_1 generations and showed an increase of 169% in the no UVB control and 17% in the mid UVB treatment (Fig. 3.2c, Table S3.6). In contrast, R_0 decreased by 4% in the low UVB treatment (Fig. 3.2c, Table S3.6). The fastest population growth rate was seen in the high UVB treatment (0.35 ± 0.08, est = 0.12 ± 0.05, t = 2.4, p = 0.03; Tables 3.5 & 3.6), and the slowest rates were seen in the low UVB treatment (0.18 ± 0.01) and the mid UVB treatment (0.21 ± 0.01) (Fig. 3.3b, Table 3.5).

Table 3.5. Effects of maternal UVB exposure on net reproductive rate (R_0), and intrinsic rate of change (r) after parental exposure to low, mid, or high UVB radiation levels (1.3, 3.7, or 5 W/m^2, respectively). Data recorded in mean± standard error (SE) days. N/A – data not recorded due to low reproduction of F_4.

	Control	**low**	**mid**	**high**
F_1 Net Reproductive rate	9.67 ± 0.50	32.33 ± 2.51	29.48 ± 6.72	8.56 ± 1.89
F_5 Net Reproductive rate	26.00 ± 4.41	30.96 ± 2.11	34.42 ± 2.19	ND
F_1 intrinsic rate of change	0.23 ± 0.01	0.18 ± 0.02	0.21 ± 0.01	0.35 ± 0.01
F_5 intrinsic rate of change	0.27 ± 0.14	0.20 ± 0.03	0.20 ± 0.01	ND

Table 3.6. Analysis of UVB exposure over three generations using a linear mix effects model (lme). *Philodina* life history traits compared to the control for net reproductive rate (R_0)and intrinsic rate of change after parental exposure to low, mid, or high UVB. Kenward-Roger correction estimate (est) ± standard error (SE).

		est ± SE	t value	Pr(>|t|)
Net reproductive rate	F_5 vs F_1	16.3 ± 2.6	6.305	< 0.0001
	F_1 low	22.7± 2.3	9.783	< 0.0001
	F_1 mid	19.8 ± 2.6	7.649	< 0.0001
	F_1 high	-1.1 ± 2.6	-0.429	0.673
	F_5 low	-17.7 ± 3.2	-5.405	< 0.0001
	F_5 mid	-11.5 ± 3.5	-3.297	0.004
	F_5 high	ND	ND	ND
The intrinsic rate of change	F_5 vs F_1	0.03 ± 0.04	0.857	0.401
	F_1low	-0.1 ± 0.1	-1.712	0.102
	F_1mid	-0.03 ± 0.1	-0.765	0.453
	F_1high	0.1 ± 0.1	3.080	0.006
	F_5low	-0.01 ± 0.1	-0.220	0.828
	F_5mid	-0.04 ± 0.1	-0.814	0.425
	F_5high	ND	ND	ND

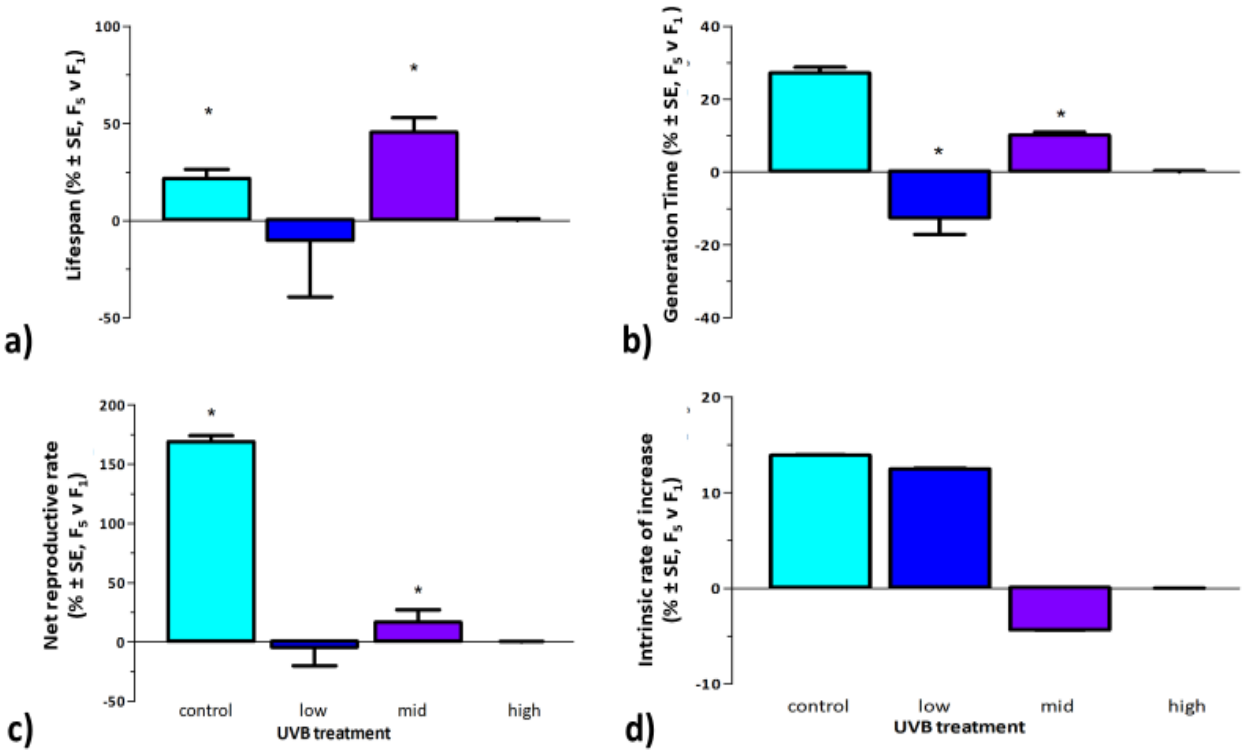

Figure 3.2. Transgenerational effects of UVB exposure on lifespan and generation time in bdelloid rotifers exposed to three levels of UVB radiation. Percent differences between F_5 and F_1 generations for a) lifespan b) generation time (T), c) net reproductive rate (R_0), d) the intrinsic rate of change (r). Significant difference ($p<0.05$) between means when comparing F_5 to F_1 are shown by *.

To interpret the effects of maternal UVB exposure, life histories from each UVB treatment were compared to the no UVB control treatment. Low UVB exposure increased lifespan by 117% in the F_1 generation (Fig. 3.3a, regression coefficient (coef) ± standard error (SE); coef = 23 ± 0.6, z = 0.003, p <0.0001; Table 3.4). In the F_5 generation, lifespan increased by ~50% in the low UVB treatment (Fig. 3a; coef = 20 ± 0.8, z = 0.003, p <0.0001; Table 3.4), and 43% in mid UVB cohorts (Fig. 3.3a, coef = 20 ± 0.8, z = 0.003, p <0.0001; Table 3.4). Generation time increased by 105% in the low UVB treatments (Fig. 3.3b, coef = 5 ± 1.1, z = 4.9, p <0.0001; Table 3.4), and by 69% in the mid (Fig. 3.3b, coef = 3 ± 1.0, z = 3.1, p = 0.01; Table 3.4).

In comparing the UVB exposed treatments to the control, net reproductive rate was positively affected in the F_1 generation under low and mid UVB treatments (Fig. 3.3c). In the

low UVB treatment R_0 increased by 235% (estimate = -23 ± 1.9, t = -12.08, p <0.0001: Table S3.6) and by 205% in the mid UVB treatment (estimate = -20 ± 2.1, t = -9.4, p <0.0001: Table S6). In the F_5 generation (Fig. 3.3c R_0 increased by 32% in the mid UVB treatment (estimate = -8 ± 1.9, t = -4.5, p = 0.009; Table S3.6). Bdelloids in the high UVB treatment had the highest rate of intrinsic increase (0.35 ± 0.04); 50% higher than the control (Fig. 3.3d) (25%: coef = -0.2 ± 0.04, z = -3.9, p = 0.002; Table 3.4). A decrease occurred in both the F_1 and F_5 generations under low and mid UVB treatments as compared to the control (Fig. 3.3d). The earliest reproduction was seen in the mid F_1 generation (5.5 ± 0.7 days) (e.g., control (8.4 ± 0.8 days) or low UVB treatments (8.8 ± 0.8 days; Fig. 3.3d).

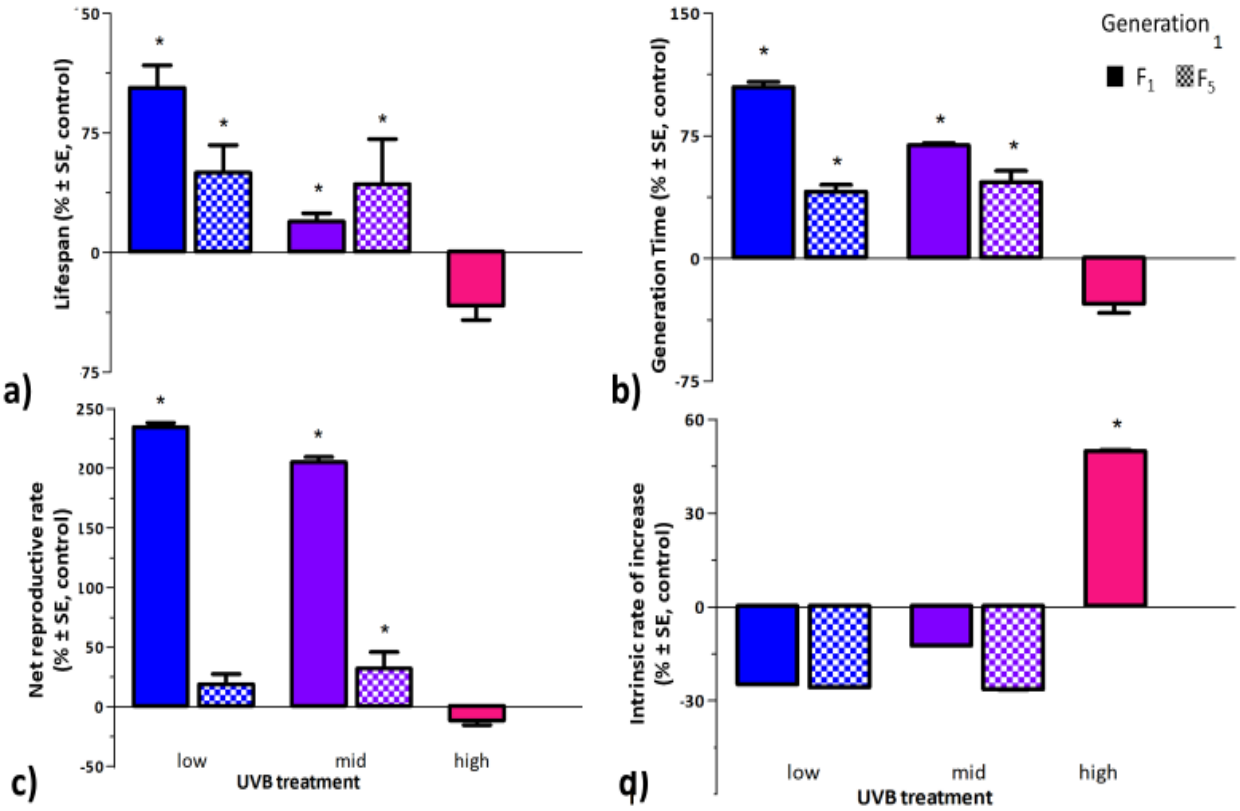

Figure 3.3. Effects of maternal UVB exposure on Philodina lifespan and generation time. Life history traits were compared between low, mid, and high UVB radiation (0, 1.3, 3.7, or 5.0 W/m^2) and control. The maternal line was exposure to UVB for one generation (F_0), or three non-consecutive generations (F_0, F_2, F_4). a) Lifespan, b) generation time. c) net reproductive rate (R_0), d) the intrinsic rate of change (r). Difference (p<0.05) between means shown by * as determined by a post-hoc Tukey (Table S3.4, S3.6).

Fecundity per female in the F_1 generation showed a peak at day 20, then a decline in fecundity per female in the controls (Fig. 3.4). Bdelloids began to reproduce on day 8 until day 72 in the low UVB treatments while reproduction started on day 3 until 52. In both low and mid UVB treatments there were multiple, brief phases of high reproductive output, followed by intervals of very few or no eggs being laid. Bdelloids exposed to high UVB intensity had the lowest fecundity with the shortest reproductive phase which began on day 3 followed by short periods of reproduction which persisted until day 38 (Fig. 3.4). In the F_5 generation, bdelloids began reproducing on day 5 in the mid UVB treatment and day 6 in the control and low UVB treatments. Overall, fecundity in the control treatment had a several periods of reproduction before it peaked and ended on day 42. *Philodina* exposed to low UVB intensity continued to reproduce up to day 73, although mean number of offspring per female was lower in this generation. The mid UVB treatment had the highest fecundity per female which peaked at day 25 days and gradually decreased until day 61 (Fig. 3.4).

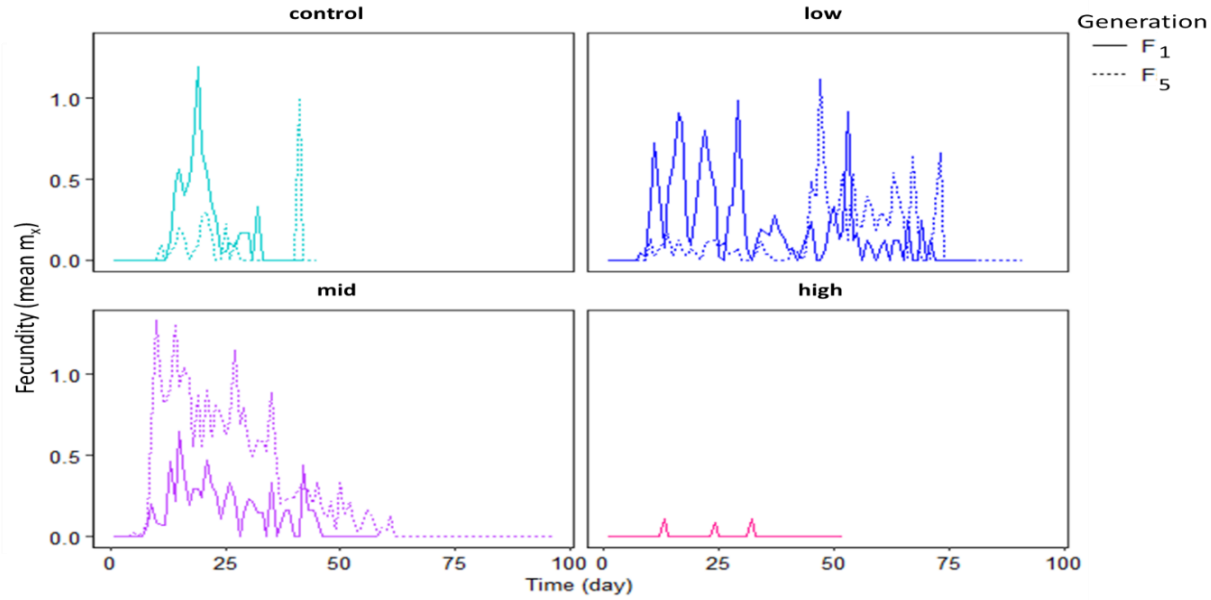

Figure 3.4. The impact of maternal UVB exposure on age-specific survivorship and fecundity per surviving *Philodina* sp. Maternal lines were exposed to environmental relevant UVB radiation (low, mid, and high UVB radiation, winter, summer, and extreme scenario, respectively), over three non-consecutive generations (F_0, F_2 and F_4).

As previously mentioned, non-fed replicates for each treatment were conducted simultaneously with the fed treatments, to ensure the results recorded were due to UVB exposure and due influenced by the food source. Similar trends as those seen in the fed treatment, the low and mid UVB exposure cohorts had a longer lifespan increased in NF when compared to the control of both low and mid UVB treatments for the F_1 generation (88 and 37%, respectively) and for the F_5 generation (low: 84%, mid:80%). This trend was also seen in the NF R_O when compared to the control for both F_1 and F_5 low (173, 250%) and mid (22, 250%) UVB treatments (Tables 3.7, S3.6 – 7).

Table 3.7. Life history traits of *Philodina*. Life history traits were recorded for the F_1 and F_5 generations after maternal exposure to low, mid, high UVB radiation (1.3, 3.7, or 5 W/m^2), as well as a no UVB control. Means ± SD, net reproductive rate (R_o), generation time (T) and intrinsic rate of change (r). [a] $p<0.05$ when compared to control; [b] $p<0.05$ when comparing F_5 to F_1.

Generation	UVB	Lifespan (days)	T	R_0	r
F1	control	24.5 ± 5.1	12.6 ± 5.2	4.0 ± 1.8	0.15 ± 0.08
	low	46.0 ± 7.8[a]	15.6 ± 1.9	11.2 ± 1.3[a,b]	0.14 ± 0.02
	mid	33.4 ± 1.0 [a,b]	16.2 ± 0.8	4.9 ± 0.8	0.10 ± 0.01
	high	20.7 ± 6.2	8.0 ± 2.8[a]	0.1 ± 0.1 [a]	-0.26 ± 0.37 [a]
F5	control	22.1 ± 2.5	11.4 ± 3.3[a]	1.1 ± 0.5	0.01 ± 0.05
	low	40.5 ± 15.3[a]	24.3 ± 12.3[a,b]	3.9 ± 2.5[a,b]	0.02 ± 0.11[b]
	mid	39.8 ± 4.3[a,b]	20.5 ± 2.3	3.9 ± 2.5	0.05 ± 0.06
	high	ND	ND	ND	ND

Discussion

Regions of the Chihuahuan Desert that are at higher elevations experience higher intensities of UVR, which could act as a selective force favoring individuals which can avoid or prevent damage. In this study, I found that lifespan and reproductive rates of bdelloids exposed to regional UVB intensities were higher as compared to unexposed individuals. In the winter in Hueco Tanks, UVB intensity is similar to the levels in the low UVB treatment. During this time, temperatures range between 1 – 20 ˚C (retrieved December 15, 2022,

https://www.weather.gov/epz/climatedataforelpaso) prolonging the filling cycle in the rock pool, thereby extending the hydrated period for *Philodina*. The low UVB intensity exposure could trigger the reallocation of resources in females toward increased lifespan as with the increased in lifespan seen in the low UVB treatment. The mid UVB treatment is reflective of summer mean UVB levels, which often is accompanied by high temperatures (~40 ˚C; retrieved December 15, 2022, https://www.weather.gov/epz/climatedataforelpaso). At these high temperatures, water evaporates faster, shortening the hydroperiod. Under these conditions, bdelloids likely reallocate resources to increase reproduction at the cost of a shorter lifespan. Animals in the mid UVB treatments lived 45% fewer days than in the low UVB treatment, however, they had nearly the same number of offspring/female (R_0 = 29.5 ± 6.7 offspring/female) as the low UVB (32 ± 2.5 offspring/female). In the high UVB treatment, which represented an extreme UVB intensity that is approximately 1.4 times greater than average levels, bdelloids often laid two eggs within 24 h and had the shortest lifespan of 21.5 ± 2.0 days.

In a non-optimal environment, it is better to produce a few larger, high-quality, and fast-developing offspring, whereas the number of offspring should be maximized under favorable conditions (Vehmaa et al. 2012). This would ensure the perseverance of the population under high UVB intensities. The trade-off between somatic maintenance and reproduction is a common strategy observed in response to various stressors, including UVB radiation (Fernández et al. 2018; Latta et al. 2019; Sha et al. 2020). For example, exposure of the monogonont rotifer *Brachionus asplanchnoidis* Charin, 1947 to low intensities of UVB showed no evidence of acclimation, and a trade-off between survival and reproduction was

found (Kan et al. 2023). At higher UVB dosages both longevity and fecundity were negatively affected. This indicated that as UVB radiation intensified, there was a deterioration in fitness.

The lifespan of most bdelloids is approximately 35 days, with the shortest lifespan of 16 days recorded in *Adineta vaga* (Davis, 1873) (Latta et al. 2019; Ricci 1983) and the longest in *Philodina gregaria* Murray, 1910 (Dartnall 1992) ranging from 60-89 days (King et al. 2005). Net reproductive rates for bdelloids average 17 offspring per female with a generation time of 10 days (Table S9). *Philodina* in the low and mid UVB treatments, of both F_1 and F_5 generations, appear to have lifespan, number of offspring produced, and net reproductive rates in in the upper ranges of those found in other *Philodina* species. In the control treatment, lifespan and reproductive rates were comparable to the lower ranges seen in *Philodina* species (King et al. 2005). In both low and mid UVB treatments, bdelloids lived longer and had greater net reproductive than in the control treatments. No significant difference was seen in reproductive rate between the high and control treatments. This suggests that both extreme and no UVB scenarios could be detrimental to the reproductive success of *Philodina*, supporting the supposition that bdelloids have locally adapted and UVR may have acted as a selective force.

In addition, there are differences in life history traits in bdelloid species found in permanent aquatic habitats and those from temporary terrestrial habitats (Ricci 1983). Species from aquatic habitats tend to have a brief reproductive phase, gradually increasing the number of offspring produced until reaching a peak, and then decreasing steadily. In contrast, bdelloids living in terrestrial habitats show multiple brief phases of high reproduction, with intervals of very few or no eggs produced (Ricci 1983). In our study, fecundity steadily increased in the low and mid UVB treatments, peaked (~20 day) then steadily decreased until senesce while in the

control and high UVB treatments fecundity had two distinct peaks. Under low UVB intensity exposure, bdelloids exhibited extended lifespans and continued reproduction up to 70 days, with intermittent phases of high reproductive output. In the mid UVB intensity treatment, the highest fecundity per female peaked within 25 days and gradually decreasing afterward. Conversely, high UVB intensity resulted in the lowest fecundity. Overall, our research suggests that regional UVB exposure positively influences bdelloid lifespan and reproductive patterns, while extreme UVB intensity negatively affects these life history traits.

Evidence of transgenerational accumulative damage was seen when the maternal line was exposed to UVB radiation. This evidence was supported when we compared bdelloids survival after multiple generations being exposed to the results of a single generational exposure after being cultured until nearly no pigment remained. However, in this study bdelloids were cultured in the laboratory for six months, which resulted in the loss of most of their pigmentation. When only one generation of *Philodina* was exposed, survival was >75% for all UVB intensities (Baeza 2023). After a second UVB exposure, bdelloid survival was ≤75% in F_2 generation. After the third exposure rotifer, survival was significantly lower in all UVB treatments (64%, 39%, 7%; low, mid and high UVB intensity, respectively). Transgenerational accumulative damage seen here, suggests that the cellular damage incurred by bdelloids due to UVB exposure impacts the fitness of offspring, even if those offspring were not directly exposed to UVB radiation. This could occur through various mechanisms, such as changes in gene expression, epigenetic modifications, or alterations in the germ cells (Dam 2013; Fox et al. 2019; White & Butlin 2021).

Another possible reason for the cumulative damage seen in *Philodina* could be the loss of the red coloration once they were cultured in laboratory. Red algal extracts, often composed of carotenoids (Fischer et al. 2013), are known to prolong lifespan in monogonont rotifers, due in part to their antioxidant properties (Snare et al. 2013). Red pigmentation in *Philodina* be an example of phenotypic plasticity, where the expression of this trait is influenced by the high UVB environment. In addition, I observed that *Philodina* eggs laid after collection were pigmented (Fig. S3). This is likely due to the mother reallocating resources to enhance the offspring's ability to survive in environments with high UV radiation (Dam 2013; Fox et al. 2019); even before the pigment source can be ingested. This plasticity allows the offspring to quickly adjust their phenotype based on environmental cues, enhancing their survival in UV-exposed habitats. Over time, such phenotypic plasticity can lay the foundation for genetic adaptation. Individuals with a genetic inclination to produce red pigmentation may have a higher fitness level as they are more likely to survive and reproduce in UVR-intense environments. As these advantageous traits are passed down from one generation to the next, genetic changes may occur, promoting a more fixed and heritable expression of pigmentation. Natural selection favors individuals with specific genetic variations that confer a survival advantage in the environment by shifting from plasticity to genetic adaptation.

Future Directions

Regional adaptation to UVB intensity was supported by this study although further research is needed to understand the mechanisms involved. One promising line of research would be to quantify gene expression of bdelloid rotifers that have been exposed to environmentally relevant levels of UVR. In addition, conducting follow-up experiments that

consider a broader range of environmental factors would help give a deeper understanding of *Philodina* adaptive strategies in shallow waters. These experiments could involve cultivating *Philodina* under regional UVR levels, while introducing variations in temperature and photoperiod. Furthermore, identification of the pigment and its source would be of value in maintaining the degree of pigmentation in the laboratory.

Chapter 4: Gene Expression in Response to Ultraviolet Radiation in a Pigmented Aquatic Microinvertebrate

Introduction

As climate changes and weather patterns become more erratic, regions close to -30˚ or 30˚ latitude or above 1,000 m in elevation are expected to experience prolonged exposure to direct sunlight, and in turn enhanced levels of ultraviolet radiation (UVR) (Bais et al. 2018; Pinceel et al. 2018; Salawitch et al. 2019; Watanabe et al. 2011). Aquatic animals have developed various behavioral and genetic adaptations that allow them to prevent, withstand, or repair damage caused by UVR (Oexle et al. 2016; Williamson et al. 2001). Some zooplankton produce their own photoprotection, usually in the form of brightly colored melanin, while other obtain photoprotectants from their food such as algae, bacteria, fungi, or smaller zooplankton (Fernández et al. 2018; Nevalainen et al. 2020; Wang et al. 2011). This results in phenotypic variation that may be due to genetic variation, availability of food, or other environmental pressures (Dan 2013).

Exposure to UVR affects all three major biomolecules (e.g., proteins, lipids, and DNA/RNA) (Schuch et al. 2013; Oexle et al. 2016; Williamson et al. 2019). Cellular injury is incurred through the absorption of UVR photons, which cause the formation of cyclobutane pyrimidine dimers (CPDs) and 6,4 photoproducts (PPs). These nucleotides are mutated in areas where two pyridine bases (cytosine, thymine, or uracil) are found next to each other or overlapping on the same polynucleotide strand (Kim et al. 2011; Ikehata & Ono 2011; Widel 2012). Radical oxygen molecules are released when thymine mutates to cytosine. The absorption of UVR photons by lipids, proteins (riboflavin, tryptophan), or other macromolecules

(porphyrin) causes peroxidation, de-esterification (Kim et al. 2011; Krisko et al. 2012; Schuch et al. 2013; Widel 2012). Free reactive oxygen species (ROS), such as superoxide anions, hydrogen peroxide, and hydroxyl free radicals, are released and can then directly attack the DNA backbone (Kim et al. 2011; Krisko et al. 2012; Schuch et al. 2013). This results in closely spaced DNA lesions that can lead to late-stage oxidative double stranded breaks (DSBs) (Hecox-Lea & Mark Welch 2018; Kim et al. 2011; Krisko et al. 2012).

The oxidation incurred during UVR exposure is comparable to the oxidation of DNA when tardigrades and bdelloid rotifers undergo quiescence (Fischer et al. 2013; Horikawa et al. 2013). As bdelloids undergo anhydrobiosis they contract their head and foot into their trunk, becoming a xerosome (Caprioli & Ricci 2001; Ricci et al. 2003; Ricci 2016). As they emerge from the desiccated state, breaks in the DNA are thought to be repaired by numerous DNA repair mechanisms (Hecox-Lea & Mark Welch 2018) and antioxidants (Fischer et al. 2013; Daly 2012). Antioxidants scavenge ROS to counter UV-induced oxidation (Oexle et al. 2016; Williamson et al. 2001).

Transcriptome analysis involves high-throughput sequencing of mRNA transcripts produced by an organism's genes at a given time, providing indirect measure of gene expression patterns (Li & Dewey 2011) and molecular responses to environmental changes (Boschetti et al. 2012; Hecox-Lea & Mark Welch 2018). Transcriptome analyses have been conducted to characterize major repair pathways active as bdelloids enter and emerging from desiccation using *Adineta ricciae* (Segers & Shiel, 2005) (Boschetti et al. 2012; Eyres et al. 2013; Nowell et al. 2018) and *Adineta vaga* Davis, 1873 (Flot et al. 2013; Wiles & Schurko 2020; Hecox-Lea & Mark Welch 2018). Additionally, various bdelloid transcriptomes have been used

to determine the size of their genomes (Hespeels et al. 2014; Mark Welch & Meselson 2000; Ricci 2016), the presence of horizontally acquired genes (Eyres et al. 2015; Nowell et al. 2021; Szydlowski, et al. 2015; Yoshida et al. 2019), and transposable elements (Nowell et al. 2021). Current research has also been focused on gaining insight on how bdelloids have successfully adapted and evolved for 40 million years with no males or hermaphrodites (Hanson et al. 2013; Simion et al. 2021; Terwagne et al. 2023). Transcriptome analysis can also reveal the activation or inhibition of specific signaling pathways, the production of stress-related proteins, and changes in metabolic processes that occur in response to environmental changes. In turn this process can uncover novel genes or regulatory elements that are involved in stress response, providing potential targets for further investigation (Li & Dewey 2011; Hecox-Lea & Mark Welch 2018).

This information can enhance our understanding of the adaptive strategies and physiological responses that allow organisms to survive and thrive in challenging environments such as ephemeral rock pools. These shallow ephemeral habitats depend on rainwater and are vulnerable to many aspects of climate change, including increases in temperatures, prolonged droughts, and alterations in dissolved organic carbon (DOC) (Joćque et al. 2010; Schröder et al. 2007; Walsh et al. 2014). Rock pool communities at Hueco Tanks State Park and Historic Site, El Paso Co., TX located in the northern Chihuahuan Desert, are at relatively high elevations (1,380 m). This high elevation means there is reduced atmospheric protection from UVR (Blumthaler & Ellinger 1997; Piazena 1996; Williamson et al. 2001). Several bdelloid species have bright red pigmentation. Nearly all these rotifers occur in temporary habitats that experience prolonged periods of desiccation, high temperatures, and exposure to intense ultraviolet radiation. They

are capable of surviving in these hostile environments by entering a dormant state and reducing their metabolic rate. This adaptation has enabled them to survive in extreme conditions for thousands of years (Cakil et al. 2021; Ricci et al. 2003; Hespeels et al. 2020).

The objectives of this study were to 1) create a *de novo* transcriptome to identify and quantify genes of a pigmented *Philodina* species and 2) to test how pigmentation affects expression of genes during response to UVR treatment. We hypotheses that highly pigmented (HP) bdelloids will likely show a milder response because of the presence of pigment. Due to this, fewer repair genes and pathways will be differentially expressed. In non-pigmented (NP) bdelloids, a broader response in the number and types of genes that are differentially expressed is expected in response to UVB radiation. Results obtained in this study will enhance our understanding of types of genes within the bdelloid rotifer and how pigmentation alters the UVR response of bdelloids.

Methods

Site, collection, and culture

Hueco Tanks State Park and Historic Site (hereafter Hueco Tanks) in El Paso Co., TX (31.93° N, 106.04°W; elevation: 1,372m), mean UVB intensities for this region range from 1.45 W/m^2 in the winter and 3.55 W/m^2 in the summer (Sengupta et al. 2018). El Paso Co., TX, has mean summer temperatures of 36 °C and receives ~22 cm of rainfall each year. Water samples were collected after a precipitation event (≳0.5 cm, https://www.weather.gov/epz/elpaso_monthly_precip). *Philodina* species (hereon: *Philodina*) were isolated in the laboratory, washed free of debris, cultured, and exposed to

environmentally relevant levels of UVB radiation. At time of collection, the *Philodina* are highly pigmented (HP). A subset of bdelloids were fed a mixture of the green algae *C. reinhardtii* and *Chlorella vulgaris* Berijerinck, 1890 (UTEX strain 30) and cultured for over six months, until only a slight trace of orange in the lining of their gut remained.

UVB exposure & RNA extraction

Environmentally relevant UVB intensities of low (1.3 W/m^2), mid (3.7 W/m^2), and an extreme UVR scenario of high (5.0 W/ m^2) were selected for exposure levels. Exposure to UVB radiation was conducted as before in chapter 2, with the modification of using 5 mm of 3% low melting point agarose (IBI Scientific IB70057) to line the glass Petri dish (60 x 15 mm: n=16 with 50 rotifers). In short, rotifers were then exposed to UVB intensities for a period of 2 hr at 25 ± 1°C. Approximately 500 µL of MBL was added to maintain rotifers hydrated during exposures. After exposure, an additional 5 mL of MBL media and 10 drops of 1X Dulbecco's phosphate-buffered saline (DPBS) was added to each Petri dish to facilitate xerosome formation. Xerosomes (n=300) were then washed free of any remaining agarose in a 9-well plate and transferred to a 1.5 mL tube with as little media as possible. Bdelloids were rinsed and pelleted using 250 µL of deionized water, before RNA extraction, this was done for each replicate (HP, n=5; NP, n=3).

Extraction of RNA was conducted immediately after UVB exposure, methods were adapted from Hecox-Lea et al. (2018) and Chomczynski et al. (1995). All solutions used for RNA extraction were chilled on ice, and samples were centrifuged (>6,000 rpm) at 2 – 8 °C to preserve RNA integrity. Briefly, 1,000 µL of TRIzol® Reagent and the xerosome pellets were transferred to a mortar and pestle, then agitated for 2 min. The TRIzol mixture was incubated

for 5 min at room temperature to separate cellular debris, after which 200 µL of chloroform was added, to separate nucleic acids from other cellular substances. The upper portion of the solutions containing nucleic acids, with equal parts 95% ethanol and 2 µL of linear acrylamide (5 mg/mL) were incubated for 18 hr at -20°C. To ensure precipitation of low concentrations of RNA, isopropyl alcohol was added the following day, and incubated at room temperature for 45 min. After the incubation period, an RNA pellet was obtained through centrifugation. Additionally, the RNA pellet was washed using ethanol, which was then removed using a pipette, with the residual ethanol allowed to evaporate. The RNA pellet was then dissolved in 62 µL of RNA-free water for RNA-seq analysis. The concentration and integrity of the extracted RNA were determined using a NanoDropTM OneC Microvolume UV-Vis Spectrophotometer (Thermo ScientificTM). To confirm RNA concentration and purity, a small aliquot of the sample (7 µL) was sent to the BBRC's Genomics Analysis Core Facility and analyzed using a Qubit® RNA High Sensitivity Assay Kit.

RNA sequencing, de novo transcriptome assembly and annotation

Total RNA was used for preparation of cDNA libraries and sequencing, which was done at UTEP's Border Biomedical Research Center (BBRC) Genomics Analysis Core Facility. Illumina TruSeq RNA Library Prep Kit v2 was used to selectively purify the poly(A)+ tail of mRNA from 4 µg of total RNA. Poly(A)+ mRNA was used to synthesize the first then the second cDNA strands following the manufacture's protocol. Sequencing was performed on an Illumina NextSeq 550 system which generated paired end reads of 500 bases. After libraries were constructed, the PCR product was purified, and quality was assessed using High Sensitivity DNA ScreenTape Analysis on Agilent TapeStation 2200.

Raw RNA-Seq reads were checked for quality using the FastQC v0.11.5 software. Trimmomatic was used to remove low quality reads. Using OmicsBox (www.biobam.com), a *de novo* transcriptome was assembled. Briefly, the steps included using Trinity v2.5.0 (Haas et al. 2013) to assemble from the combined reads of all the HP and NP samples. The Trinity pipeline consists of the following steps: 1) sequences from each treatment are assembled into unique transcripts or contigs, 2) contigs are then clustered to represent isoforms for any gene and 3) contigs are then spliced into a full-length transcriptome (Grabherr et al. 2011). To minimize contamination and misassembly of transcripts following mapping, the sequence reads were aligned back to the de novo assembly using RSEM (Li & Dewey 2011) and Bowtie2 (Langmead et al. 2019); the transcripts with fewer than ten counts were removed from the assembly. The quality of the transcriptome assembly was determined using quality assessment tool (QUAST) which evaluates and compares the assembly's contiguity (Gurevich et al. 2013). The transcriptomes completeness in terms of the expectation of finding a single copy of every gene is determined by using the software benchmarking universal single-copy orthologs (BUSCO) (Simão et al. 2015).

To functionally characterize nucleotide sequences, annotation was performed within OmicBox's Functional Annotation module using both InterProScan and Basic Local Alignment Search Tool (BLAST) search against the NCBI non-redundant protein database (Nr). Transcripts were then mapped to a Gene Ontology (GO terms) annotation database (Götz et al. 2008). Additionally, metabolic, genetic, biological, and chemical pathways were mapped using (GHOAST KOALA) Kyoto Encyclopedia of Genes and Genomes (KEGG) orthology (Kanehisa et al. 2022).

Transcriptome Comparisons

To validate the genes identified in the *Philodina* transcriptome assembly, transcriptome sequences of *Philodina acuticornis* and *P. roseola* were downloaded from GenBank (https://www.ncbi.nlm.nih.gov/datasets/genome/?taxon=44578, April 6, 2022). The downloaded sequences were in the form of nucleotide sequences, to validate the identified genes, and the nucleotide sequences were translated into protein sequences using OmicsBox. This step helps ensure that the predicted genes can produce functional proteins. Moreover, to maximize the number of transcripts verified using other bdelloids species, protein sequences were obtained from complete genome assemblies which had been used as a reference genome or showed high coverage genomes (Nowell et al. 2021) (Table S4.1) of *Adineta ricciae* (Segers & Shiel, 2005), *Adineta vaga* (Davis, 1873), *Didymodactylos carnosus* Milne, 1916, *Macrotrachela quadricornifera,* Milne 1886*, Rotaria* sp. Silwood1, *R. magnacalcarata,* Hudson 1884, and *R. sordida,* Scopoli, 1777, were included to serve as references for comparison and validation of the identified genes. Combining the information from nucleotide sequences, protein sequences, and comparative analyses allows for the validation and verification of the presence, functionality, and conservation of genes, functions, and pathways in the transcriptome assembly of *Philodina*.

Differential Gene expression

Gene expression was quantified in both HP and NP pigment groups to study how red pigmentation would affect genes that respond to UVB exposure. The trimmed reads were again aligned to the filtered transcriptome using Bowtie2. The aligned reads were then counted using RSEM (RNA-Seq by Expectation-Maximization) version 1.3.0, which estimates the abundance of

transcripts. Using the raw count data obtained from RSEM, Venn diagrams were created using R-studio VennDiagram package (Chen 2011). Within R, DESeq2 was used to normalize and determine differential expression of genes between the different exposures and pigmentation groups (Love & Anders 2014). Differentially expressed genes were considered as those with log2-fold change greater than 2 or less than -2 and with an adjusted p-value of < 0.05.

Log2-transformed fold changes are commonly used to represent the magnitude of gene expression differences between conditions or treatments. For example, a log2 fold change of +1 indicates a two-fold increase in gene expression, while a log2 fold change of -1 indicates a two-fold decrease. In addition, the p-values represent the probability of obtaining the observed gene expression differences or more extreme results under the assumption of the null hypothesis (no differential expression). However, when performing thousands of statistical tests simultaneously, the chance of obtaining a high false discovery rate (FDR) increase. Thus, a Benjamini-Hochberg adjustment was applied. Transformed expression values of genes within specific GO terms and KEGG were determined using R version 3.4.3 and RStudio version 1.0.136 (R Core Team 2022).

Results

UVB exposure and RNA extraction

The high pigmentation seen in field collected *Philodina* was retained for 5-7 days, so bdelloids were exposed to UVB radiation within 3 days of collection. After more than 20 weeks and multiple generations in culture, an orange tint remained in the lining of the inner gut. After RNA extraction, concentrations ranging from 17 – 117 ng/mL for highly pigmented samples and

10 – 31 ng/mL in non-pigmented bdelloids were obtained (Table S4.1). The RNA integrity number equivalent (RINe) was greater than 5.3 for all samples (Table S4.1).

RNA sequencing, de novo transcriptome assembly and annotation

After filtering out reads of poor quality, the transcriptome consisted of nearly 360,000,000 reads which formed 109,868 contigs, and with a size of 139.8 mb (Table S4.2). Contig size ranged up to 24 kb, with a mean of 1,498 bp, N50 of 1,500 bp, L50 of 25,442 bp, and GC content of 41.7% (Table S4.2). Transcriptome sequencing showed an acceptable contig quality as well as good transcriptome coverage with a likelihood of having identified 95.3% of the total genes present, based on a total of 255 BUSCO markers (Table S4.2).

Among the top ten species in the *Philodina* transcriptome BLAST results were seven bdelloid species: *A. steineri, Rotaria* sp. Silwood2, *R. sordida* , *A. vaga*, *D. carnosus*, *P. citrina,* and *M. quadricornifera* (Fig S4.1). KEGG analysis showed approximately 22% of proteins having a significant sequence similarity with either: mollusks, arthropods, vertebrates, brachiopods, or cnidarians. Approximately 7% of the sequences matched “others” taxon while, and 71% of the protein sequences were considered “undefined” (Fig S4.2).

Transcriptome comparison

Philodina transcriptome nucleotide sequences were compared to 13 bdelloid genomes (Fig. 4.1), some of which were identified as being red pigmented, or clear and originating from either desiccating or permanently hydrated habitats. For *P. acuticornis* and *P. roseola* only transcriptomes were available. It should be noted that these may include redundant sequences, however the sequence with the highest similarity was for *M. quadricornifera*. The least similar sequence was *Didymodactylos carnosus* (<5%; Fig. 4.1a), overall >15% of the sequences in

Philodina transcriptome were found in 13 other bdelloid genomes (Fig. 4.1a). Nine of the bdelloid species were selected to further validate the transcriptome using amino acid sequences (Fig. 4.1b). The amino acid sequences that showed the highest similarity to our *Philodina*, were *P. acuticornis* and *P. roseola*, followed by *R. sordida*, *R.* Silwood sp1, *A. ricciae*, and *A. vaga* (Fig. 4.1b). Genes and proteins identified in at least one bdelloids species that are associated with repair were: RAD23, RAD26, RAD50, RAD51, excision repair homologs, late embryogenesis abundant proteins, superoxide dismutase, glutathione transferase, heat shock protein, carotenoids, and melanocytes found in at least one other bdelloid species. As well as

housekeeping genes such as cytochrome, or those associated with ATP production and transcript were also identified (Table S4.3)

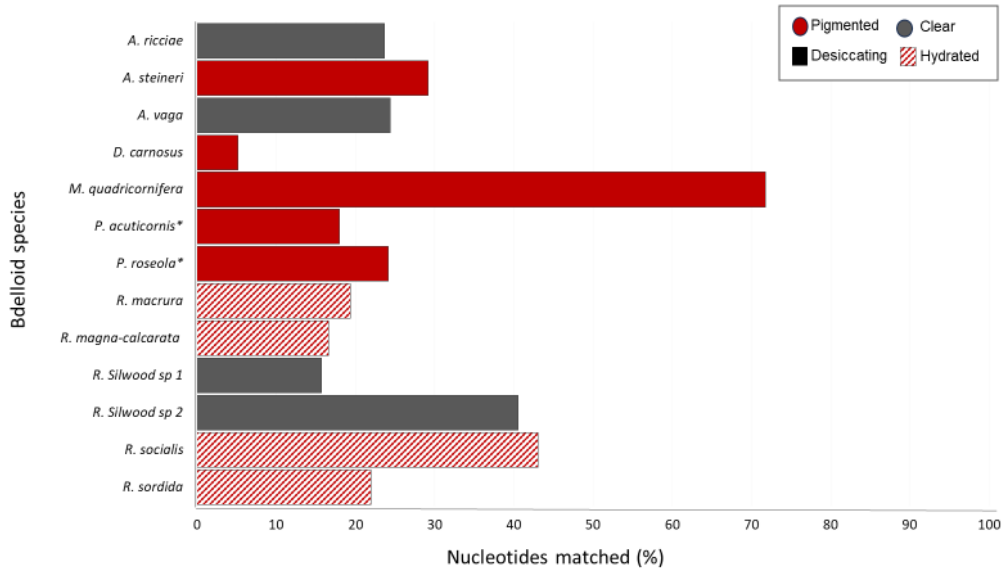

a)

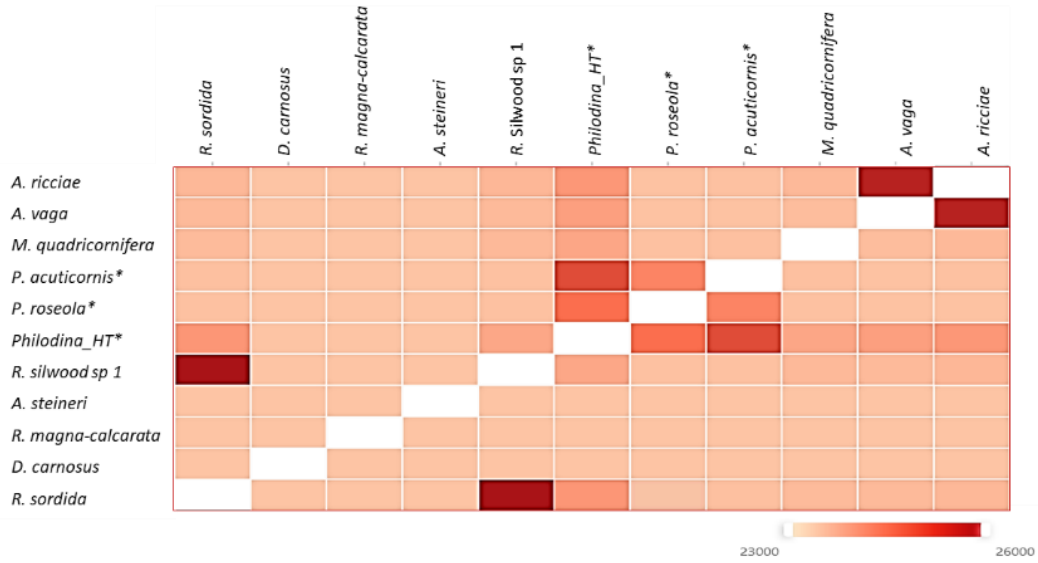

b)

Figure 4.1. *Philodina* sp. transcriptome gene validation. Genes assembled in *Philodina* transcriptome were compared to a) nucleotide sequences from 13 other bdelloids species; and b) amino acid sequences were compared to nine bdelloid genome- or transcriptome-predicted proteins. *Indicate analysis done using transcriptomes instead of genome, which may include redundant gene sequences.

Comparison of transcripts from Highly and Non-Pigmented *Philodina*

Transcripts that responded to UVB exposure were identified in each of the four UVB treatments and compared to one another (Fig. 4.2). In HP bdelloids 88% of all transcripts were shared across all HP treatment groups with <5% transcripts being uniquely identified in a single UVB treatment (Fig. 4.2a). Nearly 80% of all transcripts were shared in NP samples, and ~ 1.5% unique transcripts in either control or mid UVB treatments; the highest number of unique transcripts, 5.54%, were identified in the low UVB treatment (Fig. 4.2b). Over 25% of transcripts were shared between pigmented groups for HP control and HP mid UV (Fig. 4.3a and 4.3c), while the HP low UV treatment shared over 30% of transcripts (Fig. 4.3b).

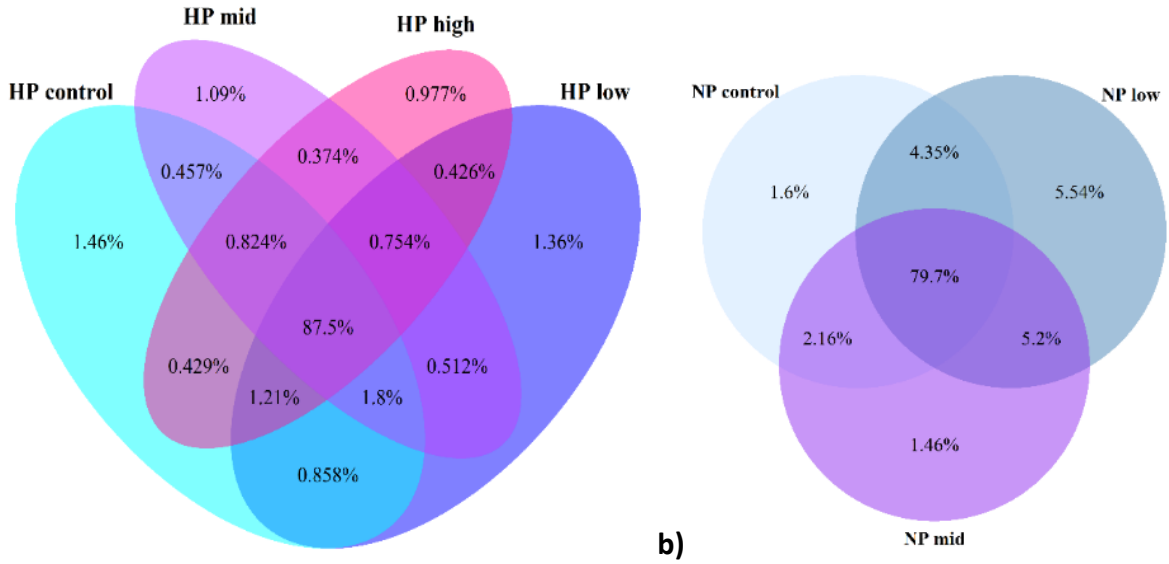

Figure 4.2. Total RNA transcripts of highly pigmented *Philodina* after exposure to UVB radiation for 2 hr (control = 0, low = 1.3, mid = 3.7, high = 5.0 w/cm^2). Transcripts that are shared by two or more UVR treatments are shown in the overlapping regions.

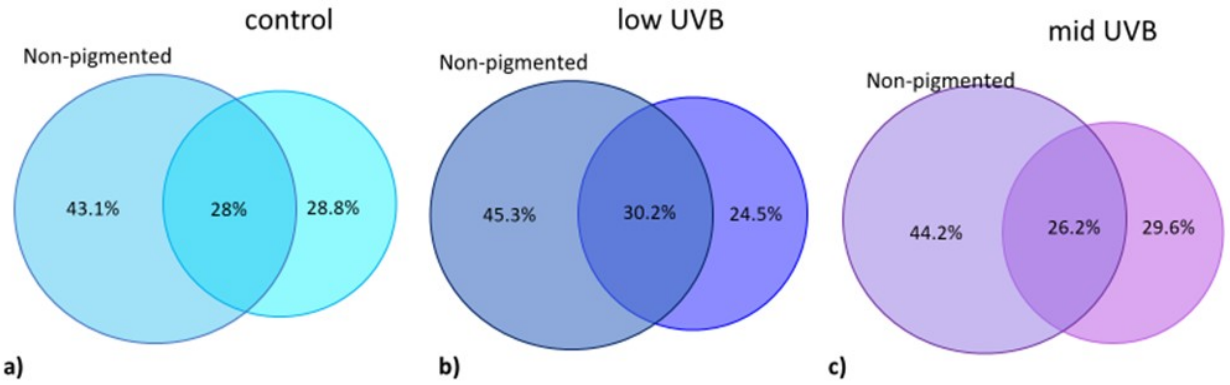

Figure 4.3. Shared transcripts between highly pigmented (HP), and non-pigmented (NP) *Philodina* transcripts. UVB intensities were a) control =0 W/m ^{2} b) low= 1.30 W/m^2 and c) mid= 3.7 W/m^2.

Differential gene expression in pigment groups

In comparing the UVR treatments to their respected control a total of 31,844 genes responded to UVB exposure and were significantly differentially expressed genes (DEGs) (adjusted p-vale ≤ 0.05, Fig. S4.3). Significantly DEGs ~32% of genes were shared in both pigment groups for control, low and mid UVB treatments, the greater majority (>67%) responded in only NP bdelloids (Fig. 4.4). In HP bdelloids, 51 genes were significant DEGs, 35 of those genes were over-expressed, and 16 were under-expressed. When HP bdelloids were exposed to mid UVB radiation, 32 genes were over-expressed and 12 were under-expressed (Table 4.1). In the NP treatments, 1,820 transcripts responded to UVB exposure. Low UVB exposure resulted in 422 DEGs being over-expressed and 202 genes being under-expressed (Fig. 4.5).

Table 4.1. Responsive transcripts of highly pigmented (HP) and non-pigmented (NP) *Philodina.* Bdelloids were exposed to UVB intensities low (1.30 W/m^2), mid (3.7 W/m^2), or high (3.7 W/m^2) for 2 hours. Differential gene expression (DEG) was determined by comparing expression from each UVB treatment to the control, log_2 fold change > +2 (over expressed), <-2 (under expressed), and adjusted p-value <0.05).

Pigment	UVB	All genes	DEG	significant DEG	Over	Under
HP	control	130,064	-	-	-	-
	low	129,903	2,171	7	4	3
	mid	128,379	2,195	44	32	12
	high	127,254	2,151	9	3	6
NP	control	162,774	-	-	-	-
	low	175,724	6,729	1,031	815	216
	mid	164,106	6,730	790	498	292

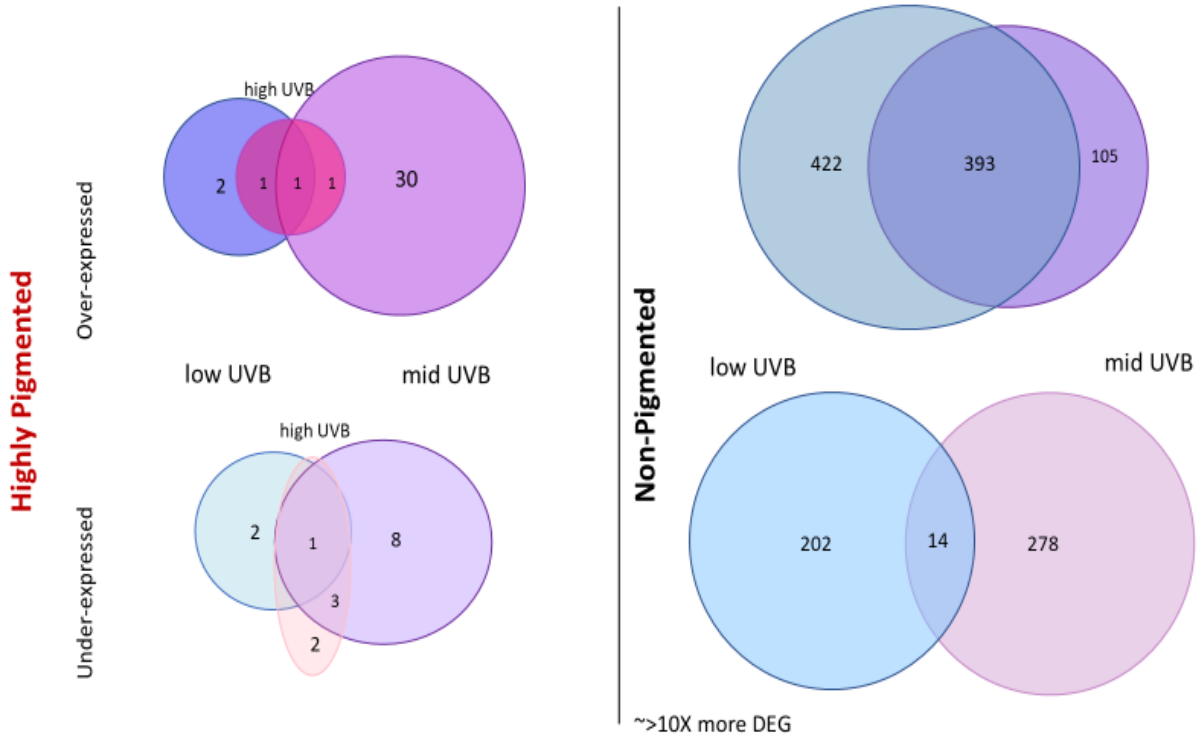

Figure 4.4. Venn diagrams of RNA transcripts from highly pigmented *Philodina* exposed to ultraviolet radiation (UVR) intensities (control= 0; low= 1.30; mid= 3.7; or high = 5.0 ± 0.05 W/m^2 UVR.) intensities for 2 hr. Genes that were significantly over-expressed (log_2 > 2) or under-express (log_2 < -2) when compared to the control for both highly and non-pigmented treatments.

The expression patterns of the 1,874 genes, which were significantly differentially expressed when in either HP or NP, revealed that over 10 times as many genes responded to

UV exposure in NP bdelloids. Of these only 5% (98/1874) of the genes were annotated back to a known function, see Table 4.1. Of these fully annotated genes only 3 were identified in the HP pigment, the remaining 48 genes had no known, predicted, nor hypothesized function (Table S4.2). In the NP treatment, 45 of the over-expressed genes and 50 of those under-expressed were identified. Of the 98,905 genes that were verified using other bdelloid genomes 79.7% where unnamed, 12% where hypothetical proteins, 0.3% belonged to unknown or uncharacterized functions, and 5.7% of genes have not been identified, annotated, or furthered studied in other species. Of the 2.3% of genes that were identified 2.0% are predicted genes (Table S4.3).

Table 4.2. Significant differentially expressed genes in response to UVB exposure. RNA transcripts from highly (HP) and non-pigmented (NP) *Philodina* exposed to ultraviolet radiation (UVR) intensities low (L), mid (M), or high (1.3, 3.7, 5.0 ± 5 W/m^2) for 2 hr. Transcripts were considered over-expressed if $\log_2 > 2$ or under-express if $\log_2 < -2$, when compared. Genes identified in other species as responsive to UVR exposure are shown in bold. *Shows genes which were verified using their corresponding genomes. GO (GO Term) identifier; UVB=pigment and UVB treatments.

Gene	Description	GO/KO	$\log_2$	UVB
TRINITY_DN512178_c0_g1	ATP synthase F0 subunit 6	GO:0015986	-2.2	HPM
TRINITY_DN6412_c0_g4	HSP70like protein	GO:0006457	4.3	HPM
TRINITY_DN191564_c1_g1	Vtype ATP synthase subunit B	GO:0003676	22.3	HPM
TRINITY_DN77728_c0_g1	protein transport protein SEC31like		6.6, 5.0	NP: L, M
TRINITY_DN266388_c0_g1	ATP dependent DNA helicase		3.8, 4.4	NP: L, M
TRINITY_DN218010_c0_g1	acid resistance repetitive basic protein Asr partial	GO:0016491	3.4, 3.5	NP: L, M
TRINITY_DN588095_c0_g1	aspartate aminotransferase		3.4, 2.7	NP: L, M
TRINITY_DN217091_c0_g1	GH3 auxinresponsive promoter family protein partial		3.3, 3.2	NP: L, M
TRINITY_DN495672_c0_g1	FADdependent oxidoreductase partial		3.2, 3.1	NP: L, M
TRINITY_DN340751_c0_g1	oxalurate catabolism protein HpxZ		3.2, 2.7	NP: L, M
TRINITY_DN80348_c0_g1	short chain dehydrogenase/reductase partial		3.0, 3.0	NP: L, M
TRINITY_DN207676_c1_g1	ATP dependent DNA helicase		2.7, 2.8	NP: L, M
TRINITY_DN10209_c1_g1	mucin2like		2.7, 2.5	NP: L, M
TRINITY_DN560059_c0_g1	DUF3492 domain containing protein	GO:0016740	2.6, 3.1	NPL
TRINITY_DN29261_c0_g1	plasma membrane calcium ATPase partial	GO:0070588	2.5, 2.6	NP: L, M
TRINITY_DN7359_c3_g1	plasma membrane calciumdependent ATPase	GO:0006431	2.4, 2.4	NP: L, M
TRINITY_DN22473_c0_g1	**acylCoA dehydrogenase partial**		2.2, 2.1	NPL
TRINITY_DN131049_c0_g1	PREDICTED: high mobility group protein DSP1like	GO:0003677	7.2	NPL
TRINITY_DN398931_c0_g1	**cytochrome b**	**GO:0022904**	**6.7**	**NPL**

TRINITY_DN23210_c0_g1	ADP ribosylation factor 1like	GO:0006886	4.6	NPL
TRINITY_DN36055_c0_g1	**Hsp70 family protein**	**GO:0006457**	**3.2**	**NPL**
TRINITY_DN131429_c1_g1	BiP protein partial	GO:0006457	2.7	NPL
TRINITY_DN154405_c0_g1	**82 kD heat shock protein 1 partial**	**GO:0006457**	**2.4**	**NPL**
TRINITY_DN15112_c1_g1	transmembrane protease serine 9like	GO:0006508	2.4	NPL
TRINITY_DN16418_c0_g1	**NAD(P)/FAD dependent oxidoreductase**	**GO:0006725**	**2.3**	**NPL**
TRINITY_DN5159_c2_g1	DUG3; glutamine amido transferase	KO:K18802	2.3	NPL
TRINITY_DN22342_c1_g1	**transglutaminase domain containing protein**		**2.2, 2.2**	NP: L, M
TRINITY_DN355488_c0_g1	MRE11; double-strand break repair protein MRE11	KO:K10865	2.2	NPL
TRINITY_DN36841_c0_g1	WFDC2; WAP four-disulfide core domain protein 2	KO:K23636	2.2	NPL
TRINITY_DN14440_c0_g1	AQP9; aquaporin 9	KO:K09877	2.2	NPL
TRINITY_DN21103_c1_g1	PMA1, PMA2; H+-transporting ATPase	KO:K01535	2.1	NPL
TRINITY_DN489617_c0_g1	ISA, treX; isoamylase	KO:K01214	2.1	NPL
TRINITY_DN12824_c0_g1	ACSL, fadD; long-chain acyl-CoA synthetase	KO:K01897	2.1	NPM
TRINITY_DN16433_c0_g1	SPG20; spartin	KO:K19366	2.1	NPL
TRINITY_DN146183_c0_g1	Elongation factor 1alpha 2 partial	GO:0097159	2.1	NPL
TRINITY_DN24282_c0_g1	ISA, treX; isoamylase	KO:K01214	2.1	NPL
TRINITY_DN37828_c0_g1	translation initiation factor eIF4A partial	GO:0006413	2.0	NPL
TRINITY_DN36978_c0_g1	katE, CAT, catB, srpA; catalase	KO:K03781	2.0	NPL
TRINITY_DN537508_c0_g1	katE, CAT, catB, srpA; catalase	KO:K03781	2.0	NPL
TRINITY_DN16324_c0_g1	FADdependent monooxygenase	GO:0006725	2.0	NPL
TRINITY_DN15907_c0_g1	PMA1, PMA2; H+-transporting ATPase	KO:K01535	2.0	NPL
TRINITY_DN4334_c1_g1	predicted protein	GO:0006457	3.5	NPL
TRINITY_DN2114_c0_g1	CTSL; cathepsin L	KO:K01365	2.2	NPM
TRINITY_DN333233_c0_g1	**aldehyde dehydrogenase (NAD(P)(+)) ald5**		**2.2**	**NPM**
TRINITY_DN7972_c1_g1	yahK; alcohol dehydrogenase (NADP+)	KO:K13979	2.2	NPL
TRINITY_DN332511_c0_g1	ISA, treX; isoamylase	KO:K01214	2.2	NPM
TRINITY_DN412110_c0_g1	ubiquitin/ribosomal S27 fusion protein partial	GO:0006412	2.2	NPL
TRINITY_DN21184_c0_g1	ATP2B; P-type Ca2+ transporter type 2B	KO:K05850	2.2	NPM
TRINITY_DN414856_c0_g1	ISA, treX; isoamylase	KO:K01214	2.2	NPM
TRINITY_DN94721_c0_g1	TBXAS1, CYP5A; thromboxane-A synthase	KO:K01832	2.2	NPM
TRINITY_DN103999_c0_g1	GCLC; glutamate--cysteine ligase catalytic subunit	KO:K11204	2.1	NPM
TRINITY_DN104748_c0_g1	KCNA1, KV1.1; potassium voltage-gated channel Shaker-related subfamily A member 1	KO:K04874	2.1	NPM
TRINITY_DN35540_c0_g1	ACSL, fadD; long-chain acyl-CoA synthetase	KO:K01897	2.1	NPM
TRINITY_DN7333_c3_g1	malQ; 4-alpha-glucanotransferase	KO:K00705	2.1	NPL
TRINITY_DN49072_c0_g1	VCP, CDC48; transitional endoplasmic reticulum ATPase	KO:K13525	2.1	NPM
TRINITY_DN466505_c0_g1	malQ; 4-alpha-glucanotransferase	KO:K00705	2.1	NPM
TRINITY_DN483550_c0_g1	malQ; 4-alpha-glucanotransferase	KO:K00705	2.1	NPM
TRINITY_DN9881_c2_g1	DHCR7; 7-dehydrocholesterol reductase	KO:K00213	2.1	NPM
TRINITY_DN464968_c295_g1	SLC35E3; solute carrier family 35, member E3	KO:K15285	2.0	NPM
TRINITY_DN276188_c0_g1	malQ; 4-alpha-glucanotransferase	KO:K00705	2.0	NPM
TRINITY_DN52856_c0_g1	katE, CAT, catB, srpA; catalase	KO:K03781	2.0	NPM
TRINITY_DN27017_c0_g1	calcium binding protein	GO:0005509	2.0	NPM

TRINITY_DN115780_c0_g1	BCAP31, BAP31; B-cell receptor-associated protein 31	KO:K14009	2.0	NPM
TRINITY_DN17523_c1_g1	tRNA (adenosine(37)N6)dimethylallyltransferase MiaA	GO:0016740	-2.0	NPM
TRINITY_DN15742_c0_g1	DUF4394 domaincontaining protein	GO:0003677	-2.0	NPM
TRINITY_DN19136_c0_g2	transaconitate 2methyltransferase	GO:0032259	-2.1, -2.1	NP: L, M
TRINITY_DN6084_c0_g1	cytochrome c oxidase subunit 1 partial	GO:0006119	-2.1	NPM
TRINITY_DN12174_c0_g1	K24129; glutaredoxin-dependent peroxiredoxin	KO:K24129	-2.2	NPM
TRINITY_DN506_c8_g1	PREDICTED: polyubiquitinC	GO:0008152	-2.2	NPM
TRINITY_DN44938_c7_g1	**cytochrome c oxidase subunit 1 partial**	**GO:0006119**	**-2.2**	**NPM**
TRINITY_DN628_c1_g1	mortalinlike protein/H2A; histone H2A	GO:0006457/KO:K11251	-2.2	NPM
TRINITY_DN465446_c1_g1	**cytochrome c oxidase subunit 3**	**GO:0019646**	**-2.2**	**NPM**
TRINITY_DN1756_c0_g1	CKAP5; cytoskeleton-associated protein 5	KO:K16803	-2.2	NPM
TRINITY_DN112095_c0_g1	MESO1, ERG25; methylsterol monooxygenase	KO:K07750	-2.3	NPL
TRINITY_DN1422_c0_g1	SQSTM1; sequestosome 1	KO:K14381	-2.3	NPM
TRINITY_DN7401_c1_g1	TTLL10; tubulin--tyrosine ligase like protein 10	KO:K23628	-2.3	NPM
TRINITY_DN2611_c15_g1	**cytochrome c oxidase subunit 2**	**GO:0006119**	**-2.3**	**NPM**
TRINITY_DN34686_c0_g1	CSG1, SUR1, CSH1; inositol phosphorylceramide mannosyltransferase catalytic subunit	KO:K22721	-2.3	NPM
TRINITY_DN70901_c0_g1	ALDH18A1, P5CS; delta-1-pyrroline-5-carboxylate synthetase	KO:K12657	-2.3	NPL
TRINITY_DN1552_c0_g1	CCNA; cyclin-A	KO:K06627	-2.3	NPM
TRINITY_DN25431_c0_g1	ANKRD17, MASK; ankyrin repeat domain-containing protein 17	KO:K16726	-2.3	NPL
TRINITY_DN55069_c0_g1	CA; carbonic anhydrase	KO:K01672	-2.4	NPL
TRINITY_DN29685_c2_g1	arcA; arginine deiminase	KO:K01478	-2.4	NPL
TRINITY_DN106239_c0_g1	ABCG2, CD338; ATP-binding cassette, subfamily G (WHITE), member 2	KO:K05681	-2.4	NPM
TRINITY_DN66246_c0_g1	PIR; quercetin 2,3-dioxygenase	KO:K06911	-2.4	NPM
TRINITY_DN99481_c0_g2	MINDY3_4; ubiquitin carboxyl-terminal hydrolase MINDY-3/4	KO:K22647	-2.4	NPM
TRINITY_DN43502_c0_g1	DUF4118 domaincontaining protein partial		-2.4	NPM
TRINITY_DN15288_c0_g1	SLC42A, RHAG, RHBG, RHCG, CD241; ammonium transporter Rh	KO:K06580	-2.4	NPL
TRINITY_DN549666_c0_g1	COX1; cytochrome c oxidase subunit 1	GO:0006119/KO:K02256	-2.4	NPM
TRINITY_DN549666_c0_g1	**cbb3type cytochrome c oxidase subunit I**	**GO:0006119**	**-2.4**	**NPM**
TRINITY_DN331397_c3_g1	**cytochrome oxidase subunit 1**	**GO:0006119**	**-2.4**	**NPM**
TRINITY_DN5348_c2_g1	phhA, PAH; phenylalanine-4-hydroxylase	KO:K00500	-2.4	NPL
TRINITY_DN14974_c0_g1	PDCD6; programmed cell death protein 6	KO:K23902	-2.4	NPM
TRINITY_DN23058_c0_g1	ALDH18A1, P5CS; delta-1-pyrroline-5-carboxylate synthetase	KO:K12657	-2.4	NPL
TRINITY_DN11844_c2_g1	ABCG2, CD338; ATP-binding cassette, subfamily G (WHITE), member 2	GO:0055085/KO:K05681	-2.4	NPM
TRINITY_DN254_c0_g2	CCNB2; G2/mitotic-specific cyclin-B2	KO:K21770	-2.4	NPM
TRINITY_DN27837_c0_g1	EDD1, UBR5; E3 ubiquitin-protein ligase EDD1	KO:K10593	-2.4	NPM
TRINITY_DN79151_c0_g2	SLC39A13, ZIP13; solute carrier family 39 (zinc transporter), member 13	KO:K14719	-2.4	NPM
TRINITY_DN68528_c0_g1	ALDH18A1, P5CS; delta-1-pyrroline-5-carboxylate synthetase	KO:K12657	-2.4	NPL
TRINITY_DN254_c3_g1	DNAH; dynein axonemal heavy chain	GO:0007018/KO:K10408	-2.4	NPM

TRINITY_DN9879_c0_g2	**NADH dehydrogenase subunit 3**	**GO:0019646**	**-2.4**	**NPM**
TRINITY_DN156610_c1_g1	**cytochrome c oxidase subunit 1 partial**	**GO:0016020**	**-2.5**	**NPM**
TRINITY_DN21529_c0_g1	ACSL, fadD; long-chain acyl-CoA synthetase	KO:K01897	-2.5	NPL
TRINITY_DN445_c0_g1	TRIM2_3; tripartite motif-containing protein 2/3	KO:K11997	-2.5	NPM
TRINITY_DN5734_c0_g1	PIR; quercetin 2,3-dioxygenase	KO:K06911	-2.5	NPM
TRINITY_DN29433_c0_g1	**cytochrome c oxidase subunit 1 partial**	GO:0006119	-2.5	NPM
TRINITY_DN29433_c0_g1	COX1; cytochrome c oxidase subunit 1	GO:0006119/KO:K02256	-2.5	NPM
TRINITY_DN5812_c0_g3	LOW QUALITY PROTEIN: polyubiquitinC		-2.5	NPM
TRINITY_DN121441_c0_g1	abfA; alpha-L-arabinofuranosidase	KO:K01209	-2.5	NPL
TRINITY_DN144546_c1_g1	**Cytochrome B**	GO:0022904	-2.5	NPM
TRINITY_DN2834_c0_g1	TRAF1; TNF receptor-associated factor 1	KO:K03172	-2.6	NPM
TRINITY_DN83439_c0_g1	CYP4V; docosahexaenoic acid omega-hydroxylase	KO:K07427	-2.6	NPL
TRINITY_DN24967_c3_g1	COL4A; collagen type IV alpha	KO:K06237	-2.6	NPM
TRINITY_DN687_c0_g1	PIR; quercetin 2,3-dioxygenase	KO:K06911	-2.6	NPM
TRINITY_DN938_c0_g1	ELF2C, AGO; eukaryotic translation initiation factor 2C	KO:K11593	-2.6	NPM
TRINITY_DN37478_c0_g1	TLN; talin	KO:K06271	-2.6	NPL
TRINITY_DN59423_c1_g1	K00666; fatty-acyl-CoA synthase	KO:K00666	-2.6	NPL
TRINITY_DN2890_c0_g1	FBXO7; F-box protein 7	KO:K10293	-2.6	NPM
TRINITY_DN23400_c0_g1	SUN1_2; SUN domain-containing protein 1/2	KO:K19347	-2.6	NPM
TRINITY_DN40275_c0_g1	ACSL, fadD; long-chain acyl-CoA synthetase	KO:K01897	-2.7	NPL
TRINITY_DN1019_c1_g1	gsp; glutathionylspermidine amidase/synthetase	KO:K01460	-2.7	NPM
TRINITY_DN6412_c1_g1	HSPA1s; heat shock 70kDa protein 1/2/6/8	KO:K03283	-2.7	NPM
TRINITY_DN95366_c0_g1	MAG: fasciclin domaincontaining protein		-2.7	NPL
TRINITY_DN43252_c0_g1	alpha/beta hydrolase	GO:0016787	-2.7	NPL
TRINITY_DN40299_c0_g1	fasciclin domaincontaining protein		-2.7	NPL
TRINITY_DN778_c3_g1	NFYC, HAP5; nuclear transcription factor Y, gamma	KO:K08066	-2.7	NPM
TRINITY_DN10345_c0_g1	GON4L; GON-4-like protein	KO:K23804	-2.7	NPM
TRINITY_DN90180_c3_g1	APTX; aprataxin	KO:K10863	-2.7	NPM
TRINITY_DN4902_c0_g1	MASTL, GW; serine/threonine-protein kinase greatwall	KO:K16309	-2.8	NPM
TRINITY_DN43441_c0_g1	DOT1L, DOT1; -lysine79 N-trimethyltransferase	KO:K11427	-2.8	NPL
TRINITY_DN58337_c0_g1	DENND2; DENN domain-containing protein 2	KO:K20161	-2.8	NPM
TRINITY_DN2611_c0_g1	**cytochrome c oxidase subunit 2**	GO:0022900/KO:K02261	-2.8	NPM
TRINITY_DN180513_c0_g2	FYVE RhoGEF and PH domaincontaining protein 2like isoform X1	GO:0000455	-2.8	NPM
TRINITY_DN236_c0_g2	EIF4E; translation initiation factor 4E	KO:K03259	-2.8	NPM
TRINITY_DN28548_c0_g1	ELSPBP1; epididymal sperm-binding protein 1	KO:K24475	-2.8	NPM
TRINITY_DN53168_c0_g1	ABCA3; ATP-binding cassette, subfamily A (ABC1), member 3	KO:K05643	-2.9	NPM
TRINITY_DN1795_c0_g1	arcA; arginine deiminase	KO:K01478	-2.9	NPM
TRINITY_DN4446_c7_g1	EFTUD2; 116 kDa U5 small nuclear ribonucleoprotein component	KO:K12852	-2.9	NPM
TRINITY_DN21265_c0_g2	PARD6; partitioning defective protein 6	KO:K06093	-2.9	NPM
TRINITY_DN59606_c0_g1	K14165; atypical dual specificity phosphatase	KO:K14165	-3.0	NPM

TRINITY_DN143658_c0_g1	SLC10A7, P7; solute carrier family 10 (sodium/bile acid cotransporter), member 7	KO:K14347	-3.0	NPL
TRINITY_DN2611_c0_g2	**cytochrome c oxidase subunit 2**	**GO:0022900**	**-3.0**	**NPM**
TRINITY_DN1047_c1_g1	CCNB2; G2/mitotic-specific cyclin-B2	KO:K21770	-3.0	NPM
TRINITY_DN4994_c1_g2	ERGIC3, ERV46; endoplasmic reticulum-Golgi intermediate compartment protein 3	KO:K20367	-3.0	NPM
TRINITY_DN19967_c0_g1	CENPE, KIF10; centromeric protein E	KO:K11498	-3.0	NPM
TRINITY_DN40740_c0_g1	ATP1A; sodium/potassium-transporting ATPase subunit alpha	KO:K01539	-3.0	NPM
TRINITY_DN5305_c5_g1	PDS5; sister chromatid cohesion protein PDS5	KO:K11267	-3.0	NPM
TRINITY_DN50354_c0_g1	ABCG2, CD338; ATP-binding cassette, subfamily G (WHITE), member 2	KO:K05681	-3.1	NPL
TRINITY_DN1987_c0_g1	BCDO2; beta,beta-carotene 9',10'-dioxygenase	KO:K10252	-3.1	NPM
TRINITY_DN962_c0_g1	RASEF, RAB45; Ras and EF-hand domain-containing protein	KO:K17199	-3.1	NPM
TRINITY_DN15862_c0_g2	MAN1A_C, MNS1_2; mannosyl-oligosaccharide alpha-1,2-mannosidase	KO:K01230	-3.1	NPM
TRINITY_DN11013_c0_g1	E1.3.3.6, ACOX1, ACOX3; acyl-CoA oxidase	KO:K00232	-3.2	NPM
TRINITY_DN468845_c0_g1	**cytochrome oxidase subunit 1**	**GO:0006119**	**-3.2**	**NPM**
TRINITY_DN32360_c0_g1	GST, gst; glutathione S-transferase	KO:K00799	-3.2	NPM
TRINITY_DN372509_c0_g1	sat, met3; sulfate adenylyltransferase	KO:K00958	-3.2	NPM
TRINITY_DN76348_c0_g1	DNAH; dynein axonemal heavy chain	KO:K10408	-3.2	NPM
TRINITY_DN468995_c0_g1	DUF2088 domaincontaining protein		-3.3	NPM
TRINITY_DN443888_c0_g1	**cytochrome c oxidase subunit 2**	GO:0022900	-3.3	NPM
TRINITY_DN4019_c2_g1	K03791; putative chitinase	KO:K03791	-3.3	NPL
TRINITY_DN63637_c0_g1	HAMP domaincontaining protein		-3.3	NPL
TRINITY_DN1638_c0_g1	PLG; plasminogen	KO:K01315	-3.3	NPM
TRINITY_DN328884_c0_g1	SLC24A6, NCKX6; solute carrier family 24 (sodium/potassium/calcium exchanger), member 6	KO:K13754	-3.3	NPM
TRINITY_DN4004_c0_g1	kup; KUP system potassium uptake protein	KO:K03549	-3.3	NPM
TRINITY_DN22247_c0_g1	OLFR; olfactory receptor	KO:K04257	-3.3	NPM
TRINITY_DN544586_c0_g1	Amyloidlike protein 2	GO:0010466	-3.4	NPM
TRINITY_DN131449_c0_g1	HMCN; hemicentin	KO:K17341	-3.4	NPM
TRINITY_DN553982_c0_g1	cbb3type cytochrome c oxidase subunit I	GO:0006119	-3.5	NPM
TRINITY_DN62073_c0_g1	alpha/beta hydrolase	GO:0016787	-3.5	NPL
TRINITY_DN61487_c3_g1	MAG: hypothetical protein LQ350_002788		-3.5	NPM
TRINITY_DN3769_c0_g1	FUT1_2; galactoside 2-L-fucosyltransferase 1/2	KO:K00718	-3.5	NPM
TRINITY_DN69961_c0_g1	magnetosomeassociated protein MamJlike	GO:0006468	-3.5	NPM
TRINITY_DN48227_c0_g1	ABCG2, CD338; ATP-binding cassette, subfamily G (WHITE), member 2	KO:K05681	-3.5	NPL
TRINITY_DN143858_c0_g1	CSLA; beta-mannan synthase	KO:K13680	-3.5	NPL
TRINITY_DN190046_c2_g1	Amyloidlike protein 2	GO:0010466	-3.6	NPM
TRINITY_DN400493_c0_g1	UDPNacetylglucosamine 1carboxyvinyl transferase	GO:0006260	-3.6	NPM
TRINITY_DN69941_c0_g2	VCL; vinculin	KO:K05700	-3.6	NPL
TRINITY_DN4124_c0_g1	DNAJC9; DnaJ homolog subfamily C member 9	KO:K09529	-3.6	NPM
TRINITY_DN72546_c0_g1	SSPO; SCO-spondin	KO:K24434	-3.6	NPM

TRINITY_DN195414_c0_g1	ABCG2, CD338; ATP-binding cassette, subfamily G (WHITE), member 2	KO:K05681	-3.7	NPL
TRINITY_DN61938_c0_g1	ABCG2, CD338; ATP-binding cassette, subfamily G (WHITE), member 2	KO:K05681	-3.7	NPL
TRINITY_DN334342_c0_g1	magnetosomeassociated protein MamJlike		-3.7	NPM
TRINITY_DN381598_c0_g1	E4.3.1.19, ilvA, tdcB; threonine dehydratase	KO:K01754	-3.7	NPM
TRINITY_DN47296_c0_g1	EEF1A; elongation factor 1-alpha	KO:K03231	-3.7	NPM
TRINITY_DN263846_c1_g1	**cytochrome c oxidase subunit I partial**	**GO:0006119**	**-3.7**	**NPM**
TRINITY_DN107557_c3_g1	SMAD3; mothers against decapentaplegic homolog 3	KO:K23605	-3.8	NPM
TRINITY_DN369877_c0_g1	**cytochrome c oxidase subunit 2**	**GO:0022900**	**-3.8**	**NPM**
TRINITY_DN6084_c0_g2	**cytochrome c oxidase subunit I**	**GO:0006119**	**-3.8**	**NPM**
TRINITY_DN175234_c0_g1	**cytochrome c oxidase subunit 2**	**GO:0022900**	**-3.9**	**NPM**
TRINITY_DN22348_c0_g1	FMRFaR; FMRFamide receptor	KO:K26201	-4.0	NPM
TRINITY_DN264985_c0_g1	keratinassociated protein 54like	GO:0016020	-4.1	NPM
TRINITY_DN44938_c1_g1	COX1; cytochrome c oxidase subunit 1	KO:K02256	-4.4	NPM
TRINITY_DN332442_c0_g1	**Cytochrome B**	**GO:0022904**	**-4.4**	**NPM**
TRINITY_DN467334_c1_g1	COX1; cytochrome c oxidase subunit 1	GO:0006119/KO:K02256	-4.5	NPM
TRINITY_DN467334_c1_g1	**cytochrome c oxidase subunit I partial**	**GO:0006119**	**-4.5**	**NPM**
TRINITY_DN466688_c2_g1	COX1; cytochrome c oxidase subunit 1	GO:0006119/KO:K02256	-4.5	NPM
TRINITY_DN466688_c2_g1	**cytochrome c oxidase subunit 1 partial**	**GO:0006119**	**-4.5**	**NPM**
TRINITY_DN6840_c0_g1	CYB5; cytochrome b5	KO:K23490	-4.7	NPM
TRINITY_DN5981_c0_g1	**cytochrome oxidase subunit 1**	**GO:0006119**	**-4.7**	**NPM**
TRINITY_DN96102_c0_g1	CALM; calmodulin	KO:K02183	-4.8	NPL
TRINITY_DN33_c0_g2	MVP; major vault protein	KO:K17266	-4.8	NPM
TRINITY_DN354704_c0_g1	**Cytochrome B**	**GO:0022904**	**-4.9**	**NPM**
TRINITY_DN120154_c0_g1	SMT1, ERG6; sterol 24-C-methyltransferase	KO:K00559	-5.5	NPL
TRINITY_DN133306_c0_g1	FDFT1; farnesyl-diphosphate farnesyltransferase	KO:K00801	-5.6	NPL
TRINITY_DN82234_c0_g1	cell wallassociated hydrolase domain protein	GO:0016787	-6.1	NPM
TRINITY_DN9782_c0_g1	SMT1, ERG6; sterol 24-C-methyltransferase	KO:K00559	-6.5	NPL
TRINITY_DN555008_c1_g1	**cytochrome c oxidase subunit 1 partial**	**GO:0006119**	**-7.1**	**NPM**

Numerous genes that did not have a known function did have a GO term association their predicted association with a GO Term. Go terms associated with guanosine triphosphate (GTP) (GO:0005525, 0003924) had the highest match with significant DEGs in the NP low UVB treatment. Other GO that governs mitochondrial inner membrane process, cytochrome-c oxidase activity, proton transmembrane transport, oxidative phosphorylation, among other has associations with genes that were both over and under expressed in the NP low UVB treatment

(Table 4.3). The response of genes associated with the DEGs for UV damage (GO:0009411), direct DNA damage (GO: 0006281), antioxidants (GO: 0016209), DNA repair (KO:002209), exonuclease activity (GO:0004527), non-homologous DNA end joining (KO:003450) was visualized as heatmaps for both HP and NP genes (Fig. S4.4). The subset of genes whose function was annotated by GO terms or KEGG terms was 12% (13,134) of total number of DEGs (109,868). The significant DEG identified via GO or KEGG were associated with genes or pathways to repair damage, while antioxidants and DEGs associated with direct damage repair were the most responsive in NP treatments.

Table 4.3. GoTerms of significantly differentiated genes. RNA transcripts from highly and non-pigmented *Philodina* exposed to UVB for 2 hr. Significant transcripts had an adjusted p-value <0.05, where either over-expressed ($log_2 > 2$) or b) under-express ($log_2 < -2$) when compared to the control for both highly (HP) and non-pigmented (NP) treatments. In grey high light are Genes that were both over and under expressed in response to UVB exposure.

Go term	Description	No. Genes	Expression	UVB	Pigment
GO:0005525	GTP binding	37	over	low	NP
GO:0003924	GTPase activity	34	over	low	NP
GO:0005743	mitochondrial inner membrane	26	over	mid	NP
GO:0004129	cytochrome-c oxidase activity	25	over	mid	NP
GO:1902600	proton transmembrane transport	25	over	mid	NP
GO:0055085	transmembrane transport	24	over	low	NP
GO:0020037	heme binding	23, 20	over	low, mid	NP
GO:0006457	protein folding	22	over	low	NP
GO:0140662	ATP-dependent protein folding chaperone	22	over	low	NP
GO:0140359	ABC-type transporter activity	19	over	low	NP
GO:0006119	oxidative phosphorylation	18	over	mid	NP
GO:0022900	electron transport chain	18	over	mid	NP
GO:0005506	iron ion binding	17	over	low	NP
GO:0005737	cytoplasm	16	over	low	NP
GO:0005788	endoplasmic reticulum lumen	15	over	low	NP
GO:0005634	nucleus	14	over	low	NP
GO:0015031	protein transport	14	over	low	NP
GO:0070469	respirasome	14	over	mid	NP
GO:0008234	cysteine-type peptidase activity	13	over	low	NP
GO:0045277	respiratory chain complex IV	13	over	mid	NP
GO:0098869	cellular oxidant detoxification	13	over	low	NP
GO:0016192	vesicle-mediated transport	12	over	low	NP
GO:0005507	copper ion binding	11	over	mid	NP
GO:0004096	catalase activity	10	over	low	NP
GO:0004497	monooxygenase activity	10	over	low	NP
GO:0005794	Golgi apparatus	10	over	low	NP
GO:0006979	response to oxidative stress	10	over	low	NP
GO:0042744	hydrogen peroxide catabolic process	10	over	low	NP
GO:0003723	RNA binding	9	over	low	NP

GO:0016705	oxidoreductase activity, acting on paired donors, with incorporation or reduction of molecular oxygen	9	over	low	NP
GO:0022904	respiratory electron transport chain	9	over	mid	NP
GO:0005388	P-type calcium transporter activity	7	over	low	NP
GO:0006869	lipid transport	7	over	low	NP
GO:0016829	lyase activity	7	over	low	NP
GO:0070588	calcium ion transmembrane transport	7	over	low	NP
GO:0004133	glycogen debranching enzyme activity	6	over	low	NP
GO:0005980	glycogen catabolic process	6	over	low	NP
GO:0006695	cholesterol biosynthetic process	6	over	low	NP
GO:0008171	O-methyltransferase activity	6	over	low	NP
GO:0016628	oxidoreductase activity, acting on the CH-CH group of donors, NAD or NADP as acceptor	6	over	low	NP
GO:0017000	antibiotic biosynthetic process	6	over	low	NP
GO:0019156	isoamylase activity	6	over	low	NP
GO:0035494	SNARE complex disassembly	6	over	low	NP
GO:0044281	small molecule metabolic process	6	over	low	NP
GO:0017154	semaphorin receptor activity	5	over	mid	NP
GO:0043170	macromolecule metabolic process	5	over	low	NP
GO:0071526	semaphorin-plexin signaling pathway	5	over	mid	NP
GO:0004057	arginyltransferase activity	4	over	low	NP
GO:0004476	mannose-6-phosphate isomerase activity	4	over	low	NP
GO:0009055	electron transfer activity	4	over	mid	NP
GO:0009298	GDP-mannose biosynthetic process	4	over	low	NP
GO:0010181	FMN binding	4	over	low	NP
GO:0016598	protein arginylation	4	over	low	NP
GO:0033179	proton-transporting V-type ATPase, V0 domain	4	over	low	NP
GO:0000506	glycosylphosphatidylinositol-N-acetylglucosaminyltransferase (GPI-GnT) complex	3	over	low	NP
GO:0003958	NADPH-hemoprotein reductase activity	3	over	low	NP
GO:0004134	4-alpha-glucanotransferase activity	3	over	low	NP
GO:0006468	protein phosphorylation	3	over	low	NP
GO:0006672	ceramide metabolic process	3	over	low	NP
GO:0006725	cellular aromatic compound metabolic process	3	over	low	NP
GO:0015721	bile acid and bile salt transport	3	over	low	NP
GO:0017040	N-acylsphingosine amidohydrolase activity	3	over	low	NP
GO:0017176	phosphatidylinositol N-acetylglucosaminyltransferase activity	3	over	low	NP
GO:0031146	SCF-dependent proteasomal ubiquitin-dependent protein catabolic process	3	over	low	NP
GO:0031409	pigment binding	3	over	low	NP
GO:0031966	mitochondrial membrane	3	over	low, mid	NP
GO:0051649	establishment of localization in cell	3	over	low	NP
GO:0070330	aromatase activity	3	over	low	NP
GO:0004364	glutathione transferase activity	2	over	low	NP
GO:0004622	lysophospholipase activity	2	over	low	NP
GO:0005874	microtubule	2	over	low	NP
GO:0019646	aerobic electron transport chain	2	over	mid	NP
GO:0034641	cellular nitrogen compound metabolic process	2	over	low	NP
GO:0045174	glutathione dehydrogenase (ascorbate) activity	2	over	low	NP
GO:0046470	phosphatidylcholine metabolic process	2	over	low	NP
GO:0046483	heterocycle metabolic process	2	over	low	NP
GO:0050610	methylarsonate reductase activity	2	over	low	NP
GO:0070973	protein localization to endoplasmic reticulum exit site	2	over	low	NP
GO:0140640	catalytic activity, acting on a nucleic acid	2	over	low	NP
GO:1901360	organic cyclic compound metabolic process	2	over	low	NP
GO:0004674	protein serine/threonine kinase activity	1	over	low	NP

GO:0005743	mitochondrial inner membrane	26	under	mid	NP
GO:0004129	cytochrome-c oxidase activity	25	under	mid	NP
GO:1902600	proton transmembrane transport	25	under	mid	NP
GO:0020037	heme binding	20	under	mid	NP
GO:0006119	oxidative phosphorylation	18	under	mid	NP
GO:0022900	electron transport chain	18	under	mid	NP
GO:0070469	respirasome	14	under	mid	NP
GO:0045277	respiratory chain complex IV	13	under	mid	NP
GO:0005507	copper ion binding	11	under	mid	NP
GO:0006508	proteolysis	10	under	low	NP
GO:0022904	respiratory electron transport chain	9	under	mid	NP
GO:0005886	plasma membrane	8	under	low	NP
GO:0005506	iron ion binding	7	under	low	NP
GO:0008233	peptidase activity	7	under	low	NP
GO:0005739	mitochondrion	6	under	low	NP
GO:0017154	semaphorin receptor activity	5	under	mid	NP
GO:0071526	semaphorin-plexin signaling pathway	5	under	mid	NP
GO:0004349	glutamate 5-kinase activity	4	under	low	NP
GO:0004350	glutamate-5-semialdehyde dehydrogenase activity	4	under	low	NP
GO:0008610	lipid biosynthetic process	4	under	low	NP
GO:0009055	electron transfer activity	4	under	mid	NP
GO:0055129	L-proline biosynthetic process	4	under	low	NP
GO:0008745	N-acetylmuramoyl-L-alanine amidase activity	3	under	low	NP
GO:0009253	peptidoglycan catabolic process	3	under	low	NP
GO:0015204	urea transmembrane transporter activity	3	under	low	NP
GO:0031966	mitochondrial membrane	3	under	low, mid	NP
GO:0042742	defense response to bacterium	3	under	low	NP
GO:0046872	metal ion binding	3	under	low	NP
GO:0071918	urea transmembrane transport	3	under	low	NP
GO:0071949	FAD binding	3	under	low	NP
GO:0003796	lysozyme activity	2	under	low	NP
GO:0004568	chitinase activity	2	under	low	NP
GO:0006032	chitin catabolic process	2	under	low	NP
GO:0006694	steroid biosynthetic process	2	under	low	NP
GO:0008519	ammonium transmembrane transporter activity	2	under	low	NP
GO:0016899	oxidoreductase activity, acting on the CH-OH group of donors, oxygen as acceptor	2	under	low	NP
GO:0016998	cell wall macromolecule catabolic process	2	under	low	NP
GO:0019646	aerobic electron transport chain	2	under	mid	NP
GO:0019835	cytolysis	2	under	low	NP
GO:0042834	peptidoglycan binding	2	under	low	NP
GO:0045087	innate immune response	2	under	low	NP
GO:0072488	ammonium transmembrane transport	2	under	low	NP
GO:0004175	endopeptidase activity	1	under	low	NP
GO:0004310	farnesyl-diphosphate farnesyltransferase activity	1	under	low	NP
GO:0004452	isopentenyl-diphosphate delta-isomerase activity	1	under	low	NP
GO:0006527	arginine catabolic process	1	under	low	NP
GO:0006552	leucine catabolic process	1	under	high	HP
GO:0015935	small ribosomal subunit	1	under	high	HP
GO:0016874	ligase activity	1	under	high	HP
GO:0016990	arginine deiminase activity	1	under	low	NP
GO:0031083	BLOC-1 complex	1	under	low	NP
GO:0050992	dimethylallyl diphosphate biosynthetic process	1	under	low	NP
GO:0051996	squalene synthase activity	1	under	low	NP

Discussion

In the study, the identification of the transcriptomic changes in *Philodina* when exposed to UVB radiation was undertaken to explore the impact of pigmentation on the stress response genes. The analysis revealed differentially expressed genes, with approximately 33% of these genes being shared between the pigment groups. Notably, more than 50% of these genes specifically respond in non-pigmented bdelloids. More than ten times as many were significant genes showed a significant differential expression in response to UVB exposure in the NP treatment than in the HP treatments and the number of responsive transcripts increased. In both treatments, approximately 30 transcripts showed a response to the treatment. These results suggest that the red pigmentation may absorb UVB radiation, thus minor changes in cellular processes are seen in response to UVB exposure.

Red pigmentation in organisms can serve as a protective mechanism against UVB damage. Carotenoids are organic pigments commonly found in plants, algae, and some bacteria (de Carvalho & Caramujo 2017). Carotenoids are typically ingested in response to UVB exposure by several zooplankton taxa such as copepods, cladocerans, tardigrades, and ciliates (Rautio et al. 2009; Rautio & Tartarotti 2010; Zagarese et al. 1997). By incorporating carotenoids from their diet, bdelloids can benefit from the antioxidant and photoprotective properties that carotenoids offer (Hairston 1976; Marcoval et al. 2021; Moeller et al 2005). When the red pigmentation absorbs UVB radiation there is less damage to cellular components. This reduced damage may lead to fewer genes being triggered or activated in response to UVB-induced stress. Consequently, organisms with effective red pigmentation may require fewer genetic responses to counteract the damage caused by UVB radiation. Carotenoid oxygenase

(TRINITY_DN540231_c0_g1, TRINITY_DN540231_c0_g1, TRINITY_DN542673_c1_g1) was identified in HP treatments. Carotenoid oxygenase is an enzyme involved in the metabolism of carotenoids. It catalyzes the oxidative cleavage or modification of carotenoid molecules. The presence of carotenoid oxygenase genes indicates an ability to metabolize and utilize carotenoids in various physiological processes (Prado-Cabrero et al. 2007).

Genes associated with stress were identified within the assembled *Philodina* transcriptome, such as RAD23 homologs (TRINITY_DN12_c5_g1, TRINITY_DN277236_c0_g1), which are involved in nucleotide excision repair (NER), which is a mechanism responsible for repairing DNA damage caused by UVR. RAD23 assists in the recognition of DNA lesions and recruits other proteins to the site of damage, initiating the repair process (Aranda et al. 2011; Hecox-Lea & Mark Welch 2018). Several isomers of late embryogenesis abundant (LEA) proteins (LEA 1A: TRINITY_DN4936_c4_g1, TRINITY_DN181607_c0_g1, LEA 1B: TRINITY_DN4936_c3_g1), which play a role in stabilizing proteins, membranes, and cellular structures by preventing aggregation or denaturation during stress, were found (Hanson et al. 2013; Hecox-Lea & Mark Welch 2018). They may also function as molecular chaperones, assisting in the refolding of damaged proteins and maintaining their proper conformation (Aranda et al. 2011; Hanson et al. 2013; Hecox-Lea & Mark Welch 2018).

Superoxide Dismutase (SOD: TRINITY_DN155886_c1_g1) plays a crucial role in protecting cells against damage caused by reactive oxygen species (ROS), particularly the superoxide radical (O^{2-}). The primary function of SOD is to neutralize and detoxify the harmful superoxide radicals, preventing them from causing oxidative damage to cells (Aranda et al. 2011; Kim et al. 2015; Singh et al. 2015). Glutathione transferase (GST) plays a crucial role in the

detoxification of xenobiotics and endogenous compounds by catalyzing the conjugation of glutathione (GSH) with these compounds. This conjugation reaction enhances the solubility and excretion of these compounds, making them less harmful to cells. GSTs are also involved in the modulation of signaling pathways and have been implicated in the protection against oxidative stress, inflammation, and cell death. Several genes were identified as GSTs (TRINITY_DN269647_c0_g1, TRINITY_DN123081_c0_g2), glutathione S-transferase (TRINITY_DN10443_c0_g1, TRINITY_DN26206_c0_g1), with a few of these showing a significant change in expression in response to low, mid, and high UVB radiation (TRINITY_DN473324_c0_g1, TRINITY_DN26206_c0_g1, TRINITY_DN57440_c0_g1).

Only 2.4% of DEGs that responded to UVB exposure in *Philodina* have been functionally annotated and identified in other animals. Of all the genes that were identified, ~80% of have not been given specific names since their function has not yet been identified. For example, the gene DUF3492 domain is a protein domain identified and characterized through bioinformatics analyses. However, its specific function and role in cellular processes are still unknown and has not have not been fully characterized. Often in non-model or less studied organisms, when genes do not have a known function, researchers attempt to narrow down their functions by identifying the gene ontology each gene may be associated with. These techniques have been used in other taxa in narrowing down genes of interest that respond to UVR exposure. Some examples include stress response (GO:0006950), SOD (GO:0004784), GST, heat sock proteins (GO:0031072) and heat shock protein (hsp) 70 kb (GO:0030544), hsp 90 (GO:0051879), endoplasmic reticulum (GO:0005783), development (GO:0032502), and apoptosis (GO:0097194). These gene ontologies were also associated with genes that responded to UVB

stress in coral (Aranda et al. 2011), cladocerans (Ulbing et al. 2019), copepods (Won et al. 2015), and monogonont rotifers (Kim et al. 2011).

In this study, ~13% of significant DEGs were associated with GO or KEGG pathways terms. GO terms associated with significantly DEGs were identified for each UVB and pigment level. None of the 51 significant DEGs identified in the HP treatment match any GO, however, several GO were identified in NP pigment such as: the electron transfer chain which was over expressed was NADH (GO:0006116, Table 4.1), Guanosine triphosphate (GTP) binding (GO:0005525), GTPase activity (GO:0003924). GTP is an energy-rich nucleotide that is necessary for protein synthesis, intracellular trafficking, cell migration, and translation (Wolinski et al.2016). GTP is also a building block for RNA and DNA. It is also an energy source for cellular activities such as

Interestingly, cytochrome b, cytochrome c oxidase subunit 1 (COX1), subunit 2, and 3 (Table 4.1) were identified to be significantly under-expressed. Cytochrome c oxidase (including its subunits) are involved in facilitating the last step of mitochondrial electron transport chain, where electrons derived from cellular respiration are passed to oxygen to produce water. This process is essential for the efficient production of adenosine triphosphate (ATP), through oxidative phosphorylation (Aranda et al. 2011; Hanson et al. 2013; Hecox-Lea & Mark Welch 2018). It has been implicated in apoptosis, a programmed cell death process that occurs in response to stress or certain signals (Atlante et al. 20000; Wang et al. 2003; Aeanda et al. 2011). Furthermore, cytochrome c oxidase has a scavenging function, helping to reduce harmful ROS generated during cellular metabolism.

Genes identified in *Philodina* were validated by comparing transcriptome sequences to 11 bdelloid genomes and two additional transcriptomes downloaded from GenBank (Table S. 2). The bdelloids used for comparisons are composed of five bdelloid families from both desiccating and non-desiccating environments. Unsurprisingly, nucleotides and predicted proteins based on *Philodina* transcriptome were most similar to *P. acuticornis* (SRX155614) and *P. roseola* (SRX155615). There was a similar transcriptome size, N50, and GC content in the three species. There appears to be a large variation in the number of unique genes across the bdelloids as highlighted in Figure 4.1b, this could be a reason so few bdelloids genes have been assigned a function (Table S4.4). Another plausible reason could be environmental factors, such pigment, UVR, temperature, and desiccation that could be driving the retention of or acquisition of different genes across bdelloids.

Chapter 5: General Discussion

This study focused on the role of pigmentation in providing the bdelloid rotifer *Philodina* with increased resistance to ultraviolet radiation (UVR). Changes in weather patterns are expected to increase UVR exposure in low to mid latitude regions (Bais et al. 2018; Neal et al. 2022). The hypothesis that red pigmentation provides protection against UVR damage was supported by (1) Pigmented *Philodina* were found in shallow rock pools with low concentrations of dissolved organic carbon (DOC). I infer that bdelloids in habitats with high concentrations of DOC do not need to produce or acquire red pigment to prevent UVR damage, (2) *Philodina* had greater odds of surviving UVB exposure when highly pigmented, (3) Evidence that pigmentation may prevent cumulative damage by repeated exposure and could have aided *Philodina* in locally adapting to UVB intensities, and (4) fewer genes showed differential gene expression in response to UVB exposure in highly pigmented rotifers. These findings point to the adaptive significance of red pigmentation in protecting *Philodina* from the detrimental effects of intense UVB radiation in the Chihuahuan Desert.

Red pigmentation is common in bdelloids from temporary habitats, found in all four bdelloid families and 13 genera. Bdelloids selectively ingest cyanobacteria which enabled them to obtain the brown-yellowish carotenoids fucoxanthin and myxoxanthophyll (Mialet et al. 2013). Given that bdelloids still expressed a level of pigmentation even after being cultured in the laboratory for >6 month, it is possible that they have the ability to produce photoprotection. Here, *de novo* transcriptome assemblies of *Philodina* after UVB exposure identified possible pathways and related to the synthesis and/or metabolism of the carotenoid zeaxanthin. Zeaxanthin is a yellow-orange pigment, like most carotenoids, commonly produced

by some plants, algae, bacteria, and fungi (Maoka 2011; Murillo et al. 2019). Zeaxanthin, like fucoxanthin and myxoxanthophyll, can absorb UVR as well as act as an antioxidant (Maoka 2011; Mialet et al. 2013; Murillo et al. 2019). It has been found in pigmented anostracans, cladocerans, copepods, and notostracods (Rautio et al. 2009). These carotenoids are β-carotenoids which contribute to the regulation of carotenoid levels and their conversion into red pigmentation (Mialet et al. 2013; Toews et al. 2017).

In animals, carotenoids are not synthesized *de novo* but are acquired through dietary sources (de Carvalho & Caramujo 2017; Prado-Cabrero et al. 2007). In this study, the culturing of pigmented *Philodina* for over six months in the laboratory bdelloids resulted in bdelloids becoming non-pigmented. Although *Philodina* was considered unpigmented, traces of red color remained lining the gut. This lining corresponds to where pigmentation was concentrated in moderately and lightly pigmented individuals. The presence pigment in bdelloids after 6 months in culture contradicts the established understanding that only photosynthetic plants, algae, bacteria, or fungi produce carotenoids (de Carvalho & Caramujo 2017; Mialet et al. 2013; Prado-Cabrero et al. 2007). Although we expected it to identify carotenoids in pigmented bdelloids, after removed from their food sourced A possible reason for the presence of some pigmentation in NP bdelloids could be that these genes have been acquired through horizontal gene transfer (HGT). Other studies have found that bdelloids exhibit one of the highest rates of horizontal gene transfer (HGT) among metazoans, ranging from 9.1% in *A. ricciae* to 6.2% in *R. macrura* (Eyres et al. 2015; Gladyshev et al. 2008, 2010). The mechanisms underlying HGT in rotifers remain a subject of ongoing investigation, and further research is needed to determine if this could be a possible source for the presence of carotenoids in bdelloids.

Populations may exhibit variability in their responses to selection pressures, despite being exposed to the same environment (Angilletta 2009; Van Dooren et al. 2016). Differences can be attributed to genotypic differences which occur when individuals within a population carry different combinations of alleles for a specific gene or set of genes (Dam 2013; Neal et al. 2023; Sha et al. 2022). Often adaptations to survive in harsh environments are promoted through genetic recombination, by facilitating the creation of new allelic combinations that may be better suited to the environment (Mousseau & Fox 1998; Vakhrusheva et al. 2020). Although bdelloids are not able to undergo meiotic recombination, a recent studies have found indications of sex in different bdelloid species based on genetic variants that suggest occasional sexual reproduction (Laine et al. 2021, Vakhrusheva et al. 2020). Another possibility is that bdelloids have made use of HGT to integrate genes from members of the same species (Bininda-Emonds et al. 2016; Debortoli et al. 2016; Flot et al. 2013; Gladyshev et al. 2010). Many of these acquired genes are functional and may be responsive to environmental stimuli, leading to differential gene expression and phenotypic outcomes in different environments (Dam 2013; Fox et al. 2019; Neale et al. 2023; Schlichting & Pigliucci 1998). Gene acquisition was shown to be more common in bdelloids prone to desiccation (Eyers et al. 2015). This is because during cryptobiosis the pores on bdelloids integument secrete a gelatinous substance, cell membranes then become permeable and reduce further water loss and protects biological components (Bininda-Emonds et al. 2016; Eyers et al. 2015; Fontaneto et al. 2007; Hinz et al. 2018; Ricci et al. 2003; Signorovitch et al. 2015; Simion et al 2021). The viscous secretion has not yet been characterized in bdelloids but may trap DNA in the environment and enable rotifers to uptake genetic material (Hinz et al. 2018; Ricci 2016).

Pigmented bdelloid rotifers, like *Philodina*, become particularly intriguing when considering the unrelenting selective pressures within rock pools. These pressures such as desiccation, high UVR, extreme temperatures, might further be influenced by environmental factors, can impact specific genes, resulting in phenotypic plasticity and potentially leading to maternal effects that affect the next generation's traits and behaviors (Joćque et al. 2010; Schröder et al. 2007; Walsh et al. 2014; White & Butlin 2021). They can act on specific genes within these pigmented rotifers, triggering phenotypic plasticity and potentially inducing maternal effects. The presence of pigmentation in these bdelloids might confer a certain degree of resilience against the harsh UVR conditions commonly found in their habitat. This could be interpreted as an adaptive strategy that helps them withstand high intensities of UVR. Consequently, enhancing their chances of survival and reproductive success within the rock pool ecosystem.

In the case of pigmented bdelloids, the mechanisms of phenotypic plasticity and maternal effects could offer substantial advantages for adaptation. Phenotypic plasticity enables pigmented bdelloids to adjust their responses to changing environmental conditions, ensuring their survival even in challenging circumstances. This flexibility can manifest in diverse ways, such as altering their physical traits, physiological processes, or behaviors (Mousseau & Fox 1998; Yampolsky et al. 2014; Wolf & Wade 2009). Additionally, maternal effects further enhance their adaptive capabilities by influencing the development and expression of traits in their offspring. This can be particularly beneficial in preparing the next generation for specific challenges like desiccation, UVR exposure, and temperature fluctuations (Fox et al. 2019; de

Villemereui et al. 2020; White & Butlin 2021). This helps *Philodina* survive and do well in their highly fluctuating habitat.

Often exposure to stressors can result in a trade-off between somatic maintenance and reproduction. When organisms are exposed to high levels of UVB radiation, they often allocate resources towards repairing damage and maintaining their own physiological functions, reducing the available resources for reproductive processes. This trade-off ensures that energy and resources are directed towards survival and self-preservation rather than reproductive efforts as seen in daphnids (Oexle et al. 2016), copepods (Heine et al. 2019; Hylander et al. 2014; Moeller et al. 2005), tardigrades (Altiero et al. 2011), and rotifers (Luijckx et al. 2018; Wang et al. 2011). As a result, there may be a decrease in reproductive output or delayed reproductive maturity in response to UVB radiation or other stressors. However, this trade-off has been seen to reverse, in response to exposure to low intensities of UVB. Such an example was seen in the increased clutch size and decreased their lifespan when the copepod *Tigriopus californicus* (Baker, 1912) was exposed to low intensities of UVB radiation (Heine et el. 2019). However, these trade-offs have been avoided by maintaining *Acartia tonsa,* Dana, 1849 on diet rich in photoprotectants UVB exposure resulted in increased lifespan and reproduction (Hylander et al. 2014). Similarly, pigmentation in *Philodina* might indicate an adaptive response to high UVR environments that ensures survival.

Adaptation refers to the process by which organisms develop traits or characteristics that enhance their survival and have reproductive success in a specific environment (Garcia et al. 2008; Brüsin et al. 2016; Ubling et al. 2019). In the case of UVR exposure, selection pressures will favor genetic variants that provide enhanced UVR tolerance without compromising

reproductive fitness (Garcia et al. 2008; Brüsin et al. 2016; Ubling et al. 2019). In this study, UVB exposure of the *Philodina* maternal line resulted in extending lifespan and increased net reproductive rates in both low and mid UVB treatments. Surprisingly, the control group and high UVB exposure group exhibited negative effects on both lifespan and reproduction in *Philodina*, implying the presence of an optimal range of UVB intensity. This suggests a positive relationship between these traits and UVB exposure, up to a certain intensity.

Regional adaptation to UVB intensity in the bdelloid rotifer *Philodina* was supported in this study. The lack of a trade-off between somatic maintenance and reproduction under low and mid UVB treatments in *Philodina* suggests the development of specific mechanisms to balance both life history traits under specific UVB conditions. These differences can involve enhanced DNA repair mechanisms, increased production of protective molecules like antioxidants. Such genotypic variance allows individuals within these populations to better cope with higher UVB exposure than populations in regions with lower UVB intensities (Dam 2013; Neal et al. 2023; Sha et al. 2022). Another possibility is that the environment in which the embryos are developing could be altered by the mother's activities or behaviors, providing specific nutrients or conditions that support the production of the protective pigments. This could include factors such as exposure to certain light wavelengths, availability of specific food sources, or other environmental cues (Alcocer et al. 2020; Marcoval et al. 2020; Oexle et al. 2016).

In *Philodina* production of red coloration may be form of phenotypic plasticity, in response to the high UVR environment. I observed that bdelloids also provided red pigments and potentially other compounds to their developing embryos. Eggs that were laid after two

weeks by a moderately pigmented *Philodina* remained tinted throughout the remainder of their lifespan. Clear eggs were produced by the F_1 generation, however, F_1 bdelloids retained a slight red tint seen in the lightly pigmented level. These observations support the hypothesis that females are reallocating of dietary pigments or other beneficial compounds to their embryos, aiding in the development of photoprotective coloration. The copepod *Leptodiaptomus minutus* (Lilljeborg 1889) uses a similar reproductive strategy, where females redistribute large amounts of carotenoids and fatty acids, they uptake from their diet to their eggs (Schneider et al. 2017). This adaptive strategy may provide offspring with photoprotection before it can be ingested, enhancing their ability to survive in environments characterized by high levels of UVR.

The advancement of spring, longer growing seasons, and delayed onset of winter due to climate change will also affect the intensity and duration of UVR exposure. Species that are not adapted to the increased UVR stress might see a reduction in fitness and possibly their ability to survive in that habitat (Bais et al. 2018; Pinceel et al. 2018; Salawitch et al. 2019; Watanabe et al. 2011). Pigmented species have an advantage in dealing with these changes as they are more equipped to handle the altered conditions. Their pigmentation protects them from UVB rays that can damage cellular structures, minimizing the negative effects of increased ultraviolet radiation (Alcocer et al. 2020; Garcia et al. 2008; Hairston 1976, 1979) and neutralizing UVB radiation (Suma et al. 2020), thus reducing cellular damage. *Philodina* may have adapted to its current environment through genetic changes, then they are more likely to possess a level of flexibility and adaptability that allows it to adjust and respond to future environmental shifts.

Future directions

Further research is necessary to understand the exact mechanisms involved in adaptation to regional UVB intensities by *Philodin*a. Further investigation of the presence and function of photoprotective compounds, such as carotenoids or melanins found in *Philodina* and *Adineta* species, are synthesized by bdelloids. The first step would be to determine if bdelloids are able to produce pigmentation themselves or if it is acquired from their food source. This could be accomplished by culturing *Philodina* under regional UVR to determine if *Philodina* can produce red pigmentation under laboratory conditions. In addition, it would be interesting to determine whether the maintenance of red pigment prevents accumulative damage.

Additional research is required to elucidate how *Philodina* responds to other regional stressors such as changes in water chemistry, and food quality and quantity. This could help clarify how these variables interact with UVB stress. Exploring the role of seasonal variables, such as temperature and photoperiod, could shed light on whether similar responses to UVB exposure occur naturally in response to regular seasonal changes. The response to UVR stress of a broad array of taxa could examine the genetic and physiological mechanisms underlying UVB stress response. Studying how various pigmented organisms respond to UVB stress could reveal the genetic and physiological mechanisms behind their reactions. Furthermore, analyzing pigmented invertebrates from Hueco Tanks, which also display signs of local adaptation to UVB intensity, could contribute to identifying common genetic pathways or shared strategies for coping with this stress in these populations. Comparative studies offer the opportunity to delve into the genetic and physiological mechanisms that underlie the response to UVB stress in

these diverse organisms, with a focus on identifying common genetic pathways or shared adaptive tactics. Such investigations would contribute to our understanding of the broader patterns of adaptation and response to UVB stress in diverse taxa, enhancing our knowledge of the evolutionary and ecological dynamics in rock pool and other high UV intensity ecosystems.

References

Altiero, T., Guidetti, R., Caselli, V., Cesari, M., Rebecchi, L. (2011). Ultraviolet radiation tolerance in hydrated and desiccated eutardigrades. Journal of Zoological Systematics and Evolutionary Research, 49, 104-110. https://doi.org/10.1111/j.1439-0469.2010.00607.x

Alcocer, J., C. N. Delgado, & R. Sommaruga. (2020). Photoprotective compounds in zooplankton of two adjacent tropical high mountain lakes with contrasting underwater light climate and fish occurrence. *J. Plankton Res.* 42: 105–118. https://doi.org/10.1093/plankt/fbaa001

Allen, D. J., Nogués, S., & Baker, N. R. (1998). Ozone depletion and increased UV-B radiation: is there a real threat to photosynthesis? *Journal of Experimental Botany* 49: 1775-1788. https://doi.org/10.1093/jxb/49.328.1775

Alonso, C., Rocco, V., Barriga, J. P., Battini, M. A., & Zagarese, H. (2004). Surface avoidance by freshwater zooplankton: Field evidence on the role of ultraviolet radiation. *Limnology and Oceanography*, *49*(1), 225-232. https://doi.org/10.4319/lo.2004.49.1.0225

Alton, L. A., & Franklin, C. E. (2017). Drivers of amphibian declines: effects of ultraviolet radiation and interactions with other environmental factors. *Climate Change Responses*, *4*(1), 1-26. https://doi.org/10.1186/s40665-017-0034-7

Andersson, M., Van Nieuwerburgh, L., & Snoeijs, P. (2003). Pigment transfer from phytoplankton to zooplankton with emphasis on astaxanthin production in the Baltic Sea food web. *Marine Ecology Progress Series*, *254*, 213-224. https://doi.org/10.3354/meps254213

Angilletta, M. J. (2009). Thermal adaptation: a theoretical and empirical synthesis. *Oxford: OUP Oxford*. ISBN:9780198570875, 0198570872

Bais, A. F., Lucas, R. M., Bornman, J. F., Williamson, C. E., Sulzberger, B., Austin, A. T., Wilson, S. R., Andrady, A. L., Bernhard, G., McKenzie, R. L., Aucamp, P. J., Madronich, S., Neale, R. E., Yazar, S., Young, A. R., de Gruijil, F. R., Norval, M., Takizawa, Y., Barnes, P. W., Robson, T. M., Robinson, S. A., Ballaré, C. L., Flint, S. D., Neale, P. J., Hylander, S., Rose, K. C., Wängberg, S. -Å., Häder, D.-P., Worrest, R. C., Zepp, R. G., Paul, N. D., Cory, R. M., Solomon, K. R., Longstreth, J., Pandey, K. K., Redhwi, H. H., Torikai, A., Heikkiä, A. M., (2018). Environmental effects of ozone depletion, UV radiation and interactions with climate change: UNEP Environmental Effects Assessment Panel, update 2017. Photochemical and photobiological sciences, 17: 127-179. https://doi.org/10.1039/C7PP90043k

Barnes, P. W., Williamson, C. E., Lucas, R. M., Robinson, S. A., Madronich, S., Paul, N. D., Bornman, J.F., Bais, A.F., Sulzberger, B., Wilson, S.R. and Andrady, A.L., & McKenzi, R. L., Neale, P.J., Austin, A.T., Bernhard, G. H., Solomon, K. R., Neale, R. E., Youbg, P. J., Norval,

M., Rhodes, L. E., Hylander S., Rose K. C., Longstreth, J., Aucamp, P. J., Ballaré C. L., Cory, R. M., Flint, S. D., de Gruijl, Häder, D-P., Heikkilä, S. M., Jansen M. A. K., Pandey, K. K., Robson M. T., Sinclair, C. A., Wängberg S-A., Worrest, R. C., Yazar, S., Young, A. R. and Zepp, R. G. (2019). Ozone depletion, ultraviolet radiation, climate change and prospects for a sustainable future. *Nature Sustainability*, *2*(7), 569-579. https://doi.org/10.1038/s41893-019-0314-2

Bashevkin, S. M., Christy, J. H., and Morgan, S. G. (2020). Costs and compensation in zooplankton pigmentation under countervailing threats of ultraviolet radiation and predation. *Oecologia* 193.1:111-123. https://doi.org/10.1007/s00442-020-04648-2

Bates, D., Maechler, M., Bolker, B., Walker, S., Christensen, R.H.B., Singmann, H., Dai, B., Scheipl, F. and Grothendieck, G. (2009). Package 'lme4'. URL: http://lme4r-forge.r-project.org

Bininda-Emonds, O. R. P., Hinz C., Ahlrichs W. H. Evidence Supporting the Uptake and Genomic Incorporation of Environmental DNA in the "Ancient Asexual" Bdelloid Rotifer *Philodina roseola*. *Life*. 2016; 6(3):38. https://doi.org/10.3390/life6030038

Blumthaler, M., Ambach, W., Ellinger, R. (1997). Increase in solar UV radiation with altitude. Journal of photochemistry and Photobiology B: Biology, 39: 130-134. https://doi.org/10.1016/S1011-1344(96)00018-8

Boeing, W. J., Leech, D. M., Williamson, C. E., Cooke, S., and Torres, L. (2004). Damaging UV radiation and invertebrate predation: conflicting selective pressures for zooplankton vertical distribution in the water column of low DOC lakes. *Oecologia* 138.4: 603-612. https://doi.org/10.1007/s00442-003-1468-0

Bonifacio, A., Guidetti, R., Altiero, T., Sergo, V., and Rebecchi, L. (2012). Nature, source and function of pigments in tardigrades: *In vivo* Raman imaging of carotenoids in *Echiniscus blumi*. *PLoS One*, 7.11: p.e50162:1-8. https://doi.org/10.1371/journal.pone.0050162

Boschetti, C., Ricci, C., Sotgia, C., & Fascio, U. (2005). The development of a bdelloid egg: a contribution after 100 years. *Hydrobiologia*, 546:323-331. https://doi.org/10.1007/s10750-005-4241-z

Brendonck, L., Joćque, M., Hulsmans, A., and Vanschoenwinkel, B. (2010). Pools "on the rocks": freshwater rock pools as model system in ecological and evolutionary research. *Limnetica* 29.1: 0025-40. ISSN: 0213-8409

Briggs, M. K., Lozano-Cavazos, E. A., Poulos, H. M., Ochoa-Espinoza, J., & Rodriguez-Pineda, J. A. (2019). The Chihuahuan Desert: a binational conservation response to protect a global treasure. *Reference Module in Earth Systems and Environmental Sciences*. https://doi.org/10.1016/B978-0-12-409548-9.11966-9

Brüsin M., Svensson, P. A., and Hylander, S. (2016). Individual changes in zooplankton pigmentation in relation to ultraviolet radiation and predator cues *Limnol. Oceanogr*. 61.4: 1337-1344. https://doi.org/10.1002/lno.10303

Brown, P. D., Schröder, T., Ríos-Arana, J. V., Rico-Martinez, R., Silva-Briano, M., Wallace, R. L., & Walsh, E. J. (2022). Processes contributing to rotifer community assembly in shallow temporary aridland waters. *Hydrobiologia* 1-17. https://doi.org/10.1007/s10750-022-04842-8

Cabrol, N. A., Feister, U., Häder, D. P., Piazena, H., Grin, E. A., and Klein, A. (2014). Record solar UV irradiance in the tropical Andes. *Front. environ. sci.* 2: 1-19. https://doi.org/10.3389/fenvS2014.00019

Cakil, Z.V., Garlasche, G., Iakovenko, N., Di Cesare, A., Eckert, E.M., Guidetti, R., Hamdan, L., Janko, K., Lukashanets, D., Rebecchi, L. and Schiaparelli, S., Sforzi, T., Štefková Kašparová, E., Velasco-Castrillón1 , A., Walsh, E.J., Fontaneta, D., (2021). Comparative phylogeography reveals consistently shallow genetic diversity in a mitochondrial marker in Antarctic bdelloid rotifers. *Journal of Biogeography*, *48*: 1797-1809. https://doi.org/10.1111/jbi.14116

Caprioli, M., Krabbe Katholm, A., Melone, G., Ramlov, H., Ricci, C., & Santo, N. (2004). Trehalose in desiccated rotifers: a comparison between a bdelloid and a monogonont species. *Comparative Biochemistry and Physiology Part A: Molecular & Integrative Physiology* 139: 527-532. https://doi.org/10.1016/j.cbpb.2004.10.019

Caprioli, M., & Ricci, C. (2001). Recipes for successful anhydrobiosis in bdelloid rotifers. *Hydrobiologia* 446/447: 13-17. https://doi.org/10.1023/a:1017556602272

Caswell, H. (1989). Analysis of life table response experiments I. Decomposition of effects on population growth rate. *Ecological Modelling*, *46*(3-4), 221-237. https://doi.org/10.1016/0304-3800(89)90019-7

Chatragadda, R., & Dufossé, L. (2021). Ecological and biotechnological aspects of pigmented microbes: A way forward in development of food and pharmaceutical grade pigments. *Microorganisms*, *9*(3), 637. https://doi.org/10.3390/microorganisms9030637

Chen, H. VennDiagram: generate high-resolution Venn and Euler plots. R package version 113, (2011). https://doi.org/10.1186/1471-2105-12-35

Chomczynski, P., Wilfinger, W. W., Eghbalnia, H. R., Kennedy, A., Rymaszewski, M., & Mackey, K. (2016). Inter-individual differences in RNA levels in human peripheral blood. *PLoS One*, 11: e0148260. https://doi.org/10.1371/journal.pone.0148260

Cockell, C. S. (1998). Ultraviolet radiation, evolution, and the π-electron system. *Biological Journal of the Linnean Society* 63: 449-457. https://doi.org/10.1111/j.1095-8312.1998.tb01528.x

Cordero, R.R., Feron, S., Damiani, A., Redondas, A., Carrasco, J., Sepúlveda, E., Jorquera, J., Fernandoy, F., Llanillo, P., Rowe, P.M. and Seckmeyer, G., . (2022). Persistent extreme ultraviolet irradiance in Antarctica despite the ozone recovery onset. *Scientific reports*, 12.1: 1266. https://doi.org/10.1038/s41598-022-05449-8

Dam, H. G. (2013). Evolutionary adaptation of marine zooplankton to global change. *Annual review of marine science*, *5*: 349-370. https://doi.org/10.1146/annurev-marine-121211-172229

Dartnall, H. J. G. (1992). The reproductive strategies of two Antarctic rotifers. *Journal of Zoology*, *227*(1), 145-162. https://doi.org/10.1111/j.1469-7998.1992.tb04350.x

de Carvalho, C. C., & Caramujo, M. J. (2017). Carotenoids in aquatic ecosystems and aquaculture: a colorful business with implications for human health. *Frontiers in Marine Science*, *4*, 93. https://doi.org/10.3389/fmars.2017.00093

de Los Rios, P., (2005). Survival of pigmented freshwater zooplankton, exposed to artificial ultraviolet radiation and two levels of dissolved organic carbon. *Pol. J. Ecol.* 53.1: 113-116. https://doi.org/https://repositoriodigital.uct.cl/handle/10925/2535

Debortoli, N., Li, X., Eyres, I., Fontaneto, D., Hespeels, B., Tang, C. Q., . Flot, J. F., Van Doninck, K. (2016). Genetic exchange among bdelloid rotifers is more likely due to horizontal gene transfer than to meiotic sex. *Current Biology* 26: 723-732. https://doi.org/10.1016/j.cub.2016.01.031

Declerck, S. A., & Papakostas, S. (2017). Monogonont rotifers as model systems for the study of micro-evolutionary adaptation and its eco-evolutionary implications. *Hydrobiologia*, 796:131-144. https://doi.org/10.1007/s10750-016-2782-y

Dinerstein, E., Olson, D., Atchley, J., Loucks, C., Contreras-Balderas, S., Abell, R., Iñigo, E., Enkerlin, E., Williams, C., & Castilleja, G. (2000). Ecoregion-based conservation in the Chihuahuan Desert: A biological assessment. *A collaborative effort by World Wildlife Fund, Comisíon National para el Conocimiento y Uso de la Biodiversidad (CONABIO), The Nature Conservancy, PRONATURA Noreste, and the Instituto Tecnologico y de Estudios Superiores de Monterrey (ITESM).*

Ekvall, M. T., Hylander, S., Walles, T., Yang, X., & Hansson, L. A. (2015). Diel vertical migration, size distribution and photoprotection in zooplankton as response to UV-A radiation. *Limnology and Oceanography*, *60*(6), 2048-2058.

Ekvall, M. T., Sha, Y., Palmér, T., Bianco, G., Bäckman, J., Åström, K., & Hansson, L. A. (2020). Behavioural responses to co-occurring threats of predation and ultraviolet radiation in Daphnia. *Freshwater Biology*, *65*(9), 1509-1517. https://doi.org/10.1111/fwb.13516

Erickson III, D. J., Sulzberger, B., Zepp, R. G., and Austin, A. T. (2015). Effects of stratospheric ozone depletion, solar UV radiation, and climate change on biogeochemical cycling:

interactions and feedbacks. *Photochemical & Photobiological Sciences,.* 14.1:127-148. https://doi.org/10.1039/C4PP90036G

Eyres, I., Boschetti, C., Crisp, A., Smith, T. P., Fontaneto, D., Tunnacliffe, A., & Barraclough, T. G. (2015). Horizontal gene transfer in bdelloid rotifers is ancient, ongoing, and more frequent in species from desiccating habitats. *BMC biology* 13: 90 - 102. https://doi.org/10.1186/s12915-015-0202-9

Fernández, C. E., Campero, M., Uvo, C., Hansson, L. A. (2018). Disentangling population strategies of two cladocerans adapted to different ultraviolet regimes. Ecology and Evolution, 8: 1995-2005. https://doi.org/10.1002/ece3.3792

Fernández, C. E., Campero, M., Bianco, G., Ekvall, M. T., Rejas, D., Uvo, C. B., and Hansson, L. A. (2020). Local adaptation to UV radiation in zooplankton: a behavioral and physiological approach. *Ecosphere* 11: e03081. https://doi.org/10.1002/ecs2.3081

Fischer, C., Ahlrichs, W. H., Buma, A. G., van de Poll, W. H., and Bininda-Emonds, O. R. (2013). How does the 'ancient' asexual *Philodina roseola* (Rotifera: Bdelloidea) handle potential UVB-induced mutations? *J. Exp. Biol.* 216.16: 3090-3095. https://doi.org/10.1242/jeb.087064

Flot, J.-F., Hespeels, B., Li, X., Noel, B., Arkhipova, I., Danchin, E. G., Hejnol, A., Henrissat, B., Koszul, R., Aury, J.-M. (2013). Genomic evidence for ameiotic evolution in the bdelloid rotifer *Adineta vaga*. *Nature*: *500*(7463), 453 - 457. https://doi.org/10.1038/nature12326, PMID: 23873043

Fontaneto, D., Herniou, E. A., Boschetti, C., Caprioli, M., Melone, G., Ricci, C., & Barraclough, T. G. (2007). Independently evolving species in asexual bdelloid rotifers. *PLoS biology*, *5*(4), e87. https://doi.org/10.1371/journal.pbio.0050087.

Fox, R. J., Donelson, J. M., Schunter, C., Ravasi, T., Gaitán-Espitia, J. D. (2019). Beyond buying time: the role of plasticity in phenotypic adaptation to rapid environmental change. *Philosophical Transactions of the Royal Society B*, *374*(1768), 20180174. http://dx.doi.org/10.1098/rstb.2018.0174

Garcia, P. E., Perez, A. P., Dieguez, M. D. C., Ferraro, M. A., & Zagarese, H. E. (2008). Dual control of the levels of photoprotective compounds by ultraviolet radiation and temperature in the freshwater copepod Boeckella antiqua. *Journal of Plankton Research*, *30*(7), 817-827. https://doi.org/10.1093/plankt/fbn041

Gilbert, J. J., Walsh, E. J. (2005). Brachionus calyciflorus is a species complex: mating behavior and genetic differentiation among four geographically isolated strains. *Hydrobiologia*, 546: 257-265. https://doi.org/10.1007/s10750-005-4205-3

Gladyshev, E. A., & Arkhipova, I. R. (2010). Genome structure of bdelloid rotifers: shaped by asexuality or desiccation? *Journal of Heredity* 101: S85-S93. https://doi.org/10.1093/jhered/esq008

Gladyshev EA, Meselson M, Arkhipova IR. (2008). Massive horizontal gene transfer in bdelloid rotifers. Science 320:1210–1213. https://doi.org/10.1126/science.1156407, PMID: 18511688

Götz, Stefan, Juan Miguel García-Gómez, Javier Terol, Tim D. Williams, Shivashankar H. Nagaraj, María José Nueda, Montserrat Robles, Manuel Talón, Joaquín Dopazo, and Ana Conesa. (2008). "High-throughput functional annotation and data mining with the Blast2GO suite." *Nucleic acids research* 36: 3420-3435. https://doi.org/10.1093/nar/gkn176

Grabherr MG, Haas BJ, Yassour M, Levin JZ, Thompson DA, Amit I, Adiconis X, Fan L, Raychowdhury R, Zeng Q, Chen Z, Mauceli E, Hacohen N, Gnirke A, Rhind N, di Palma F, Birren BW, Nusbaum C, Lindblad-Toh K, Friedman N, Regev A. (2011) Full-length transcriptome assembly from RNA-seq data without a reference genome. *Nature biotechnology* 29:644-52. https://doi.org/10.1038/nbt.1883, PubMed PMID: 21572440

Goutam, S. P., Kumar, A., & Kumar, D. (2022). Impacts of UV radiation and interactions with climate change. In *Microbiome Under Changing Climate* 271-288. Woodhead Publishing. https://doi.org/10.1016/B978-0-323-90571-8.00012-2

Grosbois, G., Mariash, H., Schneider, T., & Rautio, M. (2017). Under-ice availability of phytoplankton lipids is key to freshwater zooplankton winter survival. *Scientific Reports*, *7*(1), 1-11. https://doi.org/10.1038/s41598-017-10956-0

Gurevich, A., Saveliev, V., Vyahhi, N., & Tesler, G. (2013). QUAST: quality assessment tool for genome assemblies. *Bioinformatics*, *29*(8), 1072-1075. https://doi.org/10.1093/bioinformatics/btt086

Haas BJ, Papanicolaou A, Yassour M, Grabherr M, Blood PD, Bowden J, Couger MB, Eccles D, Li B, Lieber M, Macmanes MD, Ott M, Orvis J, Pochet N, Strozzi F, Weeks N, Westerman R, William T, Dewey CN, Henschel R, Leduc RD, Friedman N, Regev A. (2013). *De novo* transcript sequence reconstruction from RNA-seq using the Trinity platform for reference generation and analysis. Nature protocols 8: 1494 - 512. Open Access in PMC https://doi.org/10.1038/nprot.2013.084

Häder, D. P. (2011). Does enhanced solar UV-B radiation affect marine primary producers in their natural habitats? Photochemistry and photobiology 87: 263-266. 263-266. https://doi.org/10.1111/j.1751-1097.2011.00888.x

Hairston Jr., N. G. (1976). Photoprotection by carotenoid pigments in the copepod *Diaptomus nevadens. Proc. Nat. Acad. Sci. USA* 83: 971-974. https://doi.org/10.1073/pnaS73.3.971

Hairston Jr., N. G. (1979). The adaptive significance of color polymorphism in two species of *Diaptomus* (Copepoda). *Limnol. Oceanogr.* 24: 15–37. https://doi.org/10.4313/lo.1979.24.1.0015

Hansson, L. A. (2004). Plasticity in pigmentation induced by conflicting threats from predation and UV radiation. *Ecology* 85.4: 1005-1016. https://doi.org/10.1890/02-0525

Hansson, L.-A., Hylander, S., and Sommaruga, R. (2007). Escape from UV threats in zooplankton: a cocktail of behavior and protective pigmentation. *Ecology,* 88.8: 1932-1939. https://doi.org/10.1890/06-2038.1

Hanson, S. J., Stelzer, C. P., Mark Welch, D. B. & Logsdon, J. M. (2013). Comparative transcriptome analysis of obligately asexual and cyclically sexual rotifers reveals genes with putative functions in sexual reproduction, dormancy, and asexual egg production. *BMC Genomics*, 14(1), 1-17. https://doi.org/10.1186/1471-2164-14-412

Havstad, K. M., Huenneke, L. F., & Schlesinger, W. H. (Eds.). (2006). *Structure and function of a Chihuahuan Desert ecosystem: the Jornada Basin long-term ecological research site*. Oxford University Press. ISBN 13 978-0-19-511776-9

Hecox-Lea, B. J., and Mark Welch, D. B. (2018). Evolutionary diversity and novelty of DNA repair genes in asexual bdelloid rotifers. *BMC Evol. Biol.* 18.177: 1-25. https://doi.org/10.1186/s12862-018-1288-9

Heine, K. B., Powers, M. J., Kallenberg, C., Tucker, V. L., Hood, W. R. (2019). Ultraviolet irradiation increases size of the first clutch but decreases longevity in a marine copepod. Ecology and Evolution, 9: 9759–9767. https://doi.org/10.1002/ece3.5510

Henry, C. D. (1981). A preliminary assessment of the geologic setting, hydrology, and geochemistry of the Hueco Tanks Geothermal Area, Texas and New Mexico. Virtual Landscapes of Texas. https://doi.org/10.2172/6811369

Hespeels, B., Fontaneto, D., Cornet, V., Penninckx, S., Berthe, J., Bruneau, L., Larrick, J. W., Rapport, E., Jérémie, B., Debortoli, N., Iakovenko, N., Janko, K., Heusin, A. C., Lucas, S., Hallet, B., & Van Doninck, K. (2023). Back to the roots, desiccation and radiation resistances are ancestral characters in bdelloid rotifers. *BMC biology*, *21*(1), 72. https://doi.org/10.1186/s12915-023-01554-w

Hespeels, B., Knapen, M., Hanot-Mambres, D., Heuskin, A. C., Pineux, F., Lucas, S., Koszul, and R. van Doninck, K. (2014). Gateway to genetic exchange? DNA double-strand breaks in the bdelloid rotifer *Adineta vaga* submitted to desiccation. *J. Evol. Biol.* 27.7: 1334-1345. https://doi.org/10.1111/jeb.12326

Hespeels, B., Penninckx, S., Cornet, V., Bruneau, L., Bopp, C., Baumlé, Redivo, B., Heuskin, A.C., Moeller, R., Fujimori, A., Lucas, S., Doninck, K. (2020). Iron ladies–How desiccated

asexual rotifer *Adineta vaga* deal with X-Rays and heavy ions? *Front in Microbiol*. 11.1792. https://doi.org/10.3389/fmicb.2020.01792

Hoffmann, S., and Beierkuhnlein, C. (2020). Climate change exposure and vulnerability of the global protected area estate from an international perspective. *Diver. Distrib.* 26.11: 1496-1509. https://doi.org/10.1111/ddi.13136

Horikawa, D.D., Cumbers, J., Sakakibara, I., Rogoff, D., Leuko, S., Harnoto, R., Arakawa, K., Katayama, T., Kunieda, T., Toyoda, A. and Fujiyama, A. (2013). Analysis of DNA repair and protection in the tardigrade *Ramazzottius varieornatus* and *Hypsibius dujardini* after exposure to UVC radiation. PloS one 8: p.e64793. https://doi.org/10.1096/fasebj.31.1_supplement.906.4

Hinz, C., Ahlrichs, W. H., & Bininda-Emonds, O. R. (2018). Immediate and heritable costs of desiccation on the life history of the bdelloid rotifer Philodina roseola. *Organisms Diversity & Evolution*, *18*, 399-406. https://doi.org/10.1007/s13127-018-0379-1

Huebner, J. D., Loadman, N. L., Wiegand, M. D., Young, D. L., & Warszycki, L.-A. (2009). The effect of chronic exposure to artificial UVB radiation on the survival and reproduction of *Daphnia magna* across two generations. Photochemistry and Photobiology, 85: 374-378. https://doi.org/10.1111/j.1751-1097.2008.00454.x

Hur, J. H., Van Doninck, K., Mandigo, M. L., & Meselson, M. (2008). Degenerate tetraploidy was established before bdelloid rotifer families diverged. Molecular Biology and Evolution 26: 375-383. https://doi.org/10.1093/molbev/msn260, PMID: 18996928

Hylander, S., Larsson, N., and Hansson, L.-A. (2009). Zooplankton vertical migration and plasticity of pigmentation arising from simultaneous UV and predation threats. *Limnol. Oceanogr.* 54.2: 483-491. https://doi.org/10.4319/lo.2009.54.2.0483

Hylander, S., Grenvald, J. C., and Kiørboe, T. (2014). Fitness costs and benefits of ultraviolet radiation exposure in marine pelagic copepods. *Funct. Ecol.* 28.1: 149-158. https://doi.org/10.1111/1365-2435.12159

Ikehata, H., and Ono, T. (2011). The mechanisms of UV mutagenesis. *Journal of Radiation Research* 52: 115-125. https://doi.org/10.1269/jrr.10175

Joćque , M. B., B. Vanschoenwinkel and L. Brendonck. (2010). Freshwater rock pools: a review of habitat characteristics, faunal diversity and conservation value. *Freshwater Biol*. 55: 1587–1602. https://doi.org/10.1111/j.1365-2427.2010.02402.x

Kadad, I. M., Kandil, K. M., and Alzanki, T. H. (2020). Impact of UVB solar radiation on ambient temperature for Kuwait Desert climate. *Smart Grid Renewable Energy* 11.8: 103-125. https://doi.org/10.4236/sgre.2020.118008

Kan, D., Zhang, Y., Zeng, J., Lian, H., Feng, L., Feng, Y., Liu, X., Han, C., & Yang, J. (2023). Physiological response and molecular mechanisms against UV-B radiation in *Brachionus asplanchnoidis* (Rotifera). *Ecotoxicology and Environmental Safety*, *262*, 115319. doi: 10.1016/j.ecoenv.2023.115319

Kanehisa, M., Sato, Y., & Morishima, K. (2016). BlastKOALA and GhostKOALA: KEGG tools for functional characterization of genome and metagenome sequences. *Journal of molecular biology*, *428*(4), 726-731. https://doi.org/10.1016/j.jmb.2015.11.006

Kim, B.-M., Rhee, J.-S., Lee, K.-W., Kim, M.-J., Shin, K.-H., Lee, S.-J., Lee, Y.-M., Lee, J.-S. (2015). UV-B radiation-induced oxidative stress and p38 signaling pathway involvement in the benthic copepod *Tigriopus japonicus*. *Comparative Biochemistry and Physiology Part C: Toxicology & Pharmacology* 167: 15-23. https://doi.org/10.1016/j.cbpc.2014.08.003

Kim, R.-O., Rhee, J.-S., Won, E.-J., Lee, K.-W., Kang, C.-M., Lee, Y.-M., & Lee, J.-S. (2011). Ultraviolet B retards growth, induces oxidative stress, and modulates DNA repair-related gene and heat shock protein gene expression in the monogonont rotifer, *Brachionus* sp. *Aquatic Toxicology* 101: 529-539. https://doi.org/10.1016/j.aquatox.2010.12.005

King, C. E., Ricci, C., Schonfeld, J., & Serra, M. (2005). Evolutionary dynamics of 'the' bdelloid and monogonont rotifer life-history patterns. *Hydrobiologia*, *546*, 55-70. https://doi.org/10.1007/s10750-005-4102-9

Kragh Andersen, P., Pohar Perme, M., van Houwelingen, H.C., Cook, R.J., Joly, P., Martinussen, T., Taylor, J.M., Abrahamowicz, M. and Therneau, T.M., (2021). Analysis of time-to-event for observational studies: Guidance to the use of intensity models. *Statistics in medicine*, *40*(1), pp.185-211. https://doi.org/10.1002/sim.8757

Krisko, A., Leroy, M., Radman, M., and Meselson, M. (2012). Extreme antioxidant protection against ionizing radiation in bdelloid rotifers. *Proc. Nat. Acad. Sci. USA* 109.7: 2354-2357. https://doi.org/10.1073/pnaS1119762109

Latta, L. C., Tucker, K. N., & Haney, R. A. (2019). The relationship between oxidative stress, reproduction, and survival in a bdelloid rotifer. *BMC Ecology,* 19:7. https://doi.org/10.1186/s12898-019-0223-2

Leech, D. M., and Williamson, C. E. (2000). Is tolerance to UV radiation in zooplankton related to body size, taxon, or lake transparency? *Ecol. Appl.* 10.5: 1530-1540. https://doi.org/10.1890/1051-0761(2000)010[1530:ITTURI]2.0.CO;2

Leach, T. H., C. E. Williamson, N. Theodore, J. M. Fischer & M. H. Olson. (2015). The role of ultraviolet radiation in the diel vertical migration of zooplankton: an experimental test of the transparency-regulator hypothesis *J. Plankton Res.* 37L 886–896 https://doi.org/10.1093/plankt/fbv061

Li, B., & Dewey, C. N. (2011). RSEM: accurate transcript quantification from RNA-Seq data with or without a reference genome. *BMC Bioinformatics* 12: 323 - 339. https://doi.org/10.1186/1471-2105-12-323

Luijckx, P., Ho, E. K. H., Stanic, A., & Agrawal, A. F. (2018). Mutation accumulation in populations of varying size: large effect mutations cause most mutational decline in the rotifer *Brachionus calyciflorus* under UV-C radiation. *Journal of Evolutionary Biology* 31: 924-932. https://doi.org/10.1111/jeb.13282

Lukashanets, D. A., & Maisak, N. N. (2023). Bdelloid rotifers (Bdelloidea, Rotifera) in shallow freshwater ecosystems of Thala Hills, East Antarctica. *Polar Biology*, *46*(1), 87-102. https://doi.org/10.1007/s00300-022-03106-4

Love, M. I., Huber, W., & Anders, S. (2014). Moderated estimation of fold change and dispersion for RNA-seq data with DESeq2. Genome biology, 15(12), 1-21. https://doi.org/10.1186/s13059-014-0550-8

Maoka, T. (2011). Carotenoids in Marine Animals. *Marine Drugs*, *9*(2), 278-293. https://doi.org/10.3390/md9020278

Marcoval, M. A., Díaz, A. C., Espino, M. L., Arzoz, N. S., Velurtas, S. M., & Fenucci, J. L. (2020). Role of dietary photoprotective compounds on the performance of shrimp *Pleoticus muelleri* under UVR stress. *Aquaculture* 515:734564. https://doi.org/10.1016/j.aquaculture.2019.734564

Marinone, M. C., Marque, S. M., Suárez, D. A., Carmen Dieguez, M. D., Perez, P., Rios, P. D. L., ... & Zagarese, H. E. (2006). Symposium-in-Print: UV Effects on Aquatic and Coastal Ecosystems-UV Radiation as a Potential Driving Force for Zooplankton Community Structure in Patagonian Lakes. *Photochemistry and Photobiology*, 82.4: 962-971. https://doi.org/10.1562/2005-09-0!3-RA-680

Mark Welch, D. B., Mark Welch, J. L., & Meselson, M. M. (2008). Evidence for degenerate tetraploidy in bdelloid rotifers. *Proceedings of the National Academy of Sciences* 105: 5145-5149. https://doi.org/10.1073/pnas.0800972105, PMID: 18362354

Mark Welch, D. B., & Meselson, M. M. (2000). Evidence for the evolution of bdelloid rotifers without sexual reproduction or genetic exchange. *Science* 288: 1211-1215. https://doi.org/10.1126/science.288.5469.1211, PMID: 10817 991

Martin, M. (2017). A comparison of UVR-Induced mortality in bdelloid rotifers. MS Thesis. Univ. of Texas at El Paso.

McKenzie, R., D. Smale, and M. Kotkamp. (2004). Relationship between UVB and erythemally weighted radiation. *Photochem. Photobiol. Sci* 3.3: 252–256. https://doi.org/10.1039/B312985C

Mialet, B., Majdi, N., Tackx, M., Azémar, F., & Buffan-Dubau, E. (2013). Selective Feeding of Bdelloid Rotifers in River Biofilms. *PLOS ONE*, *8*(9), e75352. https://doi.org/10.1371/journal.pone.0075352

Michaloudi, E., Papakostas, S., Stamou, G., Neděla, V., Tihlaříková, E., Zhang, W., & J. Declerck, S. A. (2018). Reverse taxonomy applied to the Brachionus calyciflorus cryptic species complex: Morphometric analysis confirms species delimitations revealed by molecular phylogenetic analysis and allows the (re)description of four species. *PLOS ONE*, *13*(9), e0203168. https://doi.org/10.1371/journal.pone.0203168

Mojib, N., Amad, M., Thimma, M., Aldanondo, N., Kumaran, M., and Irigoien, X. (2014). Carotenoid metabolic profiling and transcriptome-genome mining reveal functional equivalence among blue-pigmented copepods and appendicularia. *Mol. Ecol*. 23.11: 2740-2756. https://doi.org/10.1111/mec.12781

Moeller, R. E., Gilroy, S., Williamson, C. E., Grad, G., & Sommaruga, R. (2005). Dietary acquisition of photoprotective compounds (mycosporine-like amino acids, carotenoids) and acclimation to ultraviolet radiation in a freshwater copepod. *Limnology and7ceanography*, 50: 427-439. https://doi.org/10.4319/lo.2005.50.2.0427 *

Mousseau, T. A., & Fox, C. W. (1998). The adaptive significance of maternal effects. *Trends in ecology & evolution*, 13: 403-407. https://doi.org/10.1016/S0169-5347(98)01472-4

Murillo, A. G., Hu, S., & Fernandez, M. L. (2019). Zeaxanthin: Metabolism, Properties, and Antioxidant Protection of Eyes, Heart, Liver, and Skin. *Antioxidants*, *8*(9). https://doi.org/10.3390/antiox8090390

Nevalainen, L., Rantala, M. V., Kivilä, E. H., Lami, A., Wauthy, M., Rautio, M., & Luoto, T. P. (2020). Biogeochemical and photobiological responses of subarctic lakes to UV radiation. *Journal of Photochemistry and Photobiology B: Biology*, *209*, 111932. https://doi.org/10.1016/j.jphotobiol.2020.111932

Nevalainen, L., Rantala, M. V., Luoto, T. P., Ojala, A. E. K., & Rautio, M. (2016). Long-term changes in pigmentation of arctic *Daphnia* provide potential for reconstructing aquatic UV exposure. *Quaternary Science Reviews* 144: 44-50. https://doi.org/10.1016/j.quascirev.2016.05.022

Nowell, R.W., Almeida, P., Wilson, C.G., Smith, T.P., Fontaneto, D., Crisp, A., Micklem, G., Tunnacliffe, A., Boschetti, C. and Barraclough, T.G., (2018). Comparative genomics of bdelloid rotifers: Insights from desiccating and nondesiccating species. PLoS biology, 16(4), e2004830. https://doi.org/10.1371/journal.pbio.2004830

Nowell, R.W., Wilson, C.G., Almeida, P., Schiffer, P.H., Fontaneto, D., Becks, L., Rodriguez, F., Arkhipova, I.R. and Barraclough, T.G., (2021). Evolutionary dynamics of transposable elements in bdelloid rotifers. *Elife*, *10*, e63194. https://doi.org/10.7554/eLife.63194

Oexle, S., Jansen, M., Pauwels, K., Sommaruga, R., De Meester, L., & Stoks, R. (2016). Rapid evolution of antioxidant defense in a natural population of *Daphnia magna*. *Journal of Evolutionary Biology* 29: 1328-1337. https://doi.org/10.1111/jeb.12873

Ono, M., Takeuchi, N., & Zawierucha, K. (2021). Snow algae blooms are beneficial for microinvertebrates assemblages (Tardigrada and Rotifera) on seasonal snow patches in Japan. *Scientific Reports*, *11*(1), 1-11. https://doi.org/10.1038/s41598-021-85462-5

Orr, H. A. (2000), "Adaptation and the cost of complexity", Evolution, 54 (1): 13–20, https://doi.org/10.1111/j.0014-3820.2000.tb00002.x, PMID 10937178, S2CID 20895396

Orr, H. A., (2005). "The genetic theory of adaptation: a brief history" (PDF). Nature Reviews Genetics. 6 (2): 119–127. https://doi.org/10.1038/nrg1523. PMID 15716908. S2CID 17772950.

Paraskevopoulou, S., Dennis, A. B., Weithoff, G., Hartmann, S., & Tiedemann, R. (2019). Within species expressed genetic variability and gene expression response to different temperatures in the rotifer *Brachionus calyciflorus* sensu stricto. *PLoS One*, *14:* e0223134. https://doi.org/10.1371/journal.pone.0223134

Paraskevopoulou, S., Dennis, A. B., Weithoff, G., & Tiedemann, R. (2020). Temperature-dependent life history and transcriptomic responses in heat-tolerant versus heat-sensitive *Brachionus* rotifers. *Scientific Reports*, 10:13281. https://doi.org/10.1038/s41598-020-70173-0

Piazena, H. (1996). The effect of altitude upon the solar UV-B and UV-A irradiance in the tropical Chilean Andes. *Solar energy*, 57: 133-140. https://doi.org/10.1016/S0038-092X(96)00049-7

Pinceel, T., Buschke, F., Weckx, M., Brendonck, L., and Vanschoenwinkel, B. (2018). Climate change jeopardizes the persistence of freshwater zooplankton by reducing both habitat suitability and demographic resilience. *BMC Ecology*. 18.1: 1-9. https://doi.org/10.1186/s12898-018-0158-z

Polvani, L. M., Previdi, M., England, M. R., Chiodo, G., & Smith, K. L. (2020). Substantial twentieth-century Arctic warming caused by ozone-depleting substances. *Nature Climate Change*, 10.2: 130-133. https://doi.org/10.1038/s41558-019-0677-4

Prado-Cabrero, A., Scherzinger, D., Avalos, J., & Al-Babili, S. (2007). Retinal biosynthesis in fungi: characterization of the carotenoid oxygenase CarX from Fusarium fujikuroi. *Eukaryotic cell*, *6*(4), 650-657. https://doi.org/10.1128/EC.00392-06

R Core Team. (2020) R: A Language and environment for statistical computing. R Foundation for Statistical Computing, Vienna, Austria. url: https://www.R-project.org

R Core Team (2022). R: A language and environment for statistical computing. R Foundation for Statistical Computing, Vienna, Austria. URL https://www.R-project.org/

Rautio M., Bonilla S., Vincent W.F. (2009). UV photoprotectants in arctic zooplankton. *Aquat Biol* 7:93-105. https://doi.org/10.3354/ab00184

Rautio, M., and Tartarotti, B. (2010). UV radiation and freshwater zooplankton: damage, protection, and recovery. *Freshw. Rev.* 3.2: 105-131. https://doi.org/10.1608/FRJ-3.2.157

Rebecchi, L., Boschetti, C., and Nelson, D. R. (2020). Extreme-tolerance mechanisms in meiofaunal organisms: a case study with tardigrades, rotifers and nematodes. *Hydrobiologia* 847.12: 2779-2799. https://doi.org/10.1007/s10750-019-04144-6

Ricci, C. (1983). Life histories of some species of Rotifera Bdelloidea. Hydrobiologia, 104: 175-180. https://doi.org/10.1007/BF00045965

Ricci, C. (1998). Anhydrobiotic capabilities of bdelloid rotifers. *Hydrobiologia* 387: 321-326. https://doi.org/10.1023/A:1017086425934

Ricci, C. (2001). Dormancy patterns in rotifers. *Hydrobiologia*, *446*, 1-11. https://doi.org/10.1023/A:1017548418201

Ricci, C. (2016). Bdelloid rotifers: 'sleeping beauties' and 'evolutionary scandals', but not only. *Hydrobiologia* 796: 277-285. https://doi.org/10.1007/s10750-016-2919-z

Ricci, C., and Caprioli, M. (2005). Anhydrobiosis in bdelloid species, populations, and individuals. *Integr. Comp. Biol.* 45.5: 759-763. https://doi.org/10.1093/icb/45.5.759

Ricci, C., Caprioli, M., and Santo, N. (2004). Feeding and anhydrobiosis in bdelloid rotifers: A preparatory study for an experiment aboard the International Space Station. *Invertebr. Biol.* 123.4: 283-288. https://doi.org/10.1111/j.1744-7410.2004.tb00162.x

Ricci, C., and Fascio, U. (1995). Life-history consequences of resource allocation of two bdelloid rotifer species. Hydrobiologia, 299: 231-239. https://doi.org/10.1007/BF00767330

Ricci, C., and Fontaneto, D. (2009). The importance of being a bdelloid: ecological and evolutionary consequences of dormancy. *Ital. J. Zool.* 76.3: 240-249. https://doi.org/10.1080/11250000902773484

Ricci, C., and Melone, G. (2000). Key to the identification of the genera of bdelloid rotifers. *Hydrobiologia*, 418:73-80. https://doi.org/10.1023/A:1003840216827

Ricci, C., Melone, G., Santo, N., and Caprioli, M. (2003). Morphological response of a bdelloid rotifer to desiccation. *J. Morphol.* 257.2: 246-253. https://doi.org/10.1002/jmor.10120

Ríos-Arana, J. V., del Carmen Agüero-Reyes, L., Wallace, R. L., and Walsh, E. J. (2019). Limnological characteristics and rotifer community composition of Northern Mexico Chihuahuan Desert Springs. *J. Arid Environ.* 160: 32-41. https://doi.org/10.1016/j.jaridenv.2018.09.005

RStudio Team. (2020). RStudio: Integrated Development Environment for R. RStudio, Inc., Boston, MA. url:http://www.rstudio.com

Salawitch, R. J., Fahey, D. W., Hegglin, M. I., McBride, L. A., Tribett, W. R., & Doherty, S. J. (2019). Twenty Questions and Answers About the Ozone Layer: 2018 Update, Scientific Assessment of Ozone Depletion: 2018. World Meteorological Organization, Geneva, Switzerland. ISBN: 978-1-7329317-2-5

SAS Institute Inc. 2017. SAS/STAT® 14.3 User's Guide. Cary, NC: SAS Institute Inc.

Schmidt, R. H., Jr. 1979. A climatic delineation of the "real" Chihuahuan Desert. Journal of Arid Environments 2:243-250. https://doi.org/10.1016/S0140-1963(18)31774-9

Schneider, C. A., Rasband, W. S., & Eliceiri, K. W. (2012). NIH Image to ImageJ: 25 years of image analysis. *Nature Methods*, *9*(7), 671–675. doi:10.1038/nmeth.2089

Schneider, T., Grosbois, G., Vincent, W. F., and Rautio, M. (2016). Carotenoid accumulation in copepods is related to lipid metabolism and reproduction rather than to UV-protection. *Limnol. Oceanogr.* 61.4: 1201-1213. https://doi.org/10.1002/lno.10283

Schröder, T., Howard, S., Arroyo, L., and Walsh, E.J. (2007). Sexual reproduction and diapause of *Hexarthra* sp. (Rotifera) in short-lived Chihuahuan Desert ponds. *Freshwater Biol.* 52.6: 1033–1042, https://doi.org/10.1111/j.1365-2427.2007.01751.x

Schuch, A. P., Garcia, C. C., Makita, K., & Menck, C. F. (2013). DNA damage as a biological sensor for environmental sunlight. *Photochemical and Photobiological Sciences* 12: 1259-1272. https://doi.org/10.1039/c3pp00004d

Schneider, T., Grosbois, G., Vincent, W. F., & Rautio, M. (2017). Saving for the future: Pre-winter uptake of algal lipids supports copepod egg production in spring. *Freshwater Biology*, *62*(6), 1063-1072. https://doi.org/10.1111/fwb.12925

Segers, H., & Shiel, R. J. (2005). Tale of a sleeping beauty: a new and easily cultured model organism for experimental studies on bdelloid rotifers. In *Rotifera X: Rotifer Research: Trends, New Tools and Recent Advances, Proceedings of the Xth International Rotifer Symposium, held in Illmitz, Austria, 7–13 June 2003* (pp. 141-145). Springer Netherlands. https://doi.org/10.1007/s10750-005-4111-8

Segers, H. (2007). Annotated checklist of the rotifers (Phylum Rotifera), with notes on nomenclature, taxonomy, and distribution. *Zootaxa* 1564: 1-104. https://doi.org/10.11646/zootaxa.1564.1.1

Sen, S., & Mallick, N. (2021). Mycosporine-like amino acids: Algal metabolites shaping the safety and sustainability profiles of commercial sunscreens. *Algal Research*, *58*, 102425. https://doi.org/10.1016/j.algal.2021.102425

Sengupta, M., Xie, Y., Lopez, A., Habte, A., Maclaurin, G., and Shelby, J. (2018). The National Solar Radiation Database (NSRDB). *Renewable Sustainable Energy Rev.* 89: 51-60. https://doi.org/10.1016/j.rser.2018.03.003

Schlichting, C. D., & Pigliucci, M. (1998). *Phenotypic evolution: a reaction norm perspective*. Sinauer associates incorporated. ISBN : 9780878937998

Schneider, T., Grosbois, G., Vincent, W. F., & Rautio, M. (2016). Carotenoid accumulation in copepods is related to lipid metabolism and reproduction rather than to UV-protection. *Limnology and Oceanography*, *61*(4), 1201-1213. https://doi.org/10.1002/lno.10283

Sha, Y., Tesson, S. V., & Hansson, L. A. (2020). Diverging responses to threats across generations in zooplankton. *Ecology*, 101:e03145. https://doi.org/10.1002/ecy.3145

Signorovitch, A., Hur, J., Gladyshev, E., & Meselson, M. (2015). Allele sharing and evidence for sexuality in a mitochondrial clade of bdelloid rotifers. *Genetics* 200: 581-590. https://doi.org/10.1534/geneticS115.176719

Simão, F. A., Waterhouse, R. M., Ioannidis, P., Kriventseva, E. V., & Zdobnov, E. M. (2015). BUSCO: assessing genome assembly and annotation completeness with single-copy orthologs. *Bioinformatics*, 31: 3210-3212. https://doi.org/10.1093/bioinformatics/btv351

Simion, P., Narayan, J., Houtain, A., Derzelle, A., Baudry, L., Nicolas, E., Arora, R., Cariou, M., Cruaud, C., Gaudray, F.R. and Gilbert, C., (2021). Chromosome-level genome assembly reveals homologous chromosomes and recombination in asexual rotifer *Adineta vaga*. *Science Advances*, *7*(41), eabg4216. https://doi.org/10.1126/sciadv.abg4216

Snare, D. J., Fields, A. M., Snell, T. W., & Kubanek, J. (2013). Lifespan extension of rotifers by treatment with red algal extracts. *Exp. Gerontol.* 48.12: 1420-1427. https://doi.org/10.1016/j.exger.2013.09.007

Snell, T. W. (2014). Rotifers as models for the biology of aging. *International review of hydrobiology*, 99.1-2: 84-95. https://doi.org/10.1002/iroh.201301707

Snell, T. W., Fields, A. M., & Johnston, R. K. (2012). Antioxidants can extend lifespan of Brachionus manjavacas (Rotifera), but only in a few combinations. *Biogerontology*, *13*, 261-275. https://doi.org/10.1007/s10522-012-9371-x

Solomon, C. T., Jones, S. E., Weidel, B. C., Buffam, I., Fork, M. L., Karlsson, J., Larson, S., Lennon, J.T., Read, J.S., Sadro, S. & Saros, J. E. (2015). Ecosystem consequences of changing

inputs of terrestrial dissolved organic matter to lakes: current knowledge and future challenges. *Ecosyst.* 18.3: 376-389. https://doi.org/10.1007/s10021-015-9848-y

Stelzer, CP. (2005) Evolution of Rotifer Life Histories. *Hydrobiologia* 546: 335–346. https://doi.org/10.1007/s10750-005-4243-x

Stábile, F., Brönmark, C., Hansson, L. A., & Lee, M. (2021). Fitness cost from fluctuating ultraviolet radiation in Daphnia magna. Biology letters, 17.8: 20210261. https://doi.org/10.1098/rsbl.2021.0261

Suma, H. R., Prakash, S., and Eswarappa, S. M. (2020). Naturally occurring fluorescence protects the eutardigrade *Paramacrobiotus* sp. from ultraviolet radiation. *Biol. Letters* 16.10: 20200391. https://doi.org/10.1098/rsbl.2020.0391

Szydlowski, L., Boschetti, C., Crisp, A., Barbosa, E. G. G., & Tunnacliffe, A. (2015). Multiple horizontally acquired genes from fungal and prokaryotic donors encode cellulolytic enzymes in the bdelloid rotifer *Adineta ricciae*. Gene, 566.2: 125-137. https://doi.org/10.1016/j.gene.2015.04.007

Tapia-Torres, Y., Elser, J.J., Souza, V. and García-Oliva, F. (2015). Ecoenzymatic stoichiometry at the extremes: how microbes cope in an ultra-oligotrophic desert soil. *Soil Biol. Biochem.* 87: 34-42. https://doi.org/10.1016/j.soilbio.2015.04.007

Tartarotti, B., N. Saul, S. Chakrabarti, F. Trattner, C. E. W. Steinberg & R. Sommaruga (2013). UV-induced DNA damage in *Cyclops abyssorum tatricus* populations from clear and turbid alpine lakes. *J. Plankton Res*. 36: 557–566. https://doi.org/10.1093/plankt/fbt109

Terwagne, M., Nicolas, E., Hespeels, B., Herter, L., Virgo, J., Demazy, C., ... & Van Doninck, K. (2022). DNA repair during nonreductional meiosis in the asexual rotifer Adineta vaga. *Science advances*, *8*(48), eadc8829. DOI: 10.1126/sciadv.adc8829

Therneau T. M. (2022). *A Package for Survival Analysis in R*. R package version 3.3-1, https://CRAN.R-project.org/package=survival.

Therneau, T. M., Grambsch, P. M., (2000A). Mixed Effects Cox Models [R package coxme version 2.2-18.1]. R package version 3.3-1, https://CRAN.R-project.org/package=survival.

Therneau, T. M., Grambsch, P. M., (2000B). *Modeling Survival Data: Extending the Cox Model*. Springer, New York. ISBN 0-387-98784-3.

Toews, D. P., Hofmeister, N. R., & Taylor, S. A. (2017). The Evolution and Genetics of Carotenoid Processing in Animals. *Trends in Genetics*, *33*(3), 171-182. https://doi.org/10.1016/j.tig.2017.01.002

Turner, P. N. (1999). A simple generic key to the Bdelloid rotifers. *Quekett Journal of Microscopy*, *38*, 351-356.

Tunnacliffe, A., Lapinski, J., & McGee, B. (2005). A putative lea protein, but no trehalose, is present in anhydrobiotic bdelloid rotifers. *Hydrobiologia, 546*(1), 315-321. https://doi.org/10.1007/s10750-005-4239-6

Ulbing, C. K., Muuse, J. M., and Miner, B. E. (2019). Melanism protects alpine zooplankton from DNA damage caused by ultraviolet radiation. *Proc. R. Soc. B* 286.1914: 20192075. https://doi.org/10.1098/rspb.2019.2075

Van Dooren T.J.M., Hoyle, R.B., and Plaistow, S.J. (2016) Maternal Effects. In: Kliman, R.M. (ed.), Oxford: Academic Press. Encyclopedia of Evolutionary Biology. 446–452. https://doi:10.1016/B978-0-12-800049-6.00051-2

Vehmaa, A., Brutemark, A., & Engström-Öst, J. (2012). Maternal effects may act as an adaptation mechanism for copepods facing pH and temperature changes. *PLoS one*, *7*(10), e48538. https://doi.org/10.1371/journal.pone.0048538

Vrekoussis, T., Chaniotis, V., Navrozoglou, I., Dousias, V., Pavlakis, K., Stathopoulos, E., and Zoras, O. (2009). Image analysis of breast cancer immunohistochemistry-stained sections using ImageJ: an RGB-based model. *Anticancer Res.* 2913: 4995-4998. PMID: 20044607

Wallace, R. L. (2002). Rotifers: exquisite metazoans. *Integrative and Comparative Biology*, 42.3, 660-667. https://doi.org/10.1093/icb/42.3.660

Wallace, R. L., Hochberg, R., & Walsh, E. J. (2023). The undiscovered country: ten grand challenges in rotifer biology. *Hydrobiologia*, 1-24. https://doi.org/10.1007/s10750-023-05247-x

Wallace, R. L., & Snell, T. W. (2010). Rotifera. In *Ecology and classification of North American freshwater invertebrates* (pp. 173-235). Academic Press. https://doi.org/10.1016/B978-0-12-374855-3.00008-X

Wallace, R. L., Snell, T. W., & Smith, H. A. (2015). Phylum rotifera. In *Thorp and Covich's freshwater invertebrates* (pp. 225-271). Academic Press. https://doi.org/10.1016/B978-0-12-385026-3.00013-9

Wallace, R. L., Walsh, E. J., Arroyo, M. L., & Starkweather, P. L. (2005). Life on the edge: rotifers from springs and ephemeral waters in the Chihuahuan Desert, Big Bend National Park (Texas, USA). *Hydrobiologia* 546.1: 147-157. https://doi.org/10.1007/s10750-005-4112-7

Wallace, R. L., Walsh, E. J., Schröder, T., Rico-Martínez, R., and Rios-Arana, J. V. (2008). Species composition and distribution of rotifers in Chihuahuan Desert waters of México: is everything everywhere? *Verh. Int. Ver. Angew. Limnol: Verh.* 30.1: 73-76. https://doi.org/10.1080/03680770.2008.11902087

Walsh, E. J., Smith, H. A., and Wallace, R. L. (2014). Rotifers of temporary waters. *International Review Hydrobiology.* 99.1-2: 3-19. https://doi.org/10.1002/iroh.201301700

Wang, J., Feng, L., & Tang, X. (2011). Effect of UV-B radiation on the population dynamics of the rotifer Brachionus urceus. Acta Oceanologica Sinica, 30: 113-119. https://doi.org/10.1007/s13131-011-0111-x

Watanabe, S., Sudo, K., Nagashima, T., Takemura, T., Kawase, H., & Nozawa, T. (2011). Future projections of surface UV-B in a changing climate. *Journal of Geophysical Research* 116: D16. https://doi.org/10.1029/2011jd015749

Widel, M. (2012). Bystander effect induced by UV radiation; why should we be interested? *Advances in Hygiene & Experimental Medicine* 66: 828-837. https://doi.org/10.5604/17322693.1019532

Wiles, J. T., and Schurko, A. (2020). Identifying Prospective Genes That Function During DNA Repair in the Bdelloid Rotifer *Adineta vaga*. *The FASEB Journal*, 34(S1), 1-1. https://doi.org/10.1096/fasebj.2020.34.s1.06480

Williamson, C. E., Neale, P. J., Grad, G., De Lange, H. J., and Hargreaves, B. R. (2001). Beneficial and detrimental effect of UV on aquatic organisms: implication of spectral variation. *Ecol. Appl.* 11.6: 1843-1857. https://doi.org/10.1890/1051-0761(2001)011[1843:BADEOU]2.0.CO;2

Williamson, C. E., Neale, P. J., Hylander, S., Rose, K. C., Figueroa, F. L., Robinson, S. A., Häder, D.-P., Wangberg, S.-A., Worrest, R. C. (2019). The interactive effects of stratospheric ozone depletion, UV radiation, and climate change on aquatic ecosystems. *Photochemical & Photobiological Sciences* 18: 717-746. https://doi.org/10.1039/c8pp90062k

Williamson, C. E., Overholt, E. P., Brentrup, J. A., Pilla, R. M., Leach, T. H., Schladow, S. G. Warren, J. D., Urmy, S. S., Sadro, S., Chandra, S., and Neale, P. J. (2016). Sentinel responses to droughts, wildfires, and floods: effects of UV radiation on lakes and their ecosystem services. *Front. Ecol. Environ.* 14.2: 102-109. doi:10.1002/fee.1228

Williamson, C. E., Stemberger, R. S., Morris, D. P., Frost, T. M., & Paulsen, S. G. (1996). Ultraviolet radiation in North American lakes: attenuation estimates from DOC measurements and implications for plankton communities. *Limnology and Oceanography* 41: 1024-1034.

Williamson, C. E., Zagarese, H. E., Schulze, P. C., Hargreaves, B. R., & Seva, J. (1994). The impact of short-term exposure to UV-B radiation on zooplankton communities in north temperate lakes. *Journal of Plankton Research* 16: 205-218.

White, N. J., and Butlin, R. K. (2021). Multidimensional divergent selection, local adaptation, and speciation. *Evolution*, 75: 2167-2178. https://doi.org/10.1111/evo.14312

Wolf, R., Andersen, T., Hessen, D. O., Hylland, K., & Pfrender, M. (2017). The influence of dissolved organic carbon and ultraviolet radiation on the genomic integrity of *Daphnia magna*. *Functional Ecology* 31: 848-855. https://doi.org/10.1111/1365-2435.12730

Wolinski, L., Souza, M. S., Modenutti, B., & Balseiro, E. (2020). Effect of chronic UVR exposure on zooplankton molting and growth. *Environmental Pollution*, 267: 115448. https://doi.org/10.1016/j.envpol.2020.115448

Yampolsky, L. Y., Schaer, T. M., & Ebert, D. (2014). Adaptive phenotypic plasticity and local adaptation for temperature tolerance in freshwater zooplankton. Proceedings of the Royal Society B: Biological Sciences, 281: 20132744. http://dx.doi.org/10.1098/rspb.2013.2744

Yoshida, Y., Nowell, R. W., Arakawa, K., & Blaxter, M. (2019). Horizontal gene transfer in Metazoa: examples and methods. *Horizontal Gene Transfer: Breaking Borders Between Living Kingdoms*, 203-226. https://doi.org/10.1007/978-3-030-21862-1_7

Zhang, W., Lemmen, K. D., Zhou, L., Papakostas, S., & Declerck, S. A. (2019). Patterns of differentiation in the life history and demography of four recently described species of the Brachionus calyciflorus cryptic species complex. *Freshwater Biology*, 64: 1994-2005. https://doi.org/10.1111/fwb.13388

Zhu, L., Huang, R., Zhou, L., Xi, Y., & Xiang, X. (2021). Responses of the ecological characteristics and antioxidant enzyme activities in *Rotaria rotatoria* to UV-B radiation. *Hydrobiologia* 848.20: 4749-4761. https://doi.org/10.1007/s10750-021-04671-1

Appendix A: Impacts of two environmental stressors on a highly pigmented bdelloid rotifer additional data (Chapter 2)

Occurrence of pigmented bdelloids

Table S2.1. Summary of red-pigmented bdelloid rotifers and where they were found.

Species	Habitat	Reference
Adineta steineri Bartoš 1951	Fresh, moss, sandy, gravel	Plewka 2010
Adineta editae Iakovenko et al. 2015	Antarctica	Iakovenko et al. 2015
Adineta barbata Janson, 1893	Fresh, ephemeral, sediment	Jersabek et al. 2003
Adineta coatsae Iakovenko 2015	Antarctica	Iakovenko et al. 2015
Adineta grandis Murray 1910	Fresh, ephemeral, sediment	Iakovenko et al. 2015
Abrochtha intermedia Bauchamp 1909	Fresh, sediment, filamentous algae	Melone & Ricci 1995
Philidinavus paradoxus Murray 1905	Fresh, sediments, moss in lakes or rivers	Michael Plewka 2009
Habrotrocha angularis Murray 1910	Fresh, ephemeral, sediment	Michael Plewka 2012
Habrotrocha antartica Iakovenko et al. 2015	Antarctica	Iakovenko et al. 2015
Habrotrocha crenata Murray 1905	Fresh, ephemeral, sediment	Plewka 2013
Scepanotrocha rubra Bryce 1910	Marine, fungus, moss	Plewka 2012
Otostephanos jolantae Iakovenko 2013	Fresh, plants, moss	Iakovenko 2013
Otostephanos donneri Bartoš 1959	Fresh, ephemeral, detritus, moss	Plewka 2013
Macrotrachela papillosa Thompson 1859	Fresh, bog, moss	Plewka 2017
Macrotrachela jankoi Iakovenko et al. 2015	Antarctica	Iakovenko et al. 2015
Macrotrachela quadricornifera Milne 1886	Fresh, sphagnum and epiphytes	Jersabek et al. 2003
Dissotrocha hertzogi Koste 1996	Fresh, creek, moss, sediment	Segers 2007
Didymodactylos carnosus Milne 1916	Fresh, ephemeral, moss	Plewka 2016
Rotaria citrina Ehrenberg 1838	Fresh, detritus, periphyton	Plewka 2009
Rotaria rotatoria Pallas 1766	Permanent and ephemeral	Plewka 2016
Rotaria tardigrada Ehrenberg 1830	Fresh, moss, sediment	Plewka 2012
Rotaria sordida Western 1893	Marine, periphyton, sediment	Michael Plewka 2016
Rotaria macrura Schrank *1803*	Fresh, ephemeral	Michael Plewka 2012
Rotaria macroceros Gosse 1851	Marine, detritus	Martin Kreutz 2014
Rotaria magna-calcarata Parsons, 1892	Marine, detritus	Michael Plewka 2014
Philodina acuticornis odiosa Milne 1916	Freshwater, ephemeral pools, detritus	Michael Plewka 2020
Philodina flaviceps Bryce 1906	Fresh, moss in lotic water	Michael Plewka 2016
Philodina dartnallis Dartnall & Hollowday 1985	Fresh, sediments	Iakovenko et al. 2015
Philodina indica Murray 1906	Fresh, ephemeral, detritus, moss	Michael Plewka 2017
Philodina roseola Ehrenberg 1832	Fresh, ephemeral, detritus	Jersabek et al. 2003
Philodina rugosa coriacea Bryce 1903	Fresh, algae, fungus, moss	Michael Plewka 2009
Philodina vorax Janson 1893	Fresh, moss	Michael Plewka 2010
Philodina convergens Murray 1908	Fresh, detritus	Michael Plewka 2014
Philodina megalotrocha Ehrenberg 1832	Fresh, detritus, periphyton	Michael Plewka 2013
Philodina gregaria Murray 1910	Fresh, ephemeral, moss	Lukashanets et al. 2019
Philodina rugosa rugosa Bryce 1903	Fresh, ephemeral, moss	Michael Plewka 2012
Philodina tranquilla Wulfert 1942	Fresh, ephemeral, moss	Michael Plewka 2012
Pleuretra humerosa Murray 1905	Fresh, ephemeral, moss	Michael Plewka 2013
Pleuretra lineata Donner 1962	Fresh, ephemeral, moss	Michael Plewka 2012
Mniobia magna Plate 1889	Fresh, ephemeral, moss	Michael Plewka 2012
Mniobia obtusicornis Murray 1911	Fresh, ephemeral, moss	Iakovenko 2008
Mniobia russeola Zelinka 1891	Marine, bark, moss	Michael Plewka 2013
Mniobia scarlatina Ehrenberg 1853	Fresh, bark, moss	Michael Plewka 2017

Dissolved organic carbon (DOC) in Chihuahuan Desert Rock Pools

Table S2.2. GPS coordinates and elevation for rock pools that were sampled for this study.

Rock pool	**GPS coordinates** (decimal degrees)	**Elevation** (m)
Al	31.9475, -106.1911	1370
Edge	31.9244, -106.0425	1390
Enrique	31.9247, -106.0427	1370
Jamie	31.9244, -106.0422	1390
Luisa	31.9247, -106.0427	1380
Paw	31.9240, -106.0425	1390
Sergio	31.9247, -106.04	1370
Walsh	31.9247, -106.0427	1380
Heart	31.9248, -106.0427	1360
Kettle 4	31.9186, -106.0403	1380
North Temp	31.9247, -106.0425	1370
South Temp	31.9247, -106.0422	1370

Table S2.3. Tukey multiple comparison tests of dissolved organic carbon concentrations (DOC) for rock pools containing bdelloid rotifers. A general linear regression was performed to compare fluctuation of DOC during the monsoon (MS) or the dry season (DS), and to determine if DOC would predict in what rock pools highly pigmented (HP) or non-pigmented (NP) bdelloid rotifers would be found. Monsoon (M; mid-June – September) or dry (D; October to early June). a) Deviance residuals, b) T-test estimates using the *Bonferron*i correction

a)	**MIN**	**1Q**	**MEDIAN**	**3Q**	**MAX**
PIGMENTED	-9.68	-2.62	-0.58	1.84	16.50
b) coefficient	estimate				
intercept	11.5				
pigmented	-7.8				
monsoon	5.7				
pigment * monsoon	-3.2				

Degrees of Freedom: 82 Total (i.e., Null); 79 Residual, Null Deviance: 5698, Residual Deviance: 3233, AIC: 549.5

Degree of pigmentation

Table S2.4. Degree of pigmentation of xerosomes produced by *Philodina* sp. collected at Hueco Tanks State Park and Historic Site, El Paso Co., TX. To determine the concentration of red color in xerosome were analyzed using ImageJ version 1.33 with RGB plug-in. The number of pixels in the red channel were determiner for each pigmentation level, highly pigmented (HP) directly after collection, moderately pigmented (MP) 2 weeks after collection, lightly pigmented (LP) 4 weeks after collection, or non-pigmented (NP) over 20 weeks in culture. Range of pigmentation level was determined by total digital numbers (DN), the sum of the means of blue, green, and red channels DN per image analyzed. n = 50, mean and standard deviation (SD) are reported.

	RED DN	**GREEN DN**	**BLUE DN**	**TOTAL DN**
HP	164.1 ± 23.0	111.4 ± 18.2	81.2 ± 15.6	358.2 ± 50.9
MP	191.3 ± 18.9	159.4 ± 12.4	136.7 ± 13.0	486.2 ± 38.3
LP	200.5 ± 14.9	179.6 ± 15.1	58.2 ± 20.6	539.9 ± 49.5
NP	223.0 ± 13.4	208.2 ± 11.9	194.6 ± 10.6	618.3 ± 28.9

Table S2.5. Differences in pigment level of *Philodina* sp. xerosome. Images of xerosomes were transformed to digital numbers composed of blue, green, and red channels for each pigmentation level: highly pigmented (HP), moderately pigmented (MP) after collection, lightly pigmented (LP), or non-pigmented (NP) using ImageJ version 1.33 with RGB plug-in. Differences in channel per pigment levels were compared using a pairwise comparison (Tukey HSD).

Pigment			
HP - MP	HP - LP	HP - NP	LP-NP
MP - LP	MP - NP		
Channel			
red -DN			
Pigment : Channel			
HP:DN-HP:red	MP:DN-LP:red	LP:DN-LP:red	NP:DN-HP:DN
HP:DN-LP:red	MP:DN-MP:red	LP:DN-NP:red	NP:DN-HP:red
HP:DN-MP:red	MP:DN-NP:red	LP:red-HP:red	NP:DN-NP:red
HP:DN-NP:red	MP:red-HP:red	LP:red-MP:red	NP:red-HP:red
MP:DN-HP:DN	LP:DN-MP:DN	NP:DN-LP:DN	NP:red-LP:red
MP:DN-HP:red	LP:DN-MP:red	NP:DN-LP:red	NP:red-MP:red
LP:DN-HP:DN	NP:DN-MP:DN		

Pigmentation, Desiccation and UVR exposure- Odds Ratio analysis

Radiation intensities used in this study were based on global, daily erythemal UVR means in North America have been recorded since 1998 by National Renewable Energy Laboratory, the National Solar Radiation Database (Sengupta et al. 2018). This data was used to create a map of the summer daily mean UV radiation in the continental USA (S. Fig. 1). Direct Normal Irradiance (DNI) is the amount of solar radiation perpendicularly received in an area, peaked at high altitudes in the Southwestern USA, (8.4 $kWh/m^2/d^1$; S. Fig. 1). UVB intensity means ranged from 1.45 W/m^2 during winter to 3.55 W/m^2 for summer (Retrieved December 2019, Sengupta et al. 2018).

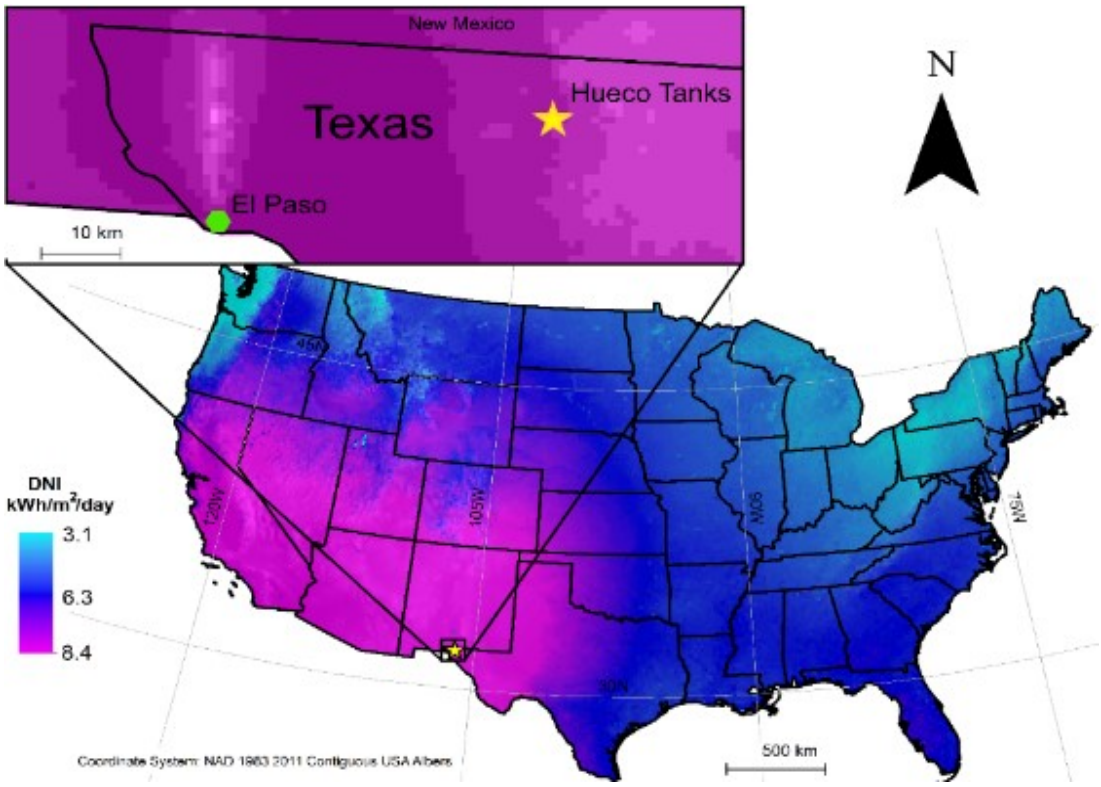

Figure S2.1. Ultraviolet radiation (UVR) intensities in the USA based on the seasonal UVR means from 1998 – 2018. The mean direct normal irradiance (DNI) was measured in $kWh/m^2/d^1$.

Explanatory variables that influence bdelloid survival, were identified used a logistic regression model, which was optimized using Fishers scoring technique. This was done using bdelloid survival as the result and pigmentation level, desiccation time, and UVB intensity as explanatory variables. The accuracy of the model as determined by receiver operating characteristic (ROC) curve was 0.86 and the calibration curve was 0.997. Supporting the use of the logistic regression model.

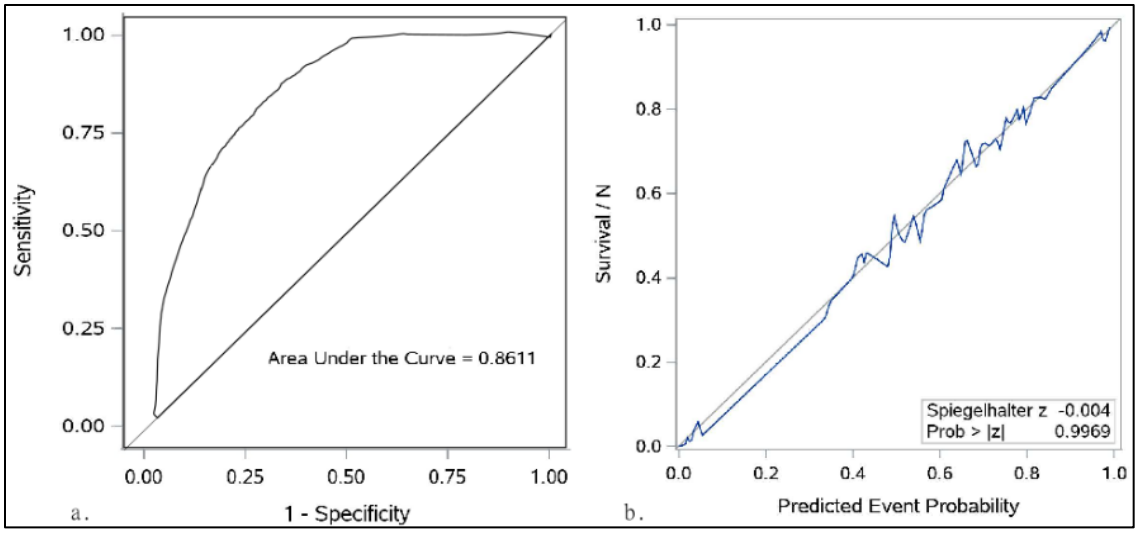

Figure S2.2. Accuracy and predictive power of the logistic regression model. **a.** Sensitivity analysis to determine the impact of pigment, desiccation time, and UVB intensity on bdelloid survival. Receiver operating characteristic (ROC) graphs are used to determine goodness of fit of the model, the area under the curve should be >80 for a model to be determined as reliable. **b.** A calibration curve was used to evaluate the predictive power of the logistic regression model to determine dead or alive status of the bdelloid rotifers, the ideal is a probability > 1.

Standardized Pearson residuals were used to detect influential observations. Replicates with a residue with > |3| are outliers and were omitted from visualizing analysis in main document.

Table S2.6. Outliers identified using Pearson residual values.

Treatment	Replicate	Survival rate	Pearson residue
HP0ctrl	1	0.94	-3.63
HP1ctrl	2	0.80	-4.48
HP1ctrl	4	0.82	-3.86
HP1mid	14	0.60	-3.23
HP32low	11	0.08	3.50
HP32low	14	0.10	3.12
MP1ctrl	5	1.00	-3.99
MP1ctrl	9	0.64	-3.59
MP1ctrl	0	0.66	-3.59
MP1ctrl	12	0.66	-3.73
MP7mid	7	0.26	3.09
MP32low	3	0.06	4.39
MP32low	5	0.08	3.09
MP32low	9	0.06	3.09
MP32mid	15	0.06	3.09
LP0ctrl	5	0.08	4.21
LP1ctrl	13	0.86	-4.99
LP1ctrl	2	0.56	-3.21
LP1ctrl	12	0.96	3.48
LP1ctrl	13	1.00	4.15

LP1ctrl	14	1.00	4.15
LP1ctrl	15	0.98	3.82
LP1ctrl	16	1.00	4.50
LP7ctrl	15	0.34	-3.28
LP7ctrl	16	0.32	-3.58
LP7low	2	0.24	-3.58
LP32mid	1	0.18	5.32
LP32mid	6	0.12	3.07
LP32mid	8	0.24	7.57
NP0ctrl	5	0.88	-4.62
NP0ctrl	8	0.86	-5.57
NP0ctrl	14	0.84	-5.52
NP0ctrl	15	0.90	-3.66
NP1ctrl	14	0.6	-3.82
NP1high	12	0.76	3.87
NP7mid	15	0.1	-3.93
NP32ctrl	4	0.3	9.53
NP32ctrl	5	0.36	11.73
NP32ctrl	6	0.32	10.26
NP32low	2	0.18	4.26
NP32mid	2	0.14	3.04

Table S2.7. Analysis of maximum likelihood estimates and Wald's Chi-square of *Philodina* sp. survival as a function of pigment level, as identified by a significant p-value of >0.05. SE = standard error; sq = square. df, degrees of freedom.

Treatment conditions			df	Estimate	SE	Wald chi-square	p-value
intercept			1	3.75	0.14	750.54	< 0.001
Pigmented	HP		1	0.87	0.12	52.61	< 0.001
Pigmented	MP		1	-0.23	0.11	4.77	0.03
Pigmented	LP		1	-0.16	0.10	2.44	0.12
Desiccation	1		1	-2.31	0.14	269.87	< 0.001
Desiccation	7		1	-3.58	0.14	685.17	< 0.001
Desiccation	32		1	-6.92	0.19	1343.06	< 0.001
UV	low		1	-2.42	0.14	292.11	< 0.001
UV	mid		1	-2.47	0.14	305.87	< 0.001
UV	high		1	-2.39	0.14	283.86	< 0.001
Pigmented Desiccation	HP	1	1	0.51	0.10	28.59	< 0.001
Pigmented Desiccation	HP	7	1	0.25	0.09	7.13	0.01
Pigmented Desiccation	HP	32	1	-1.60	0.20	62.33	< 0.001
Pigmented Desiccation	MP	1	1	0.46	0.09	28.62	< 0.001
Pigmented Desiccation	MP	7	1	0.88	0.09	-106.15	< 0.001
Pigmented Desiccation	MP	32	1	-1.12	0.22	25.23	< 0.001
Pigmented Desiccation	LP	1	1	-0.17	0.09	3.76	0.05
Pigmented Desiccation	LP	7	1	0.26	0.09	8.99	0.003
Pigmented Desiccation	LP	32	1	-0.21	0.16	1.70	0.19
Pigmented UV	HP	low	1	-0.40	0.11	12.59	< 0.001

Pigmented UV	MP	mid	1	-0.53	0.11	22.93	< 0.001
Pigmented UV	MP	high	1	-0.74	0.11	44.62	< 0.001
Pigmented UV	MP	low	1	-0.10	0.10	1.01	0.32
Pigmented UV	MP	mid	1	-0.01	0.10	0.00	0.95
Pigmented UV	LP	high	1	-0.28	0.10	7.64	0.01
Pigmented UV	LP	low	1	0.13	0.10	1.82	0.18
Pigmented UV	LP	mid	1	0.12	0.10	1.50	0.22
Pigmented UV	LP	high	1	-0.04	0.10	0.17	0.68
Desiccation UV	1	low	1	1.76	0.14	152.14	< 0.001
Desiccation UV	1	mid	1	1.47	0.14	-106.74	< 0.001
Desiccation UV	1	high	1	0.91	0.14	41.79	< 0.001
Desiccation UV	7	low	1	1.98	0.14	204.37	< 0.001
Desiccation UV	7	mid	1	1.74	0.14	157.98	< 0.001
Desiccation UV	7	high	1	1.54	0.14	124.61	< 0.001
Desiccation UV	32	low	1	2.66	0.20	173.66	< 0.001
Desiccation UV	32	mid	1	2.68	0.20	174.25	< 0.001
Desiccation UV	32	high	1	-10.95	93.94	0.01	0.91

Table S2.8. Odds ratio estimates for all pigmentation, desiccation and UVB survival data.

Pigment	Desiccation (days)	UVB	Estimates	95% confidence interval	
HP vs LP	32	control	0.7	0.5	1.0
HP vs LP	32	low	0.4	0.3	0.6
HP vs LP	32	mid	0.4	0.2	0.5
HP vs LP	32	high	0.4	0.2	0.5
HP vs MP	32	control	1.9	1.1	3.1
HP vs MP	32	low	1.4	0.8	2.3
HP vs MP	32	mid	1.1	0.7	1.8
HP vs MP	32	high	1.2	0.7	1.9
HP vs NP	32	control	0.5	0.3	0.7
HP vs NP	32	low	0.3	0.2	0.5
HP vs NP	32	mid	0.3	0.2	0.4
HP vs NP	32	high	0.2	0.2	0.3
LP vs NP	32	control	0.7	0.5	0.9
LP vs NP	32	low	0.8	0.6	1.1
LP vs NP	32	mid	0.8	0.6	1.0
LP vs NP	32	high	0.7	0.5	0.9
MP vs LP	32	control	0.4	0.2	0.6
MP vs LP	32	low	0.3	0.2	0.5
MP vs LP	32	mid	0.3	0.2	0.5
MP vs LP	32	high	0.3	0.2	0.5
MP vs NP	32	control	0.3	0.2	0.4
MP vs NP	32	low	0.2	0.2	0.4
MP vs NP	32	mid	0.3	0.2	0.4
MP vs NP	32	high	0.2	0.1	0.3

HP	32	low vs control	0.9	0.6	1.2
HP	32	mid vs control	0.7	0.5	1.0
HP	32	high vs control	<0.001	<0.001	>999
HP	32	low vs mid	1.2	0.9	1.6
HP	32	low vs high	>999	<0.001	>999
HP	32	mid vs high	>999	<0.001	>999
MP	32	low vs control	1.2	0.8	1.6
MP	32	mid vs control	1.2	0.9	1.7
MP	32	high vs control	<0.001	<0.001	>999
MP	32	low vs mid	0.9	0.7	1.3
MP	32	low vs high	>999	<0.001	>999
MP	32	mid vs high	>999	<0.001	>999
LP	32	low vs control	1.5	1.0	2.0
LP	32	mid vs control	1.4	1.0	1.9
LP	32	high vs control	<0.001	<0.001	>999
LP	32	low vs mid	1.1	0.8	1.4
LP	32	low vs high	>999	<0.001	>999
LP	32	mid vs high	>999	<0.001	>999
NP	32	low vs control	1.3	0.9	1.7
NP	32	mid vs control	1.2	0.9	1.7
NP	32	high vs control	<0.001	<0.001	>999
NP	32	low vs mid	1.0	0.8	1.4
NP	32	low vs high	>999	<0.001	>999
NP	32	mid vs high	>999	<0.001	>999
HP	1 vs 32	control	833.4	570.4	>999
HP	1 vs 32	low	339.5	233.2	494.3
HP	1 vs 32	mid	248.1	169.6	363.0
HP	1 vs 32	high	>999	<0.001	>999
LP	1 vs 32	control	105.3	76.9	144.2
LP	1 vs 32	low	42.9	32.2	57.2
LP	1 vs 32	mid	31.4	23.5	41.9
LP	1 vs 32	high	>999	<0.001	>999
MP	1 vs 32	control	489.8	318.9	752.3
MP	1 vs 32	low	199.5	131.5	302.8
MP	1 vs 32	mid	145.8	96.3	220.8
MP	1 vs 32	high	>999	<0.001	>999
NP	1 vs 32	control	100.8	75.1	135.2
NP	1 vs 32	low	41.1	31.3	53.8
NP	1 vs 32	mid	30.0	22.8	39.4
NP	1 vs 32	high	>999	<0.001	>999
HP	7 vs 32	control	177.8	123.3	256.3
HP	7 vs 32	low	90.0	62.3	130.0
HP	7 vs 32	mid	69.4	47.7	100.9
HP	7 vs 32	high	>999	<0.001	>999
LP	7 vs 32	control	45.1	33.1	61.5
LP	7 vs 32	low	22.9	17.2	30.4
LP	7 vs 32	mid	17.6	13.2	23.5
LP	7 vs 32	high	>999	<0.001	>999

MP	7 vs 32	control	207.1	135.5	316.5
MP	7 vs 32	low	104.9	69.3	158.7
MP	7 vs 32	mid	80.9	53.5	122.2
MP	7 vs 32	high	>999	<0.001	>999
NP	7 vs 32	control	28.1	21.1	37.4
NP	7 vs 32	low	14.2	10.9	18.6
NP	7 vs 32	mid	11.0	8.3	14.4
NP	7 vs 32	high	>999	<0.001	>999
HP	32 vs 0	control	<0.001	<0.001	<0.001
HP	32 vs 0	low	0.0	0.0	0.0
HP	32 vs 0	mid	0.0	0.0	0.0
HP	32 vs 0	high	<0.001	<0.001	>999
LP	32 vs 0	control	<0.001	<0.001	0.0
LP	32 vs 0	low	0.0	0.0	0.0
LP	32 vs 0	mid	0.0	0.0	0.0
LP	32 vs 0	high	<0.001	<0.001	>999
MP	32 vs 0	control	<0.001	<0.001	<0.001
MP	32 vs 0	low	0.0	0.0	0.0
MP	32 vs 0	mid	0.0	0.0	0.0
MP	32 vs 0	high	<0.001	<0.001	>999
NP	32 vs 0	control	<0.001	<0.001	0.0
NP	32 vs 0	low	0.0	0.0	0.0
NP	32 vs 0	mid	0.0	0.0	0.0
NP	32 vs 0	high	<0.001	<0.001	>999

Appendix B: Local adaptation? Enhanced fitness under regional UVB intensities in a rock pool bdelloid rotifer (Chapter 3)

Generational UVB exposure

Table S3.1. Three nonconsecutive generations of *Philodina* sp. were exposed to low, mid, high UVB intensity (*1.3*, 3.7, or 5.0 W/m^2) and a no UVB control. The offspring of exposed mother were used for life table (LT) experiments.

	control	low	mid	high
Collected	2/14/2020	1/24/2021	10/29/2020	9/10/2019
F_0 exposed	2/16/2020	1/27/2021	11/2/2020	9/15/2019
F_1 – LT	2/24/2020	2/5/2021	11/9/2020	9/21/2019
F_2 exposed	4/1/2020	2/20/2021	11/30/2020	10/22/2019
F_3 hatched	5/10/2020	2/27/2021	12/9/2020	10/30/2019
F_4 exposed	5/27/2020	4/12/2021	1/11/2021	11/27/2019
F_5 – LT	6/1/2020	4/20/2021	1/19/2021	12/05-18/2019*

* F_5 bdelloids in the high UVB treatment began to hatch on 12/05/2019. It took nearly 2 weeks for 60 individuals to hatch, due to the slow reproduction F_5 high UVB life table experiments were not carried out.

Table S3.2. Pigmentation levels in *Philodina* sp. xerosomes. Images of xerosomes were captured and analyzed using # of pixels of the red channel in each image. Pigment levels were determined based on % red digital number (DN)); highly pigmented (HP: > 45%), moderately (MP: 38 – 42%), lightly pigmented (LP: 36 – 37.4%), and non-pigmented (NP: <36). n = 25, means ± standard deviation (SD) is reported.

Pigment	Mean ± SD total DN	Mean ± SD red DN	% red DN	Pigment level
F_0	367.9 ± 31	172.1 ± 26	46.8	HP
F_2	419.8 ± 26	157.1 ± 15	37.4	MP/LP
F_4	642.3 ± 12	227.9 ± 18	35.5	LP/NP

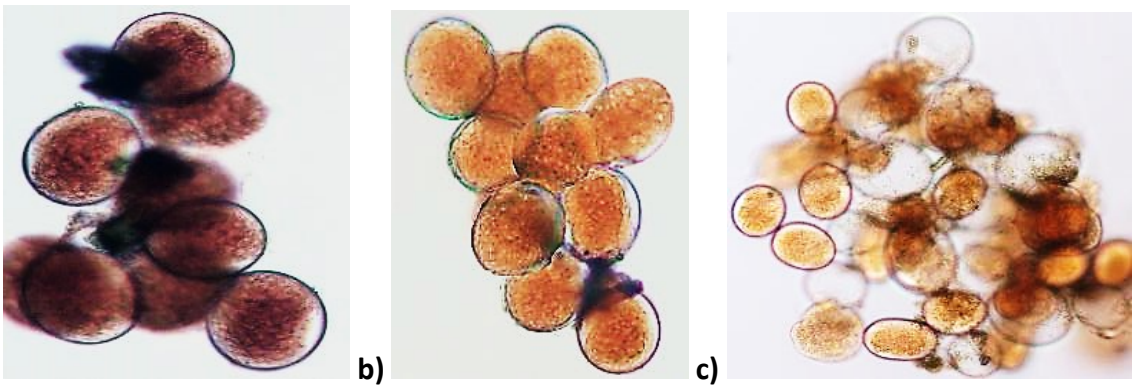

Figure S3.1: Pigmented eggs. Eggs were laid by F_0 generation **a)** 1st week in culture **b)** 2nd week in culture, **c)** pigmented neonates and leave behind clear eggshells.

Table S3.3. Pairwise comparison of survival of. *Philodina* sp. survival post exposure to 0, 1.3, 3.7, or 5.0 W/m^2 of UVB intensity, of three non-consecutive generations (F_0, F_2, F_4) using Tukey tests.

Generation	**diff**	**lwr**	**upr**	**p adj**
F2-F0	-0.0527	-0.09056	-0.01485	0.0034851
F4-F0	-0.15491	-0.19277	-0.11706	0.0000000
F4-F2	-0.10221	-0.14215	-0.06227	0.0000000
UVB	**diff**	**lwr**	**upr**	**p adj**
130-0	-0.2352	-0.28038	-0.19001	0.0000000
370-0	-0.35435	-0.39953	-0.30916	0.0000000
500-0	-0.2998	-0.35679	-0.24281	0.0000000
370-130	-0.11915	-0.16434	-0.07397	0.0000000
500-130	-0.0646	-0.1216	-0.00761	0.0193751
500-370	0.054546	-0.00245	0.111537	0.0661268
Generation: UVB	**diff**	**lwr**	**upr**	**p adj**
F2:0-F0:0	0.019927	-0.08008	0.119935	0.9999516
F4:0-F0:0	-0.02564	-0.12565	0.074365	0.9994336
F0:130-F0:0	-0.15957	-0.25957	-0.05956	0.0000256
F2:130-F0:0	-0.21899	-0.319	-0.11898	0.0000000
F4:130-F0:0	-0.33274	-0.43275	-0.23273	0.0000000
F0:370-F0:0	-0.19805	-0.29805	-0.09804	0.0000000
F2:370-F0:0	-0.31649	-0.4165	-0.21648	0.0000000
F4:370-F0:0	-0.55422	-0.65422	-0.45421	0.0000000
F0:500-F0:0	-0.21399	-0.314	-0.11398	0.0000000
F2:500-F0:0	-0.57566	-0.75362	-0.39769	0.0000000
F4:500-F0:0	-0.19566	-0.37362	-0.01769	0.0180321
F4:0-F2:0	-0.04557	-0.14558	0.054438	0.9350908
F0:130-F2:0	-0.17949	-0.2795	-0.07949	0.0000011
F2:130-F2:0	-0.23892	-0.33893	-0.13891	0.0000000

F4:130-F2:0	-0.35267	-0.45268	-0.25266	0.0000000
F0:370-F2:0	-0.21797	-0.31798	-0.11797	0.0000000
F2:370-F2:0	-0.33642	-0.43643	-0.23641	0.0000000
F4:370-F2:0	-0.57414	-0.67415	-0.47414	0.0000000
F0:500-F2:0	-0.23392	-0.33393	-0.13391	0.0000000
F2:500-F2:0	-0.59559	-0.77355	-0.41762	0.0000000
F4:500-F2:0	-0.21559	-0.39355	-0.03762	0.0049956
F0:130-F4:0	-0.13392	-0.23393	-0.03392	0.0009916
F2:130-F4:0	-0.19335	-0.29336	-0.09334	0.0000001
F4:130-F4:0	-0.3071	-0.40711	-0.20709	0.0000000
F0:370-F4:0	-0.1724	-0.27241	-0.0724	0.0000034
F2:370-F4:0	-0.29085	-0.39086	-0.19084	0.0000000
F4:370-F4:0	-0.52857	-0.62858	-0.42857	0.0000000
F0:500-F4:0	-0.18835	-0.28836	-0.08834	0.0000002
F2:500-F4:0	-0.55002	-0.72798	-0.37205	0.0000000
F4:500-F4:0	-0.17002	-0.34798	0.007949	0.0758993
F2:130-F0:130	-0.05943	-0.15943	0.040582	0.7112685
F4:130-F0:130	-0.17318	-0.27318	-0.07317	0.0000030
F0:370-F0:130	-0.03848	-0.13849	0.061528	0.9808341
F2:370-F0:130	-0.15693	-0.25693	-0.05692	0.0000381
F4:370-F0:130	-0.39465	-0.49466	-0.29464	0.0000000
F0:500-F0:130	-0.05443	-0.15443	0.045582	0.8121804
F2:500-F0:130	-0.41609	-0.59406	-0.23813	0.0000000
F4:500-F0:130	-0.03609	-0.21406	0.141873	0.9999423
F4:130-F2:130	-0.11375	-0.21376	-0.01374	0.0118439
F0:370-F2:130	0.020946	-0.07906	0.120954	0.9999204
F2:370-F2:130	-0.0975	-0.19751	0.002508	0.0634106
F4:370-F2:130	-0.33522	-0.43523	-0.23522	0.0000000
F0:500-F2:130	0.005	-0.09501	0.105008	1.0000000
F2:500-F2:130	-0.35667	-0.53463	-0.1787	0.0000000
F4:500-F2:130	0.023333	-0.15463	0.201298	0.9999994
F0:370-F4:130	0.134696	0.034689	0.234704	0.0008949
F2:370-F4:130	0.01625	-0.08376	0.116258	0.9999940
F4:370-F4:130	-0.22147	-0.32148	-0.12147	0.0000000
F0:500-F4:130	0.11875	0.018742	0.218758	0.0066506
F2:500-F4:130	-0.24292	-0.42088	-0.06495	0.0007023
F4:500-F4:130	0.137083	-0.04088	0.315048	0.3138924
F2:370-F0:370	-0.11845	-0.21845	-0.01844	0.0068929
F4:370-F0:370	-0.35617	-0.45618	-0.25616	0.0000000
F0:500-F0:370	-0.01595	-0.11595	0.084061	0.9999950

F2:500-F0:370	-0.37761	-0.55558	-0.19965	0.0000000
F4:500-F0:370	0.002387	-0.17558	0.180352	1.0000000
F4:370-F2:370	-0.23772	-0.33773	-0.13772	0.0000000
F0:500-F2:370	0.1025	0.002492	0.202508	0.0391662
F2:500-F2:370	-0.25917	-0.43713	-0.0812	0.0001985
F4:500-F2:370	0.120833	-0.05713	0.298798	0.5140242
F0:500-F4:370	0.340223	0.240216	0.440231	0.0000000
F2:500-F4:370	-0.02144	-0.19941	0.156522	0.9999997
F4:500-F4:370	0.358557	0.180592	0.536522	0.0000000
F2:500-F0:500	-0.36167	-0.53963	-0.1837	0.0000000
F4:500-F0:500	0.018333	-0.15963	0.196298	1.0000000
F4:500-F2:500	0.38	0.149042	0.610958	0.0000119

Post-Hoc Analysis of bdelloids fed daily

Table S3.4. Cox proportional hazards regression analysis. Results show the effects of parental exposure low, mid, or high UVB (1.3, 3.7, or 5.0 W/m^2). Results are given on the log (not the response) scale; p-value adjustment: Tukey method for comparing a family of 4 estimates. a) compared to F_1 control. b) comparing F_5 to F_1 generation. df = degrees of freedom; Inf= infinite number the model complex, allowing it to fit the data very closely; ND = no data

a)

coefficient ± SE		z value	Pr(>|z|)
Gen	-1.6. ± 1.0	-1.621	0.105
F1 low	-24.5 ± 9.6 E3	-0.003	0.998
F_1 mid	-1.9 ± 1.1	-1.071	0.081
F_1 high	22.1 ± 2.3 E4	0.001	0.999
F_5l ow	2.5 ± 1.3	2.017	0.044
F_5 mid	-19.9 ± 9.6 E3	-0.002	0.998
F_5 high	ND	ND	ND

b) F_5 v F_1

	estimate ± SE	df	z ratio	p value
control	1.6 ± 1.0	Inf	1.621	0.105
low	-0.9 ± 0.7	Inf	-1.201	0.229
mid	21.5 ± 1.2	Inf	0.002	0.998
high	-1.6 ± 1.0	Inf	1.621	0.105

c)

F_1					F_5				
	estimate ± SE	df	z ratio	p value	contrast	estimate ± SE	df	z ratio	p value
control - low	5.7 ± 1.6	Inf	3.53	0.002	control - low	6.1 ± 1.7	Inf	3.58	0.002
control - mid	1.9 ± 1.2	Inf	1.59	0.38	control - mid	5.0 ± 1.6	Inf	3.08	0.01
control - high	-0.7 ± 0.9	Inf	-0.80	0.86	control - high	-20.5 ± 7E3	Inf	-0.003	1.000
low - mid	-3.8 ± 1.3	Inf	-2.93	0.018	low - mid	-1.1 ± 0.7	Inf	-1.44	0.475
low - high	-6.4 ± 1.7	Inf	-3.85	0.001	low - high	-26.5 ± 7E3	Inf	-0.004	1.00

mid - high	-2.6 ± 1.3	Inf	-2.06	0.17	mid - high	-25.4 ± 7E3	Inf	-0.004	1.000

Table S3.5. General linear model of *Philodina* sp. life history traits. Analysis of mean lifespan, generation time, net reproductive rate, intrinsic rate of change of F_1 and F_5 generations. After maternal exposure to UVB radiation, intensities used were low, mid, or high UVR (l1.3, 3.7, or 5.0 W/m^2) and a no UVB control. df = degrees of freedom; Inf= infinite number the model complex, allowing it to fit the data very closely; ND = no data

	F_1				F_5			
	Lifespan (days)							
	estimate (SE)	df	z ratio	p-value	estimate (SE)	df	z ratio	p-value
control - low	23 ± 0.6	Inf	0.003	<0.0001	20 ± 0.8	0.003	Inf	<0.0001
control - mid	2 ± 0.5	Inf	1.745	0.0003	20 ± 0.8	0.003	Inf	<0.0001
control - high	ND	ND	ND	ND	ND	ND	ND	ND
low - mid	-21 ± 0.8	Inf	-0.003	<0.0001	-0.2 ± 1.1	-0.327	Inf	0.98
low - high	ND	ND	ND	ND	ND	ND	ND	ND
mid - high	ND	ND	ND	ND	ND	ND	ND	ND
	Generation time (T, days)							
control - low	5 ± 1.1	Inf	4.90	< 0.0001	21 ± 6.5E8	Inf	0.003	1.00
control - mid	3 ± 1.0	Inf	3.09	0.01	22 ± 6.5E8	Inf	0.003	1.00
control - high	-0.2 ± 0.8	Inf	-0.21	1.00	nonEst	ND	ND	ND
low - mid	-2 ± 0.8	Inf	-2.44	0.07	0.5 ± 0.7	Inf	1.074	0.71
low - high	-5. ± 1.0	Inf	-5.19	< 0.0001	nonEst	ND	ND	ND
mid - high	-3 ± 1.0	Inf	-3.35	0.004	nonEst	ND	ND	ND
	Net reproductive rate (avg offspring per female)							
contrast	estimate (SE)	df	t ratio	p.value	estimate (SE)	df	t ratio	p.value
control - low	-23 ± 1.9	39.9	-12.08	<.0001	-5 ± 1.9	39.9	-2.64	*0.055*
control - mid	-20 ± 2.1	39.9	-9.44	<.0001	-8 ± 1.9	39.9	-4.45	0.0004
control - high	1 ± 2.1	39.9	0.53	0.95	ND	ND	ND	ND
low - mid	3 ± 1.9	39.9	1.52	0.44	-3 ± 1.6	39.9	-2.092	0.17
low - high	24 ± 1.9	39.9	12.67	<.0001	ND	ND	ND	ND
mid - high	21 ± 2.1	39.9	9.97	<.0001	ND	ND	ND	ND
	Rate of change (change in population size)							
control - low	0.06 ± 0.04	32	1.31	0.57	0.07 ± 0.04	32.0	1.54	0.42
control - mid	0.03 ± 0.05	32	0.58	0.94	0.07 ± 0.04	32.0	1.58	0.40
control - high	-0.12 ± 0.05	32	-2.35	0.11	ND	ND	ND	ND
low - mid	-0.03 ± 0.04	32	-0.65	0.91	0.002 ± 0.04	32.0	0.05	1.00
low - high	-0.18 ± 0.04	32	-3.93	0.002	ND	ND	ND	ND
mid - high	-0.15 ± 0.05	32	-2.93	0.03	ND	ND	ND	ND

*Cox proportional-Hazards Model used for analysis; results are given on the log (not the response) scale; p-value adjustment: Tukey method for comparing a family of 4 estimates

**Linear model used for analysis; degrees-of-freedom method: Kenward-roger comparing a family of 4 estimates; p- value adjustment: Tukey method for n = 53 (7 observations deleted due to missingness).

NOT Fed life histories

To ensure the results recorded were not affected by the food source, non-fed replicates for each treatment were conducted simultaneously with the fed treatments. Similar patterns were seen in the NF treatments when comparing life history traits to the no UVB control. Lifespan and net reproductive rate increased in the low and mid UVB treatments when compared to the no UVB control. The primary exception being seen in the control. Lifespan increased in the F_5 control when compared to the F_1 generation in the fed treatments, this was not the case in the not fed counterpart.

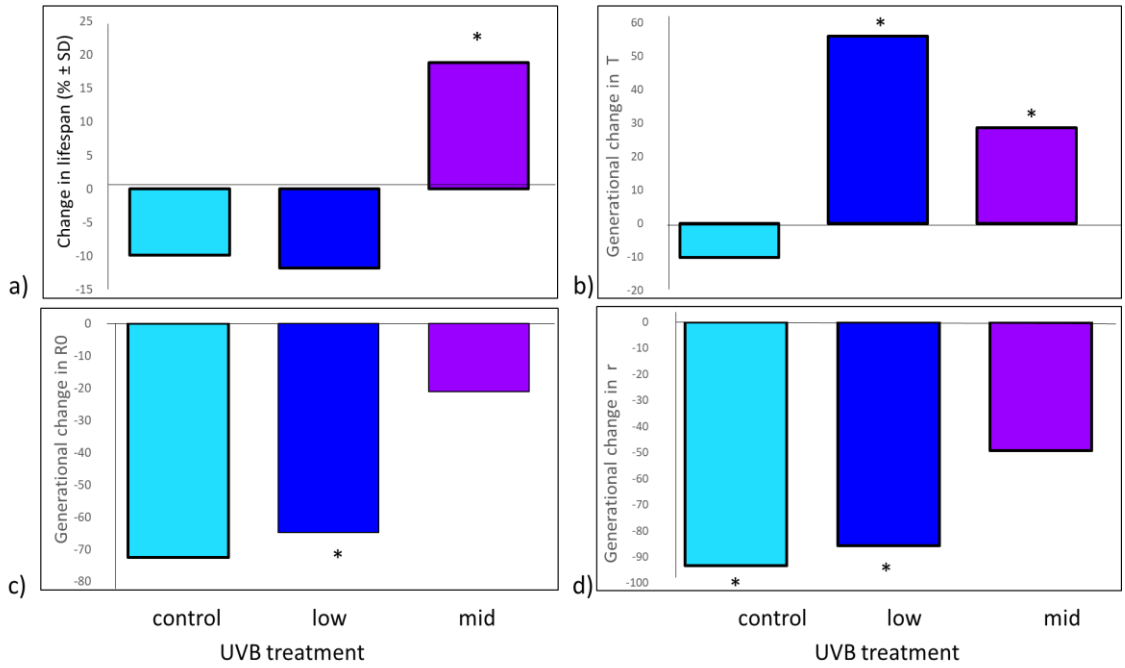

Figure S3.2. Generational differences in life history traits of *Philodina* sp. Life history traits were recorded for after maternal exposure to low, mid, high and a control UVB radiation (0, low, 3.7, or 5.0 W/m^2) for three non-consecutive generations a) lifespan b) net reproductive rate (R_0), c) generation time (T), d) intrinsic rate of change (*r*). Inf= infinite number the model complex, allowing it to fit the data very closely.

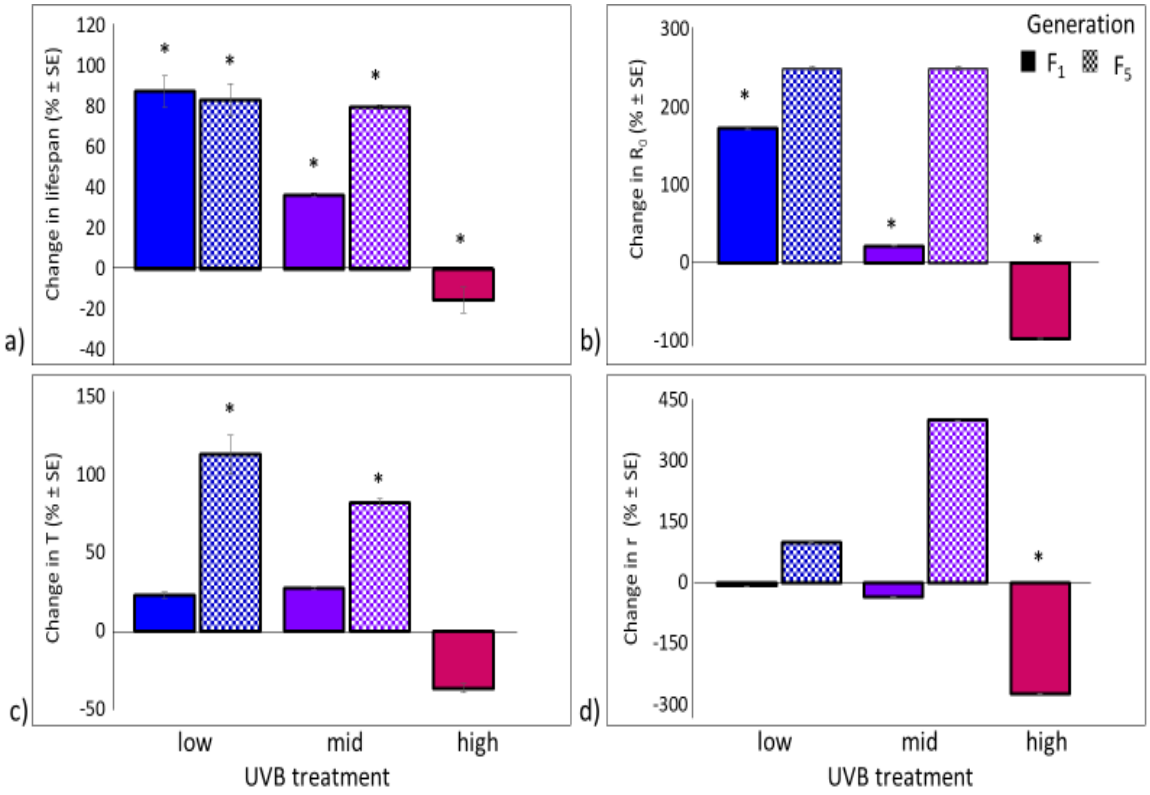

Figure S3.3. Differences in life history traits of *Philodina* sp. After exposure of one or three nonconsecutive maternal generations, life histories of F1 and F5 generation were recorded. Intensities comparable to regional levels of UVB were used. low, mid, high UVB radiation (0, 1.3, 3.7, or 5.0 W/m^2), and control. a) lifespan b) net reproductive rate (R_0), c) generation time (T), d) intrinsic rate of change (*r*).

Table S3.6. Post-hoc test of general linear model of Philodina sp. demographics. Analysis of mean lifespan, generation time, net reproductive rate, intrinsic rate of change of F1 and F5 generations. After maternal exposure to UVB radiation, intensities used were low, mid, or high UVR (l1.3, 3.7, or 5.0 W/m2) and a no UVB control. Linear model used for analysis; degrees-of-freedom method: Kenward-Roger comparing a family of 4 estimates; p- value adjustment: Tukey method for n = 53 number of events= 53 (7 observations deleted due to missingness). Inf = infinite number of degrees of freedom; ND = no data

		coef ±SE	exp(coef)	z value	Pr (>|z|)			estimate ±SE	t value	Pr (>|z|)
lifespan						**R_0****	Intercept	4.03 ± 1.0	3.944	< 0.0001
	Gen	0.7 ± 1	2.01	-3.19	0.001		Gen	-2.9 ± 1.4	-2.021	0.057
	low	-5.7 ± 2	0.003	-39.03	<0.0001		low	7.0 ± 1.3	5.395	< 0.0001
	mid	-1.8 ± 2	0.16	-3.90	<0.0001		mid	0.9 ± 1.4	0.614	0.546
	high	-	-	-	-		high	-3.9 ± 1.4	-2.712	0.013
	Gen: low	-0.4 ± 1	0.68	4.28	<0.0001		Gen: low	-4.2 ± 1.8	-2.298	0.032
	Gen: mid	-3.2 ± 2	0.04	-31.09	<0.0001		Gen: mid	1.9 ± 1.9	-0.973	0.342
	Gen: high	N/A	ND	ND	ND		Gen: high	ND	ND	ND
T*						**r****	Intercept	0.12 ± 0.04	2.912	< 0.0001
	Gen	1.4 ± 1.0	4.15	1.46	0.14		Gen	0.12 ± 0.04	-5.686	0.074
	low	0.2 ± 0.8	1.18	0.20	0.84		low	-0.11 ± 0.06	-1.894	0.561
	mid	0.3 ± 0.9	1.31	0.29	0.77		mid	0.03 ± 0.06	0.592	0.676
	high	2.3 ± 1.1	9.51	2.02	0.04		high	-0.03 ± 0.07	-0.424	<0.0001
	Gen: low	-3.9 ± 1.5	0.02	-2.57	0.01		Gen: low	-0.02 ± 0.08	-0.273	0.788

	Gen: mid	-3.0 ± 1.5	0.05	-2.11	0.04	Gen: mid	0.07 ± 0.08	-0.862	0.399
	Gen: high	N/A	ND	ND	ND	Gen: high	ND	ND	ND

Table S3.7. Post-hoc analysis of Cox proportional-Hazards regression of lifespan and generation time (T). After parental exposure low, mid, or high UVB (1.3, 3.7, or 5.0 W/m2). N/A – data not recorded due to low reproduction of F4. Results are given on the log (not the response) scale; p-value adjustment: Tukey method for comparing a family of 4 estimates. a) compared to UVB treatments, b) comparing F_5 to F_1 generation. . df = degrees of freedom; Inf= infinite number the model complex, allowing it to fit the data very closely; ND = no data

a) F_5 v F_1

	contrast	estimate ± SE	df	z ratio	p value
Lifespan	control	-0.65 ± 0.9	Inf	-0.712	0.476
	low	-0.31 ± 0.7	Inf	-0.462	0.644
	mid	2.46 ± 1.2	Inf	2.049	0.041
	high	-20.3 ± 7E3	Inf	-0.003	0.998
T*	control	-2.2 ± 1.3	Inf	1.715	0.09
	low	-2.0 ± 0.9	Inf	-2.821	0.023
	mid	-3.4 ± 1.0	Inf	-3.35	0.004
	high	non-Est	NA	NaN	NA

b)

	F_1 contrast	estimate ± SE	df	t ratio	p value	F_5 contrast	estimate ± SE	df	z ratio	p value
Lifespan*	control - low	5.7 ± 1.6	Inf	3.53	0.001	control - low	6.1 ± 1.7	Inf	3.58	0.001
	control - mid	1.9 ± 1.2	Inf	1.59	0.38	control - mid	5.0 ± 1.6	Inf	3.08	0.01
	control - high	-0.7 ± 0.9	Inf	-0.80	0.86	control - high	-	-	-	-
	low - mid	-3.8 ± 1.3	Inf	-2.93	0.018	low - mid	-1.1 ± 0.7	Inf	-1.44	0.32
	low - high	-6.4 ± 1.7	Inf	-3.85	0.001	low - high	-	-	-	-
	mid - high	-2.6 ± 1.3	Inf	-2.06	0.17	mid - high	-	-	-	-
T*	control - low	-0.2 ± 0.82	Inf	-0.20	0.99	control - low	3.8 ± 1.2	Inf	3.21	0.01
	control - mid	-0.3 ± 0.92	Inf	-0.29	0.99	control - mid	2.8 ± 1.0	Inf	3.90	0.02
	control - high	-2.3 ± 1.1	Inf	-2.02	0.18	control - high	nonEst	NA	NA	NA
	low - mid	-0.11 ± 0.7	Inf	-0.142	0.99	low - mid	-1.1 ± 0.9	Inf	-1.12	0.68
	low - high	-2.1 ± 1.0	Inf	-2.12	0.14	low - high	nonEst	NA	NA	NA
	mid - high	-2.0 ± 1.1	Inf	-1.89	0.23	mid - high	nonEst	NA	NA	NA

Table S3.8. Post-hoc test of general linear model of Philodina sp. demographics. Analysis of mean lifespan, generation time, net reproductive rate, intrinsic rate of change of F1 and F5 generations. After maternal exposure to UVB radiation, intensities used were low, mid, or high UVR (l1.3, 3.7, or 5.0 W/m^2) and a no UVB control. Linear model used for analysis; degrees-of-freedom method: Kenward-roger.) compared to UVB treatments, b) comparing F_5 to F_1 generation. . df = degrees of freedom; Inf= infinite number the model complex, allowing it to fit the data very closely; ND = no data

a) F_5 v F_1

	contrast	estimate ± SE	df	t ratio	p value
R_0	control	2.93 ± 1.5	20	2.021	0.056
	low	7.13 ± 1.12	20	6.362	<0.0001
	mid	1.04 ± 1.29	20	-0.801	0.433
	high	non-Est	20	NA	NA
r	control	0.11 ± 0.06	19	1.894	0.074
	low	0.13 ± 0.05	19	2.89	0.009
	mid	0.04 ± 0.05	19	0.824	0.420

	high	non-Est	NA	NA	NA				
	F_1					F_5				
b)	contrast	estimate ± SE	df	t ratio	p value	contrast	estimate ± SE	df	t ratio	p value
R_0	control - low	-7.0 ± 1.3	20	-5.395	0.0002	control - low	-2.8 ± 1.3	20	-1.48	0.46
	control - mid	-0.9 ± 1.5	20	-0.614	0.926	control - mid	-2.8 ± 1.3	20	-1.48	0.46
	control - high	3.9 ± 1.5	20	1650	0.060	control - high	nonEst	NA	NA	NA
	low - mid	6.1 ± 1.3	20	3.278	0.0007	low - mid	0.000	20	0	1.00
	low - high	10.9 ± 1.3	20	12.707	<0.0001	low - high	nonEst	NA	NA	NA
	mid - high	4.8 ± 1.5	20	8.434	0.016	mid - high	nonEst	NA	NA	NA
r	control - low	-0.03± 0.05	19	-0.592	0.933	control - low	-0.01 ± 0.05	19	-0.206	0.997
	control - mid	0.03 ± 0.06	19	0.424	0.974	control - mid	-0.04 ± 0.05	19	-0.820	0.844
	control - high	0.38 ± 0.07	19	5.686	0.0001	control - high	nonEst	NA	NA	NA
	low - mid	0.41 ± 0.06	19	1.065	0.714	low - mid	-0.03 ± 0.05	19	-0.709	0.892
	low - high	0.41 ± 0.06	19	6.720	<0.0001	low - high	nonEst	NA	NA	NA
	mid - high	0.36 ± 0.07	19	5.307	0.0002	mid - high	nonEst	NA	NA	NA

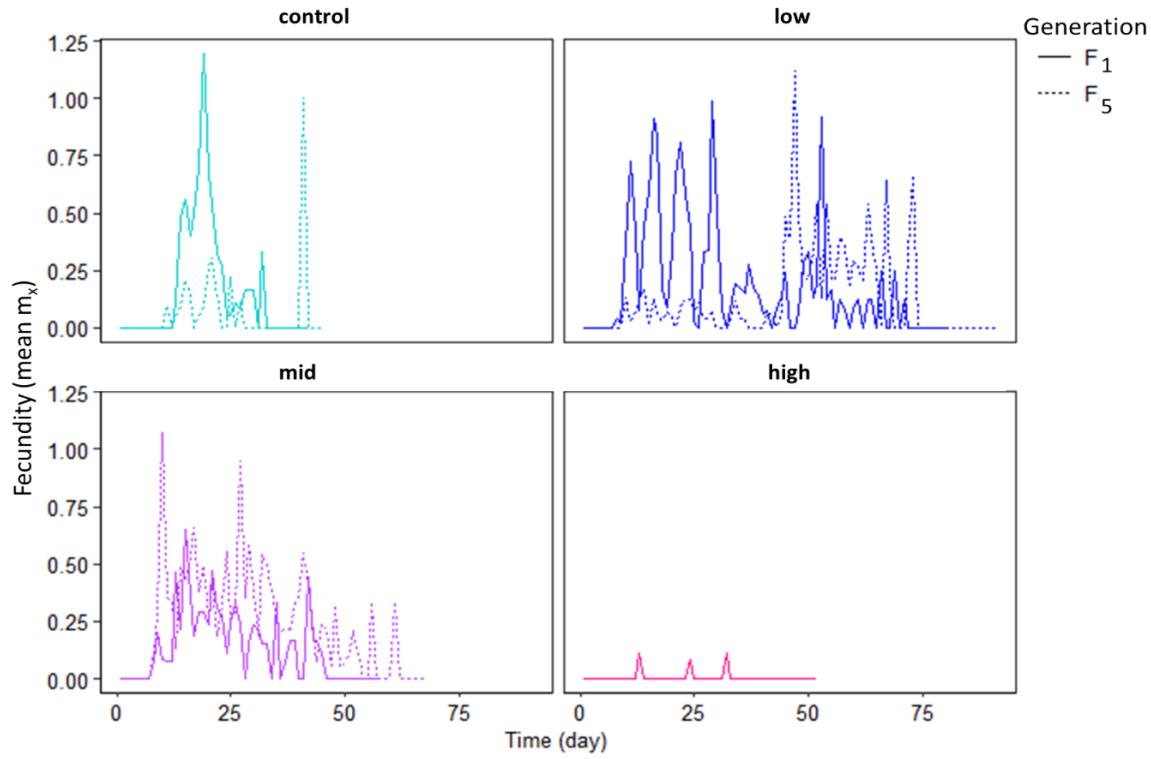

Figure S3.4. The effects of maternal *Philodina* sp. UVB exposure on age-specific survivorship and fecundity per female. Effects of F_0, F_2 and F_4 UVB exposure (low, mid, and high UVB radiation, 1.3, 3.7, or 5.0 W/m^2, respectively) and a no UVB control, on offspring (F_1 and F_5).

Bdelloid life history traits based on life table experiments

Table S3.9. Life history traits of 17 bdelloid rotifer gathered from various sources. Temperatures used for experiment are maintained on a 16L:8D [a:] 4 ˚C, [b:] 20 ˚C, [c:]22 ˚C, [d:]23 ˚C, [e] 24 ˚C, [f:]25 ˚C, [g:] 28˚C [h:] °C [i:] not reported. Expanding on which has been previously published (King et al. 2005; Ricci 2001; Zhu et al. 2021). Lived (days), Offspring (mean offspring female), Age of first reproduction (FR, day), net reproductive rate mean offspring per female (R_0), generation time (T), d. intrinsic rate of change (r).

Species	Lived	Offspring	FR	R_0	T	r	Source
Adineta grandis[a]	40 - 48	4 - 6	40	5	2	0.04	Dartnall 1992
Adineta ricciae[c]	38	32	–	–	–	0.39	Ricci & Covino 2005
Adineta vaga[e]	17	14	3	14	8	0.34	Ricci 1983
Adineta vaga[e]	16	–	3	21	7	0.45	Latta et al. 2019
Embata laticeps[e]	27	20	4	20	10	0.30	Ricci 1983
Habrotrocha constricta[e]	38	21	10	21	10	0.31	Ricci 1983
Habrotrocha elusa vegeta[e]	32	22	2	22	11	0.28	Ricci 1983
Habrotrocha sylvestris[e]	40	26	4	26	12	0.27	Ricci 1983
Habrotrocha tranquilla[c]	29	–	–	–	–	–	Ricci 2001
Macrotrachela inermis[i]	31	24	3	24	10	0.32	Ricci 1983
Macrotrachela insolita[i]	76	22	9	22	30	0.10	Ricci 1983
Macrotrachela quadricornifera[c]	26	27-29	5	21	8.8	0.35	Ricci & Fascio 1995
Macrotrachela vanoyei[f]	29-40	15-26	–	–	–	–	Ricci 2001
Otostephanos monteti[d]	44	–	–	–	–	–	Ricci 2001
Otostephanos torquatu[e]	45	10	7-8	10	23	0.10	Ricci 1983
Philodina acuticornis[e]	23	49	3	–	–	–	Meadow & Barrows 1971
Philodina citrina [b]	22	26	5	–	–	–	Lansing 1947
Philodina gregaria[a]	60-89	15-18	36	–	2.5	0.16	Dartnall 1992
Philodina rapida[c]	32	–	–	–	–	–	Ricci 2001
Philodina roseola[b, 1]	48	45	3	–	–	–	Lebedeva & Gerasimova 1987
Philodina roseola[e, 1]	27	35	3	30	8	0.43	Ricci 1983
Philodina roseola[c, 1]	20	22	3	–	–	0.14	Moreira et al. 2016
Philodina vorax[c]	22	13	6	13	9.2	0.28	Ricci & Fascio 1995
Philodina sp[e,3] F_1	31	10	8.4	9.7	10	0.23	This study
Philodina sp[e,4] F_1	70	27	8.8	32	20	0.18	This study
Philodina sp[e,5] F_1	38	20	5.5	30	16	0.21	This study
Philodina sp[e,6] F_1	22	1	6.4	9	7	0.35	This study
Philodina sp[e,3] F_5	39	26	7.5	26	12	0.27	This study
Philodina sp[e,4] F_5	59	31	6.8	31	17	0.20	This study
Philodina sp[e,5] F_5	56	34	6.6	34	18	0.20	This study
Rotaria rotatoria HX4[h, 2]	25	10	3	10	6.7	0.39	Xiang et al. 2016
Rotaria rotatoria HX8[h, 2]	27	10	3	11	6.7	0.41	Xiang et al. 2016
Rotaria rotatoria HX19[h, 2]	21	11	3	11	7.8	0.36	Xiang et al. 2016
Rotaria rotatoria [g,7] (0)	27	11	2.7	–	–	–	Zhu et al. 2021
Rotaria rotatoria [g,7] (2)	20	9	3.5	–	–	–	Zhu et al. 2021
Rotaria rotatoria [g,7] (4)	15	6	3.7	–	–	–	Zhu et al. 2021
Rotaria rotatoria [g,7] (6)	17	6	4.5	–	–	–	Zhu et al. 2021
Rotaria rotatoria [g,7] (8)	14	4	5.7	–	–	–	Zhu et al. 2021
Rotaria rotatoria [g,7] (10)	11	2	6.3	–	–	–	Zhu et al. 2021
Rotaria rotatoria [g,7] (12)	9	2	6.5	–	–	–	Zhu et al. 2021
Rotaria rotatoria [g,7] (14)	8	1	7.6	–	–	–	Zhu et al. 2021

[1] demographics recorded at different temperatures optimal temperature for the species. [2] life histories of 3 possible cryptic species. Demographics based on [3]no UVB, winter, [5]summer, [6]extreme or [7] low UVB exposure with increase time (min).

Appendix C: Gene Expression in Response to Ultraviolet Radiation in a Pigmented Aquatic Microinvertebrate (Chapter 4)

RNA Extraction Details

Table S4.1. Concentration and integrity of RNA from *Philodina.* RNA was extracted immediately after exposure to one of four intensities of ultraviolet radiation (UVR). RINe, RNA integrity # equivalent

Pigment	**Sample**	**UVR** (W/m^2)	**Concentration** (ng/mL)	RINe
Highly	control 1	0	95	8.2
Highly	control 2	0	58	8.9
Highly	control 3	0	117	8.4
Highly	control 4	0	42	9
Highly	control 5	0	26	9.1
Highly	low 1	1.3	105	8.8
Highly	low 2	1.3	74	8.6
Highly	low 3	1.3	29	9.3
Highly	low 4	1.3	18	9.8
Highly	low 5	1.3	25	9.8
Highly	mid 1	3.7	111	9.0
Highly	mid 2	3.7	64	8.7
Highly	mid 3	3.7	87	8.5
Highly	mid 4	5.0	17	8.4
Highly	mid 5	5.0	32	9.1
Highly	high 1	5.0	108	8.5
Highly	high 2	5.0	78	8.7
Highly	high 3	5.0	26	9.5
Highly	high 4	5.0	20	8.9
Highly	high 5	5.0	17	8.8
None	control 1	0	16	8.9
None	control 2	0	21	9.1
None	control 3	0	16	8.9
None	low 1	1.3	31	7.9
None	low 2	1.3	20	7.5
None	low 3	1.3	16	5.9
None	mid 1	3.7	20	7.8
None	mid 2	3.7	10	5.3
None	mid 3	3.7	10	8.1
None	mid 4	3.7	18	8.3

Table S4.2. Bdelloid genome and transcriptome comparisons. Quality Assessment Tool (QUAST) & Benchmarking Universal Single Copy Orthologs (BUSCO) score. Temporary habitat, temp; N50, N50 scaffold length (kb); L50, N50 index. BUSCO score based on eukaryote set (n = 303/255); codes: C, complete; S, complete and single copy; D, complete and duplicated; F, fragmented; M, missing. NN, number of sequences; Table modified from King et al. 2005. *NOT pigmented species; ø has not been used as a reference. NR shown for values not reported by the authors.

species	temp	pigment	sz (mb)	N50 (kb)	L50	GC (%)	coverage (x	CDS	genome BUSCO score	GenBank accession
Adineta ricciae	Yes	No	136	284	129	36	89	49,015	C:97%[S:5%, D:39%],F:2%, n:303	GCA_905250025.1
Adineta steineri	Yes	Yes	171	200	163	29	198	50,321	C:95%[S:6%, D:33%],F:%, n:303	GCA_905250115.1
*Adineta vaga**	Yes	No	101	147	3	33	NR	31,335	C:87%[S:7%, D:13%],F:7%, n:255	GCA_021613535.1
Didymodactylos carnosus	Yes	Yes	369	12	7695	34	76	46,863	C:95%[S:7%, D:25%],F:%	GCA_905250885.1
*Macrotrachela quadricornifera**	Yes	Yes	525	33	3725	30	57	25,514	C:82%[S:1%, D:64%],F:%, n:255	GCA_022393335.1
*Rotaria sordida**	No	Yes	361	37	2593	30	69	59,060	C:86%[S:1%, D:70%],F:%, n:255	GCA_905250125.1
Rotaria macrura	No	Yes	235	56	1087	33	210	NR	C:85%[S:173%,D:13%],F:7%, n:255	GCA_900239685.1
Rotaria magnacalcarata	Yes	NR	18	40	1141	32	63	40,289	C:98%[S:8%, D:17%],F:%, n:303	GCA_905273325.1
Rotaria sp. Silwood-1'	Yes	NR	310	212	211	31	53	44,241	C:95%,[S:7%,D:20%],F:1%, n:303	GCA_905250055.1
Rotaria sp. 'Silwood-2'	No	Yes	297	103	381	31	35	48,378	C:93%,[S:7%,D:21%],F:4%, n:303	GCA_905329745.1
Rotaria socialis	No	Yes	147	140	296	32	43	33,717	C:97%,[S:8%,D:18%],F:0%, n:303	GCA_905331475.1

species	temp	pigment	sz (mb)	N50 (bp)	L50	GC (%)	contigs (≥(bp)	contigs (≥1kb)	transcriptome BUSCO score	GenBank accession
*Philodina acuticornis**	Yes	Yes	187	1145	5408	44.4	7045	17757	C:82%,[S:7%, D:8%],F:11%, M:7%, n:255	SRX155614
*Philodina roseola**	Yes	Yes	205	1193	5476	38	7448	19003	C:86%,[S:6%, D:21%],F:9%, M:5%, n:255	SRX155615
Philodina sp.	Yes	Yes	260	1386	49535	41	527419	84236	C:99%,[S:3%, D:64%], F:0.4%, M:0.8%, n:255	TBD

RNA sequencing: de novo transcriptome assembly

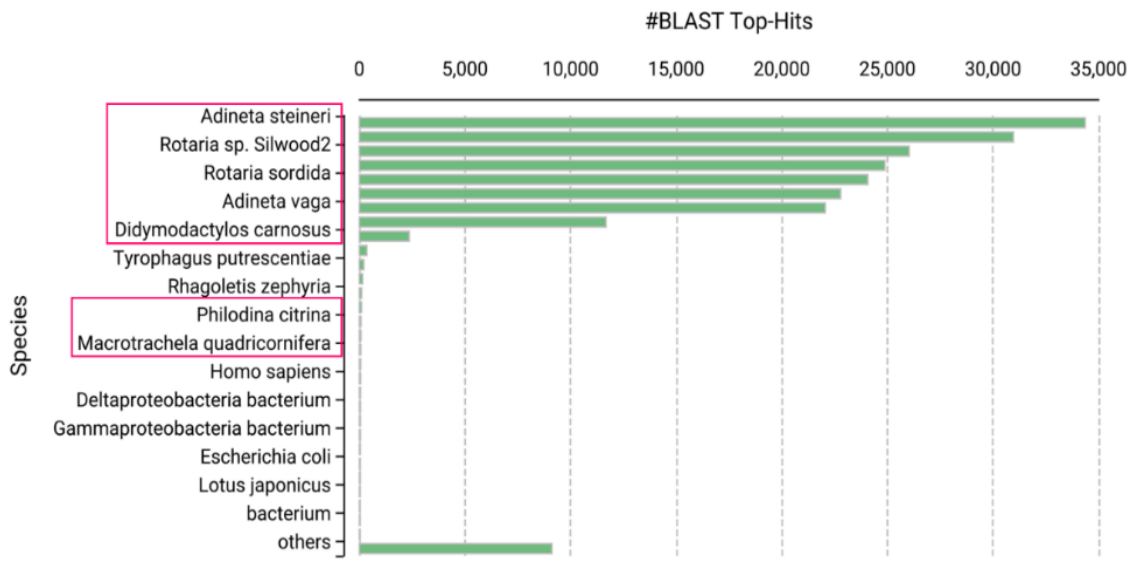

Figure S4.1. Blast2Go results. Shows species that closely resembled *Philodina* transcriptome.

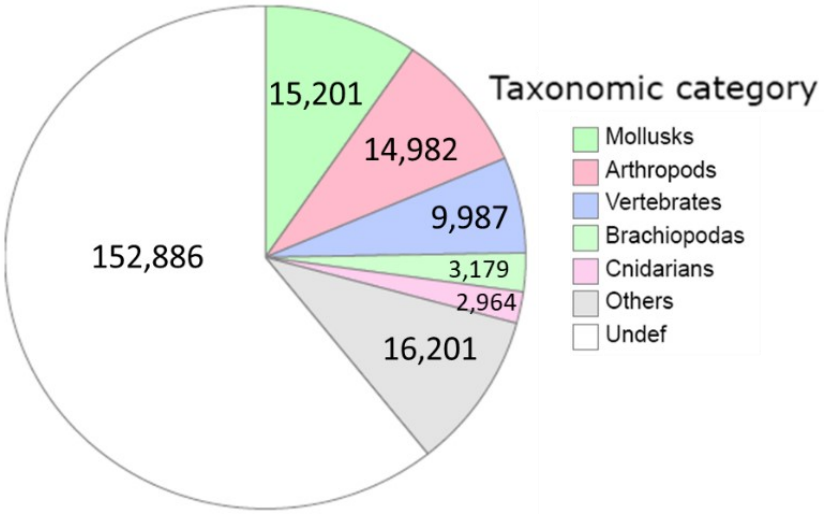

Figure S4.2. Top taxonomic matches. Pie charts are taxonomic category based on Kyoto Encyclopedia of Genes and Genomes (KEGG) pathway analysis.

Table S4.3. Genes verified using 13 bdelloid species. Gene function or pathway were determined using Kyoto Encyclopedia of Genes and Genomes (KEGG) and Gene Ontology then blasted against 11 bdelloid genomes and 2 transcriptomes.

GENE/PATHWAY DESCRIPTION	NO. GENES
AADAT, KAT2; kynurenine/2-aminoadipate aminotransferase	5
aarC, cat1; succinyl-CoA:acetate CoA-transferase	5
ABAT; 4-aminobutyrate aminotransferase / (S)-3-amino-2-methylpropionate transaminase	10

ACAA2; acetyl-CoA acyltransferase 2	5
ACAT, atoB; acetyl-CoA C-acetyltransferase	12
ADHFE1; hydroxyacid-oxoacid transhydrogenase	5
AGBL2_3, CCP2_3; cytosolic carboxypeptidase protein 2/3	6
AGBL4, CCP6; cytosolic carboxypeptidase protein 6	6
AGPAT3_4; lysophosphatidic acid acyltransferase / lysophosphatidylinositol acyltransferase	4
AGXT; alanine-glyoxylate transaminase / serine-glyoxylate transaminase / serine-pyruvate transaminase	5
AGXT2; alanine-glyoxylate transaminase / (R)-3-amino-2-methylpropionate-pyruvate transaminase	3
ALG1; beta-1,4-mannosyltransferase	2
ALG11; alpha-1,2-mannosyltransferase	4
ALG14; beta-1,4-N-acetylglucosaminyltransferase	2
ALG5; dolichyl-phosphate beta-glucosyltransferase	5
ALG6; alpha-1,3-glucosyltransferase	2
ALG8; alpha-1,3-glucosyltransferase	2
ALKBH8, TRM9; alkylated DNA repair protein alkB homolog 8	3
amt, AMT, MEP; ammonium transporter, Amt family	16
AOC3, AOC2, tynA; primary-amine oxidase	10
APRT, apt; adenine phosphoribosyltransferase	3
ARGLU1; arginine and glutamate-rich protein 1	2
ARNT; aryl hydrocarbon receptor nuclear translocator	6
ARNTL2, BMAL2; aryl hydrocarbon receptor nuclear translocator-like protein 2	3
arsA, ASNA1, GET3; arsenite/tail-anchored protein-transporting ATPase	3
ART1, CD296; ADP-ribosyltransferase 1	4
AS3MT; arsenite methyltransferase	4
ASH1L; -lysine4 N-trimethyltransferase ASH1L	2
ASH2; Set1/Ash2 histone methyltransferase complex subunit ASH2	5
asnB, ASNS; asparagine synthase (glutamine-hydrolysing)	12
ASPSCR1, ASPL; tether containing UBX domain for GLUT4	3
ATAT1, MEC17; alpha-tubulin N-acetyltransferase 1	3
ATE1; arginyl-tRNA---protein transferase	2
ATF6A; cyclic AMP-dependent transcription factor ATF-6 alpha	5
ATP13A1, SPF1; manganese-transporting P-type ATPase	14
ATP13A3_4_5; cation-transporting P-type ATPase 13A3/4/5	4
ATP1A; sodium/potassium-transporting ATPase subunit alpha	73
ATP1B, CD298; sodium/potassium-transporting ATPase subunit beta	11
ATP23, XRCC6BP1; mitochondrial inner membrane protease ATP23	3
ATP2A; P-type Ca2+ transporter type 2A	56
ATP2B; P-type Ca2+ transporter type 2B	49
ATP2C; P-type Ca2+ transporter type 2C	13
ATPeF0B, ATP5F1, ATP4; F-type H+-transporting ATPase subunit b	12
ATPeF0C, ATP5G, ATP9; F-type H+-transporting ATPase subunit c	10
ATPeF0F, ATP5J2; F-type H+-transporting ATPase subunit f	6
ATPeF0F6, ATP5J; F-type H+-transporting ATPase subunit 6	5
ATPeF0O, ATP5O, ATP5; F-type H+-transporting ATPase subunit O	3

ATPeF1A, ATP5A1, ATP1; F-type H+-transporting ATPase subunit alpha	27
ATPeF1B, ATP5B, ATP2; F-type H+-transporting ATPase subunit beta	20
ATPeF1D, ATP5D, ATP16; F-type H+-transporting ATPase subunit delta	5
ATPeF1G, ATP5C1, ATP3; F-type H+-transporting ATPase subunit gamma	12
ATPeFG, ATP5L, ATP20; F-type H+-transporting ATPase subunit g	8
ATPeV0A, ATP6N; V-type H+-transporting ATPase subunit a	30
ATPeV0B, ATP6F; V-type H+-transporting ATPase 21kDa proteolipid subunit	5
ATPeV0C, ATP6L; V-type H+-transporting ATPase 16kDa proteolipid subunit	9
ATPeV0D, ATP6D; V-type H+-transporting ATPase subunit d	13
ATPeV0E, ATP6H; V-type H+-transporting ATPase subunit e	2
ATPeV1A, ATP6A; V-type H+-transporting ATPase subunit A	15
ATPeV1B, ATP6B; V-type H+-transporting ATPase subunit B	20
ATPeV1C, ATP6C; V-type H+-transporting ATPase subunit C	4
ATPeV1D, ATP6M; V-type H+-transporting ATPase subunit D	6
ATPeV1E, ATP6E; V-type H+-transporting ATPase subunit E	3
ATPeV1F, ATP6S14; V-type H+-transporting ATPase subunit F	3
ATPeV1G, ATP6G; V-type H+-transporting ATPase subunit G	7
ATPeV1H; V-type H+-transporting ATPase subunit H	8
ATPeVS1, ATP6S1; V-type H+-transporting ATPase S1 subunit	4
ATRX; transcriptional regulator ATRX	16
AUH; methylglutaconyl-CoA hydratase	3
B4GALT4; beta-1,4-galactosyltransferase 4	2
B4GALT7; xylosylprotein 4-beta-galactosyltransferase	2
B4GAT1; beta-1,4-glucuronyltransferase 1	2
BRF1, GTF3B; transcription factor IIIB 90 kDa subunit	2
BUD23; 18S rRNA (guanine1575-N7)-methyltransferase	5
C1GALT1; glycoprotein-N-acetylgalactosamine 3-beta-galactosyltransferase	5
CAB39, MO25; calcium binding protein 39	5
CACNA1B, CAV2.2; voltage-dependent calcium channel N type alpha-1B	4
CACNA1D, CAV1.3; voltage-dependent calcium channel L type alpha-1D	10
CACNA1G, CAV3.1; voltage-dependent calcium channel T type alpha-1G	4
CACNA1H, CAV3.2; voltage-dependent calcium channel T type alpha-1H	5
CACNA1S, CAV1.1; voltage-dependent calcium channel L type alpha-1S	3
CACNA2D3; voltage-dependent calcium channel alpha-2/delta-3	3
CACNA2D4; voltage-dependent calcium channel alpha-2/delta-4	2
CACNB2; voltage-dependent calcium channel beta-2	3
CAD; carbamoyl-phosphate synthase / aspartate carbamoyltransferase / dihydroorotase	6
CADPS; calcium-dependent secretion activator	15
CAMK2; calcium/calmodulin-dependent protein kinase (CaM kinase) II	18
CARM1, PRMT4; type I protein arginine methyltransferase	16
CASD1; N-acetylneuraminate 9-O-acetyltransferase	3
CASK; calcium/calmodulin-dependent serine protein kinase	4
CBP3, UQCC; cytochrome b pre-mRNA-processing protein 3	2
cca; tRNA nucleotidyltransferase (CCA-adding enzyme)	6

CCBL; kynurenine---oxoglutarate transaminase / cysteine-S-conjugate beta-lyase / glutamine---phenylpyruvate transaminase	3
CCDC56, COA3; cytochrome c oxidase assembly factor 3, animal type	2
CD2BP2, PPP1R59; CD2 antigen cytoplasmic tail-binding protein 2	4
CDIPT; CDP-diacylglycerol--inositol 3-phosphatidyltransferase	6
CEPT1; choline/ethanolamine phosphotransferase	7
CERS1, LASS1; sphingoid base N-stearoyltransferase	3
CERS5_6, LASS5_6; sphingoid base N-palmitoyltransferase	5
CHERP; calcium homeostasis endoplasmic reticulum protein	2
CHM, CHML; Rab proteins geranylgeranyltransferase component A	2
CHO1, pssA; CDP-diacylglycerol---serine O-phosphatidyltransferase	4
CIAO2, CIA2, FAM96; cytosolic iron-sulfur assembly component 2	2
CIAO3; cytosolic iron-sulfur assembly component 3	2
CIC; capicua transcriptional repressor	2
CKAP5; cytoskeleton-associated protein 5	7
CML; calcium-binding protein CML	5
CMTR1, FTSJD2, MTR1; cap1 methyltransferase	4
CNDP2; cytosolic nonspecific dipeptidase	11
CNNM; metal transporter CNNM	12
CNOT1, NOT1; CCR4-NOT transcription complex subunit 1	12
CNOT2, NOT2; CCR4-NOT transcription complex subunit 2	4
CNOT3, NOT3; CCR4-NOT transcription complex subunit 3	7
CNOT4, NOT4, MOT2; CCR4-NOT transcription complex subunit 4	8
CNOT6, CCR4; CCR4-NOT transcription complex subunit 6	5
CNOT7_8, CAF1, POP2; CCR4-NOT transcription complex subunit 7/8	8
COA4; cytochrome c oxidase assembly factor 4	2
COASY; phosphopantetheine adenylyltransferase / dephospho-CoA kinase	4
copA, ctpA, ATP7; P-type Cu+ transporter	9
COQ3; polyprenyldihydroxybenzoate methyltransferase / 3-demethylubiquinol 3-O-methyltransferase	2
corA; magnesium transporter	6
COX1; cytochrome c oxidase subunit 1	6
COX2; cytochrome c oxidase subunit 2	3
COX4; cytochrome c oxidase subunit 4	3
COX5A; cytochrome c oxidase subunit 5a	7
COX5B; cytochrome c oxidase subunit 5b	4
COX6B; cytochrome c oxidase subunit 6b	5
COX6C; cytochrome c oxidase subunit 6c	3
coxA, ctaD; cytochrome c oxidase subunit I	2
CPEB, ORB; cytoplasmic polyadenylation element-binding protein	26
CPK; calcium-dependent protein kinase	3
CPT1A; carnitine O-palmitoyltransferase 1, liver isoform	21
CPT2; carnitine O-palmitoyltransferase 2	6
CSG1, SUR1, CSH1; inositol phosphorylceramide mannosyltransferase catalytic subunit	5
CTCF, CTCFL; transcriptional repressor CTCF	7
CTU2, NCS2; cytoplasmic tRNA 2-thiolation protein 2	2

CYB5; cytochrome b5	7
CYB561; transmembrane ascorbate-dependent reductase	4
CYB5R; cytochrome-b5 reductase	13
CYBA, P22PHOX; cytochrome b-245, alpha polypeptide	3
CYC; cytochrome c	9
CYC1, CYT1, petC; ubiquinol-cytochrome c reductase cytochrome c1 subunit	13
CYFIP; cytoplasmic FMR1 interacting protein	8
CYP20A; cytochrome P450 family 20 subfamily A	3
CYP3A; cytochrome P450 family 3 subfamily A	5
CYP55; fungal nitric oxide reductase	2
cypD_E, CYP102A, CYP505; cytochrome P450 / NADPH-cytochrome P450 reductase	2
CYTB, petB; ubiquinol-cytochrome c reductase cytochrome b subunit	2
CYTH; cytohesin	6
D2HGDH; D-2-hydroxyglutarate dehydrogenase	3
DAD1, OST2; dolichyl-diphosphooligosaccharide---protein glycosyltransferase subunit DAD1/OST2	4
DAO, aao; D-amino-acid oxidase	2
DBT, bkdB; 2-oxoisovalerate dehydrogenase E2 component (dihydrolipoyl transacylase)	9
DCLRE1C, ARTEMIS, SCIDA; DNA cross-link repair 1C protein	3
DDO; D-aspartate oxidase	2
DDOST, WBP1; dolichyl-diphosphooligosaccharide---protein glycosyltransferase subunit DDOST/WBP1	17
DECR2, SPS19; 2,4-dienoyl-CoA reductase , peroxisomal	2
DGAT1; diacylglycerol O-acyltransferase 1	2
DGLUCY; D-glutamate cyclase	2
DHDDS, RER2, SRT1; ditrans,polycis-polyprenyl diphosphate synthase	3
DIM1; 18S rRNA (adenine1779-N6/adenine1780-N6)-dimethyltransferase	7
DIO1; type I thyroxine 5'-deiodinase	3
DIRC2, SLC49A3; MFS transporter, FLVCR family, disrupted in renal carcinoma protein 2	2
DLAT, aceF, pdhC; pyruvate dehydrogenase E2 component (dihydrolipoyllysine-residue acetyltransferase)	10
DLST, sucB; 2-oxoglutarate dehydrogenase E2 component (dihydrolipoamide succinyltransferase)	7
dltE; uncharacterized oxidoreductase	3
DMAP1, SWC4, EAF2; DNA methyltransferase 1-associated protein 1	2
DMRT4_5, DMRTA; doublesex- and mab-3-related transcription factor 4/5	3
DOCK1; dedicator of cytokinesis protein 1	4
DOCK2; dedicator of cytokinesis protein 2	2
DOCK4; dedicator of cytokinesis protein 4	3
DOCK6_7_8; dedicator of cytokinesis protein 6/7/8	17
DOCK9_10_11; dedicator of cytokinesis protein 9/10/11	2
DOT1L, DOT1; -lysine79 N-trimethyltransferase	3
DPEP; membrane dipeptidase	5
DPM1; dolichol-phosphate mannosyltransferase	4
DRG, RBG; developmentally regulated GTP-binding protein	13
DRS2, ATP8A; phospholipid-transporting ATPase	12
DTWD2, tapT; tRNA-uridine aminocarboxypropyltransferase	2
DYNC1H; dynein cytoplasmic 1 heavy chain	52

DYNC1I, DNCI; dynein cytoplasmic 1 intermediate chain	4
DYNC1LI, DNCLI; dynein cytoplasmic 1 light intermediate chain	6
DYNC2H, DNCH2; dynein cytoplasmic 2 heavy chain	28
DYNC2LI; dynein cytoplasmic 2 light intermediate chain	2
E1.10.3.3; L-ascorbate oxidase	2
E1.11.1.5; cytochrome c peroxidase	9
E1.3.3.6, ACOX1, ACOX3; acyl-CoA oxidase	13
E1.4.1.4, gdhA; glutamate dehydrogenase (NADP+)	8
E2.1.1.103, NMT; phosphoethanolamine N-methyltransferase	14
E2.1.1.77, pcm; protein-L-isoaspartate(D-aspartate) O-methyltransferase	5
E2.2.1.1, tktA, tktB; transketolase	14
E2.3.1.158; phospholipid:diacylglycerol acyltransferase	4
E2.3.1.7; carnitine O-acetyltransferase	5
E2.6.1.42, ilvE; branched-chain amino acid aminotransferase	6
E2.7.7.41, CDS1, CDS2, cdsA; phosphatidate cytidylyltransferase	3
E2F4_5; transcription factor E2F4/5	2
E4.1.1.32, pckA, PCK; phosphoenolpyruvate carboxykinase (GTP)	52
E7.6.2.1; phospholipid-translocating ATPase	54
EARS, gltX; glutamyl-tRNA synthetase	3
ECM4, yqjG; glutathionyl-hydroquinone reductase	2
EEF1AKMT1, EFM5; EEF1A lysine methyltransferase 1	4
EEF1AKMT2, EFM4, METTL10; EEF1A lysine methyltransferase 2	2
EEF1AKNMT, METTL13; eEF1A lysine and N-terminal methyltransferase	2
EFCAB11; EF-hand calcium-binding domain-containing protein 11	2
EGH; beta-1,4-mannosyltransferase	7
EGR1; early growth response protein 1	2
EIF1, SUI1; translation initiation factor 1	5
EIF1A; translation initiation factor 1A	8
EIF2A; translation initiation factor 2A	5
EIF2AK3; eukaryotic translation initiation factor 2-alpha kinase 3	3
EIF2B1; translation initiation factor eIF-2B subunit alpha	3
EIF2B2; translation initiation factor eIF-2B subunit beta	2
EIF2B5; translation initiation factor eIF-2B subunit epsilon	2
EIF2S1; translation initiation factor 2 subunit 1	7
EIF2S2; translation initiation factor 2 subunit 2	9
EIF2S3; translation initiation factor 2 subunit 3	18
EIF3A; translation initiation factor 3 subunit A	13
EIF3B; translation initiation factor 3 subunit B	10
EIF3C; translation initiation factor 3 subunit C	20
EIF3D; translation initiation factor 3 subunit D	6
EIF3E, INT6; translation initiation factor 3 subunit E	10
EIF3F; translation initiation factor 3 subunit F	4
EIF3G; translation initiation factor 3 subunit G	4
EIF3H; translation initiation factor 3 subunit H	7
EIF3I; translation initiation factor 3 subunit I	6

EIF3K; translation initiation factor 3 subunit K	4
EIF3L; translation initiation factor 3 subunit L	10
EIF3M; translation initiation factor 3 subunit M	3
EIF4A; translation initiation factor 4A	40
EIF4B; translation initiation factor 4B	7
EIF4E; translation initiation factor 4E	16
EIF4EBP1; eukaryotic translation initiation factor 4E binding protein 1	3
EIF4G; translation initiation factor 4G	16
EIF4H; translation initiation factor 4H	2
EIF5; translation initiation factor 5	5
EIF5A; translation initiation factor 5A	9
EIF5B; translation initiation factor 5B	23
EIF6; translation initiation factor 6	5
ELF2C, AGO; eukaryotic translation initiation factor 2C	42
ELOF1, ELF1; transcription elongation factor 1	2
EMC1; ER membrane protein complex subunit 1	2
EMC3, TMEM111; ER membrane protein complex subunit 3	7
EMC4, TMEM85; ER membrane protein complex subunit 4	4
EMC7; ER membrane protein complex subunit 7	3
ENPEP, CD249; glutamyl aminopeptidase	4
ENY2, DC6, SUS1; enhancer of yellow 2 transcription factor	3
EOGT; EGF domain-specific O-GlcNAc transferase	2
EPHX1; microsomal epoxide hydrolase	4
EPHX4; epoxide hydrolase 4	7
EPRS; bifunctional glutamyl/prolyl-tRNA synthetase	29
EPS15; epidermal growth factor receptor substrate 15	3
EPS8; epidermal growth factor receptor kinase substrate 8	8
EPT1; ethanolaminephosphotransferase	6
ERCC2, XPD; DNA excision repair protein ERCC-2	3
ERCC3, XPB; DNA excision repair protein ERCC-3	12
ERCC4, XPF; DNA excision repair protein ERCC-4	3
ERCC5, XPG, RAD2; DNA excision repair protein ERCC-5	2
ERCC6, CSB, RAD26; DNA excision repair protein ERCC-6	4
ERV1, GFER, ALR; mitochondrial FAD-linked sulfhydryl oxidase	2
ESCO, ECO1; N-acetyltransferase	3
ETFDH; electron-transferring-flavoprotein dehydrogenase	10
ETV6_7, yan; ETS translocation variant 6/7	5
EXT1; glucuronyl/N-acetylglucosaminyl transferase EXT1	2
EZH2; -lysine27 N-trimethyltransferase EZH2	3
fabD, MCAT, MCT1; S-malonyltransferase	2
FCY1; cytosine/creatinine deaminase	2
fic, FICD, HYPE; cell filamentation protein, protein adenylyltransferase	2
fixA, etfB; electron transfer flavoprotein beta subunit	4
fixB, etfA; electron transfer flavoprotein alpha subunit	3
FMO; dimethylaniline monooxygenase (N-oxide forming) / hypotaurine monooxygenase	2

FNTA; protein farnesyltransferase/geranylgeranyltransferase type-1 subunit alpha	5
FNTB; protein farnesyltransferase subunit beta	2
FOLH1, GCPII; glutamate carboxypeptidase II (folate hydrolase 1)	2
FOXRED1; FAD-dependent oxidoreductase domain-containing protein 1	2
FPGS; folylpolyglutamate synthase	2
FPGT; fucose-1-phosphate guanylyltransferase	3
frmA, ADH5, adhC; S-(hydroxymethyl)glutathione dehydrogenase / alcohol dehydrogenase	9
frmB, ESD, fghA; S-formylglutathione hydrolase	4
FTSJ1, TRM7; tRNA (cytidine32/guanosine34-2'-O)-methyltransferase	2
FUT10; alpha-1,3-fucosyltransferase 10	5
FUT8; glycoprotein 6-alpha-L-fucosyltransferase	6
GALNT; polypeptide N-acetylgalactosaminyltransferase	56
galT, GALT; UDPglucose--hexose-1-phosphate uridylyltransferase	4
GATAD2; transcriptional repressor p66	4
GCDH, gcdH; glutaryl-CoA dehydrogenase	6
GCLC; glutamate--cysteine ligase catalytic subunit	21
GCLM; glutamate--cysteine ligase regulatory subunit	2
gcvT, AMT; glycine cleavage system T protein (aminomethyltransferase)	2
GFI1; growth factor independent 1	3
GGH; gamma-glutamyl hydrolase	4
ggt; gamma-glutamyltranspeptidase / glutathione hydrolase	3
GGT1_5, CD224; gamma-glutamyltranspeptidase / glutathione hydrolase / leukotriene-C4 hydrolase	12
glgC; glucose-1-phosphate adenylyltransferase	3
glmS, GFPT; glutamine---fructose-6-phosphate transaminase (isomerizing)	22
glnA, GLUL; glutamine synthetase	36
GLO1, gloA; lactoylglutathione lyase	2
gloB, gloC, HAGH; hydroxyacylglutathione hydrolase	2
GLUD1_2, gdhA; glutamate dehydrogenase (NAD(P)+)	31
glyA, SHMT; glycine hydroxymethyltransferase	12
GMPP; mannose-1-phosphate guanylyltransferase	17
GNPNAT1, GNA1; glucosamine-phosphate N-acetyltransferase	4
GOT1; aspartate aminotransferase, cytoplasmic	8
GOT2; aspartate aminotransferase, mitochondrial	11
GPAT3_4, AGPAT9, AGPAT6; glycerol-3-phosphate O-acyltransferase 3/4	9
GPT, ALT; alanine transaminase	12
gpx, btuE, bsaA; glutathione peroxidase	8
GRB2; growth factor receptor-bound protein 2	4
GRIA1; glutamate receptor 1	4
GRIK4; glutamate receptor, ionotropic kainate 4	2
GRIN; glutamate receptor, ionotropic, invertebrate	15
GRIN1; glutamate receptor ionotropic, NMDA 1	7
GRIN2B; glutamate receptor ionotropic, NMDA 2B	2
GRIP; glutamate receptor, ionotropic, plant	4
GRIP; glutamate receptor-interacting protein	7
GRM1; metabotropic glutamate receptor 1	2

GRM3; metabotropic glutamate receptor 3	3
grxC, GLRX, GLRX2; glutaredoxin 3	4
grxD, GLRX5; monothiol glutaredoxin	2
gsp; glutathionylspermidine amidase/synthetase	30
GSR, gor; glutathione reductase (NADPH)	5
GSS; glutathione synthase	4
GST, gst; glutathione S-transferase	31
GTF3C2; general transcription factor 3C polypeptide 2	4
guaA, GMPS; GMP synthase (glutamine-hydrolysing)	5
GUF1; translation factor GUF1, mitochondrial	3
HADHB; acetyl-CoA acyltransferase	4
HAT1, KAT1; histone acetyltransferase 1	4
HCCS; cytochrome c heme-lyase	6
HEATR5, LAA1; HEAT repeat-containing protein 5	4
HGS, HRS, VPS27; hepatocyte growth factor-regulated tyrosine kinase substrate	11
HGSNAT; heparan-alpha-glucosaminide N-acetyltransferase	4
HMGCL, hmgL; hydroxymethylglutaryl-CoA lyase	5
HMGCR; hydroxymethylglutaryl-CoA reductase (NADPH)	5
HMGCS; hydroxymethylglutaryl-CoA synthase	7
hmp, YHB1; nitric oxide dioxygenase	3
HOGA1; 4-hydroxy-2-oxoglutarate aldolase	3
HPGDS; prostaglandin-H2 D-isomerase / glutathione transferase	20
hprT, hpt, HPRT1; hypoxanthine phosphoribosyltransferase	6
HSF1; heat shock transcription factor 1	5
HSP110; heat shock protein 110kDa	6
HSP90B, TRA1; heat shock protein 90kDa beta	24
HSPA1s; heat shock 70kDa protein 1/2/6/8	104
HSPA4; heat shock 70kDa protein 4	9
HSPG2; basement membrane-specific heparan sulfate proteoglycan core protein	7
HTATIP2; oxidoreductase	3
HUGT; UDP-glucose:glycoprotein glucosyltransferase	5
hutG; formiminoglutamase	2
HXT; MFS transporter, SP family, sugar:H+ symporter	2
HYOU1; hypoxia up-regulated 1	10
IFT122; intraflagellar transport protein 122	2
IFT172; intraflagellar transport protein 172	5
IFT46; intraflagellar transport protein 46	4
IFT57, HIPPI, ESRRBL1; intraflagellar transport protein 57	3
IFT81; intraflagellar transport protein 81	2
IFT88; intraflagellar transport protein 88	2
IGF2BP1; insulin-like growth factor 2 mRNA-binding protein 1	6
IK, RED, RER; IK cytokine	3
IL4I1; L-amino-acid oxidase	3
ING1; inhibitor of growth protein 1	3
ITM2B; integral membrane protein 2B	2

JEN; MFS transporter, SHS family, lactate transporter	2
JUN; transcription factor AP-1	2
K05303; O-methyltransferase	2
K07010; putative glutamine amidotransferase	2
K07058; membrane protein	3
K24129; glutaredoxin-dependent peroxiredoxin	2
kbl, GCAT; glycine C-acetyltransferase	5
KCNMA1, KCA1.1; potassium large conductance calcium-activated channel subfamily M alpha member 1	6
KCNN3, KCA2.3; potassium intermediate/small conductance calcium-activated channel subfamily N member 3	4
KIAA1109; transmembrane protein KIAA1109	10
KIDINS220, ARMS; ankyrin repeat-rich membrane spanning protein	7
L2HGDH; 2-hydroxyglutarate dehydrogenase	2
LAMP1_2, CD107; lysosomal-associated membrane protein 1/2	4
LANCL1; glutathione transferase	3
LAPTM; lysosomal-associated transmembrane protein	2
LCLAT1, AGPAT8; lysocardiolipin and lysophospholipid acyltransferase	5
LDHD, dld; D-lactate dehydrogenase (cytochrome)	5
LEMD3; inner nuclear membrane protein Man1	5
LRMDA; leucine-rich melanocyte differentiation-associated protein	2
LRRTM1_2; leucine-rich repeat transmembrane neuronal protein 1/2	2
LYER; cell growth-regulating nucleolar protein	4
maa; maltose O-acetyltransferase	2
MAF1; repressor of RNA polymerase III transcription MAF1	2
MAGT1, TUSC3; dolichyl-diphosphooligosaccharide---protein glycosyltransferase subunit MAGT1/TUSC3	10
malQ; 4-alpha-glucanotransferase	7
MAO, aofH; monoamine oxidase	3
MBF1; putative transcription factor	7
MBOAT1_2; lysophospholipid acyltransferase 1/2	10
MBTPS1; membrane-bound transcription factor site-1 protease	2
MCU; calcium uniporter protein, mitochondrial	2
MECOM, EVI1, PRDM3; -lysine9 N-methyltransferase (ecotropic virus integration site 1 protein)	2
MECR, NRBF1; mitochondrial enoyl- reductase / trans-2-enoyl-CoA reductase	3
MED13; mediator of RNA polymerase II transcription subunit 13	2
MED14, RGR1; mediator of RNA polymerase II transcription subunit 14	2
MED19; mediator of RNA polymerase II transcription subunit 19	2
MED22; mediator of RNA polymerase II transcription subunit 22	3
MED23; mediator of RNA polymerase II transcription subunit 23	2
MED30; mediator of RNA polymerase II transcription subunit 30	3
MED31, SOH1; mediator of RNA polymerase II transcription subunit 31	2
MED7; mediator of RNA polymerase II transcription subunit 7	2
MEF2A; MADS-box transcription enhancer factor 2A	5
MEGF10_11; multiple epidermal growth factor-like domains protein 10/11	3
MEGF6; multiple epidermal growth factor-like domains protein 6	3

metE; 5-methyltetrahydropteroyltriglutamate--homocysteine methyltransferase	3
metH, MTR; 5-methyltetrahydrofolate--homocysteine methyltransferase	12
METTL14; mRNA m6A methyltransferase non-catalytic subunit	2
METTL2; tRNA N(3)-methylcytidine methyltransferase METTL2	3
MFI2, CD228; melanoma-associated antigen p97	2
MFSD11; MFS transporter, NAG-T family, sugar:H+ symporter	2
MFSD5; MFS transporter, MFS domain-containing protein family, molybdate-anion transporter	2
MGAT2; alpha-1,6-mannosyl-glycoprotein beta-1,2-N-acetylglucosaminyltransferase	3
MGAT4A_B; alpha-1,3-mannosylglycoprotein beta-1,4-N-acetylglucosaminyltransferase A/B	2
miaA, TRIT1; tRNA dimethylallyltransferase	3
MICU1; calcium uptake protein 1, mitochondrial	2
MICU3; calcium uptake protein 3, mitochondrial	2
MITF; microphthalmia-associated transcription factor	2
MLH1; DNA mismatch repair protein MLH1	2
MLL1; -lysine4 N-trimethyltransferase MLL1	2
MLL3; -lysine4 N-trimethyltransferase MLL3	5
MMP14; matrix metalloproteinase-14 (membrane-inserted)	4
MOCS3, UBA4; adenylyltransferase and sulfurtransferase	4
MPO; myeloperoxidase	2
MRE11; double-strand break repair protein MRE11	3
MROH1, HEATR7A; maestro heat-like repeat-containing protein family member 1	2
MRS2, MFM1; magnesium transporter	2
MSFD7, SLC49A4; MFS transporter, FLVCR family, MFS-domain-containing protein 7	2
MSFD8, CLN7; MFS transporter, ceroid-lipofuscinosis neuronal protein 7	7
MSH2; DNA mismatch repair protein MSH2	7
MSH6; DNA mismatch repair protein MSH6	9
msrA; peptide-methionine (S)-S-oxide reductase	8
msrB; peptide-methionine (R)-S-oxide reductase	4
MTFMT, fmt; methionyl-tRNA formyltransferase	2
MYST1, MOF, KAT8; histone acetyltransferase MYST1	3
MYST3, KAT6A; histone acetyltransferase MYST3	4
MYST4, KAT6B; histone acetyltransferase MYST4	2
NAA10_11, ARD1_2; N-alpha-acetyltransferase 10/11	10
NAA15_16; N-alpha-acetyltransferase 15/16, NatA auxiliary subunit	14
NAA20, NAT3; N-terminal acetyltransferase B complex catalytic subunit	2
NAA35, MAK10; N-alpha-acetyltransferase 35, NatC auxiliary subunit	2
NAA50, NAT5; N-alpha-acetyltransferase 50	3
NAA60; N-alpha-acetyltransferase 60	2
NAMPT; nicotinamide phosphoribosyltransferase	4
NAT10, KRE33; N-acetyltransferase 10	4
NCOAT, MGEA5; protein O-GlcNAcase / histone acetyltransferase	10
NCS1; neuronal calcium sensor 1	15
ND5; NADH-ubiquinone oxidoreductase chain 5	3
NFX1; transcriptional repressor NF-X1	7
NFYA, HAP2; nuclear transcription factor Y, alpha	6

NFYB, HAP3; nuclear transcription Y subunit beta	10
NFYC, HAP5; nuclear transcription factor Y, gamma	8
ninaB; carotenoid isomerooxygenase	2
NIPA, SLC57A2S; magnesium transporter	2
NME8, TXNDC3; thioredoxin domain-containing protein 3	5
NMT; glycylpeptide N-tetradecanoyltransferase	7
NNMT; nicotinamide N-methyltransferase	2
NNT; H+-translocating NAD(P) transhydrogenase	30
NOP1, FBL; rRNA 2'-O-methyltransferase fibrillarin	8
NOP2; 25S rRNA (cytosine2870-C5)-methyltransferase	6
NOSIP; nitric oxide synthase-interacting protein	3
NOX2, GP91, CYBB; NADPH oxidase 2	2
NOX5; NADPH oxidase 5	14
NR2F2, TFCOUP2; COUP transcription factor 2	2
NSUN2, TRM4; tRNA (cytosine34-C5)-methyltransferase	10
NXN; nucleoredoxin	10
OGDH, sucA; 2-oxoglutarate dehydrogenase E1 component	32
OGT; protein O-GlcNAc transferase	6
ORAI1; calcium release-activated calcium channel protein 1	6
osmC, ohr; lipoyl-dependent peroxiredoxin	2
OSTC; oligosaccharyltransferase complex subunit OSTC	4
OXCT; 3-oxoacid CoA-transferase	10
PAM16, TIM16; mitochondrial import inner membrane translocase subunit TIM16	6
patA; putrescine aminotransferase	19
PBX1; pre-B-cell leukemia transcription factor 1	5
PCYT1; choline-phosphate cytidylyltransferase	9
PCYT2; ethanolamine-phosphate cytidylyltransferase	12
PDE1; calcium/calmodulin-dependent 3',5'-cyclic nucleotide phosphodiesterase	11
pdxH, PNPO; pyridoxamine 5'-phosphate oxidase	4
pdxK, pdxY; pyridoxine kinase	3
PEX11B; peroxin-11B	3
PEX12, PAF3; peroxin-12	2
PEX13; peroxin-13	2
PEX5, PXR1; peroxin-5	6
PEX6, PXAAA1; peroxin-6	2
PGRMC1_2; membrane-associated progesterone receptor component	3
pgsA, PGS1; CDP-diacylglycerol---glycerol-3-phosphate 3-phosphatidyltransferase	4
PGTB1; geranylgeranyl transferase type-1 subunit beta	2
PHF12, RCO1; transcriptional regulatory protein PHF12/RCO1	2
PIGG, GPI7; ethanolamine phosphate transferase 2 subunit G	4
PIGK; GPI-anchor transamidase subunit K	3
PIGM; GPI mannosyltransferase 1 subunit M	2
PIGO; GPI ethanolamine phosphate transferase 3 subunit O	2
PIGT; GPI-anchor transamidase subunit T	3
PIGU; GPI-anchor transamidase subunit U	2

PIN1; peptidyl-prolyl cis-trans isomerase NIMA-interacting 1	3
PIN4; peptidyl-prolyl cis-trans isomerase NIMA-interacting 4	2
PIPOX; sarcosine oxidase / L-pipecolate oxidase	2
PITPNM; membrane-associated phosphatidylinositol transfer protein	6
PKMYT; membrane-associated tyrosine- and threonine-specific cdc2-inhibitory kinase	3
PLA2G4, CPLA2; cytosolic phospholipase A2	3
PLB1, PLB; phospholipase B1, membrane-associated	26
PMA1, PMA2; H+-transporting ATPase	18
PMS2; DNA mismatch repair protein PMS2	3
pncB, NAPRT1; nicotinate phosphoribosyltransferase	5
pnp, PNPT1; polyribonucleotide nucleotidyltransferase	2
PNPLA8; calcium-independent phospholipase A2-gamma	3
POFUT; peptide-O-fucosyltransferase	4
POU3F, OTF; POU domain transcription factor, class 3	6
POU6F; POU domain transcription factor, class 6	3
PPIB, ppiB; peptidyl-prolyl cis-trans isomerase B (cyclophilin B)	4
PPIL1; peptidyl-prolyl cis-trans isomerase-like 1	4
PPIL2, CYC4, CHP60; peptidyl-prolyl cis-trans isomerase-like 2	4
PPIL4; peptidyl-prolyl cis-trans isomerase-like 4	2
PQBP1, NPW38; polyglutamine-binding protein 1	9
PRDX1; peroxiredoxin 1	7
PRDX2_4, ahpC; peroxiredoxin 2/4	11
PRDX6; peroxiredoxin 6	7
PRMT1; type I protein arginine methyltransferase	18
PRMT3; type I protein arginine methyltransferase	4
PRMT5, HSL7; type II protein arginine methyltransferase	3
PRMT7; type III protein arginine methyltransferase	4
PRMT8; type I protein arginine methyltransferase	3
PTGES3; cytosolic prostaglandin-E synthase	6
PURA; transcriptional activator protein Pur-alpha	5
PXDN, VPO1; peroxidase	13
PYROXD1; pyridine nucleotide-disulfide oxidoreductase domain-containing protein 1	2
QARS, glnS; glutaminyl-tRNA synthetase	17
QCR2, UQCRC2; ubiquinol-cytochrome c reductase core subunit 2	9
QCR6, UQCRH; ubiquinol-cytochrome c reductase subunit 6	3
QCR7, UQCRB; ubiquinol-cytochrome c reductase subunit 7	3
QCR9, UCRC; ubiquinol-cytochrome c reductase subunit 9	2
QRICH2; glutamine-rich protein 2	7
RABGGTB; geranylgeranyl transferase type-2 subunit beta	3
RAC1; Ras-related C3 botulinum toxin substrate 1	8
RAC3; Ras-related C3 botulinum toxin substrate 3	2
RAD23, HR23; UV excision repair protein RAD23	7
RAD50; DNA repair protein RAD50	3
RAD51; DNA repair protein RAD51	12
RAD54L, RAD54; DNA repair and recombination protein RAD54 and RAD54-like protein	10

RCD1, CNOT9, CAF40; CCR4-NOT transcription complex subunit 9	8
RERE; arginine-glutamic acid dipeptide repeats protein	4
rfbA, rmlA, rffH; glucose-1-phosphate thymidylyltransferase	2
RIMS2, RIM2; regulating synaptic membrane exocytosis protein 2	2
RMND5; E3 ubiquitin-protein transferase RMND5	3
RNMT; mRNA (guanine-N7-)-methyltransferase	2
rocD, OAT; ornithine--oxo-acid transaminase	4
RPN1, OST1; dolichyl-diphosphooligosaccharide---protein glycosyltransferase subunit 1 (ribophorin I)	6
RPN2, SWP1; dolichyl-diphosphooligosaccharide---protein glycosyltransferase subunit 2 (ribophorin II)	10
RUNX1, AML1; runt-related transcription factor 1	3
RUVBL1, RVB1, INO80H; RuvB-like protein 1	9
RUVBL2, RVB2, INO80J; RuvB-like protein 2	8
SAM50, TOB55, bamA; outer membrane protein insertion porin family	5
SARAF; store-operated calcium entry-associated regulatory factor	3
SCAMP; secretory carrier-associated membrane protein	8
SCARB2, LIMP2, CD36L2; lysosome membrane protein 2	9
SDCCAG10; peptidyl-prolyl cis-trans isomerase SDCCAG10	3
SDHC, SDH3; succinate dehydrogenase (ubiquinone) cytochrome b560 subunit	3
SDHD, SDH4; succinate dehydrogenase (ubiquinone) membrane anchor subunit	6
SDR16C5; all-trans-retinol dehydrogenase (NAD+)	14
SEC13; protein transport protein SEC13	6
SEC14, SEC14L; phosphatidylinositol/phosphatidylcholine transfer protein	7
SEC22; vesicle transport protein SEC22	5
SEC23; protein transport protein SEC23	21
SEC24; protein transport protein SEC24	17
SEC31; protein transport protein SEC31	7
SEC61A; protein transport protein SEC61 subunit alpha	21
SEC61B, SBH2; protein transport protein SEC61 subunit beta	2
SEC61G, SSS1, secE; protein transport protein SEC61 subunit gamma and related proteins	4
SEC62; translocation protein SEC62	6
SEC63, DNAJC23; translocation protein SEC63	12
SELENBP1; methanethiol oxidase	7
SELENOO, selO; protein adenylyltransferase	12
SELENOT; thioredoxin reductase-like selenoprotein T	3
serA, PHGDH; D-3-phosphoglycerate dehydrogenase / 2-oxoglutarate reductase	8
serC, PSAT1; phosphoserine aminotransferase	7
SETD1, SET1; -lysine4 N-trimethyltransferase SETD1	3
SETD8; -lysine20 N-methyltransferase SETD8	5
SETDB1; -N6,N6-dimethyl-lysine9 N-methyltransferase	8
SETMAR; -lysine36 N-dimethyltransferase SETMAR	9
SFPQ, PSF; splicing factor, proline- and glutamine-rich	3
SGTA; small glutamine-rich tetratricopeptide repeat-containing protein alpha	3
SIDT1; SID1 transmembrane family member 1	3
SKI3, TTC37; superkiller protein 3	2
SLC10A3_5; solute carrier family 10 (sodium/bile acid cotransporter), member 3/5	3

SLC10A7, P7; solute carrier family 10 (sodium/bile acid cotransporter), member 7	3
SLC12A4_6, KCC1_3; solute carrier family 12 (potassium/chloride transporter), member 4/6	3
SLC13A2_3_5; solute carrier family 13 (sodium-dependent dicarboxylate transporter), member 2/3/5	6
SLC15A3_4, PHT; solute carrier family 15 (peptide/histidine transporter), member 3/4	2
SLC17A5; MFS transporter, ACS family, solute carrier family 17 (sodium-dependent inorganic phosphate cotransporter), member 5	13
SLC18A1_2, VMAT; MFS transporter, DHA1 family, solute carrier family 18 (vesicular amine transporter), member 1/2	5
SLC1A1, EAAT3; solute carrier family 1 (neuronal/epithelial high affinity glutamate transporter), member 1	2
SLC1A2, EAAT2; solute carrier family 1 (glial high affinity glutamate transporter), member 2	2
SLC20A, PIT; solute carrier family 20 (sodium-dependent phosphate transporter)	6
SLC22A4_5, OCTN; MFS transporter, OCT family, solute carrier family 22 (organic cation transporter), member 4/5	22
SLC24A3, NCKX3; solute carrier family 24 (sodium/potassium/calcium exchanger), member 3	2
SLC24A6, NCKX6; solute carrier family 24 (sodium/potassium/calcium exchanger), member 6	2
SLC25A1, CTP; solute carrier family 25 (mitochondrial citrate transporter), member 1	4
SLC25A10, DIC; solute carrier family 25 (mitochondrial dicarboxylate transporter), member 10	3
SLC25A11, OGC; solute carrier family 25 (mitochondrial oxoglutarate transporter), member 11	5
SLC25A12_13, AGC; solute carrier family 25 (mitochondrial aspartate/glutamate transporter), member 12/13	9
SLC25A18_22, GC; solute carrier family 25 (mitochondrial glutamate transporter), member 18/22	3
SLC25A20_29, CACT, CACL, CRC1; solute carrier family 25 (mitochondrial carnitine/acylcarnitine transporter), member 20/29	10
SLC25A23S; solute carrier family 25 (mitochondrial phosphate transporter), member 23/24/25/41	9
SLC25A28_37, MFRN; solute carrier family 25 (mitochondrial iron transporter), member 28/37	9
SLC25A3, PHC, PIC; solute carrier family 25 (mitochondrial phosphate transporter), member 3	15
SLC25A32, MFT; solute carrier family 25 (mitochondrial folate transporter), member 32	2
SLC25A4S, ANT; solute carrier family 25 (mitochondrial adenine nucleotide translocator), member 4/5/6/31	41
SLC25A51_52; solute carrier family 25 (mitochondrial nicotinamide adenine dinucleotide transporter), member 51/52	2
SLC27A1_4, FATP1_4; solute carrier family 27 (fatty acid transporter), member 1/4	7
SLC29A1_2_3, ENT1_2_3; solute carrier family 29 (equilibrative nucleoside transporter), member 1/2/3	2
SLC2A1, GLUT1; MFS transporter, SP family, solute carrier family 2 (facilitated glucose transporter), member 1	8
SLC2A5, GLUT5; MFS transporter, SP family, solute carrier family 2 (facilitated glucose/fructose transporter), member 5	2
SLC30A1, ZNT1; solute carrier family 30 (zinc transporter), member 1	7
SLC30A2, ZNT2; solute carrier family 30 (zinc transporter), member 2	4
SLC30A5_7, ZNT5_7, MTP, MSC2; solute carrier family 30 (zinc transporter), member 5/7	5
SLC30A6, ZNT6; solute carrier family 30 (zinc transporter), member 6	3
SLC30A9, ZNT9; solute carrier family 30 (zinc transporter), member 9	5
SLC31A1, CTR1; solute carrier family 31 (copper transporter), member 1	3
SLC33A1, ACATN; MFS transporter, PAT family, solute carrier family 33 (acetyl-CoA transportor), member 1	3
SLC35A1_2_3; solute carrier family 35 (UDP-sugar transporter), member A1/2/3	6
SLC35A4; solute carrier family 35 (probable UDP-sugar transporter), member A4	3
SLC35B1; solute carrier family 35 (UDP-galactose transporter), member B1	2
SLC35C1, FUCT1; solute carrier family 35 (GDP-fucose transporter), member C1	6

SLC37A1_2; MFS transporter, OPA family, solute carrier family 37 (glycerol-3-phosphate transporter), member 1/2	2
SLC37A3; MFS transporter, OPA family, solute carrier family 37 (glycerol-3-phosphate transporter), member 3	4
SLC39A10, ZIP10; solute carrier family 39 (zinc transporter), member 10	3
SLC39A11, ZIP11; solute carrier family 39 (zinc transporter), member 11	2
SLC39A13, ZIP13; solute carrier family 39 (zinc transporter), member 13	4
SLC39A14, ZIP14; solute carrier family 39 (zinc transporter), member 14	2
SLC39A7, KE4, ZIP7; solute carrier family 39 (zinc transporter), member 7	5
SLC39A9, ZIP9; solute carrier family 39 (zinc transporter), member 9	3
SLC42A, RHAG, RHBG, RHCG, CD241; ammonium transporter Rh	5
SLC44A2_4_5; solute carrier family 44 (choline transporter-like protein), member 2/4/5	3
SLC4A10, NCBE; solute carrier family 4 (sodium bicarbonate transporter), member 10	6
SLC4A11, BTR1; solute carrier family 4 (sodium borate transporter), member 11	5
SLC4A5, NBC4; solute carrier family 4 (sodium bicarbonate cotransporter), member 5	2
SLC4A7, NBC3; solute carrier family 4 (sodium bicarbonate cotransporter), member 7	4
SLC4A8; solute carrier family 4 (sodium bicarbonate cotransporter), member 8	2
SLC50A, SWEET; solute carrier family 50 (sugar transporter)	2
SLC52A3, RFT2; riboflavin transporter 2	4
SLC5A3, SMIT; solute carrier family 5 (sodium/myo-inositol cotransporter), member 3	2
SLC5A6, SMVT; solute carrier family 5 (sodium-dependent multivitamin transporter), member 6	5
SLC5A7, CHT1; solute carrier family 5 (high affinity choline transporter), member 7	2
SLC5A8_12, SMCT; solute carrier family 5 (sodium-coupled monocarboxylate transporter), member 8/12	2
SLC5A9, SGLT4; solute carrier family 5 (sodium/glucose cotransporter), member 9	2
SLC6A1, GAT1; solute carrier family 6 (neurotransmitter transporter, GABA) member 1	2
SLC6A3, DAT; solute carrier family 6 (neurotransmitter transporter, dopamine) member 3	6
SLC6A4, SERT; solute carrier family 6 (neurotransmitter transporter, serotonin) member 4	7
SLC6A5_9, GLYT; solute carrier family 6 (neurotransmitter transporter, glycine) member 5/9	7
SLC7A3, ATRC3; solute carrier family 7 (cationic amino acid transporter), member 3	2
SLC7A8, LAT2; solute carrier family 7 (L-type amino acid transporter), member 8	3
SLC7A9_15, BAT1; solute carrier family 7 (L-type amino acid transporter), member 9/15	2
SLC8A, NCX; solute carrier family 8 (sodium/calcium exchanger)	18
SMAP; stromal membrane-associated protein	8
SMOX, PAO5; spermine oxidase	2
SMT1, ERG6; sterol 24-C-methyltransferase	7
SOAT; sterol O-acyltransferase	6
SOD1; superoxide dismutase, Cu-Zn family	14
SOD2; superoxide dismutase, Fe-Mn family	7
SOX1S; transcription factor SOX1/3/14/21 (SOX group B)	5
SOX2; transcription factor SOX2 (SOX group B)	3
SOX4; transcription factor SOX4 (SOX group C)	7
SOX7S; transcription factor SOX7/8/10/18 (SOX group E/F)	3
SOX9; transcription factor SOX9 (SOX group E)	2
SPB1, FTSJ3; AdoMet-dependent rRNA methyltransferase SPB1	14
SPECC1; cytospin	2

speG, SAT; diamine N-acetyltransferase	3
SPN1, IWS1; transcription factor SPN1	3
SPNS; MFS transporter, Spinster family, sphingosine-1-phosphate transporter	5
SPOUT1; methyltransferase	2
SPT; serine palmitoyltransferase	35
SQOR; eukaryotic sulfide quinone oxidoreductase	2
SREBP1, SREBF1; sterol regulatory element-binding transcription factor 1	2
SREK1, SFRS12; splicing regulatory glutamine/lysine-rich protein 1	4
SSR1; translocon-associated protein subunit alpha	7
SSR2; translocon-associated protein subunit beta	3
SSR3; translocon-associated protein subunit gamma	3
STAM; signal transducing adaptor molecule	8
STARD10; StAR-related lipid transfer protein 10	3
STRA6; vitamin A receptor/transporter (stra6) family protein	3
STT3; dolichyl-diphosphooligosaccharide---protein glycosyltransferase	34
SUOX; sulfite oxidase	4
SUPT4H1, SPT4; transcription elongation factor SPT4	2
SUPT5H, SPT5; transcription elongation factor SPT5	14
SUPT6H, SPT6; transcription elongation factor SPT6	10
SUPV3L1, SUV3; ATP-dependent RNA helicase SUPV3L1/SUV3	6
SVIL; supervillin	5
TACC3, maskin; transforming acidic coiled-coil-containing protein 3	3
TAF1; transcription initiation factor TFIID subunit 1	4
TAF10; transcription initiation factor TFIID subunit 10	2
TAF13; transcription initiation factor TFIID subunit 13	3
TAF2; transcription initiation factor TFIID subunit 2	2
TAF3; transcription initiation factor TFIID subunit 3	2
TAF4; transcription initiation factor TFIID subunit 4	2
TAF6; transcription initiation factor TFIID subunit 6	3
TAF7; transcription initiation factor TFIID subunit 7	2
TAF9; transcription initiation factor TFIID subunit 9	3
TAGLN; transgelin	12
TALDO1, talB, talA; transaldolase	14
TAT; tyrosine aminotransferase	6
TAZ; monolysocardiolipin acyltransferase	2
TBL1; transducin (beta)-like 1	13
TBL2; transducin beta-like protein 2	3
TBP, tbp; transcription initiation factor TFIID TATA-box-binding protein	15
TC.POT; proton-dependent oligopeptide transporter, POT family	5
TCERG1, CA150; transcription elongation regulator 1	5
TCF25, RQC1; transcription factor 25	3
TCF4_12; transcription factor 4/12	5
TCF7L2; transcription factor 7-like 2	6
TEAD; transcriptional enhancer factor	5
TENT5A_B, FAM46A_B; terminal nucleotidyltransferase 5A/B	2

TENT5C, FAM46C; terminal nucleotidyltransferase 5C	4
TFAP4; transcription factor AP-4	3
TFCP2; transcription factor CP2 and related proteins	2
TFE3; transcription factor E3	4
TFIIA1, GTF2A1, TOA1; transcription initiation factor TFIIA large subunit	2
TFIIA2, GTF2A2, TOA2; transcription initiation factor TFIIA small subunit	2
TFIIB, GTF2B, SUA7, tfb; transcription initiation factor TFIIB	6
TFIIF1, GTF2F1, TFG1; transcription initiation factor TFIIF subunit alpha	4
TFIIF2, GTF2F2, TFG2; transcription initiation factor TFIIF subunit beta	4
TFIIH1, GTF2H1, TFB1; transcription initiation factor TFIIH subunit 1	6
TFIIH2, GTF2H2, SSL1; transcription initiation factor TFIIH subunit 2	5
TFIIH3, GTF2H3, TFB4; transcription initiation factor TFIIH subunit 3	2
TFIIH4, GTF2H4, TFB2; transcription initiation factor TFIIH subunit 4	5
TFIIS; transcription elongation factor S-II	4
TIM17; mitochondrial import inner membrane translocase subunit TIM17	7
TIM22; mitochondrial import inner membrane translocase subunit TIM22	2
TIM23; mitochondrial import inner membrane translocase subunit TIM23	3
TIM44; mitochondrial import inner membrane translocase subunit TIM44	3
TIM50; mitochondrial import inner membrane translocase subunit TIM50	4
TIM8; mitochondrial import inner membrane translocase subunit TIM8	3
TIM9; mitochondrial import inner membrane translocase subunit TIM9	2
TIP60, KAT5, ESA1; histone acetyltransferase HTATIP	4
TM9SF1; transmembrane 9 superfamily member 1	9
TM9SF2_4; transmembrane 9 superfamily member 2/4	28
TM9SF3; transmembrane 9 superfamily member 3	18
TMA16; translation machinery-associated protein 16	3
TMCO1; calcium load-activated calcium channel	2
TMEM106A; transmembrane protein 106A	2
TMEM127; transmembrane protein 127	3
TMEM132; transmembrane protein 132	3
TMEM150; transmembrane protein 150	2
TMEM222; transmembrane protein 222	3
TMEM230; transmembrane protein 230	4
TMEM258; transmembrane protein 258	3
TMEM33; transmembrane protein 33	2
TMEM63, CSC1; calcium permeable stress-gated cation channel	7
TMEM8A_B; transmembrane protein 8A/B	3
TMEM9; proton-transporting V-type ATPase complex assembly regulator	5
TMPRSS11B; transmembrane protease serine 11B	2
TMPRSS4; transmembrane protease serine 4	4
TMPRSS6; transmembrane protease serine 6	2
TMPRSS9; transmembrane protease serine 9	8
TMUB; transmembrane and ubiquitin-like domain-containing protein	3
TNPO1, IPO2, KPNB2; transportin-1	9
TOM1, TOM1L1_2; target of Myb membrane trafficking protein 1 and related proteins	8

TPCN2; two pore calcium channel protein 2	2
TPST; protein-tyrosine sulfotransferase	3
TRA2; transformer-2 protein	6
TRAM1; translocating chain-associated membrane protein 1	9
TRK, HKT; Trk/Ktr/HKT type cation transporter	3
TRM112, TRMT112; multifunctional methyltransferase subunit TRM112	2
TRM6, GCD10; tRNA (adenine58-N1)-methyltransferase non-catalytic subunit	2
TRM61, GCD14; tRNA (adenine57-N1/adenine58-N1)-methyltransferase catalytic subunit	3
trmB, METTL1, TRM8; tRNA (guanine-N7-)-methyltransferase	3
TRMT1, trm1; tRNA (guanine26-N2/guanine27-N2)-dimethyltransferase	3
TRMT10, TRM10, RG9MTD; tRNA (guanine9-N1)-methyltransferase	2
TRMT2A; tRNA (uracil-5-)-methyltransferase	6
TRPA1, ANKTM1; transient receptor potential cation channel subfamily A member 1	7
TRPC4; transient receptor potential cation channel subfamily C member 4	10
TRPC7; transient receptor potential cation channel subfamily C member 7	2
TRPM2; transient receptor potential cation channel subfamily M member 2	6
TRPM3; transient receptor potential cation channel subfamily M member 3	6
TRPM5; transient receptor potential cation channel subfamily M member 5	2
TRPO3, MTR10; transportin-3	2
TRPT1, TPT1; 2'-phosphotransferase	2
TRPV5; transient receptor potential cation channel subfamily V member 5	6
TRPV6; transient receptor potential cation channel subfamily V member 6	6
TRRAP; transformation/transcription domain-associated protein	7
trxA; thioredoxin 1	3
TSPO, BZRP; translocator protein	3
TST, MPST, sseA; thiosulfate/3-mercaptopyruvate sulfurtransferase	4
TTF2; transcription termination factor 2	4
TTLL1; tubulin polyglutamylase TTLL1	4
TTLL11; tubulin polyglutamylase TTLL11	3
TTLL5; tubulin polyglutamylase TTLL5	2
TTLL6_13; tubulin polyglutamylase TTLL6/13	4
TTLL9; tubulin polyglutamylase TTLL9	2
TUT; terminal uridylyltransferase	3
TXNDC10; thioredoxin domain-containing protein 10	2
TXNRD; thioredoxin reductase (NADPH)	16
uaZ; urate oxidase	3
UGCG; ceramide glucosyltransferase	6
UGP2, galU, galF; UTP--glucose-1-phosphate uridylyltransferase	27
UPF1, RENT1; regulator of nonsense transcripts 1	10
UPF2, RENT2; regulator of nonsense transcripts 2	5
UPF3, RENT3; regulator of nonsense transcripts 3	2
UQCRFS1, RIP1, petA; ubiquinol-cytochrome c reductase iron-sulfur subunit	10
uvrD, pcrA; ATP-dependent DNA helicase UvrD/PcrA	5
VAMP2; vesicle-associated membrane protein 2	10
VAMP3; vesicle-associated membrane protein 3	3

VAPA; vesicle-associated membrane protein-associated protein A	7
VAPB, ALS8; vesicle-associated membrane protein-associated protein B	2
VAT1; synaptic vesicle membrane protein VAT-1	4
VCP, CDC48; transitional endoplasmic reticulum ATPase	54
VEGFC_D; vascular endothelial growth factor C/D	3
VKORC1; vitamin-K-epoxide reductase (warfarin-sensitive)	3
VMP1; vacuole membrane protein 1	6
VTI1; vesicle transport through interaction with t-SNAREs 1	2
WHSC1, MMSET, NSD2; -lysine36 N-dimethyltransferase NSD2	2
WHSC1L1, NSD3; -lysine4 N-dimethyltransferase / -lysine27 N-dimethyltransferase	2
WHT; ATP-binding cassette, subfamily G (WHITE), eye pigment precursor transporter	12
XDH; xanthine dehydrogenase/oxidase	11
XRCC1; DNA-repair protein XRCC1	2
YAT; yeast amino acid transporter	8
yghU, yfcG; GSH-dependent disulfide-bond oxidoreductase	2
yhdR; aspartate aminotransferase	2
yidC, spoIIIJ, OXA1, ccfA; YidC/Oxa1 family membrane protein insertase	5
YIF1; protein transport protein YIF1	2
YY; transcription factor YY	4
ZDHHC; palmitoyltransferase	7
ZDHHC13_17, HIP14; palmitoyltransferase ZDHHC13/17	3
ZDHHC14_18; palmitoyltransferase ZDHHC14/18	2
ZDHHC2_15_20; palmitoyltransferase ZDHHC2/15/20	8
ZDHHC3_7_25; palmitoyltransferase ZDHHC3/7/25	2
ZDHHC5_8; palmitoyltransferase ZDHHC5/8	7

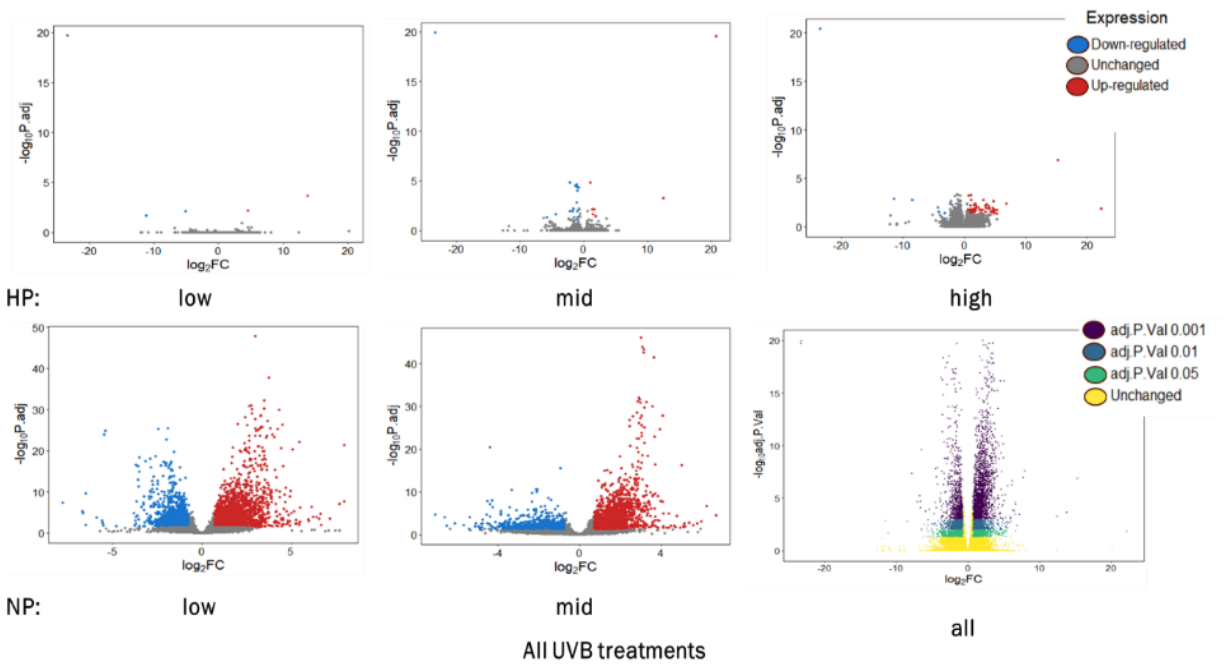

Figure S4.3. Volcano plot of genes expression in response to UVB exposure in *Philodina*. Plots show differentially expressed genes that responded to a 2 hr low, mid, or high (1.3, 3.7, 5.0 W/m^2) for either highly pigmented (HP) or non-pigmented (NP) bdelloids.

Table S4.4. Go Terms with >10 transcripts in highly pigmented samples. Differentially expressed genes responding to UVB radiation exposure in a) highly pigmented bdelloids and b) non-pigmented bdelloids.

a)

GoTerm	ontology	description	No. genes
GO:0005525	mf	GTP binding	98
GO:0005509	mf	calcium ion binding	83
GO:0005975	bp	carbohydrate metabolic process	62
GO:0006457	bp	protein folding	62
GO:0003924	mf	GTPase activity	61
GO:0016491	mf	oxidoreductase activity	56
GO:0140662	mf	ATP-dependent protein folding chaperone	55
GO:0005788	cc	endoplasmic reticulum lumen	39
GO:0020037	mf	heme binding	38
GO:0015031	bp	protein transport	36
GO:0005743	cc	mitochondrial inner membrane	33
GO:1902600	bp	proton transmembrane transport	29
GO:0016192	bp	vesicle-mediated transport	28
GO:0006468	bp	protein phosphorylation	27
GO:0005794	cc	Golgi apparatus	26
GO:0008152	bp	metabolic process	25
GO:0030170	mf	pyridoxal phosphate binding	23

GO:0004553	mf	hydrolase activity, hydrolyzing O-glycosyl compounds	23
GO:0004129	mf	cytochrome-c oxidase activity	20
GO:0006119	bp	oxidative phosphorylation	18
GO:0022900	bp	electron transport chain	16
GO:0005507	mf	copper ion binding	14
GO:0005978	bp	glycogen biosynthetic process	13
GO:0070469	cc	respirasome	13
GO:0006914	bp	autophagy	12
GO:0006094	bp	gluconeogenesis	12
GO:0003756	mf	protein disulfide isomerase activity	12
GO:0045277	cc	respiratory chain complex IV	11
GO:0022904	bp	respiratory electron transport chain	11
GO:0019902	mf	phosphatase binding	11
GO:0010923	bp	negative regulation of phosphatase activity	11
GO:0050661	mf	NADP binding	11
GO:0006888	bp	endoplasmic reticulum to Golgi vesicle-mediated transport	11

b)

GoTerm	ontology	description	No. genes
GO:0016020	cc	membrane	1530
GO:0005524	mf	ATP binding	481
GO:0005634	cc	nucleus	214
GO:0005737	cc	cytoplasm	200
GO:0016491	mf	oxidoreductase activity	156
GO:0005975	bp	carbohydrate metabolic process	148
GO:0055085	bp	transmembrane transport	145
GO:0003723	mf	RNA binding	111
GO:0016740	mf	transferase activity	109
GO:0020037	mf	heme binding	95
GO:0006457	bp	protein folding	94
GO:0003677	mf	DNA binding	86
GO:0003824	mf	catalytic activity	81
GO:0140662	mf	ATP-dependent protein folding chaperone	77
GO:0140359	mf	ABC-type transporter activity	75
GO:0005506	mf	iron ion binding	73
GO:0006412	bp	translation	70
GO:0006468	bp	protein phosphorylation	69
GO:0004553	mf	hydrolase activity, hydrolyzing O-glycosyl compounds	59
GO:0008233	mf	peptidase activity	54
GO:1990904	cc	ribonucleoprotein complex	54
GO:0005840	cc	ribosome	53
GO:0003735	mf	structural constituent of ribosome	51
GO:0005788	cc	endoplasmic reticulum lumen	50
GO:0005874	cc	microtubule	50
GO:0030170	mf	pyridoxal phosphate binding	49
GO:0006869	bp	lipid transport	47
GO:0008234	mf	cysteine-type peptidase activity	47
GO:0004672	mf	protein kinase activity	46
GO:0004497	mf	monooxygenase activity	43
GO:0008152	bp	metabolic process	43

GO:0016705	mf	oxidoreductase activity, acting on paired donors, with incorporation or reduction of molecular oxygen	41
GO:0050790	bp	regulation of catalytic activity	38
GO:0098869	bp	cellular oxidant detoxification	36
GO:0004129	mf	cytochrome-c oxidase activity	33
GO:0005978	bp	glycogen biosynthetic process	31
GO:0006119	bp	oxidative phosphorylation	30
GO:0004674	mf	protein serine/threonine kinase activity	29
GO:0007186	bp	G protein-coupled receptor signaling pathway	27
GO:0005507	mf	copper ion binding	26
GO:0006979	bp	response to oxidative stress	25
GO:0071704	bp	organic substance metabolic process	25
GO:0006914	bp	autophagy	24
GO:0051537	mf	2 iron, 2 sulfur cluster binding	23
GO:0007018	bp	microtubule-based movement	23
GO:0070469	cc	respirasome	23
GO:0004930	mf	G protein-coupled receptor activity	22
GO:0050661	mf	NADP binding	22
GO:0004096	mf	catalase activity	21
GO:0042744	bp	hydrogen peroxide catabolic process	21
GO:0003779	mf	actin binding	20
GO:0045277	cc	respiratory chain complex IV	18
GO:0008569	mf	minus-end-directed microtubule motor activity	18
GO:0008610	bp	lipid biosynthetic process	17
GO:0003756	mf	protein disulfide isomerase activity	17
GO:0006281	bp	DNA repair	17
GO:0004613	mf	phosphoenolpyruvate carboxy kinase (GTP) activity	17
GO:0003993	mf	acid phosphatase activity	15
GO:0004134	mf	4-alpha-glucanotransferase activity	15
GO:0019902	mf	phosphatase binding	15
GO:0010923	bp	negative regulation of phosphatase activity	15
GO:0043169	mf	cation binding	15
GO:0022904	bp	respiratory electron transport chain	14
GO:0030976	mf	thiamine pyrophosphate binding	14
GO:0003774	mf	cytoskeletal motor activity	13
GO:0005730	cc	nucleolus	13
GO:0008017	mf	microtubule binding	13
GO:0008171	mf	O-methyltransferase activity	13
GO:0008184	mf	glycogen phosphorylase activity	13
GO:0003724	mf	RNA helicase activity	12
GO:0006352	bp	DNA-templated transcription initiation	12
GO:0003983	mf	UTP:glucose-1-phosphate uridylyl transferase activity	12
GO:0006011	bp	UDP-glucose metabolic process	12
GO:0030248	mf	cellulose binding	12
GO:0016459	cc	myosin complex	11
GO:0008745	mf	N-acetyl muramoyl-L-alanine amidase activity	11
GO:0009253	bp	peptidoglycan catabolic process	11

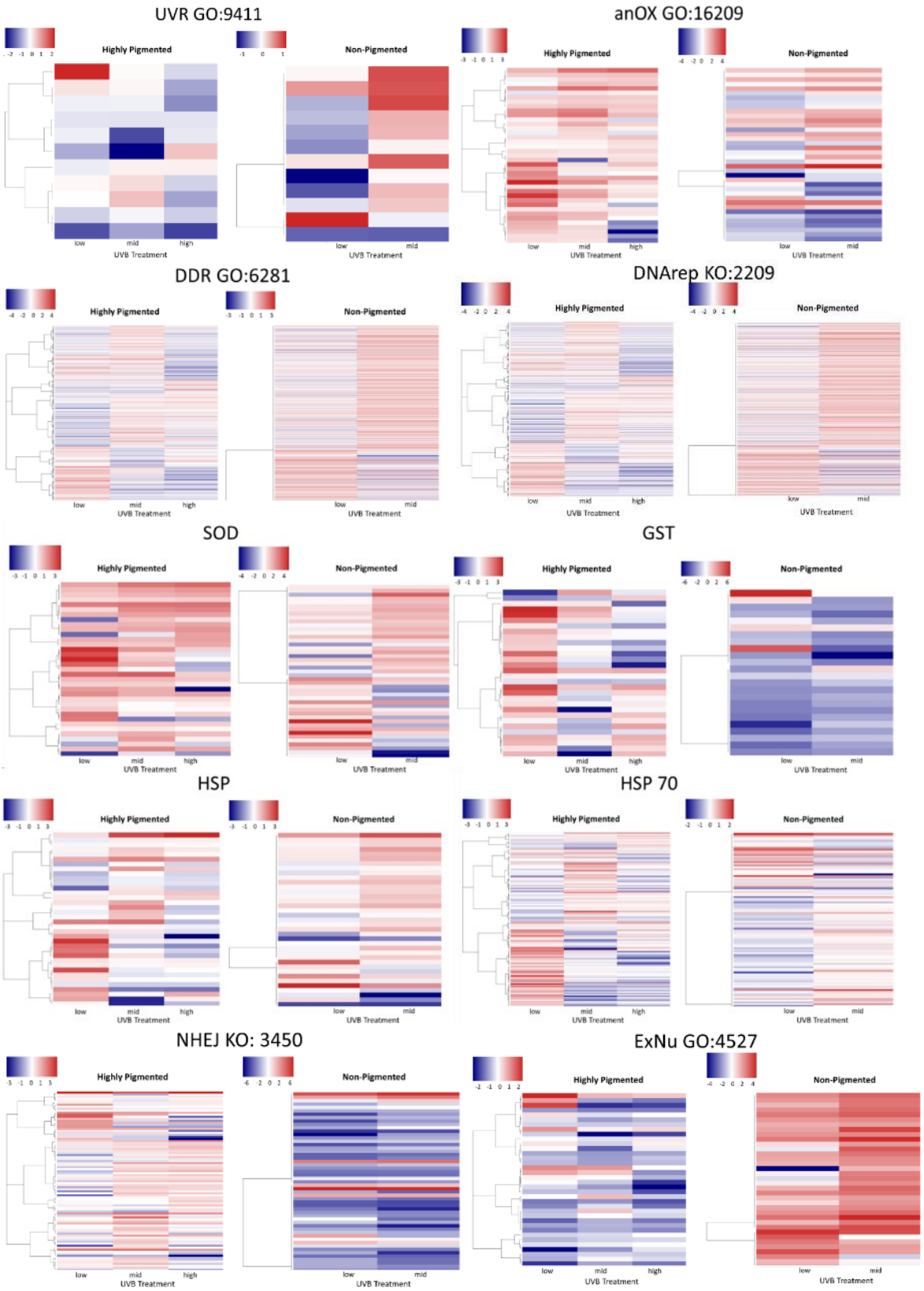

Figure S4.4. Responsive transcripts identified through Gene Ontology (Go terms) annotation database and Kyoto Encyclopedia of Genes and Genomes Orthology (KEGG) pathways.

Curriculum Vita

I obtained a Bachelor of Science in Biology and defended a thesis for a Master of Science in Biology with an emphasis in Ecology from New Mexico Institute of Mining and Technology. After earning my Master's degree, I worked as a part-time biology professor add where, and then as a research assistant for two start-up companies developing innovative medical devices. In 2016, I began working towards a Ph.D. under Dr. Elizabeth Walsh's mentorship at the University of Texas at El Paso (UTEP) in the Ecology and Evolutionary Biology doctoral program. In May 2021, I completed the requirements for a graduate degree in Geospatial Information Science and Technology (GIST) Graduate Certificate from UTEP. I have also received financial support from various outlets. These grants include two UTEP Dodson grants, a College of Science Research Award supported by a grant from NIH, Research Assistant Fellowship from the University of Texas at El Paso Office of the Provost and Graduate School, UTEP Frank B. Cotton Trust Scholarship, and a 3-year fellowship from the Hispanic Alliance for the Professoriate in Environmental Sciences and Engineering Fellowship.

Several local and national conferences have provided me with opportunities to present my doctoral research in person and virtually, including the Association for Limnology and Oceanography, Environmental Society of America, Minority Science and Engineering Improvement Program, and International Rotifer Symposium. Along with research, I taught Introductory Biology laboratories, which strengthened my knowledge and multitasking skills. I also participated in numerous local science outreach programs for students and adults alike to inspire. more individuals with backgrounds similar to mine to pursue higher education in science.